



Universiteit
Leiden
The Netherlands

Investigations on the role of impaired lysosomes of macrophages in disease

Lienden, M.J.C. van der

Citation

Lienden, M. J. C. van der. (2021, March 18). *Investigations on the role of impaired lysosomes of macrophages in disease*. Retrieved from <https://hdl.handle.net/1887/3152425>

Version: Publisher's Version

License: [Licence agreement concerning inclusion of doctoral thesis in the Institutional Repository of the University of Leiden](#)

Downloaded from: <https://hdl.handle.net/1887/3152425>

Note: To cite this publication please use the final published version (if applicable).

Cover Page



Universiteit Leiden



The handle <https://hdl.handle.net/1887/3152425> holds various files of this Leiden University dissertation.

Author: Lienden, M.J.C. van der

Title: Investigations on the role of impaired lysosomes of macrophages in disease

Issue Date: 2021-03-18

Investigations on the role of impaired lysosomes of macrophages in disease

Proefschrift

Ter verkrijging van de graad van Doctor aan de Universiteit Leiden, op gezag
van Rector Magnificus prof. dr. ir. H. Bijl, volgens het besluit van het College
voor promoties te verdedigen op 18 maart 2021 klokke 11:15

Door

Martijn Johan Christiaan van der Lienden
Geboren te Gouda, Nederland, 1990

Promotiecomissie

Promotor: Prof. dr. J.M.F.G. Aerts *Universiteit Leiden*

Copromotor: Dr. M. van Eijk *Universiteit Leiden*

Overige leden: Prof. dr. T.M. Cox *University of Cambridge*

Prof. dr. M. van Eck *Universiteit Leiden*

Prof. dr. J.D. Laman *Rijksuniversiteit Groningen*

Prof. dr. H.S. Overkleeft *Universiteit Leiden*

Prof. dr. M. van der Stelt *Universiteit Leiden*

Investigations on the role of impaired lysosomes of macrophages in disease

Martijn van der Lienden

Doctoral thesis, 209 pages, Leiden University 2021

ISBN: 978-94-6421-228-0

Printed by: Ipskamp printing

©2021, Martijn van der Lienden, All rights reserved. No part of this thesis may be reproduced in any matter or by any means without permission from the author.

Table of contents

General introduction	Lysosome function and macrophage lysosomes	1
Chapter 1	HEPES activates a MiT/TFE-dependent lysosomal-autophagic gene network in cultured cells: a call for caution	23
Chapter 2	Glucocerebrosidase in cultured cells: extreme sensitivity for medium conditions	49
Chapter 3	Localization of active endogenous and exogenous GBA by correlative light-electron microscopy in human fibroblasts	75
Chapter 4	Glycoprotein non metastatic protein B: An Emerging Biomarker for Lysosomal Dysfunction in Macrophages	101
Chapter 5	GCase and LIMP2 abnormalities in the liver of Niemann Pick type C mice	127
Chapter 6	Transcriptional regulation of macrophage lysosome biogenesis in vitro and in the obese adipose	145
Discussion and summary		169
Appendices	Summary in Dutch	191
	List of publications	
	Curriculum Vitae	
	Acknowledgements	

‘The effect that each component of the pathway has on the pathway flux under a particular condition is indicated by its flux control coefficient, defined as the $\delta J/J / \delta E_i/E_i$ ($\delta J/J$, the relative change in flux caused by a small relative change in enzyme I activity, $\delta E_i/E_i$ (e.g., a particular Atg); the activity of the other enzymes in the pathway must be kept constant).’

Klionsky, D. J. & Meijer, A. J. From the urea cycle to autophagy: Alfred J. Meijer. Autophagy vol. 7 805–813 (2011).

General introduction

Lysosome function and macrophage lysosomes

Introduction

The lysosome is a membrane enclosed organelle that contains at least 60 hydrolases and mediates degradation of macromolecules. Macromolecules are delivered to lysosomes through endocytosis, macropinocytosis, phagocytosis and autophagy. Hydrolysis of macromolecules is generally facilitated by low pH. Consistently, the luminal pH of the lysosome ranges between 4.0 and 5.0 and is generated at the expense of ATP via the lysosomal proton pump. This allows for optimal activity of lysosomal hydrolases. The lysosomal enzymes are in turn subjected to proteolytic degradation in lysosomes. Their ongoing synthesis and delivery to lysosomes is therefore crucial. Upon synthesis and N-glycosylation in the endoplasmic reticulum (ER), lysosomal enzymes traverse the Golgi apparatus and are sorted to lysosomes by shuttling protein receptors that recognize lysosomal sorting motifs. The major sorting mechanism for soluble acid hydrolases is via mannose-6-phosphate receptors, which recognize unique mannose-6-phosphate moieties on lysosomal glycoproteins attached in the Golgi system. In specific cells alternative lysosomal routing occurs, for example via progranulin and sortilin.¹ A fraction of most soluble acid hydrolases is secreted by cells and may subsequently be delivered to lysosomes by receptor-mediated endocytosis. The mannose-6-phosphate receptor and additional receptors can mediate this re-uptake.¹

Glucocerebrosidase (GBA)

One of the lysosomal hydrolases is the retaining beta-glucosidase named glucocerebrosidase, encoded by the *GBA* gene. GBA catalyses the fragmentation of the ubiquitous glycosphingolipid glucosylceramide (GlcCer) in lysosomes (**Figure 1**). The enzyme is assisted in its activity by saposin C, which promotes activity towards lipid substrate. GBA is uniquely sorted to lysosomes by binding to the membrane protein LIMP2 in the ER. Together, these proteins are routed to lysosomes where the acidic environment triggers dissociation of the complex. GBA can be detected and visualized by means of its enzymatic activity towards fluorogenic substrates. GBA-specific antisera also available. Relatively novel detection methods are fluorescent activity-based probes (ABPs) that allow selective labelling and visualization of catalytically active GBA molecules in cells and organisms.²⁻⁵ These ABPs are based on a cyclophellitol scaffold to which a fluorophore is covalently attached. Cyclophellitol, and the related conduritol B epoxide, are known suicide inhibitors of GBA that covalently link to its catalytic nucleophile, glutamate 340, in mechanism-based manner. Modified cyclophellitols with a hydrophobic extension at C6 have been designed as suicide inhibitors, allowing generation of enzyme deficiency on demand.⁶

Lysosomal storage disease (LSD)

Deficiency of GBA due to mutations in the encoding gene forms the molecular basis of Gaucher disease (GD).⁷ In rare cases, GBA activity is reduced due to inherited defects in LIMP2 (Action Myoclonus Renal Failure Syndrome; AMRF), or in saposin C or its precursor protein prosaposin.⁸⁻¹⁰ The clinical presentation of GBA deficiency in GD patients is remarkably heterogeneous and ranges from neonatal lethality due to skin barrier abnormalities to a virtual asymptomatic course of disease.^{11,12} The GBA genotype and concomitant residual enzyme activity correlates to some extent with severity of disease but is only partly predictive in milder cases that do not develop neurological complications, the so-called type 1 variant of GD.^{13,14} A hallmark of GD is accumulation

of GlcCer in storage tubules inside lysosomes of tissue macrophages that transform into swollen Gaucher cells. These lipid-laden macrophages are viable and show features of alternatively activated macrophages.¹⁵ Gaucher cells are thought to underly typical GD symptoms such as hepatosplenomegaly and hematologic abnormalities, but the pathophysiological basis for other symptoms (e.g. neurological complications and osteoporosis) is still enigmatic. Adaptive metabolism of GlcCer during GBA deficiency is considered to produce toxic factors such as glucosylsphingosine.^{5,16}

Inherited deficiencies of other lysosomal enzymes also occur and lead to lysosomal accumulation of their corresponding substrates in one or many cell types. These disorders, more than 60 discrete entities, are collectively named lysosomal storage diseases (LSDs) and constitute a major part of the inherited metabolic disorders.^{17,18} Lysosomal storage may also be caused by defects in lysosomal proteins that are responsible for metabolite export or by defects in accessory proteins that assist lysosomal hydrolases in their activity or stability. One example of this is Niemann Pick disease type C (NPC), which is caused by inherited defects in either the lysosomal transporter NPC1 or NPC2, proteins involved in the export of cholesterol from the lysosome to the ER.^{19,20} NPC cells show a lysosomal accumulation of cholesterol that is accompanied by a secondary, partial deficiency of GBA.²¹

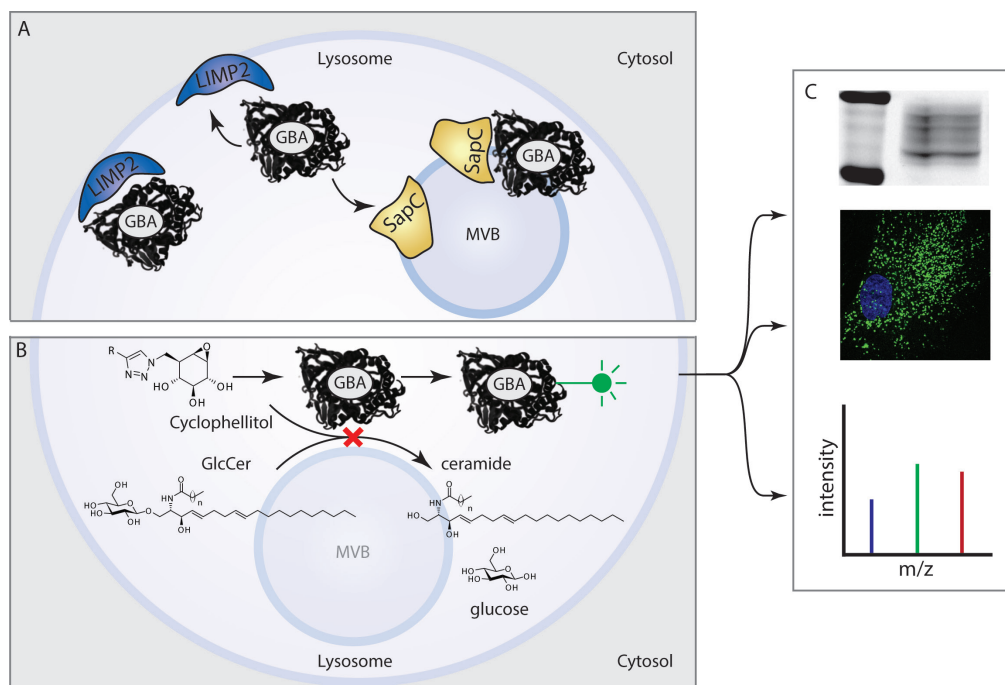


Figure 1. Localisation and function of GBA in the lysosome; (A) Lysosomal targeting of GBA is dependent on LIMP2. Luminal pH facilitates dissociation of the GBA-LIMP2 complex. GBA is assisted by Saposin C in its hydrolytic function at intraluminal membranes. (B) GBA catalyses the hydrolysis of glucosylceramide into ceramide and glucose. Cyclophellitol competes with the endogenous substrate of GBA and binds irreversibly in the active site. To visualize or isolate active GBA, cyclophellitol can be attached via a linker (R) to a detection group such as a fluorophore or a biotin. (C) Properties of GBA can be analysed through several methods including SDS-PAGE, fluorescence microscopy

Introduction

and LC-MS/MS (depicted from top to bottom); GBA, glucocerebrosidase; LIMP2, lysosomal integral protein 2; SapC, saposin C; GlcCer, glucosylceramide, MVB, multivesicular body.

Regulation of lysosomes

Cells contain on average 100-200 lysosomes which can change in composition and position.²² A fraction of a cell's lysosomes is found in the periphery and controlled movement towards the nucleus can occur along microtubules. Vice versa, the large proportion of perinuclear lysosomes reside near the microtubule-organising centre (MTOC) and may move outward. Autophagosomes and endosomes also move along the same microtubules and can peripherally exchange content through organelle fusion.²³ The morphology of individual lysosomes is influenced by their actual content, which includes membranes and macromolecules that are destined for degradation.²² In addition, external factors impact on lysosomes. One example of this is the major effect of the buffer compound HEPES in cell culture medium (see chapter 1 and 2).²⁴

Functions of lysosomes in signalling

The importance of the lysosome in cellular metabolism is illustrated by the progressive pathology that is observed in inherited LSDs.^{25,26} Of note, extracellular functions for lysosomes and their hydrolases have recently been discovered and are subjected to specific regulatory processes. Secreted lysosomal hydrolases exhibit physiological functions in certain biological processes such bone remodelling (Cathepsin K) and lipid barrier formation in the stratum corneum (GBA).^{27,28} The discovery of protein complexes at the lysosome membranes has revealed a nutrient sensing mechanism that impacts on the metabolic state of the cell. A key role is fulfilled in this respect by the mechanistic target of rapamycin complex 1 (mTORC1). Its activity is regulated by the combined presence of lysosomal nutrients and cytosolic signalling as triggered by growth factors.²⁹ For example, the reciprocal presence of AMPK at the surface of lysosomes during nutrient shortage provides the cell with a switch for anabolic and catabolic processes, respectively.³⁰ A general mode of action for mTORC1 has been proposed. Upon nutrient rich conditions, active mTORC1 localizes to the lysosomal membrane. In this state mTORC1 promotes cell growth and protein synthesis. It simultaneously inhibits transcriptional processes that promote catabolism, such as autophagy and lysosomal biogenesis.²⁹ Nutrient poor conditions inhibit mTORC1 and allow a transcriptionally regulated switch towards degradation of macromolecules.

Transcriptional control of lysosomal apparatus

Identification of a common sequence upstream of lysosomal genes named Coordinated Lysosomal Expression and Regulation (CLEAR) element, led to the discovery of Transcription factor EB (TFEB) as master regulator of lysosomal biogenesis.³¹ TFEB is a basic helix-loop-helix (bHLH) transcription factor that belongs to the microphthalmia-transcription factor E (MiT/TFE) subfamily.³² The family furthermore contains the transcription factors MITF, TFE3 and TFEC. The subfamily classification is based on exclusive heterodimerization among MiT/TFE members, but not with other bHLH transcription factors.³² It has become apparent that the status of lysosomes has impact on transcription factors that regulate expression of genes encoding lysosomal proteins and essential components of autophagy (**Figure 2**). These transcription factors (TFs) couple

lysosome status and the related ability to supply nutrients with lysosome biogenesis and autophagy.^{33,34} Under nutrient-rich conditions, serine phosphorylation of TFEB prevents its translocation to the nucleus.^{34,35} A homologous serine residue is found in MITF, which renders cytosolic retention in phosphorylated state.³⁶ TFEB, MITF and TFE3 are sequestered in the cytosol by Rag GTPases and 14-3-3 proteins and drive lysosomal biogenesis upon nuclear translocation.^{34,37-39} Upon perturbation of lysosomal function by increasing lysosomal pH, employing the lysosomotropic compound chloroquine, or by depletion of amino acids, TFEB is dephosphorylated and translocates into the nucleus.^{34,40} Similarly, exposure of cells to chloroquine induces translocation of MITF and TFE3 into the nucleus.³⁴ The transcriptional activity of various MiT/TFE transcription factors is highly cell type and context dependent.⁴¹ Of note, TFEC is assumed to counteract transcription due to a lack of an activation domain, but its exact function remains enigmatic.⁴² MTORC1 has been shown to regulate MiT/TFE factors, providing a direct link between lysosomal nutrient status and the transcription of lysosome genes.^{43,44} In addition, alternative regulation of MiT/TFE members exists and involves signaling proteins such as MAPK, PKC and AKT.⁴⁵ Complicating the regulation of lysosomal biogenesis, additional transcription factors that have been found to modulate expression of lysosomal and autophagy genes, such as MYC, STAT3 and zinc finger with KRAB and SCAN domains 3 (ZKSCAN3).⁴⁶⁻⁴⁹

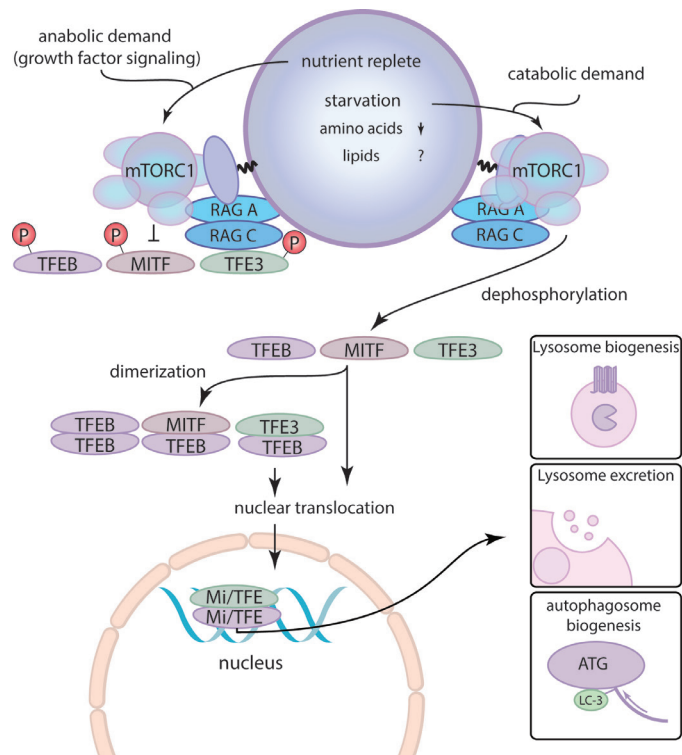


Figure 2. The role of the lysosome in regulating transcription of lysosome -and autophagy genes; Upon sufficient nutrient availability mTORC1 is sequestered at the cytosolic side of the lysosomal membrane by Rag GTPases. This location favours the catalytic activity of mTORC1. MiT/TFE members are likewise sequestered in the cytosol by Rag GTPases and close proximity to active

Introduction

mTORC1 renders MiT/TFE members in an inactive, phosphorylated state. Upon high catabolic demand or reduced lysosomal amino acid content, mTORC1 is inactivated. Dephosphorylated MiT/TFE members may homo- or heterodimerize and translocate into the nucleus to initiate transcription of lysosome and autophagy genes and lysosome excretion. Mechanisms through which alternative metabolites such as lipids and sugars influence mTORC1 activity are less characterized.

Role of lysosomes in lipid metabolism.

Although *de novo* synthesis and lipid-driven ATP-production (through beta-oxidation) takes place in other cellular compartments, lysosomes are important in releasing free fatty acids and cholesterol from esterified lipid substrates. The sources of lysosomal lipid substrates can be endogenous (being delivered by autophagy processes) or exogenous (being delivered by endocytosis). Lysosome mediated degradation of lipids is highly dynamic.⁵⁰ In view of this, it is not surprising that the transcription factor TFEB can trigger transcription of proliferator-activated receptor α (PPAR α) as well as PPAR- γ Coactivator 1 Alpha (PGC1 α), key regulators of lipid catabolism.⁵¹ The role of lysosomes in fragmentation of various types of complex lipids, including sphingolipids and cholesterol, warrants further introduction.

Sphingolipids

Sphingolipids are a class of lipids characterized by a ceramide lipid moiety existing of a variable fatty acyl moiety linked via an amide bond to a C18 sphingosine. A prominent and ubiquitous sphingolipid is sphingomyelin (SM) in which a phosphorylcholine moiety is linked to ceramide. Glycosphingolipids (GSLs) are a class of sphingolipids in which sugars are attached to the ceramide backbone. Numerous distinct glycosphingolipids exist due to variations in the sugar moiety. The simplest GSLs are galactosylceramide (GalCer) and glucosylceramide (GlcCer) with a single sugar beta-linked to ceramide. Complex GSLs have additional sugars (or sulfates) attached to the primary sugar. Sphingolipids are synthesized by multi-step formation of ceramide from serine and palmitoyl CoA followed by sequential attachments of moieties to generate the head groups.^{52,53} Together with cholesterol, SM and GSLs are major components of lipid rafts, highly specialized compartments in the cell membrane that facilitate cell signalling, polarization and movement.⁵⁴ Glycan composition on sphingolipids determines protein-lipid and lipid-lipid interactions at the plasma membrane as well as on intracellular membrane structures such as the Golgi-network.⁵⁴⁻⁵⁶ Knock-out models lacking enzymes that synthesize specific subsets of glycosphingolipids revealed their importance in a wide variety of processes such as neuronal development and function, skin permeability, immune function, pathogen-host interactions and intracellular protein trafficking.^{53,55,57-62} GSLs and SM are ongoingly synthesized and fragmented in lysosomes. The lysosomal degradation involves stepwise removal of terminal moieties (phosphorylcholine, sulfate, sugars) rendering ceramide that is cleaved into a fatty acid and sphingosine. The lysosomal degradation products are exported to the cytosol and may be re-used or enter re-synthesis routes for other purposes. Deficiencies in sphingomyelinase and GSL degrading glycosidases give rise to sphingolipidoses (diseases characterized by lysosomal storage of sphingolipids).^{17,25} The glycosphingolipidoses such as Gaucher disease, are the most prevalent among the LSDs.⁶³⁻⁶⁶ Besides the turnover of various cellular membranes via autophagy pathways, the recycling of plasma membrane and uptake of lipoproteins

via endocytosis provides lysosomes with sphingolipid substrates for fragmentation.

Cholesterol

Cholesterol is a major constituent of cellular membranes. Excessive cholesterol in cells is converted to cholesterol-ester that is relatively inert and accumulates in lipid droplets (LD). Lipoproteins, particularly low-density lipoproteins (LDL), are rich in cholesterol ester. Other important membrane lipids are the diglyceride-based structures such as the various phospholipids that contain distinct polar head group composition. Attachment of another fatty acyl to diglyceride results in triglyceride that similarly to cholesterol ester does not incorporate in membranes but in LDs. Cholesterol-esters and diglyceride-based lipids undergo lysosomal fragmentation by lipase activity, releasing free fatty acids that are subsequently exported to the cytosol. Other degradation products (monoacylglycerol, cholesterol) are similarly exported from lysosomes. Lysosomal acid lipase (LAL) hydrolyses triglycerides and cholesterol-esters.^{67,68} Deficiency in LAL results in two lysosomal storage disorders (LSDs): Cholesteryl Ester Storage Disease (CESD) is characterized by hypercholesterolemia and high blood LDL, whereas Wolman Disease (WD) is characterized by dramatic increases in triglycerides and cholesteryl esters. CESD is a heterogenous disease with predominant hepatic complications, whereas WD is lethal within the first five years due to massive lipid storage in most organs.⁶⁹ Defects in the export of cholesterol due to deficiencies in NPC1 or NPC2 cause endolysosomal cholesterol accumulations, as well as dramatic secondary elevations in neutral and acidic glycosphingolipids.^{19,20,70} Recently, the lysosomal membrane protein LIMP-2 has been reported to also facilitate cholesterol transport, but this pathway is apparently insufficient to compensate NPC1-mediated sterol export.⁷¹

Endocytosis of lipoproteins supplies lysosomes with cholesterol-ester and diglyceride-based lipids destined for fragmentation.⁶⁸ Importantly, lipophagy, a specialized form of autophagy, mediates the transfer of LDs to lysosomes.⁷² LDs are specialized structures that contain triacylglycerols and sterol esters and are surrounded by a phospholipid monolayer containing membrane proteins such as perilipins (PLIN), lipid synthesizing proteins, lipid degrading proteins (lipases) and proteins involved in vesicular transport.⁷³ The degree of lipid storage and composition of LDs depends on cell type, cellular metabolic status and whole-body metabolism. Primary LD storing cells include hepatocytes and adipocytes and serve as crucial regulators of lipid storage in other organs.^{50,74}

Lipotoxicity

The toxicity of excessive fatty acids has been appreciated for a long time and has led to the concept of lipotoxicity, initially formulated by Unger.^{75,76} During the last decades, several lipids have been proposed to play a pivotal role in obesity-induced insulin resistance, including excessive diacylglycerol (DAG), ceramide and acyl carnitines.⁷⁷ Impaired insulin sensitivity has indeed been linked to elevation of DAG species and their ability to activate protein kinase C subvariants.⁷⁷ Moreover, excessive ceramide has been shown to be a major cause for insulin sensitivity in various cell types and tissues, an effect ascribed to the sphingolipid's interaction with atypical PKC ζ and AKT.^{78,79} Levels of glycosphingolipids are similarly increased in obese individuals and rodents. Reduction of glycosphingolipid levels through inhibition of glucosylceramide synthase, the enzymatic reaction that

Introduction

catalyses the formation of glucosylceramide from ceramide, has been found to markedly improve insulin sensitivity in obese rodents.⁸⁰ These findings are consistent with other observations regarding detrimental effects of excessive gangliosides, in particular GM3, on insulin sensitivity.⁸¹ This effect is ascribed to disturbed lipid rafts in which the insulin receptor preferentially resides.⁵ Of note, it has been proposed that in some cell types (such as muscle) excessive ceramide is the primary cause for insulin resistance, whereas in adipocytes glycosphingolipids are the major underlying cause.⁸²

Macrophages

The primary function of the tissue resident macrophage is to maintain tissue homeostasis and the basal physiological state of these macrophages will therefore predominantly be of an anti-inflammatory nature. Hence, gut, adipose tissue, and spleen resident macrophages show anti-inflammatory expression profiles. Interference with, or change in their function, results in widespread (low grade) inflammation and auto-immune reactions.⁸³⁻⁸⁵ These tissue-associated macrophages are generally termed alternatively activated macrophages or M2-macrophages, as opposed to pro-inflammatory, classically activated M1-macrophages. The dichotomous M1/M2-classification may however be too simplified, as differentiated macrophage subsets have been suggested to exist that exhibit varying stages of inflammatory states. A main distinction between different populations of tissue resident macrophages is between those that differentiate from hematopoietic progenitor cells that reside in the yolk sac or foetal liver and infiltrate the tissue during development (e.g. microglia and hepatocytes), and those derived from circulating monocytes that are recruited into the tissue after development (Figure 3).^{86,87,88,89} Intrinsic and environmental factors, such as a bidirectional interaction with tissue, further trigger epigenetic changes and determine the chromatin status of macrophages.⁸⁸ A recent study by Glass and co-workers revealed that following acute depletion of Kupffer cells, peripheral monocytes are recruited to the liver where they can differentiate in response to local stimuli into Kupffer cell-like macrophages.⁹⁰ Transcriptome profiling and single-cell sequencing techniques have indeed unravelled a highly diverse mix of distinct macrophage populations within tissues, occurring in a spectrum of inflammatory states rather than a dichotomy among macrophage subtypes (Figure 3).^{87,91,92} These populations respond differently to external stimuli such as pathogens, tissue damage and metabolic stress, and contribute differently to disorders in which the macrophage (or microglia) are known to play a crucial role, such as cancer, neurodegeneration and diabetes type 2.^{93,94} Despite these phenotypical differences, the macrophage is in general a professional phagocyte, which clears pathogens and removes apoptotic cells through phagocytosis and efferocytosis respectively.⁹⁵ These processes occur at steady state under physiological circumstances and rapidly increase upon tissue damage or exposure to pathogen associated molecules.⁹⁶

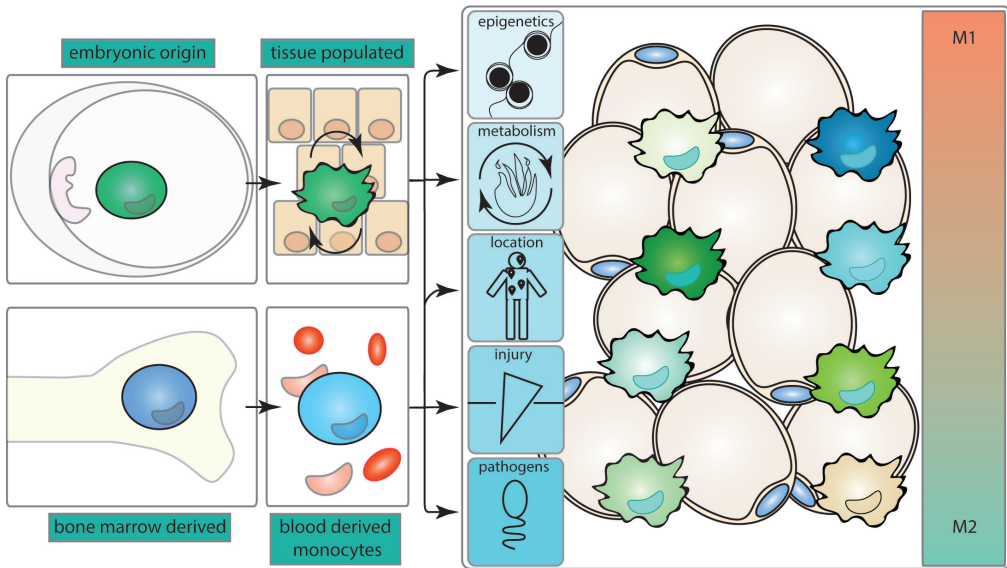


Figure 3. The ontology and heterogeneity of tissue resident macrophages; Embryonic hematopoietic cells from the yolk sac and foetal liver give rise to a macrophage population that infiltrate the developing tissue and self-sustain locally throughout life. Adult hematopoietic stem cells that reside in the bone marrow differentiate into circulating monocytes which upon recruitment into the tissue give rise to a distinct pool of tissue resident macrophages. Both groups of macrophages are subjected to a variety of intrinsic and environmental factors such as epigenetics, tissue type, metabolism, injury, pathogens that determines the function of each macrophage within the tissue, giving rise to a high heterogeneity. This function can be placed within the spectrum between pro-inflammatory M1-macrophages and anti-inflammatory M2-macrophages.

The macrophage plays an important role in lysosomal degradation of lipids. This is best illustrated by the occurrence of lipid-laden macrophages during deficiencies of lysosomal hydrolases and the spectacular clinical improvements upon correction of these cells.^{70,95} One example offers WD, where bone marrow transplantation, or macrophage specific re-introduction of LIPA⁹⁸⁻¹⁰⁰, renders major improvements. Another example is Gaucher disease where macrophage targeted enzyme replacement therapy (ERT) rapidly corrects hepatosplenomegaly and hematologic abnormalities such as anaemia and thrombocytopenia.^{11,66} Immunological characterization of a Gaucher patients' spleen identified the lipid-laden macrophage (Gaucher cell) to be predominantly of a M2-nature.¹⁵ Strikingly, Gaucher cells were found to be surrounded by pro-inflammatory M1-macrophages without an overt storage phenotype. Circulating pro-inflammatory factors are likely derived from M1-inflammatory macrophages. In a proposed model, a systemic low-grade inflammatory state is sustained through a vicious cycle in which tissue damage recruits lytic, pro-inflammatory macrophages that cause further tissue damage.

Gaucher cells are viable macrophages that, in response to their lysosomal distress, produce and secrete unique proteins. These include chitotriosidase, CCL18 and GPNMB (described extensively in chapter 4). The markedly elevated plasma chitotriosidase, CCL18 and GPNMB in GD patients are exploited to monitor disease progression and correction following ERT and substrate reduction therapy (SRT) with small compound

inhibitors of glucosylceramide synthase.¹⁰¹⁻¹⁰³ Elevated plasma levels of macrophage-derived chitotriosidase are documented for various lysosomal lipid storage disorders, that in addition to glycosphingolipidoses also include Wolman disease and NPC.¹⁰⁴ This illustrates the common occurrence of lysosomal distress in macrophages in disorders with quite distinct primary defects.

In adaptation to GlcCer accumulation in lysosomes of Gaucher cells, excessive glycosphingolipids are de-acylated by acid ceramidase, thereby producing glucosylsphingosine. This bioactive sphingoid base can leave storage cells and it is more than hundred-fold elevated in plasma of symptomatic GD patients. It is assumed that the chronic increase in glucosylsphingosine contributes to specific symptoms of Gaucher disease.⁵ In the acid sphingomyelinase deficiencies Niemann Pick types A and B (NPA, NPB), lipid-laden macrophages are also a hallmark of pathology. The so-called Pick cells resemble Gaucher cells both morphologically and molecularly, and excessively produce chitotriosidase and CCL18, which can be exploited for diagnostic and monitoring purposes.¹⁰⁵ Moreover, acid ceramidase converts accumulating SM in lysosomes to its deacylated form, phosphocholinesphingosine, which is dramatically elevated in the patient's plasma. The same phenomenon is observed with other sphingolipidoses like Fabry disease and Krabbe disease. Toxic deacylated forms of accumulating lipids are generated in these disorders and are utilized as biomarkers.⁵

Moreover, lipid-laden macrophages are present in spleen and liver of NPC patients. The primary storage lipid is considered to be cholesterol, but profound accumulation of (glyco)sphingolipids occurs concomitantly. This is attributed to secondary perturbation of lysosomal hydrolase function due to the NPC1-deficiency. Apparently, the aberrant lysosomal lipid composition exerts pleiotropic effects within the lysosome, which causes multiple deficiencies to develop simultaneously. This may explain some similarities among NPC, other inherited sphingolipidoses and possibly acquired metabolic disorders with respect to biomarker and clinical representation.¹⁰⁶

Acquired metabolic disorders

A group of macrophages that is typically exposed to high lipid load are adipose tissue macrophages (ATMs). These ATMs can acquire a storage phenotype during obesity when the adipose tissue (AT) hypertrophies and adipocytes become dysfunctional. A systemic low-grade inflammation accompanies this AT change, which contributes to impaired insulin sensitivity in adipocytes and other organs. Consequently, glucose uptake by AT and muscle is impaired, along with insulin mediated suppression of glucose secretion by the liver. Blood glucose levels progressively increase during the development of obesity. Insulin resistance (IR) is a major risk factor for the development of type 2 diabetes mellitus and cardiovascular complications.^{107,108} These acquired metabolic disorders pose an increasing threat to global health. Estimates of the world health organisation indicated that 39% (1.9 billion) of adults were overweight in 2016, and 13% (650 million) of the global population was obese.¹⁰⁹ The prevalence of diabetes has similarly increased in the last 20 years, and has entered the top ten of global causes of deaths.¹¹⁰

For a long time, a low-grade inflammatory state has been associated with perturbed whole-body metabolism as during obesity. Early work revealed a causal relationship between TNF α , then alternatively called cachectin, and insulin homeostasis.^{111,112} Administration of neutralizing antibodies against TNF α was employed to improve

metabolic stress as a consequence of acute elevations of TNF α and of chronic levels as induced by obesity.^{113,114} Reduction of elevated circulating TNF α in obese mice restores insulin sensitivity, demonstrating a relationship between insulin resistance and inflammation.^{114,115} In obese AT, the amount of macrophages is dramatically increased and apoptotic adipocytes are surrounded by aggregates of macrophages, termed crown-like structures.^{116–119} Indeed, the ATM was identified as the primary source of TNF α during obesity.⁸⁵ Upon excessive nutritional intake, the properties of ATMs change from an anti-inflammatory (M2-like) to a pro-inflammatory (M1-like) profile.¹²⁰ The bidirectional communication between macrophages and adipocytes is a major determinant in the phenotypic switch that macrophages undergo, and many stimuli have been identified, including hormones, cytokines, chemokines as well as lipid mediators released from hypertrophied adipocytes.¹²¹ For example, adipocytes communicate by secreting the hormone adiponectin, which acts as potent systemic insulin sensitizer and reducer of inflammation.¹²² Conceivably, obese ATMs are stressed by lipids and undergo differentiation to a specific phenotype. Recent data indicated a foamy appearance of obese ATMs on an ultrastructural level, which was associated with an increased lipid degradation by a lysosome driven program.¹²³ Moreover, GPNMB was recently identified as a potentially novel biomarker of these obese ATMs.¹¹⁹ The storage cell marker has been found to be under transcriptional control of MiT/TFE subfamily of transcription factors and expression could be potently induced *in vitro* upon application of lysosomal stress through palmitate feeding or chloroquine exposure.¹²⁴ These data suggest that lysosomal storage in macrophages is a hallmark of obesity and that adaptation to a storage phenotype is at least partly mediated by MiT/TFE family members.

Atherosclerosis is another pathology that is characterized by lipid laden macrophages. Incomplete clearance of oxidized LDL-apolipoprotein B particles gives rise to a storage phenotype.¹²⁵ These storage cells contribute to the chronic, non-resolving inflammation that occurs in the intima and are assumed to be crucial in the progression of the lesion. Expression of lipid-laden macrophage markers are strongly elevated in atherosclerotic lesion macrophages and include chitotriosidase and GPNMB.^{126–128} Additional similarities can be found in lipid laden microglia, which are considered to contribute to progression of neurodegenerative diseases.^{129,130} Again, typical storage markers identified in LSDs such as GPNMB are elevated in these lipid-filled microglia.

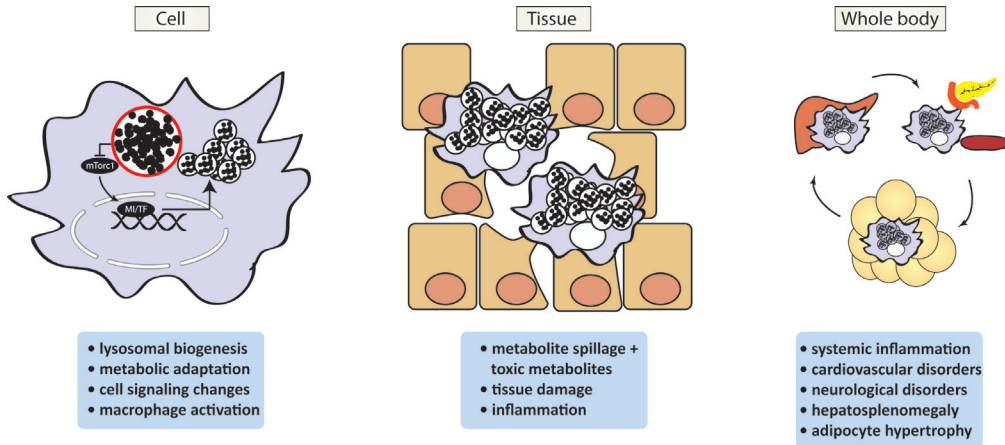


Figure 4. Proposed impact of lysosomal stress at a molecular level, within the tissue and on the whole body. On a cellular level lysosomal stress triggers a molecular response, involving increased lysosomal biogenesis and autophagy through transcription factor family MiT/TFE. In macrophages this induces a differentiation associated with the nature of metabolic and inflammatory triggers. In organs containing cells with lysosomal stress, storage cells drive disease progression through recruitment of lytic immune cells causing further damage to the affected tissue. Systemically, a low-grade inflammation can arise in pathologies characterized by lipid-laden macrophages, which drives chronic multi-organ pathology.

Relevance of lysosomal biogenesis for disease

Perturbation of the lysosome can lead to a coordinated signalling cascade that changes metabolism and signalling in cells, tissues and whole body, as is illustrated by the lysosomal accumulation of lipids in inborn errors of lysosomal lipid metabolism (**Figure 4**). Prominent in these diseases are lipid-laden macrophages, which secrete markers that are connected to disease burden and could be exploited as biomarkers. Importantly, storage cells have emerged as a hallmark in acquired metabolic pathologies such as obesity and atherosclerosis. It remains largely unclear however, how canonical regulators of lysosome biogenesis, the family of MiT/TFE, contribute to the storage-cell phenotype in response to lipid-laden lysosomes. Moreover, it is of therapeutic relevance to study whether increased lysosomal biogenesis in storage cells is beneficial to the cell and to its surrounding tissue.

Scope of thesis

This thesis aims to explore the pathophysiological role of the lysosome with a focus on the macrophage. The studies employ an integrated approach that involves biochemical and transcriptional analysis to combine data on hydrolytic capacity with lysosomal signalling. In addition, ultrasensitive visualization by activity-based probe labelling enabled in depth studies on glucocerebrosidase in controlled cellular models as well as in metabolic pathologies.

Chapter 1 characterizes the lysosome integrity and the following cellular response in cultured cells. It identifies HEPES as a potent inducer of a MiT/TFE mediated transcriptional program in cultured macrophage-like cells that affects lysosomal function, as well as the immunological phenotype of the macrophage.

Chapter 2 characterizes the maturation of acid hydrolase in cultured cells. It identifies a perturbed maturation of glucocerebrosidase (GBA) by use of the zwitterionic buffers HEPES and illustrates the importance of culture conditions when using cultured cells for diagnosis.

Chapter 3 investigates the localization of lysosomal enzymes and delivery of recombinant lysosomal enzyme by combining ultrasensitive activity-based probe labeling (ABP) with the high spatial resolution of electron microscopy through correlative light electron microscopy (CLEM).

Chapter 4 explores the recent developments in storage cell characterization. The potential is discussed of a recently identified transmembrane protein glycoprotein non metastatic protein B (GPNMB) as biomarker in lipid laden macrophage associated disorders.

Chapter 5 identifies tissue specific adaptation upon lysosomal deficiency in cholesterol efflux transporter NPC1 in mice. A hepatocyte specific upregulation of LIMP2 is identified without concomitant upregulation of known NPC biomarkers, as opposed to biomarkers that are upregulated in lipid laden Kupffer cells.

Chapter 6 characterizes the contribution of lysosome signalling in lipid-laden macrophages in the adipose tissue present during obesity, an acquired metabolic disorder. Glucan encapsulated particles (Gerps) were employed to perform an siRNA mediated knock down of MiT/TFE genes in adipose tissue macrophages.

References

1. Braulke, T. & Bonifacino, J. S. Sorting of lysosomal proteins. *Biochim Biophys. Acta. Mol. Cell. Res.* **1793**, 605–614 (2009).
2. Witte, M. D., Kallemeyjn, W. W., Aten, J., Li, K.-Y., Strijland, A., Donker-Koopman, W. E., van den Nieuwendijk, A. M. C. H., Bleijlevens, B., Kramer, G., Florea, B. I., Hooibrink, B., Hollak, C. E. M., Ottenhoff, R., Boot, R. G., van der Marel, G. A., Overkleeft, H. S. & Aerts, J. M. F. G. Ultrasensitive in situ visualization of active glucocerebrosidase molecules. *Nat. Chem. Biol.* **6**, 907–13 (2010).
3. Kallemeyjn, W. W., Scheij, S., Hoogendoorn, S., Witte, M. D., Herrera Moro Chao, D., van Roomen, C. P. A. A., Ottenhoff, R., Overkleeft, H. S., Boot, R. G. & Aerts, J. M. F. G. Investigations on therapeutic glucocerebrosidases through paired detection with fluorescent activity-based probes. *PLoS One* **12**, e0170268 (2017).
4. Chao, D. H. M., Kallemeyjn, W. W., Marques, A. R. A., Orre, M., Ottenhoff, R., Van Roomen, C., Foppen, E., Renner, M. C., Moeton, M., Van Eijk, M., Boot, R. G., Kamphuis, W., Hol, E. M., Aten, J., Overkleeft, H. S., Kalsbeek, A. & Aerts, J. M. F. G. Visualization of active glucocerebrosidase in rodent brain with high spatial resolution following in situ labeling with fluorescent activity based probes. *PLoS One* **10**, (2015).
5. Aerts, J. M. F. G., Kuo, C. L., Lelieveld, L. T., Boer, D. E. C., van der Lienden, M. J. C., Overkleeft, H. S. & Artola, M. Glycosphingolipids and lysosomal storage disorders as illustrated by gaucher disease. *Curr. Opin. Chem. Biol.* **53** 204–215 (2019).
6. Artola, M., Kuo, C. L., Lelieveld, L. T., Rowland, R. J., Van Der Marel, G. A., Codée, J. D. C., Boot, R. G., Davies, G. J., Aerts, J. M. F. G. & Overkleeft, H. S. Functionalized cyclophellitols are selective glucocerebrosidase inhibitors and induce a bona fide neuropathic Gaucher model in zebrafish. *J. Am. Chem. Soc.* **141**, 4214–4218 (2019).
7. Brady, R. O., Kanfer, J. N., Bradley, R. M. & Shapiro, D. Demonstration of a deficiency of glucocerebrosidase-cleaving enzyme in Gaucher's disease. *J. Clin. Invest.* **45**, 1112–1115 (1966).
8. Berkovic, S. F., Dibbens, L. M., Oshlack, A., Silver, J. D., Katerelos, M., Vears, D. F., Lüllmann-Rauch, R., Blanz, J., Zhang, K. W., Stankovich, J., Kalnins, R. M., Dowling, J. P., Andermann, E., Andermann, F., Faldini, E., D'Hooge, R., Vadlamudi, L., Macdonell, R. A., Hodgson, B. L., Bayly, M. A., Savige, J., Mulley, J. C., Smyth, G. K., Power, D. A., Saftig, P., Bahlo, M. Array-based gene discovery with three unrelated subjects shows SCARB2/ LIMP-2 deficiency causes myoclonus epilepsy and glomerulosclerosis. *Am. J. Hum. Genet.* **82**, 673–684 (2008).
9. Balreira, A., Gaspar, P., Caiola, D., Chaves, J., Beirão, I., Lima, J. L., Azevedo, J. E. & Miranda, M. C. S. A nonsense mutation in the LIMP-2 gene associated with progressive myoclonic epilepsy and nephrotic syndrome. *Hum. Mol. Genet.* **17**, 2238–2243 (2008).
10. Tylki-Szymańska, A., Czartoryska, B., Vanier, M. T., Poorthuis, B. J. M. H., Groener, J. A. E., Ługowska, A., Millat, G., Vaccaro, A. M. & Jurkiewicz, E. Non-neuronopathic Gaucher disease due to saposin C deficiency. *Clin. Genet.* **72**, 538–542 (2007).
11. Beutler, E. & Grabowski, G. Gaucher Disease. In Scriver CR, Valle D, Beaudet A, Sly WS, eds. *The Metabolic and Molecular Bases of Inherited Diseases* **8** 3635–3668 (2001).
12. Boer, D. E. C., van Smeden, J., Bouwstra, J. A. & Aerts, J. M. F. . Glucocerebrosidase: functions in and beyond the lysosome. *J. Clin. Med.* **9**, 736 (2020).
13. Aerts, J. M., Hollak, C., Boot, R. & Groener, A. Biochemistry of glycosphingolipid storage disorders: implications for therapeutic intervention. *Philos. Trans. R. Soc. Lond. B. Biol. Sci.* **358**, 905–14 (2003).
14. Boot, R. G., Hollak, C. E. M., Verhoek, M., Sloof, P., Poorthuis, B. J. H. M., Kleijer, W. J., Wevers, R. A., Van Oers, M. H. J., Mannens, M. M. A. M., Aerts, J. M. F. G. & van Weely, S. Glucocerebrosidase genotype of Gaucher patients in the Netherlands: limitations in prognostic value. *Hum. Mutat.* **10**, 348–358 (1997).

15. Boven, L. A., van Meurs, M., Boot, R. G., Mehta, A., Boon, L., Aerts, J. M. & Laman, J. D. Gaucher cells demonstrate a distinct macrophage phenotype and resemble alternatively activated macrophages. *Am. J. Clin. Pathol.* **122**, 359–369 (2004).
16. Ferraz, M. J., Marques, A. R. A., Appelman, M. D., Verhoek, M., Strijland, A., Mirzaian, M., Scheij, S., Ouairy, C. M., Lahav, D., Wisse, P., Overkleeft, H. S., Boot, R. G. & Aerts, J. M. Lysosomal glycosphingolipid catabolism by acid ceramidase: formation of glycosphingoid bases during deficiency of glycosidases. *FEBS Lett.* **590**, 716–725 (2016).
17. Neufeld, E. F. Lysosomal storage diseases. *Annu. Rev. Biochem.* **60**, 257–280 (1991).
18. Platt, F. M. Sphingolipid lysosomal storage disorders. *Nature* **510**, 68–75 (2014).
19. Sleat, D. E., Wiseman, J. A., El-Banna, M., Price, S. M., Verot, L., Shen, M. M., Tint, G. S., Vanier, M. T., Walkley, S. U. & Lobel, P. Genetic evidence for nonredundant functional cooperativity between NPC1 and NPC2 in lipid transport. *Proc. Natl. Acad. Sci. USA.* **101**, 5886–5891 (2004).
20. Infante, R. E., Wang, M. L., Radhakrishnan, A., Hyock, J. K., Brown, M. S. & Goldstein, J. L. NPC2 facilitates bidirectional transfer of cholesterol between NPC1 and lipid bilayers, a step in cholesterol egress from lysosomes. *Proc. Natl. Acad. Sci. U. S. A.* **105**, 15287–15292 (2008).
21. Marques, A. R. A., Aten, J., Ottenhoff, R., van Roomen, C. P. A. A., Herrera Moro, D., Claessen, N., Vinueza Veloz, M. F., Zhou, K., Lin, Z., Mirzaian, M., Boot, R. G., De Zeeuw, C. I., Overkleeft, H. S., Yildiz, Y. & Aerts, J. M. F. G. Reducing GBA2 activity ameliorates neuropathology in Niemann-Pick Type C mice. *PLoS One* **10**, e0135889 (2015).
22. Johnson, D. E., Ostrowski, P., Jaumouillé, V. & Grinstein, S. The position of lysosomes within the cell determines their luminal pH. *J. Cell Biol.* **212**, 677–692 (2016).
23. Hesketh, G. G., Wartosch, L., Davis, L. J., Bright, N. A. & Luzio, J. P. The lysosome and intracellular signalling. *Prog. Mol. Subcell. Biol.* **57**, 151–180 (2018).
24. Tol, M. J., van der Lienden, M. J. C. C., Gabriel, T. L., Hagen, J. J., Scheij, S., *et al.* HEPES activates a Mit/TFE-dependent lysosomal-autophagic gene network in cultured cells: A call for caution. *Autophagy* **14**, 1–13 (2018).
25. Platt, F. M., d'Azzo, A., Davidson, B. L., Neufeld, E. F. & Tiffit, C. J. Lysosomal storage diseases. *Nat. Rev. Dis. Prim.* **4**, 27 (2018).
26. Parenti, G., Andria, G., Ballabio, A. & Duncan, D. Lysosomal storage diseases: from pathophysiology to therapy. *Annu. Rev. Med.* **66**, 471–486 (2015).
27. Vaes, G. On the mechanisms of bone resorption. The action of parathyroid hormone on the excretion and synthesis of lysosomal enzymes and on the extracellular release of acid by bone cells. *J. Cell Biol.* **39**, 676–697 (1968).
28. Van Smeden, J., Dijkhoff, I. M., Helder, R. W. J., Al-Khakany, H., Boer, D. E. C., Schreuder, A., Kallemeijn, W. W., Absalah, S., Overkleeft, H. S., Aerts, J. M. F. G. & Bouwstra, J. A. In situ visualization of glucocerebrosidase in human skin tissue: zymography versus activity-based probe labeling. *J. Lipid Res.* **58**, 2299–2309 (2017).
29. Condon, K. J. & Sabatini, D. M. Nutrient regulation of mTORC1 at a glance. *J. Cell Sci.* **132**, (2019).
30. Zhang, C. S., Jiang, B., Li, M., Zhu, M., Peng, Y., *et al.* The lysosomal v-ATPase-regulator complex is a common activator for AMPK and mTORC1, acting as a switch between catabolism and anabolism. *Cell Metab.* **20**, 526–540 (2014).
31. Sardiello, M., Palmieri, M., Ronza, A. di, Medina, D. L., Valenza, M., *et al.* A gene network regulating lysosomal biogenesis and function. *Science* **325**, 473–477 (2009).
32. Steingrímsson, E., Copeland, N. G. & Jenkins, N. A. Melanocytes and the *Microphthalmia* transcription factor network. *Annu. Rev. Genet.* **38**, 365–411 (2004).
33. Yu, L., McPhee, C. K., Zheng, L., Mardones, G. A., Rong, Y., Peng, J., Mi, N., Zhao, Y., Liu, Z., Wan, F., Hailey, D. W., Oorschot, V., Klumperman, J., Baehrecke, E. H. & Lenardo, M.

- J. Termination of autophagy and reformation of lysosomes regulated by mTOR. *Nature* **465**, 942–6 (2010).
34. Rocznik-Ferguson, A., Petit, C. S., Froehlich, F., Qian, S., Ky, J., Angarola, B., Walther, T. C. & Ferguson, S. M. The transcription factor TFEB links mTORC1 signaling to transcriptional control of lysosome homeostasis. *Sci. Signal.* **5**, ra42 (2012).
35. Martina, J. A., Chen, Y., Gucek, M. & Puertollano, R. MTORC1 functions as a transcriptional regulator of autophagy by preventing nuclear transport of TFEB. *Autophagy* **8**, 903–914 (2012).
36. Bronisz, A., Sharma, S. M., Hu, R., Godlewski, J., Tzivion, G., Mansky, K. C. & Ostrowski, M. C. Microphthalmia-associated transcription factor interactions with 14-3-3 modulate differentiation of committed myeloid precursors. *Mol. Biol. Cell* **17**, 3897–3906 (2006).
37. Jin, J., Smith, F. D., Stark, C., Wells, C. D., Fawcett, J. P., Kulkarni, S., Metalnikov, P., O'Donnell, P., Taylor, P., Taylor, L., Zougman, A., Woodgett, J. R., Langeberg, L. K., Scott, J. D. & Pawson, T. Proteomic, functional, and domain-based analysis of in vivo 14-3-3 binding proteins involved in cytoskeletal regulation and cellular organization. *Curr. Biol.* **14**, 1436–1450 (2004).
38. Martina, J. A., Diab, H. I., Lishu, L., Jeong-A, L., Patange, S., Raben, N. & Puertollano, R. The nutrient-responsive Transcription factor TFE3, Promotes autophagy, lysosomal biogenesis, and clearance of cellular debris. *Sci. Signal.* **7**, ra9 (2014).
39. Napolitano, G. & Ballabio, A. TFEB at a glance. *J. Cell Sci.* **129**, 2475–2481 (2016).
40. Settembre, C., Di Malta, C., Polito, V. A., Arencibia, M. G., Vetrini, F., Erdin, S., Erdin, S. U., Huynh, T., Medina, D., Colella, P., Sardiello, M., Rubinsztein, D. C. & Ballabio, A. TFEB links autophagy to lysosomal biogenesis. *Science* **332**, 1429–1433 (2011).
41. Peña-Llopis, S., Vega-Rubin-de-Celis, S., Schwartz, J. C., Wolff, N. C., Tran, T. A. T., Zou, L., Xie, X.-J., Corey, D. R. & Brugarolas, J. Regulation of TFEB and V-ATPases by mTORC1. *EMBO J.* **30**, 3242–58 (2011).
42. Zhao, G. Q., Zhao, Q., Zhou, X., Mattei, M. G. & de Crombrughe, B. TFEC, a basic helix-loop-helix protein, forms heterodimers with TFE3 and inhibits TFE3-dependent transcription activation. *Mol. Cell. Biol.* **13**, 4505–4512 (1993).
43. Martina, J. A. & Puertollano, R. Rag GTPases mediate amino acid-dependent recruitment of TFEB and MITF to lysosomes. *J. Cell Biol.* **200**, 475–491 (2013).
44. Settembre, C., Fraldi, A., Medina, D. L. & Ballabio, A. Signals from the lysosome: a control centre for cellular clearance and energy metabolism. *Nat. Rev. Mol. Cell Biol.* **14**, 283–296 (2013).
45. Yang, M., Liu, E., Tang, L., Lei, Y., Sun, X., Hu, J., Dong, H., Yang, S.-M. M., Gao, M. & Tang, B. Emerging roles and regulation of MiT/TFE transcriptional factors. *Cell Commun. Signal.* **16**, 31 (2018).
46. Martínez-Fábregas, J., Prescott, A., van Kasteren, S., Pedrioli, D. L., McLean, I., Moles, A., Reinheckel, T., Poli, V. & Watts, C. Lysosomal protease deficiency or substrate overload induces an oxidative-stress mediated STAT3-dependent pathway of lysosomal homeostasis. *Nat. Commun.* **9**, 1–16 (2018).
47. Chauhan, S., Goodwin, J. G., Chauhan, S., Manyam, G., Wang, J., Kamat, A. M. & Boyd, D. D. ZKSCAN3 is a master transcriptional repressor of autophagy. *Mol. Cell* **50**, 16–28 (2013).
48. Annunziata, I., van de Vlekkert, D., Wolf, E., Finkelstein, D., Neale, G., Machado, E., Mosca, R., Campos, Y., Tillman, H., Roussel, M. F., Andrew Weesner, J., Ellen Fremuth, L., Qiu, X., Han, M. J., Grosveld, G. C. & D'Azzo, A. MYC competes with MiT/TFE in regulating lysosomal biogenesis and autophagy through an epigenetic rheostat. *Nat. Commun.* **10**, 3623 (2019).
49. d'Azzo, A. & Annunziata, I. Transcription factor competition regulates lysosomal biogenesis and autophagy. *Mol. Cell. Oncol.* **7**, 1685840 (2020).

50. Jaishy, B. & Abel, E. D. Lipotoxicity: Many roads to cell dysfunction and cell death lipids, lysosomes, and autophagy. *J. Lipid Res.* **57**, 1619–1635 (2016).
51. Settembre, C., De Cegli, R., Mansueto, G., Saha, P. K., Vetrini, F., *et al.* TFEB controls cellular lipid metabolism through a starvation-induced autoregulatory loop. *Nat. Cell Biol.* **15**, 647–658 (2013).
52. Wennekes, T., van den Berg, R. J. B. H. N., Boot, R. G., van der Marel, G. A., Overkleeft, H. S. & Aerts, J. M. F. G. Glycosphingolipids—nature, function, and pharmacological modulation. *Angew. Chem. Int. Ed. Engl.* **48**, 8848–8869 (2009).
53. Aerts, J. M. F. G., Artola, M., van Eijk, M., Ferraz, M. J. & Boot, R. G. Glycosphingolipids and Infection. Potential New Therapeutic Avenues. *Front. Cell. Dev. Biol.* **7** 324 (2019).
54. Lingwood, D. & Simons, K. Lipid rafts as a membrane-organizing principle. *Science* **327** 46–50 (2010).
55. Klemm, R. W., Ejsing, C. S., Surma, M. A., Kaiser, H. J., Gerl, M. J., Sampaio, J. L., De Robillard, Q., Ferguson, C., Proszynski, T. J., Shevchenko, A. & Simons, K. Segregation of sphingolipids and sterols during formation of secretory vesicles at the trans-Golgi network. *J. Cell Biol.* **185**, 601–612 (2009).
56. Varki, A. Biological roles of glycans. *Glycobiology* **27**, 3–49 (2017).
57. Furukawa, K., Tokuda, N., Okuda, T., Tajima, O. & Furukawa, K. Glycosphingolipids in engineered mice: insights into function. *Semin. Cell Dev. Biol.* **15**, 389–396 (2004).
58. Lingwood, C. A. Glycosphingolipid functions. *Cold Spring Harb. Perspect. Biol.* **3**, 1–26 (2011).
59. Holleran, W. M., Takagi, Y. & Uchida, Y. Epidermal sphingolipids: metabolism, function, and roles in skin disorders. *FEBS Lett.* **580**, 5456–5466 (2006).
60. Schengrund, C.-L. L. Gangliosides: glycosphingolipids essential for normal neural development and function. *Trends Biochem. Sci.* **40**, 397–406 (2015).
61. Yu, R. K., Nakatani, Y. & Yanagisawa, M. The role of glycosphingolipid metabolism in the developing brain. *J. Lipid Res.* **50**, S440–S445 (2009).
62. Iwabuchi, K. Gangliosides in the immune system: Role of glycosphingolipids and glycosphingolipid-enriched lipid rafts in immunological functions. in *Methods in Molecular Biology* **1804** 83–95 (Humana Press Inc., 2018).
63. Aerts, J. M. F. G., Kallemeijn, W. W., Wegdam, W., Joao Ferraz, M., van Breemen, M. J., Dekker, N., Kramer, G., Poorthuis, B. J., Groener, J. E. M., Cox-Brinkman, J., Rombach, S. M., Hollak, C. E. M., Linthorst, G. E., Witte, M. D., Gold, H., van der Marel, G. A., Overkleeft, H. S. & Boot, R. G. Biomarkers in the diagnosis of lysosomal storage disorders: proteins, lipids, and inhibodies. *J. Inherit. Metab. Dis.* **34**, 605–19 (2011).
64. Gold, H., Mirzaian, M., Dekker, N., Joao Ferraz, M., Lugtenburg, J., Codée, J. D. C., van der Marel, G. A., Overkleeft, H. S., Linthorst, G. E., Groener, J. E. M., Aerts, J. M. & Poorthuis, B. J. H. M. Quantification of globotriaosylsphingosine in plasma and urine of fabry patients by stable isotope ultraperformance liquid chromatography-tandem mass spectrometry. *Clin. Chem.* **59**, 547–56 (2013).
65. Mirzaian, M., Wisse, P., Ferraz, M. J., Gold, H., Donker-Koopman, W. E., Verhoek, M., Overkleeft, H. S., Boot, R. G., Kramer, G., Dekker, N. & Aerts, J. M. F. G. Mass spectrometric quantification of glucosylsphingosine in plasma and urine of type 1 Gaucher patients using an isotope standard. *Blood Cells, Mol. Dis.* **54**, 307–314 (2015).
66. Ferraz, M. J., Kallemeijn, W. W., Mirzaian, M., Herrera Moro, D., Marques, A., Wisse, P., Boot, R. G., Willems, L. I., Overkleeft, H. S. & Aerts, J. M. Gaucher disease and Fabry disease: New markers and insights in pathophysiology for two distinct glycosphingolipidoses. *Biochim. Biophys. Acta - Mol. Cell Biol. Lipids* **1841**, 811–825 (2014).
67. Goldstein, J. L., Dana, S. E., Faust, J. R., Beaudet, A. L. & Brown, M. S. Role of lysosomal acid lipase in the metabolism of plasma low density lipoprotein. Observations in

- cultured fibroblasts from a patient with cholesteryl ester storage disease. *J. Biol. Chem.* **250**, 8487–8495 (1975).
68. Brown, M. S. & Goldstein, J. L. A receptor-mediated pathway for cholesterol homeostasis. *Science* **232**, 34–47 (1986).
69. Pastores, G. M. & Hughes, D. A. Lysosomal acid lipase deficiency: therapeutic options. *Drug. Des. Devel. Ther.* **14** 591–601 (2020).
70. Vanier, M. T. Niemann-Pick disease type C. *Orphanet J. Rare Dis.* **5**, 16 (2010).
71. Heybrock, S., Kanerva, K., Meng, Y., Ing, C., Liang, A., *et al.* Lysosomal integral membrane protein-2 (LIMP-2/SCARB2) is involved in lysosomal cholesterol export. *Nat. Commun.* **10**, (2019).
72. Singh, R., Kaushik, S., Wang, Y., Xiang, Y., Novak, I., Komatsu, M., Tanaka, K., Cuervo, A. M. & Czaja, M. J. Autophagy regulates lipid metabolism. *Nature* **458**, 1131–1135 (2009).
73. Guo, Y., Cordes, K. R., Farese, R. V. & Walther, T. C. Lipid droplets at a glance. *J. Cell Sci.* **122**, 749–752 (2009).
74. Zechner, R., Madeo, F. & Kratky, D. Cytosolic lipolysis and lipophagy: two sides of the same coin. *Nat Rev. Mol. Cell. Biol.* **18** 671–684 (2017).
75. Unger, R. H. Lipotoxicity in the pathogenesis of obesity-dependent NIDDM: Genetic and clinical implications. *Diabetes* **44** 863–870 (1995).
76. Unger, R. H. Lipotoxic diseases. *Annu. Rev. Med.* **53**, 319–336 (2002).
77. Petersen, M. C. & Shulman, G. I. Mechanisms of insulin action and insulin resistance. *Physiol. Rev.* **98** 2133–2223 (2018).
78. Summers, S. A., Chaurasia, B. & Holland, W. L. Metabolic messengers: ceramides. *Nat. Metab.* **1** 1051–1058 (2019).
79. ter Horst, K. W., Gilihamse, P. W., Versteeg, R. I., Ackermans, M. T., Nederveen, A. J., la Fleur, S. E., Romijn, J. A., Nieuwdorp, M., Zhang, D., Samuel, V. T., Vatner, D. F., Petersen, K. F., Shulman, G. I. & Serlie, M. J. Hepatic diacylglycerol-associated protein Kinase C ϵ translocation links hepatic steatosis to hepatic insulin resistance in humans. *Cell Rep.* **19**, 1997–2004 (2017).
80. Aerts, J. M., Ottenhoff, R., Powlson, A. S., Grefhorst, A., van Eijk, M., Dubbelhuis, P. F., Aten, J., Kuipers, F., Serlie, M. J., Wennekes, T., Sethi, J. K., O’Rahilly, S. & Overkleeft, H. S. Pharmacological inhibition of glucosylceramide synthase enhances insulin sensitivity. *Diabetes* **56**, 1341–1349 (2007).
81. Inokuchi, J. GM3 and diabetes. *Glycoconj. J.* **31**, 193–197 (2014).
82. Chavez, J. A., Siddique, M. M., Wang, S. T., Ching, J., Shayman, J. A. & Summers, S. A. Ceramides and glucosylceramides are independent antagonists of insulin signaling. *J. Biol. Chem.* **289**, 723–734 (2014).
83. Maloy, K. J. & Powrie, F. Intestinal homeostasis and its breakdown in inflammatory bowel disease. *Nature* **474** 298–306 (2011).
84. McGaha, T. L., Chen, Y., Ravishankar, B., Rooijen, N. Van & Karlsson, M. C. I. Marginal zone macrophages suppress innate and adaptive immunity to apoptotic cells in the spleen. *Blood* **117** 5403–5412 (2011).
85. Lumeng, C. N., Bodzin, J. L. & Saltiel, A. R. Obesity induces a phenotypic switch in adipose tissue macrophage polarization. *J. Clin. Invest.* **117** 175–184 (2007).
86. Sawai, C. M., Babovic, S., Upadhaya, S., Knapp, D. J. H. F., Lavin, Y., Lau, C. M., Goloborodko, A., Feng, J., Fujisaki, J., Ding, L., Mirny, L. A., Merad, M., Eaves, C. J. & Reizis, B. Hematopoietic stem cells are the major source of multilineage hematopoiesis in adult animals. *Immunity* **45** 597–609 (2016).
87. Bian, Z., Gong, Y., Huang, T., Lee, C., Bian, L., Bai, Z., Shi, H., Zeng, Y., Liu, C., He, J., Zhou, J., Li, X., Li, Z., Ni, Y., Ma, C., Cui, L., Zhang, R., Chan, J., Ng, L. G., Lan, Y., Ginhoux, F.,

- Liu, B. Deciphering human macrophage development at single-cell resolution. *Nature* **582**, 571–576 (2020).
88. Locati, M., Curtale, G. & Mantovani, A. Diversity, mechanisms, and significance of macrophage plasticity. *Annu. Rev. Pathol. Mech. Dis.* **15** 123–147 (2020).
 89. Kracht, L., Borggrewe, M., Eskandar, S., Brouwer, N., Chuva de Sousa Lopes, S. M., Laman, J. D., Scherjon, S. A., Prins, J. R., Kooistra, S. M. & Eggen, B. J. L. Human fetal microglia acquire homeostatic immune-sensing properties early in development. *Science* **369** 530–537 (2020).
 90. Sakai, M., Troutman, T. D., Seidman, J. S., Ouyang, Z., Spann, N. J., Abe, Y., Ego, K. M., Bruni, C. M., Deng, Z., Schlachetzki, J. C. M., Nott, A., Bennett, H., Chang, J., Vu, B. T., Pasillas, M. P., Link, V. M., Texari, L., Heinz, S., Thompson, B. M., McDonald, J. G., Geissmann, F., Glass, C. K. Liver-derived signals sequentially reprogram myeloid enhancers to initiate and maintain Kupffer cell identity. *Immunity* **51** 655–670.e8 (2019).
 91. Willemsen, L. & de Winther, M. P. J. Macrophage subsets in atherosclerosis as defined by single-cell technologies. *J. Pathol.* **250**, 705–714 (2020).
 92. Russo, L. & Lumeng, C. N. Properties and functions of adipose tissue macrophages in obesity. *Immunology* **155**, 407–417 (2018).
 93. Matejuk, A. & Ransohoff, R. M. Crosstalk Between Astrocytes and Microglia: An Overview. *Frontiers in Immunology* **11**, 1416 (2020).
 94. Cox, N. & Geissmann, F. Macrophage ontogeny in the control of adipose tissue biology. *Current Opinion in Immunology* **62**, 1–8 (2020).
 95. Doran, A. C., Yurdagul, A. & Tabas, I. Efferocytosis in health and disease. *Nat. Rev. Immunol.* **20**, 254–267 (2020).
 96. Flannagan, R. S., Jaumouillé, V. & Grinstein, S. The cell biology of phagocytosis. *Annu. Rev. Pathol. Mech. Dis.* **7**, 61–98 (2012).
 97. Ries, M. Enzyme replacement therapy and beyond—in memoriam Roscoe O. Brady, M.D. (1923–2016). *J. Inherit. Metab. Dis.* **40**, 343–356 (2017).
 98. Krivit, W., Peters, C., Dusenbery, K., Ben-Yoseph, Y., Ramsay, N. K. C., Wagner, J. E. & Anderson, R. Wolman disease successfully treated by bone marrow transplantation. *Bone Marrow Transplant.* **26**, 567–570 (2000).
 99. Qu, P., Yan, C., Blum, J. S., Kapur, R. & Du, H. Myeloid-specific expression of human lysosomal acid lipase corrects malformation and malfunction of myeloid-derived suppressor cells in *lal* $-/-$ mice. *J. Immunol.* **187**, 3854–3866 (2011).
 100. Tolar, J., Petryk, A., Khan, K., Bjoraker, K. J., Jessurun, J., Dolan, M., Kivisto, T., Charnas, L., Shapiro, E. G. & Orchard, P. J. Long-term metabolic, endocrine, and neuropsychological outcome of hematopoietic cell transplantation for Wolman disease. *Bone Marrow Transplant.* **43**, 21–27 (2009).
 101. Platt, F. M., Jeyakumar, M., Andersson, U., Priestman, D. A., Dwek, R. A., Butters, T. D., Cox, T. M., Lachmann, R. H., Hollak, C., Aerts, J. M. F. G., Van Weely, S., Hrebícek, M., Moyses, C., Gow, I., Elstein, D. & Zimran, A. Inhibition of substrate synthesis as a strategy for glycolipid lysosomal storage disease therapy. *J. Inherit. Metab. Dis.* **24**, 275–290 (2001).
 102. Shayman, J. A. & Larsen, S. D. The development and use of small molecule inhibitors of glycosphingolipid metabolism for lysosomal storage diseases. *J. Lipid Res.* **55** 1215–1225 (2014).
 103. Mistry, P. K., Balwani, M., Baris, H. N., Turkia, H. Ben, Burrow, T. A., *et al.* Safety, efficacy, and authorization of eliglustat as a first-line therapy in Gaucher disease type 1. *Blood Cells Mol. Dis.* **71** 71–74 (2018).
 104. Aerts, J. M., van Breemen, M. J., Bussink, A. P., Ghauharali, K., Sprenger, R., Boot, R. G., Groener, J. E., Hollak, C. E., Maas, M., Smit, S., Hoefsloot, H. C., Smilde, A. K., Vissers, J. P., de Jong, S., Speijer, D. & de Koster, C. G. Biomarkers for lysosomal storage disorders: identification and application as exemplified by chitotriosidase in Gaucher disease. *Acta*

- Paediatr.* **97**, 7–14 (2008).
105. Eskes, E. C. B., Sjouke, B., Vaz, F. M., Goorden, S. M. I., van Kuilenburg, A. B. P., Aerts, J. M. F. G. & Hollak, C. E. M. Biochemical and imaging parameters in acid sphingomyelinase deficiency: Potential utility as biomarkers. *Mol. Genet. Metab.* **130** 16–26 (2020).
106. Marques, A. R. A., Gabriel, T. L., Aten, J., Van Roomen, C. P. A. A., Ottenhoff, R., Claessen, N., Alfonso, P., Irún, P., Giraldo, P., Aerts, J. M. F. G. & Van Eijk, M. Gpnmb is a potential marker for the visceral pathology in Niemann-Pick type C disease. *PLoS One* **11**, e0147208 (2016).
107. Abdelaal, M., le Roux, C. W. & Docherty, N. G. Morbidity and mortality associated with obesity. *Ann. Transl. Med.* **5** 8 (2017).
108. Li, Z., Bowerman, S. & Heber, D. Health ramifications of the obesity epidemic. *Surg. Clin. North Am.* **85** 681–701 (2005).
109. Obesity and overweight. <https://www.who.int/news-room/fact-sheets/detail/obesity-and-overweight>; accessed: 2020-05-17.
110. The top 10 causes of death. <https://www.who.int/news-room/fact-sheets/detail/the-top-10-causes-of-death>; accessed: 2020-05-17.
111. Beutler, B. & Cerami, A. Tumor necrosis, cachexia, shock, and inflammation: a common mediator. *Annu Rev Biochem.* **57** 505–18 (1988).
112. Filkins, J. P. Reticuloendothelial system function and glucose-insulin dyshomeostasis in sepsis. *Am. J. Emerg. Med.* **2**, 70–73 (1984).
113. Tracey, K. J., Fong, Y., Hesse, D. G., Manogue, K. R., Lee, A. T., Kuo, G. C., Lowry, S. F. & Cerami, A. Anti-cachectin/TNF monoclonal antibodies prevent septic shock during lethal bacteraemia. *Nature* **330**, 662–664 (1987).
114. Hotamisligil, G. S., Shargill, N. S. & Spiegelman, B. M. Adipose expression of tumor necrosis factor- α : Direct role in obesity-linked insulin resistance. *Science* **259**, 87–91 (1993).
115. Hotamisligil, G. S., Murray, D. L., Choy, L. N. & Spiegelman, B. M. Tumor necrosis factor α inhibits signaling from the insulin receptor. *Proc. Natl. Acad. Sci. USA* **91**, 4854–4858 (1994).
116. Weisberg, S. P., McCann, D., Desai, M., Rosenbaum, M., Leibel, R. L. & Ferrante, A. W. Obesity is associated with macrophage accumulation in adipose tissue. *J. Clin. Invest.* **112**, 1796–1808 (2003).
117. Xu, H., Barnes, G. T., Yang, Q., Tan, G., Yang, D., Chou, C. J., Sole, J., Nichols, A., Ross, J. S., Tartaglia, L. A. & Chen, H. Chronic inflammation in fat plays a crucial role in the development of obesity-related insulin resistance. *J. Clin. Invest.* **112**, 1821–1830 (2003).
118. Cinti, S., Mitchell, G., Barbatelli, G., Murano, I., Ceresi, E., Faloia, E., Wang, S., Fortier, M., Greenberg, A. S. & Obin, M. S. Adipocyte death defines macrophage localization and function in adipose tissue of obese mice and humans. *J. Lipid Res.* **46**, 2347–2355 (2005).
119. Gabriel, T. L., Tol, M. J., Ottenhof, R., van Roomen, C., Aten, J., *et al.* Lysosomal stress in obese adipose tissue macrophages contributes to MITF-dependent Gpnmb induction. *Diabetes* **63**, 3310–3323 (2014).
120. Lackey, D. E. & Olefsky, J. M. Regulation of metabolism by the innate immune system. *Nat. Rev. Endocrinol.* **12**, 15–28 (2016).
121. Lee, Y. S., Wollam, J. & Olefsky, J. M. An integrated view of immunometabolism. *Cell* **172** 22–40 (2018).
122. Wang, Z. V & Scherer, P. E. Adiponectin, the past two decades. *J. Mol. Cell. Biol.* **8** 93–100 (2016).
123. Xu, X., Grijalva, A., Skowronski, A., van Eijk, M., Serlie, M. J. J., Ferrante, A. W. W., van Eijk, M., Serlie, M. J. J. & Ferrante, A. W. W. Obesity activates a program of lysosomal-

- dependent lipid metabolism in adipose tissue macrophages independently of classic activation. *Cell Metab.* **18**, 816–830 (2013).
124. Van Der Lienden, M. J. C., Gaspar, P., Boot, R., Aerts, J. M. F. G. & Van Eijk, M. Glycoprotein non-metastatic protein B: an emerging biomarker for lysosomal dysfunction in macrophages. *Int. J. Mol. Sci.* **20** 66 (2019).
 125. Moore, K. J. & Tabas, I. Macrophages in the pathogenesis of atherosclerosis. *Cell* **145**, 341–355 (2011).
 126. Boot, R. G., van Achterberg, T. A. E., van Aken, B. E., Renkema, G. H., Jacobs, M. J. H. M., Aerts, J. M. F. G. & de Vries, C. J. M. Strong induction of members of the chitinase family of proteins in atherosclerosis. *Arterioscler. Thromb. Vasc. Biol.* **19**, 687–694 (1999).
 127. Bietrix, F., Lombardo, E., van Roomen, C. P. A. A., Ottenhoff, R., Vos, M., Rensen, P. C. N., Verhoeven, A. J., Aerts, J. M. & Groen, A. K. Inhibition of glycosphingolipid synthesis induces a profound reduction of plasma cholesterol and inhibits atherosclerosis development in APOE*3 Leiden and low-density lipoprotein receptor-/- mice. *Arterioscler. Thromb. Vasc. Biol.* **30**, 931–7 (2010).
 128. Xu, J., Jüllig, M., Middleditch, M. J. & Cooper, G. J. S. Modelling atherosclerosis by proteomics: Molecular changes in the ascending aortas of cholesterol-fed rabbits. *Atherosclerosis* **242**, 268–76 (2015).
 129. Krasemann, S., Madore, C., Cialic, R., Baufeld, C., Calcagno, N., *et al.* The TREM2-APOE pathway drives the transcriptional phenotype of dysfunctional microglia in neurodegenerative diseases. *Immunity* **47**, 566–581.e9 (2017).
 130. Hendrickx, D. A. E., van Scheppingen, J., van der Poel, M., Bossers, K., Schuurman, K. G., van Eden, C. G., Hol, E. M., Hamann, J. & Huitinga, I. Gene expression profiling of multiple sclerosis pathology identifies early patterns of demyelination surrounding chronic active lesions. *Front. Immunol.* **8**, 1810 (2017).

Chapter 1

HEPES activates a MiT/TFE-dependent lysosomal-autophagic gene network in cultured cells: a call for caution

Manuscript published as:

Tol, M. J., **van der Lienden, M. J. C.**, Gabriel, T. L., Hagen, J. J., Scheij, S., Veenendaal, T., Klumperman, J., Donker-Koopman, W.E., Verhoeven A.J., Overkleeft, H., Aerts, J.M.F.G., Armann, C.A. & Van Eijk, M. HEPES activates a MiT/TFE-dependent lysosomal-autophagic gene network in cultured cells: A call for caution. *Autophagy* **14**, 1–13 (2018).

Abstract

In recent years, the lysosome has emerged as a highly dynamic, transcriptionally regulated organelle that is integral to nutrient-sensing and metabolic rewiring. This is coordinated by a lysosome-to-nucleus signaling nexus in which MTORC1 controls the subcellular distribution of the microphthalmia-transcription factor E (MiT/TFE) family of “master lysosomal regulators”. Yet, despite the importance of the lysosome in cellular metabolism, the impact of traditional in vitro culture media on lysosomal dynamics and/or MiT/TFE localization has not been fully appreciated. Here, we identify HEPES, a chemical buffering agent that is broadly applied in cell culture, as a potent inducer of lysosome biogenesis. Supplementation of HEPES to cell growth media is sufficient to decouple the MiT/TFE family members-TFEB, TFE₃ and MITF-from regulatory mechanisms that control their cytosolic retention. Increased MiT/TFE nuclear import in turn drives the expression of a global network of lysosomal-autophagic and innate host-immune response genes, altering lysosomal dynamics, proteolytic capacity, autophagic flux, and inflammatory signaling. In addition, siRNA-mediated MiT/TFE knockdown effectively blunted HEPES-induced lysosome biogenesis and gene expression profiles. Mechanistically, we show that MiT/TFE activation in response to HEPES requires its macropinocytic ingestion and aberrant lysosomal storage/pH, but is independent of MTORC1 signaling. Altogether, our data underscore the cautionary use of chemical buffering agents in cell culture media due to their potentially confounding effects on experimental results.

Introduction

Lysosomes are ubiquitous membrane-bound organelles that were first described by de Duve and colleagues.¹ These catabolic structures contain a selection of acid hydrolases capable of degrading a vast repertoire of biological substrates. The lysosomal membrane harbors many multimeric protein complexes involved in transport of metabolites in and out of the lysosome, lumen acidification, trafficking, and fusion with other intracellular structures.^{2,3} Both endocytic and autophagic pathways converge on the lysosomal apparatus for content degradation. The autophagic-lysosomal axis plays a key role in cellular quality control and recycling of building blocks. Macroautophagy/autophagy facilitates the removal of aggregated or misfolded proteins and the removal of either damaged or functionally redundant organelles under stress conditions.⁴ As a result, lysosomal dysfunction has been coupled to a wide range of inherited⁵⁻⁷ and acquired metabolic disorders.⁸⁻¹¹

Over the past decade, the view of the lysosome has evolved radically from a static recycling center into a highly dynamic, transcriptionally regulated organelle that is integral to nutrient-sensing and metabolic adaptation.²⁻⁴ In 2009, Sardiello et al. defined a conserved lysosome-to-nucleus signaling nexus controlled by the basic helix-loop-helix leucine zipper TFEB (transcription factor EB).¹² TFEB is a member of the microphthalmia-transcription factor E (MiT/TFE) subfamily, to which TFE3 (transcription factor E3) and MITF (melanogenesis associated transcription factor) also belong.¹³ In response to starvation or metabolic stress, TFEB undergoes cytosol-to-nucleus shuttling where it activates a coherent transcriptional program that controls major steps of the autophagic-lysosomal system, such as lysosome biogenesis, autophagosome formation, autophagosome-lysosome fusion, and content degradation.^{12,14} TFEB recognizes a specific coordinated lysosomal expression and regulation (CLEAR) motif (GTCACGTGAC) enriched in the promoter regions of certain lysosomal and autophagic genes.¹⁵ A similar mode of action has been ascribed to TFE3 through binding the E-box sequence motif (CANNTG), which partially overlaps with the CLEAR sequence.^{16,17} Conversely, MITF regulates only a subset of lysosomal-autophagic genes, but lacks the ability to promote the formation of functional lysosomes.^{16,18} It is unknown whether MiT/TFE family members have cooperative, complementary, or nonredundant roles in tailoring the lysosomal system to cell-type or metabolic stress-specific needs.

The first clues for a direct role of the lysosomal apparatus in nutrient sensing emerged from a pioneering study by Sancak et al.¹⁹ They uncovered that the MTORC1 (mechanistic target of rapamycin [serine/threonine kinase] complex 1), a master regulator of cell growth, localized to RAB7/RAS-related GTP-binding protein 7-positive vesicular structures in an amino acid-sensitive fashion.¹⁹ This localization depends on a heterodimeric RRAF/RAG (Ras-related GTP binding) GTPase signaling complex that relays amino acid sufficiency to MTORC1. Recent advances in this field have uncovered that active RRAF heterodimers target MTORC1 to the lysosomal surface via a mechanism that requires the vacuolar-type H⁺-translocating adenosine triphosphatase (v-ATPase) and Ragulator, a pentameric scaffolding complex that anchors RRAF GTPases to the lysosomal surface.²⁰⁻²² These components allow MTORC1 to interact with its upstream activator RHEB (Ras homolog enriched in brain), and in turn control key biosynthetic and catabolic processes.²³⁻²⁵ In addition to stimulating cell growth under nutrient-rich conditions, MTORC1 acutely

inhibits autophagy by phosphorylating a range of autophagy effectors.²⁶⁻²⁸ Moreover, MTORC1 signaling has recently been linked to the transcriptional regulation of autophagy by controlling the subcellular localization of MiT/TFE proteins.²⁹⁻³² Active RRAF GTPases direct MiT/TFE family members to the lysosomal surface, where they undergo MTORC1-mediated phosphorylation, resulting in their cytosolic retention. During starvation or lysosomal stress, MTORC1 is turned off and MiT/TFE proteins localize to the nucleus and promote lysosomal-autophagic gene expression.²⁹⁻³¹

The recently defined lysosome-based nutrient-sensing apparatus governed by MTORC1 and MiT/TFE family members has positioned the lysosome at the forefront of metabolic research. Indeed, aberrant lysosomal-autophagic transcriptional biology and nutrient sensing has now been implicated in a range of acquired disease states.⁵⁻¹¹ Yet, despite the upsurge of interest in the lysosome as a major nutrient gateway, it is hitherto largely unexplored whether specific *in vitro* cell culture conditions affect lysosomal function and MiT/TFE subcellular localization. Here, we identify HEPES, a widely applied chemical buffering agent in cell culture—we found >800,000 hits in a Google Scholar search (using “HEPES” AND “in vitro” AND “cell culture”)—as a potent activator of MiT/TFE-dependent lysosomal-autophagic gene networks. Our data emphasize the importance of understanding how cell culture media with its varying chemical, nutrient, and buffer compositions, affect lysosomal homeostasis and cellular metabolism in general.

Results

HEPES Drives Lysosome Biogenesis in Cultured Cells

Macrophages are specialized phagocytic cells that rely on a dynamic endo-lysosomal system to cope with varying substrate fluxes that enter through endocytic and autophagic routes. As part of our ongoing studies aimed at unraveling the transcriptional regulation of the lysosomal stress reporter GPNMB (glycoprotein [transmembrane] NMB)³³ in the RAW264.7 (RAW) cell line, we observed a robust on/off state when using distinct growth media. RAW cells cultured in RPMI-1640 medium (22409; Dutch modification; see Materials and Methods) showed a marked induction of GPNMB expression as well as its secreted form, relative to DMEM (31966) (**Supplemental figure 1A-C**). In addition, by using the LysoTracker Green (LTG) dye, a specific marker for acidic organelle compartments, we measured an ~3.5-fold increase in the number of acidic organelles in RPMI-grown cells by flow cytometry (**Supplemental figure 1D**). Parallel studies using MitoTracker Green demonstrated no evident changes in mitochondrial number (**Supplemental figure 1E**).

To identify the nutrient/chemical in RPMI initiating lysosomal biogenesis in cultured cells, we systematically compared the formulations of the 2 respective growth media. This revealed notable changes in glucose, amino acid, vitamin and inorganic salt concentrations. The most striking discrepancy was the inclusion of the zwitterionic biological buffer HEPES (25 mM) in the RPMI recipe, which was lacking in DMEM. Notably, we confirmed HEPES as the elusive factor driving the induction of acidic organelles by recreating the lysosomal stress phenotype in RAW cells cultured in a HEPES-containing DMEM variant (32430) (**Figure 1A**). Conversely, switching cells to HEPES-free RPMI (61870) completely abolished lysosomal biogenesis. In line with these results,

supplementing DMEM with culture-grade HEPES (DMEM^{+H}) elicited a progressive and dose-dependent increase of LTG signal and *Gpnmb* gene expression and protein (**Figure 1B-C** and **Supplemental figure 1F-I**). Moreover, this lysosomal stress signature fully resolved upon the withdrawal of HEPES from cell culture media (**Figure 1D-E**). To further characterize the impact of HEPES on an ultrastructural level, we resorted to transmission electron microscopy (TEM). This analysis unveiled a striking vacuolation phenotype in DMEM^{+H}-grown cells (**Figure 1F**). These vacuoles were readily visible by phase-contrast microscopy and stained positive for LAMP1 (lysosomal-associated membrane protein 1) (**Figure 1G**), suggesting that they correspond to late endosomes and/or lysosomes. Additionally, it is important to note that HEPES supplementation to culture media did not adversely affect cell viability (**Supplemental figure 1J-K**).

To determine whether the LAMP1-positive structures represent functional lysosomes, we first measured the activities of lysosomal enzymes using a 4-MU assay and activity-based probes (ABP).^{34, 35} Indeed, DMEM^{+H}-grown cells displayed a significant increase in active GBA1/glucocerebrosidase 1 (glucosidase, beta, acid) and cysteine cathepsin enzymes (**Figure 1H** and **Supplemental figure 1L-M**). We next determined lysosomal proteolytic activity using the dequenched (DQ)-BSA reagent³⁶, which is readily incorporated by cells via fluid-phase endocytosis. Upon fusion with endo-lysosomes, DQ-BSA is digested into smaller fragments, thereby relieving its self-quenching properties and generating a fluorescent signal that reflects lysosomal degradative capacity (**Figure 1I**). Of interest, HEPES supplementation to RAW cell culture media led to a marked increase in DQ-BSA cleavage (**Figure 1J**), signifying that these LAMP1-positive structures are, at least in part, functional lysosomes. Lastly, given the highly integrated nature of the autophagy-lysosomal pathway, we explored the impact of HEPES on the conversion of cytosolic MAP1LC3/LC3 (microtubule-associated protein 1 light chain 3)-I to lipidated autophagic membrane-bound LC3-II.³⁷ The steady-state level of autophagosomes depends on both *de novo* synthesis and their lysosomal turnover. We therefore measured autophagic flux in the presence and absence of bafilomycin A₁, a potent v-ATPase inhibitor that blocks autophagosome-lysosome fusion and thus LC3-II degradation. Under both normal and lysosome-inhibited conditions, LC3-II levels were significantly elevated in DMEM^{+H}-grown RAW cells (**Figure 1K-L**), indicating that HEPES drives biogenesis of the autophagic-lysosomal pathway.

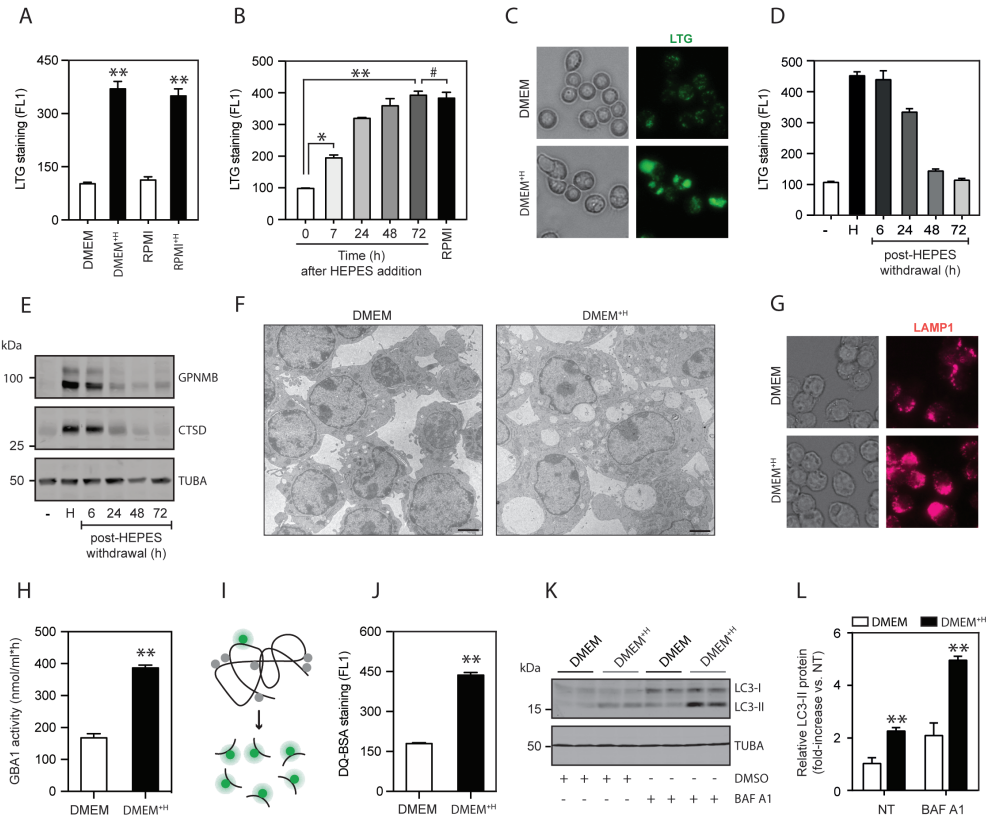


Figure 1. HEPES drives lysosomal biogenesis in cultured RAW264.7 macrophages. (A) Flow cytometric analysis (FL1) of LTG-stained RAW cells grown in either DMEM (31966), DMEM (32430; containing HEPES), RPMI (61870), or RPMI (22409; containing HEPES). (B) Time-course analysis of LTG staining in cells grown in DMEM supplemented with HEPES (25 mM) for 6-72 h. RPMI-grown cells served as a positive control. (C) Fluorescence microscopy analysis of LTG-stained RAW cells cultured in DMEM or DMEM^{HEPES} for 24 h. (D-E) RAW cells were adapted to grow in DMEM (32430; containing HEPES) for 7 days, after which culture media were replaced by HEPES-free DMEM (31966) for 6-72 h. A time course for (D) LTG staining and (E) Immunoblot analysis of GPNMB and CTSD protein levels. (F) Transmission electron microscopy (TEM) analysis of RAW cells grown in either DMEM or DMEM^{HEPES} for 24 h. Scale bar: 1 μ m. (G) Phase-contrast and immunofluorescence microscopy analysis of LAMP1-stained cells. (H) Analysis of GBA1 enzymatic activity using a 4-MU-based assay in RAW cells grown in DMEM or DMEM^{HEPES} for 24 h. (I) Schematic illustration of the DQ-BSA reagent used for quantifying lysosomal proteolytic activity. DQ-BSA added to culture media is rapidly endocytosed, but only emits a fluorescent signal after cleavage by proteases inside lysosomes. (J) Flow cytometric analysis of DQ-BSA cleavage (FL1) in RAW cells grown in DMEM or DMEM^{HEPES} for 24 h. (K) Western blot analysis and (L) quantification of LC3-II protein levels in RAW cells grown in DMEM or DMEM^{HEPES} for 24 h, and where indicated treated with bafilomycin A₁ (BAF A1; 100 nM) for the last 2 h. Values are expressed as mean \pm SEM, n=3-4 in A-L. **P<0.01.

HEPES affects MiT/TFE Cytoplasmic-Nuclear Distribution

Of interest, the lysosomal phenotype induced by HEPES closely mirrors a previously defined sucrose-driven vacuolation model.³⁸⁻⁴⁰ In addition, sucrose supplementation induces the nuclear translocation of TFEB and activation of the lysosomal-autophagic gene program.¹² This prompted us to study the subcellular distribution of MiT/TFE family members in response to HEPES. Immunofluorescence analysis showed mainly cytosolic localization of endogenous TFEB, TFE3 and MITF in standard DMEM-grown RAW cells (**Figure 2A**). Notably, HEPES supplementation to cell culture media induced a dramatic nuclear translocation of all three MiT/TFE family members (**Figure 2A-B**). In line with prior studies^{12, 29-32}, sucrose (80 mM) and the MTOR catalytic site inhibitor Torin1 (400 nM) were equally potent in driving the nuclear localization of MiT/TFE family proteins (**Figure 2A-B**). These observations were further verified by immunoblotting performed after nuclear-cytosolic fractionation (**Figure 2C**). In addition, treating DMEM⁺-grown cells with an siRNA cocktail targeting *Tfeb*, *Tfe3*, and *Mitf*, significantly blunted lysosome biogenesis and gene expression (**Supplemental figure 2A-C**), thus directly coupling the HEPES-dependent lysosomal stress response to MiT/TFE activity. In agreement, omitting HEPES from RAW culture media led to a prompt MiT/TFE redistribution back to the cytosol (**Supplemental figure 2D**).

We next aimed to clarify the molecular basis of MiT/TFE activation in DMEM⁺-cultured RAW cells. In recent years, MTORC1 has emerged as the major repressor of lysosomal-autophagic transcriptional biology under nutrient-replete conditions via directly phosphorylating MiT/TFE proteins on multiple conserved residues, leading to their cytosolic sequestration.²⁹⁻³² Similar to Torin1, HEPES or sucrose supplementation to culture media changed the electrophoretic mobility of TFEB to a fast-migrating form (**Figure 2D**), signifying dephosphorylated TFEB that is present in the nucleus.^{29, 30} Yet, both buffering agents did not alter MTORC1 signaling, as measured by phosphorylation of its substrates RPS6/S6 (ribosomal protein S6) and EIF4EBP1/4E-BP1 (eukaryotic translation initiation factor 4E binding protein 1) (**Figure 2D** and **Supplemental figure 2E**), suggesting that HEPES affects MiT/TFE localization via an MTORC1-independent mode of action. To evaluate whether the effects of HEPES rely on active ingestion and delivery to the lysosome, we made use of LY294002 (LY2), a potent inhibitor of the class III phosphatidylinositol 3-kinase (PtdIns3K) and fluid-phase endocytosis⁴¹ (confirmed by monitoring the uptake of FITC-labeled dextran; **Supplemental figure 2F**). A potential caveat of studying the relevance of HEPES uptake is that well-known inhibitors of endocytic trafficking either perturb lysosomal pH or MTORC1 activity^{30, 42}, both of which trigger MiT/TFE redistribution to the nucleus. Notably, although LY2 inhibited MTORC1 signaling to the same extent as Torin1, this was not followed by a significant TFEB molecular weight shift (**Figure 2D**). Moreover, LY2 pre-treatment largely prevented the TFEB mobility shift induced by HEPES or sucrose, but not by Torin1 (**Figure 2D**). In line with these observations, LY2 strongly blunted the ability of HEPES to drive MiT/TFE nuclear transport and lysosome biogenesis (**Figure 2E-G**), whereas the response to Torin1 was unaffected (**Supplemental figure 2G**).

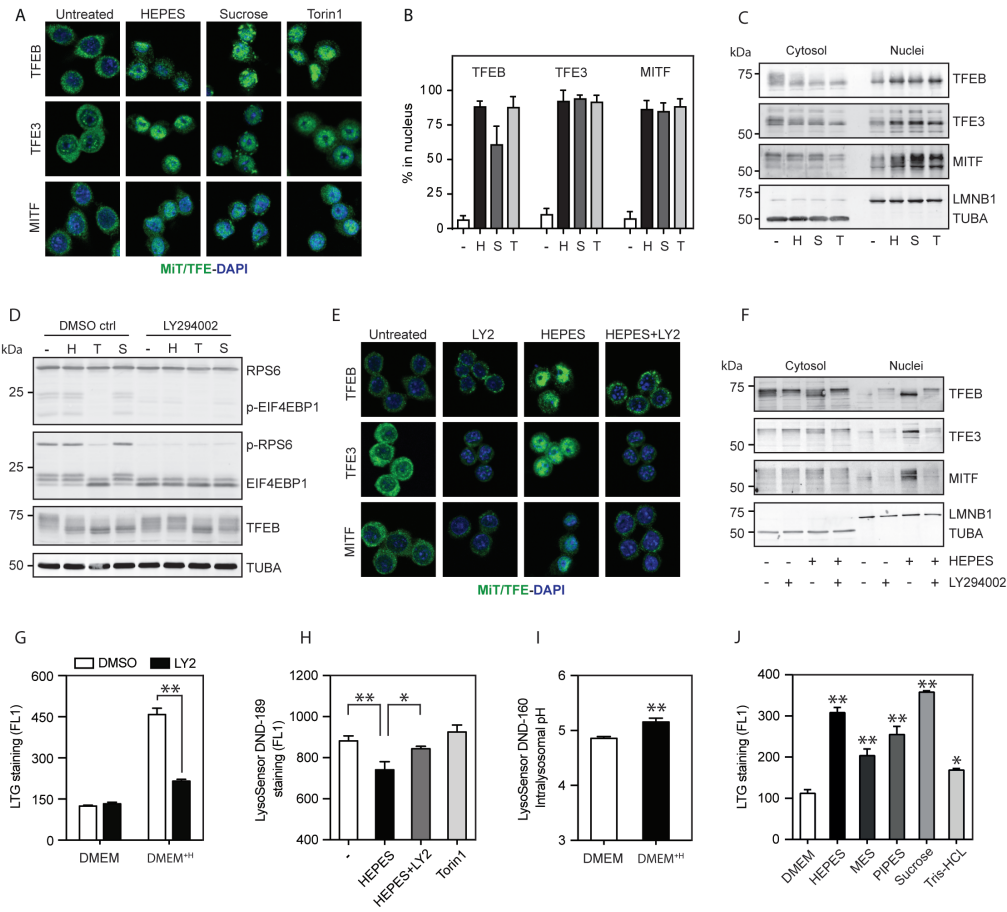


Figure 2. HEPES promotes MiT/TFE nuclear translocation independent of MTORC1 activity. (A) Representative images and (B) quantified MiT/TFE nuclear import in RAW cells treated with HEPES (H), sucrose (S), or Torin1 (T) for 6 h, stained for endogenous TFEB, TFE3, or MITF levels (in green) and counterstained with DAPI (in blue). Values are expressed as percent of cells counted (>100 per experiment). (C) Western blot analysis on cytosolic and nuclear fractions isolated from RAW macrophages treated for 6 h, as indicated. Membranes were probed with antibodies against MiT/TFE family members. TUBA and LMNB1 were used as controls for the cytosolic and nuclear fractions, respectively. (D) HEPES and sucrose supplementation to RAW cell culture media does not inhibit MTORC1 signaling. Western blot analysis on protein extracts isolated from RAW cells treated for 6 h as indicated in the presence and absence of the PtdIns3K inhibitor LY294002 (LY2; 50 μ M). Membranes were probed with antibodies against p-EIF4EBP1 (Thr37/46), p-RPS6 (Ser235/236), and TFEB. (E-G) LY2 prevents HEPES-dependent MiT/TFE nuclear redistribution and lysosome biogenesis. (E) Representative images and (F) western blot analysis of MiT/TFE relocation in RAW cells pretreated with LY2 for 30 min and subsequently cultured in either DMEM or DMEM^H for 6 h. (G) Flow cytometric analysis of LTG-stained cells pre-treated with LY2 and grown in DMEM or DMEM^H for another 16 h. (H-I) HEPES perturbs lysosomal pH/acidification. (H) Flow cytometric analysis of fluorescent intensity (FL1) in LysoSensorTM DND-189 stained RAW cells treated for 2 h, as indicated. (I) Quantified lysosomal pH using LysoSensorTM Yellow/Blue DND-160 in cells grown in DMEM or DMEM^H for 4 h. (J) Flow cytometric analysis of LTG-stained RAW cells grown in DMEM supplemented with HEPES (20 mM), MES (20 mM), PIPES (10 mM), sucrose (80 mM), and Tris-HCl (20 mM) for 16 h. Values are expressed as mean \pm SEM, n=3-4 in A-J. *P < 0.05, **P < 0.01.

The MiT/TFE factors mobilize to the nucleus in response to inhibitors of the v-ATPase.^{29-31, 33} We thus reasoned that aberrant HEPES storage may interfere with lysosomal pH regulation. To test this hypothesis, we used LysoSensor™ Green DND-189 (LSG) to measure lysosomal acidification. LSG fluorescence intensity increases in more acidic cellular compartments.⁴³

We opted for a short-term (2.5 h) exposure to HEPES to exclude MiT/TFE-related compensatory effects aimed at correcting the defective pH status of the lysosome. Flow cytometric analysis of LSG-stained DMEM⁺H-grown cells showed an LY2-sensitive reduction in fluorescent signal relative to RAW controls (**Figure 2H**), reflecting a higher lysosomal pH. In contrast, treating cells with Torin1 had little effect on LSG signal (**Figure 2H**). The increase in lysosomal pH was validated by using LysoSensor™ Yellow/Blue DND-160 (**Figure 2I**), a ratiometric probe that allows for pH analysis in acidic organelles. These data support a model of aberrant lysosomal pH and/or storage as a mechanism for HEPES-dependent MiT/TFE activation. LY2 blocks the full lysosomal signature in DMEM⁺H-grown RAW cells, most likely by its ability to suppress macropinocytosis, a nonselective mode of fluid-phase endocytosis.⁴⁴ Supporting this view, supplementing RAW cell culture media with a number of chemical buffering agents (pH 7.4) recapitulated HEPES-driven lysosome biogenesis (**Figure 2J**). Lastly, it is important to note that macropinocytosis is a ubiquitous cellular process, although the pinocytic rate varies between distinct cell types.⁴⁵ This led us to explore whether HEPES-related lysosomal stress is a universal feature in mammalian cell culture. Indeed, multiple widely used fibroblastic and cancerous cell lines adapted to grow in DMEM⁺H showed a significant increase in LTG signal, albeit less robust as observed in RAW cells (**Supplemental figure 2H**). Similarly, this was accompanied by a progressive nuclear redistribution of endogenous MiT/TFE proteins (**Supplemental figure 2G**), as shown by immunostaining. Together, these results suggest that HEPES inclusion in cell culture media drives a MiT/TFE-related lysosomal stress pathway.

HEPES Disrupts Global Cellular Transcriptional Profiles

To study the global molecular consequence of HEPES on cellular transcriptional profiles, we conducted RNA-Seq on the RAW cell line. Overall, HEPES supplementation to culture media significantly affected the expression of ~1738 genes (15.5% of the total; **Figure 3A**). The molecular changes induced by HEPES corroborated our phenotypic observations because Kyoto encyclopedia of genes and genomes (KEGG) pathway enrichment analysis unveiled upregulation of genes associated with the lysosome (**Figure 3B**). Similarly, gene-set enrichment analysis (GSEA) confirmed our findings that HEPES affects MiT/TFE transcriptional biology, as illustrated by a robust enrichment of numerous lysosome-autophagic genes harboring CLEAR⁵ and/or E-box⁴⁶ consensus motifs (**Figure 3C-D** and **Supplemental figure 3**). Additionally, classical pro-inflammatory pathways were significantly overrepresented among the genes induced by HEPES, for example those involving TNF/TNFA, NFκB/NF-κB, and TLR (toll-like receptor) (**Figure 3A**). This outcome is befitting, as MiT/TFE members have recently also been defined as key transcriptional regulators of the host-immune response.^{33, 46-48}

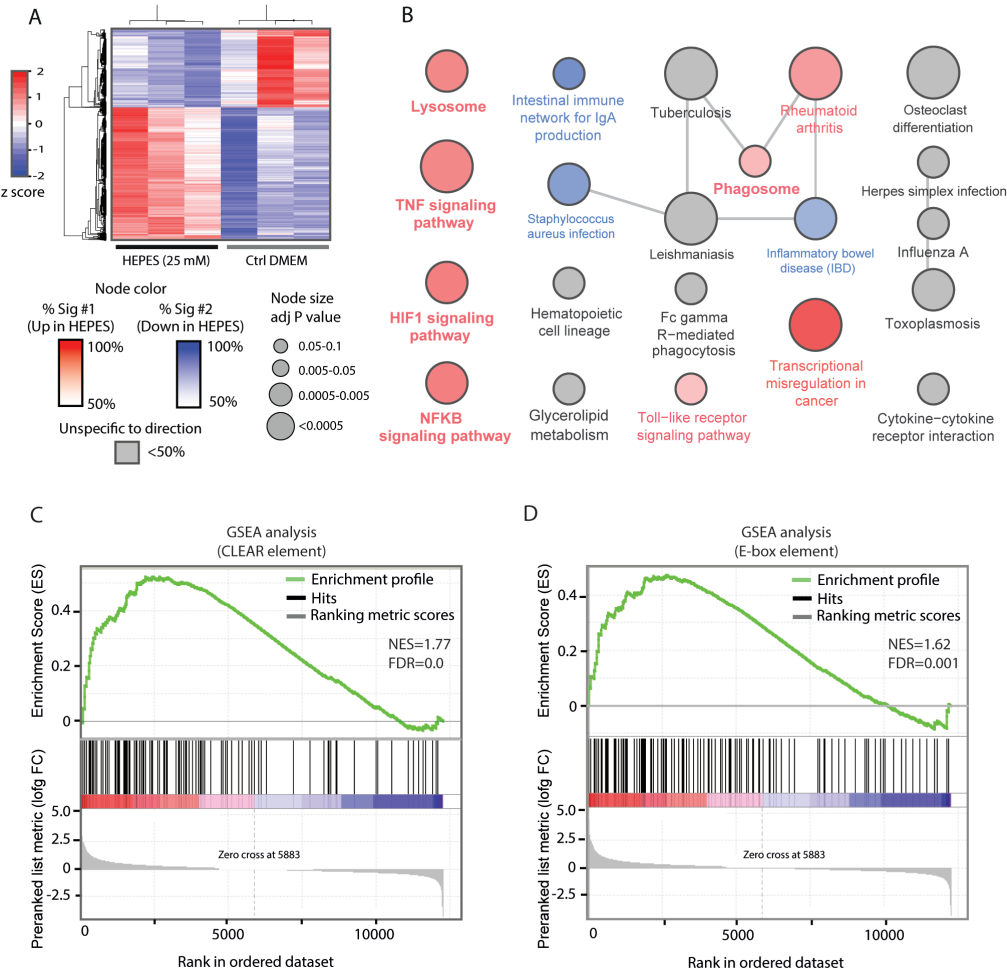


Figure 3. Global molecular consequence of HEPES on the RAW264.7 macrophage cell line. (A) A heatmap transformation of the z-score normalized levels of the top ~1738 differentially expressed genes (log FC > |0.5| with adj p-value of <0.01) following HEPES supplementation to RAW cell culture media for 24 h. (B) Kyoto Encyclopedia of Genes and Genomes (KEGG) pathway enrichment analysis on 2 lists with either up- or downregulated genes in response to HEPES. Node color indicates cellular pathways that were mostly enriched in upregulated (more red) or downregulated (more blue) genes or nonspecific to direction of the expression change (gray). (C-D) HEPES drives a MiT/TFE-mediated gene signature in RAW cells. Gene set enrichment analysis (GSEA) on the RAW transcriptome following exposure to HEPES for 24 h. Graphs show enrichment plots of ranked gene expression data (red, upregulated; blue, downregulated). The enrichment score is depicted as a green line, and the vertical black bars below indicate the position of lysosomal-autophagic and innate host-immune response genes carrying either validated (C) CLEAR sequences bound by TFE^{12, 15} or (D) E-box consensus motifs bound by TFE₃⁴⁶.

We next sought to identify whether the HEPES-associated inflammatory signature mirrored a known macrophage polarization state. M1 or 'classically activated' macrophages are induced by pro-inflammatory mediators such as lipopolysaccharide (LPS), whereas M2 or the 'alternatively activated' state is typically generated after exposure to IL4. To define how the global transcriptional changes in response to HEPES-induced lysosomal stress compared to M1 or M2 polarization states, we conducted parallel RNA-seq on RAW cells treated with 100 ng/ml LPS or 50 ng/ml IL4 for 24 h. We subsequently applied a rank-rank hypergeometric overlap (RRHO) algorithm that enables a global comparison of the molecular consequence of HEPES with those defined by the polarization states. Notably, an RRHO map of the HEPES vs. LPS differentially expressed genes uncovered a significant overlap, as shown by a bright red intensity along the diagonal axis (**Figure 4A**).

This overlap was further evidenced by a positive correlation ($r = 0.54$) in the scatter plot of the corresponding Log2FC values (**Figure 4A**). Conversely, the RRHO map and scatter plot comparing HEPES and IL4 showed a less conserved correlation pattern (**Figure 4B**). Hence, these results indicate that HEPES addition to culture media triggers a lysosomal stress-related inflammatory phenotype that molecularly resembles an M1-like activation state.

To explore the functional consequence of HEPES on cytokine and interleukin biology in more detail, we evaluated the cytokine/chemokine secretion profile using a cytokine array blot (**Figure 4C**). This analysis supported an increased capacity of DMEM^H-grown RAW cells to produce and secrete a number of cytokines (**Figure 4C**), such as TNF and CCL2. Of interest, both M1 and M2 stimuli have recently been linked to the induction of specific lysosomal gene programs in RAW macrophages.^{46, 49} This led us to hypothesize that HEPES-related lysosomal priming affects macrophage polarization in response to M1 or M2 stimuli. To this end, RAW cells were grown in the presence or absence of HEPES for 48 h, and pulsed with either LPS or IL4 for the last 24 h. HEPES potentiated the capacity of LPS to induce M1-specific markers, including *Tnf*, *Ccl2*, and *Ilrn* (**Figure 4D**). Moreover, the presence of HEPES also enhanced the IL4 (M2 like) response, as shown by amplified transcript levels of the M2-specific marker *Arg1* (**Figure 4D**). Notably, *Cstd* expression was similarly upregulated in both HEPES and LPS-treated cells (**Figure 4E**). The lack of a synergistic effect between HEPES and LPS implies that both stimuli converge on the same effector pathway. In line with this, LPS-mediated TLR signaling in RAW macrophages has recently been shown to drive nuclear import of TFEB and TFE3.⁴⁶ Finally, we observed a distinct pattern for *Gpnmb* transcript levels, which was selectively induced in DMEM^H-grown cells (**Figure 4E**). Together, these data suggest that HEPES supplementation to culture media alters the RAW polarization response. Additionally, whereas HEPES and LPS both converge on MiT/TFE signaling, specific triggers may govern a tailored transcriptional outcome.

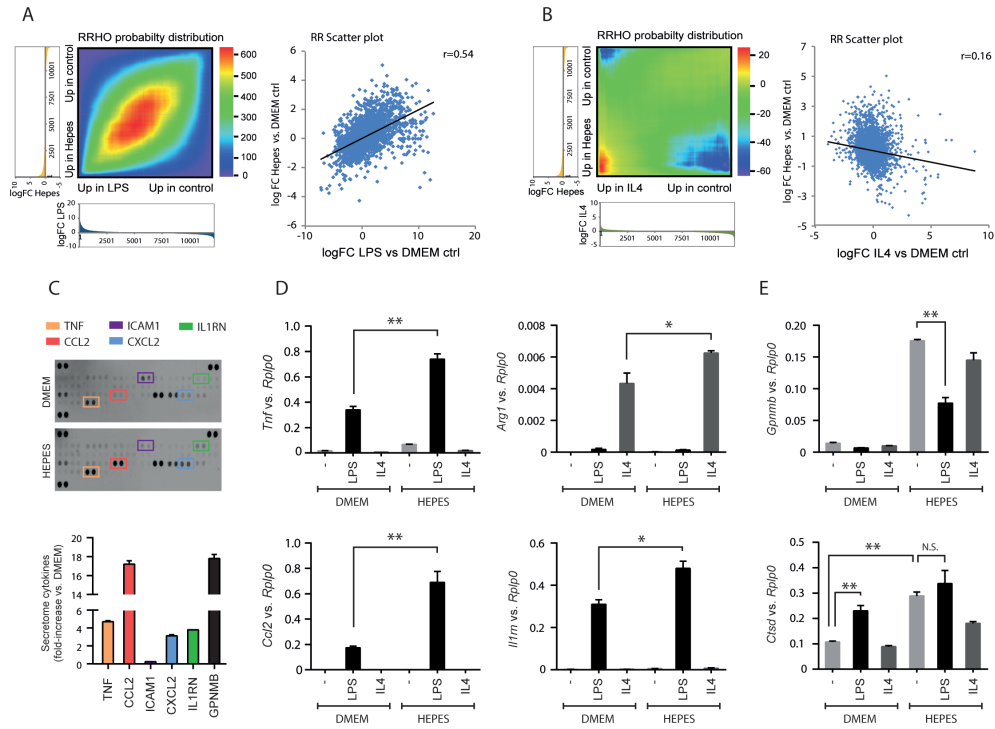


Figure 4. HEPES affects host-immune gene programs in RAW macrophages. (A-B) Rank-rank hypergeometric overlap (RRHO) analysis comparing the gene ranking (log FC) affected by HEPES (relative to DMEM) to an (A) M1 polarization state induced by LPS (100 ng/ml), or an (B) M2-specific state induced by IL4 (50 ng/ml). Pixel values in the RRHO map represent the \log_{10} -transformed hypergeometric overlap of subsections of 2 ranked gene lists (step size 100 genes). Red values indicate a higher than expected number of overlapping genes in the subsections, and blue values signify a lower than expected overlapping gene number. Below the heatmaps, the metric values (log FC) used for the differential expression levels are plotted in a bar graph along x- and y-axes. A scatter plot (A-B) of the datasets is shown for comparing the RRHO map to a standard metric of correlation (Pearson). The RRHO result and Pearson correlation coefficient reflect a similar relationship. (C) Cytokine array blots on culture media derived from DMEM or DMEM^{HL}-grown cells for 24 h. Secreted cytokines and chemokines in culture media were detected using a Mouse Cytokine Array kit and quantified with the Odyssey V3.0 software (fold-increase relative to DMEM ctrl). Secreted GPNMB levels were measured as a positive control. (D-E) RT-PCR analysis of the specified (D) M1- and M2-specific markers and (E) MiT/TFE target genes in RAW cells grown in DMEM or DMEM^{HL} for 24 h and pulsed with either vehicle Ctrl (-), LPS (100 ng/ml) or IL4 (50 ng/ml) for another 24 h. Gene expression was normalized to Rplp0. Values are expressed as mean \pm SEM, $n=3-4$ in A-E. * $P < 0.05$, ** $P < 0.01$. N.S., nonsignificant.

Discussion

In recent years, the lysosome has evolved from a static recycling center into a dynamic, transcriptionally regulated organelle integral to nutrient sensing.^{12, 19} This involves a highly integrated signaling nexus governed by MTORC1 and the MiT/TFE family members. Indeed, deregulated lysosomal function has now been implicated in a wide range of acquired disease states, including obesity, inflammation, ageing, and cancer.⁸⁻¹¹ This underscores the importance of using a well-defined set of *in vitro* cell culture conditions in order to accurately study cellular metabolism and disease pathogenesis. Our study defines HEPES, a chemical buffering agent that is broadly applied in culture media, as a potent inducer of transcriptional changes leading to lysosome biogenesis. The HEPES-dependent lysosomal stress signature is mechanistically coupled to activation of the MiT/TFE family members. Increased nuclear import drives a global network of lysosome-autophagic and innate host-immune genes in the monocytic RAW cell line. This reflects an adaptive metabolic response to cope with aberrant lysosomal pH and/or storage upon active HEPES ingestion.

Work in the 1980s first described a HEPES-driven vacuolation phenotype in cultured cells, although the underlying mechanism(s) remained elusive.^{50, 51} The MiT/TFE family members—TFEB, TFE3, and MITF—have recently been defined as “master regulators” of the lysosomal-autophagic transcriptional biology.^{12, 14-16} Here, we present several lines of evidence supporting a MiT/TFE dependency of the HEPES-induced lysosomal stress response. First, HEPES supplementation to cell culture media induced a dramatic nuclear translocation of MiT/TFE family members. Second, HEPES withdrawal from culture media led to MiT/TFE redistribution back to the cytosol. Third, siRNA-mediated MiT/TFE knockdown blunted lysosomal biogenesis and gene expression profiles in DMEM⁺^H-grown cells. Fourth, inhibition of fluid-phase endocytosis largely prevented the HEPES-driven TFEB mobility shift, MiT/TFE nuclear translocation, and the associated increase in LTG signal. Fifth, a GSEA on RNA-seq datasets showed that direct TFEB and TFE3 target genes were overrepresented in the fraction of genes upregulated by HEPES.

The MiT/TFE members, in particular TFEB and TFE3, are key effectors in cellular adaptation to starvation or lysosomal stress.¹⁴⁻¹⁶ It is widely accepted that both stressors trigger MiT/TFE nuclear transport by virtue of their ability to suppress MTORC1.²⁹⁻³¹ The emerging concept of MTORC1 activation status as a gating factor in determining MiT/TFE localization has recently been questioned by Pastore et al.⁴⁶ They have reported that TLR signaling in macrophages drives TFE3 nuclear import under conditions of sustained MTORC1 activity. Consistently, HEPES-dependent MiT/TFE nuclear redistribution was independent of changes in MTORC1 activity, as judged by the phosphorylation status of its downstream targets RPS6 and EIF4EBP1. Thus, MiT/TFE activation by HEPES appears to be mechanistically distinct from the response to starvation or MTORC1 inhibition. Reinforcing this view, LY2 prevented the ability of HEPES to drive MiT/TFE translocation, whereas the response to Torin1 was insensitive to PtdIns3K inhibition. We speculate that aberrant lysosomal pH and/or storage triggered by HEPES is sensed by a hitherto unknown signaling node (e.g. a lysosome-resident phosphatase or PRKC^{52, 53}) that converges on MiT/TFE localization.

Our data uncover an apparent nonlinearity between MTORC1 activation status and MiT/TFE subcellular distribution. Treating RAW macrophages with the PtdIns3K

inhibitor LY2 led to a near-complete suppression of MTORC1 activity, but this was not accompanied by MiT/TFE nuclear relocalization. This observation is in contrast to a previous study by Martina et al.³⁰ showing that LY2 triggers a TFEB mobility shift to a fast-migrating form and concomitant cytosol-to-nucleus shuttling in ARPE-19 cells. Importantly, experiments using the MTOR kinase inhibitor Torin1 verified that MTORC1-MiT/TFE regulation is intact in RAW cells. The inability of LY2 to prevent Torin1-mediated MiT/TFE redistribution to the nucleus suggests that their cytosolic retention in LY2-treated cells may still be MTORC1 dependent. This is based on the premise that LY2 impairs the activity of MTORC1 on only a subset of downstream targets, such as RPS6 and EIF4EBP1. Future studies will be required to determine whether MiT/TFE family members are in fact LY2-resistant MTORC1 substrates in RAW cells. Alternatively, MiT/TFE localization may be subject to cell type-specific regulatory mechanisms that act in parallel with MTOR.

We have previously reported that GPNMB is highly induced in RAW cells following exposure to chemical inhibitors of lysosome acidification (e.g., by targeting v-ATPase) and MTORC1, or physiological stressors such as palmitate.³³ Here, we extend these observations by showing that GPNMB is similarly induced in response to HEPES and sucrose. However, it is intriguing to note that although numerous lysosomal-autophagic genes are highly upregulated by LPS, *Gpnmb* was not one of them. This implies that LPS-induced TLR activation drives only a specific subset of the MiT/TFE transcriptional network. In light of this, the data presented here exhibit parallels with the study by Pastore et al.⁴⁶, delineating synergistic roles of TFEB and TFE3 in the regulation of innate host-immune genes in RAW macrophages.⁴⁶ Our RNA-Seq analysis of DMEM^{+H}-grown RAW cells confirmed a global induction of host-immune genes, supporting a functional role for the lysosome as a critical integrator of metabolic-inflammatory cross-talk in macrophages.^{9, 33, 46, 48} Defining how distinct stimuli such as lysosomal stress, starvation/MTORC1 inhibition, or TLR signaling inhibition, induce a tailored MiT/TFE transcriptional program requires further investigation.

By eliciting a MiT/TFE-driven feed-forward loop in lysosomal-autophagic biogenesis, HEPES could potentially affect the outcome of studies in diverse research disciplines. For example, numerous studies have demonstrated that autophagy induction counteracts the deposition of aggregate-prone proteins, such as mutant H (huntingtin), SNCA/ α -synuclein, and the pathological PRNP (prion protein; PRNP^{Sc}).^{54, 55} In fact, HEPES has recently been shown to interfere with the build-up of PRNP^{Sc} in cultured cells.⁵⁶ Similarly, by virtue of its ability to induce endo-lysosomal biogenesis, HEPES may pose a confounding factor in cancer stem cell research by potentiating the WNT signaling pathway.^{18, 57} In addition, as shown here, the impact of HEPES is most penetrant in scavenging cell types such as macrophages, leading to altered host-immune responses and polarization state. Lastly, HEPES supplementation to culture media likely alters the outcome of high-throughput screenings and lysosomal storage disorder diagnostics via boosting the lysosomal machinery. It should however be noted that the confounding effects of HEPES depend on the cell type (e.g., the intrinsic rate of fluid-phase endocytosis) and duration of the incubation period.

In conclusion, our study calls for caution when utilizing zwitterionic buffering agents in culture media. We have shown here that HEPES addition to cell growth media

affects core aspects of the lysosomal-autophagic machinery and inflammatory signaling. Given that the lysosome is at the very center of nutrient-sensing and stress adaptation, this has major implications for studying a wide range of metabolic processes, such as autophagy, immunology, cancer, and neurodegeneration.

Material and Methods

Cell culture and siRNAs

The RAW264.7 cell line (ATCC, TIB-71) was cultured in DMEM (Thermo Fisher Scientific, 31966), DMEM (32430; containing HEPES), RPMI (61870), or RPMI (22409; Dutch modification), supplemented with 10% fetal calf serum (Invitrogen, 10270106) and antibiotics (pen-strep) in a humidified incubator at 37°C and 5% CO₂. Where indicated, culture-grade HEPES (Thermo Fisher Scientific, 15630) was added to DMEM. HEK293T (CRL-3216), HepG2 (HB-8065), 3T3-L1 (CL-173), C2C12 (CRL-1772) and HeLa (CCL-2) cells (all from ATCC) were grown in DMEM (31966) or DMEM (32430); containing HEPES. For buffer comparison, PIPES disodium salt (Sigma, P3768) and MES (Sigma, M3671) were added to DMEM as indicated. For the siRNA experiments, RAW cells were seeded at a density of 3×10^5 cells/ml 3 h prior to transfection. Cells were transfected with 2 siRNA sequences per gene target. The used siRNA sequences were as follows: *Tfeb* (QIAGEN: SI01444394, SI01444408), *Tfe3* (SI01444415, SI05181435), *Mitf* (SI02687692, SI02709637), and control (CTRL) siRNA (SI03650318) at a final concentration of 50 nM according to manufacturer's instructions. Gene expression analysis was performed 48 h post transfection.

Cell viability assays

Cell viability was determined using the WST1 reagent (Sigma, 5015944001) according to the manufacturer's instructions. The absorbance at 450 nm was measured using an ELISA plate reader (Synergy BioTek). The propidium iodide (PI; Thermo Fisher Scientific, P1304MP) exclusion assay was performed as follows: RAW264.7 cells were gently scraped and washed in phosphate-buffered saline (PBS; Gibco, 70011044). A cell suspension ($1 \times 10^6/100 \mu\text{L}$) was incubated with 5 μL PI (10 $\mu\text{g/ml}$) for 2 min prior to flow cytometric analysis (FL2).

Western blot analysis and antibodies

Cell lysates were prepared in RIPA buffer (150 mM NaCl, 50 mM Tris-HCl, pH 7.4, 2 mM EDTA, 10 mM NaF, 1 mM Na₃VO₄, 1 mM PMSF (Sigma, P7626), 0.5% sodiumdeoxycholate 1% Triton X-100 (Sigma, X100), supplemented with protease (Sigma, 11697498001) and phosphatase (Sigma, 4906845001) inhibitors. Lysates were cleared by centrifugation at 4°C for 15 min at 12,000 x *g* and protein concentrations were determined using the BCA method (Thermo Fisher Scientific, 23225). Samples were boiled, separated by SDS-PAGE, and transferred to nitrocellulose. Membranes were saturated with 5% (w:v) bovine serum albumin (Sigma, A1906) in PBS-0.1% Tween-20 (Sigma, P1379) for 2 h at room temperature (RT), and probed overnight at 4°C with the following antibodies: GPNMB (R&D systems, AF2330), LC3B (Cell Signaling Technology, 4108), CTSD (house made), MITF (Exalpha Biologicals Inc, X1405M), TFEB (Bethyl Lab Inc, A303-673A), TUBA (α -tubulin; Cedarlane, CLT9002), LMNB1 (Lamin B; Santa Cruz Biotechnology, SC6216), total RPS6 (Cell Signaling, 2217S), phosphorylated RPS6 (Cell Signaling Technology, 4856S), total EIF4EBP (Cell Signaling Technology, 69445S), and phosphorylated EIF4EBP (Cell Signaling Technology, 94595). For detection, membranes were exposed to matching IRdye-conjugated antibodies (Westburg BV, 926-23313/-32214/-32210/-32211) and analyzed with the Odyssey V3.0 Infrared Imaging System (LI-COR Biosciences).

Immunofluorescence

RAW264.7 cells were cultured on glass coverslips in the presence of HEPES (25 mM), sucrose (80 mM, Sigma, S7903), or Torin1 (400 nM, Tocris, 4247) for 6 h. Cells were fixed in ice-cold methanol (Biosolve, 13680502) for 10 min at -20°C. Cells were then stained with primary abs for TFEB, MITF or TFE3, and detected with Alexa Fluor 488 targeting mouse or rabbit IgG (Invitrogen, A2102 and A21206 resp.). Representative images were captured with a Confocal SP5 LEICA (Leica Microsystem, USA) with a 63x objective, using an excitation wavelength of 488 nm. For LAMP1 staining, cells were fixed in 4% (w:v) paraformaldehyde in PBS (pH 7.4), for 30 min at RT. Primary antibodies against LAMP1 (Abcam, ab24170) were detected with Alexa Fluor 647 and visualized using an EVOS microscope (Thermo Fisher Scientific). To monitor fluid-phase endocytosis, RAW cells were cultured in serum-free DMEM for 4 h followed by LY294002 (50 μ M; Sigma, L9908) treatment for 30 min. Thereafter, FITC-labeled dextran (Sigma, 46944) was added to the culture media (1 mg/ml) for a final 30 min. Cells were rinsed in ice-cold PBS and monitored using the EVOS microscope.

Real-time PCR

Total RNA was isolated using the NucleoSpin II extraction kit (Macherey Nagel, 740955-250). Equal amounts of total RNA were used to synthesize cDNA according to the manufacturer's method (Invitrogen, 18091200). Analysis of gene expression was performed with the iCycler MyiQTM system (Bio-Rad) with initial denaturation at 95°C for 10 min, followed by 40 PCR cycles, each consisting of 95°C for 15 sec, 60°C for 1 min, and 72°C for 1 min. mRNA expression was calculated using the $\Delta\Delta$ Ct method, relative to *Rplp0*. Oligonucleotide sequences are available upon request.

RNA-seq analysis

RAW cells were cultured in DMEM in the presence of either HEPES (25 mM), IL4 (50 ng/ml; R&D systems, 404-ML-010), and LPS (50 ng/ml; Salmonella Minnesota R595; Enzo Life Sciences), for 24 h. RNA was isolated with the NucleoSpin II extraction kit, and was submitted for sequencing at the Genomics Core Facility at the Icahn Institute and Department of Genetics (<http://icahn.mssm.edu/research/genomics/core-facility>). cDNA libraries were prepared with the Illumina Ribo-Zero Gold rRNA (MRZG126) removal kit. Samples were run on Illumina HiSeq 2000 at a read-length of 100 nucleotides single end, and at a sequencing depth of ~50 million reads per sample. Raw and processed data were returned and count files were generated by aligning to mouse genome mm10 (GRCm38.75) with STAR.⁵⁸ Counting overlaps with exons were grouped at the gene level with featureCounts.⁵⁹ A differential expression study was conducted with R package limma (Voom transformation).⁶⁰ Low count genes were removed in the limma analysis, genes were kept if they had at least 1 count per million in at least 3 samples. The cut-off value for differential expression was chosen at an adjusted p-value (Benjamini-Hochberg) of <0.05 unless otherwise stated.

In silico analysis

GSEA was performed using a desktop software application (v2.2.2)⁶¹ on a pre-ranked list of differentially expressed genes (based on the log-fold change of HEPES vs.

DMEM Ctrl incubations) using custom gene sets for lysosomal-autophagic and host-immune response genes carrying either validated CLEAR-consensus elements^{12, 15} or E-box consensus motifs.⁴⁶ Additional options selected included 1000 permutations and a weighted enrichment statistic. The Rank-rank hypergeometric overlap test was performed using software implemented on <http://systems.crupp.ucla.edu/rankrank/rankranksimple.php>.⁶² From each set of treatments—HEPES, LPS, IL4—a pre-ranked list of genes was generated based on the log fold change differences in gene expression between the treated and nontreated condition. The following parameters were selected: step size of 100; Bejamini-Yekutieli p-value correction; and rank and metric scatter plot generation. Pathway enrichment analysis on differentially expressed genes was performed using ClueGo (v2.1.7) and CluePedia (v1.1.7) plug-ins in Cytoscape (v3.1.0) with the KEGG pathway database (10.04.2016 download).^{63, 64, 65} The pathways with a Benjamin-Hochberg corrected p-value <0.005 are shown. The heatmap was generated using heatmap.2 function in gplots R package (<http://CRAN.R-project.org/package=gplots>).

Secretome analysis

RAW264.7 cells were cultured in 25mM HEPES containing DMEM or in DMEM alone for 48h. Secreted cytokine levels blotted and analyzed using a Mouse Cytokine Array Panel A Kit (R&D Systems, ARY006) using manufacturer's instructions.

Analysis of lysosomal parameters

RAW cells were rinsed 3 times and gently scraped in PBS. Following centrifugation and cell counting, equal cell suspensions were stained with 50 nM LysoTracker Green DND-26 (Thermo Fisher Scientific, L7526) for 10 min or exposed to 50 µg/ml DQTM Green BSA (Thermo Fisher Scientific, D12050) for 3 h at 37°C, washed in PBS, and analyzed by flow cytometry (FACS Calibur, BD Biosciences) to evaluate lysosomal mass and proteolytic activity. Lysosomal acidification was assayed using 1 µM LysoSensorTM Green DND-189 (Thermo Fisher Scientific, L7535) for 30 min at 37°C, and lysosomal pH was assayed with LysoSensorTM Yellow/Blue DND-160 (Thermo Fisher Scientific, L7545) at 37°C for 1 h. RAW cells were analyzed directly or equilibrated in MES buffer (25 mM MES, 5 mM NaCl, 115 mM KCl, 1.2 mM MgSO₄) supplemented with monensin (10 µM; Sigma, M5273) and nigericin (10 µM; Sigma, N7142); pH ranging from 4.0-6.0. Excitation and emission spectra (329 and 440; 384 and 540) were determined in a Perkin-Elmer LS55 spectrometer. The yellow:blue ratio emission was plotted against the pH calibration curve and pH values were calculated.

Lysosomal enzymatic activity

For GBA1-related glucosidase activity, 4-methylumbelliferyl (4-MU)-β-D-glucopyranoside (Sigma, M3633) was utilized as an artificial substrate at 37°C, in 150 mM citric acid-Na₂HPO₄ (pH 5.2) buffer supplemented with 0.2% sodium taurocholate (Sigma, T0557), 0.1% Triton X-100 and 0.1% BSA. The enzymatic reaction was stopped with NaOH-glycine (pH 10.6) and fluorescence of liberated 4-MU was determined with a fluorometer LS55 (Perkin Elmer) using λ_{ex} 366 nm and λ_{em} 445 nm.

Activity-based probe analysis

ABP-MDW941/Inhibody Red³⁴ was used (1 nM for 16 h; synthesized in reference³⁴) to

label active endogenous GBA₁ molecules in RAW cells. Images were taken with a confocal SP5 Leica with a 63x objective using an excitation wavelength of 561 nm. For cysteine cathepsin labeling, ABP DCG-04³⁵ was added (500 nM for 2 h; synthesized in reference ³⁵) to cells. After rinsing in PBS, cell homogenates were prepared in KPi lysis buffer (25mM K₂HPO₄/KH₂PO₄ pH6.5, 0.1%(v/v) Triton X-100) supplemented with protease inhibitors. After protein separation with SDS-PAGE (10%), fluorescence was subsequently monitored in wet slab gels with a Typhoon Variable Mode Imager (Amersham Biosciences) using λ_{ex} 488 nm and λ_{em} 520 nm (bandpass 40).

GPNMB ELISA

Secreted GPNMB levels in culture media were determined using a mouse GPNMB ELISA according to the instructions of the manufacturer (R&D systems, DY2330).

Transmission electron microscopy

RAW cells were maintained as described and fixed at RT by addition of Karnovsky fixative (2.5% glutaraldehyde, 2% formaldehyde solution in 0.2 M cacodylate buffer, pH 7.4) 1:1 to growth media for 10 min. This was replaced by fresh fixative for 2 h at RT. Thereafter, cells were post-fixed with 1% OsO₄, 1.5% K₃Fe(III)(CN)₆ in 0.1 M cacodylate buffer, for 2 h at RT. Cells were then dehydrated and embedded in Epon epoxy resin (Polysciences, 02334-500). Ultrathin sections of 60 nm were contrasted with uranyl acetate and lead citrate using the AC20 (Leica) and studied with a Jeol 1010 electron microscope (Jeol Europe).

Statistics

Values are presented as mean \pm SEM. Statistical significance was analyzed with a two-tailed unpaired Student's *t*-test. Criterion for statistical significance was set on $P < 0.05$, unless stated otherwise.

References

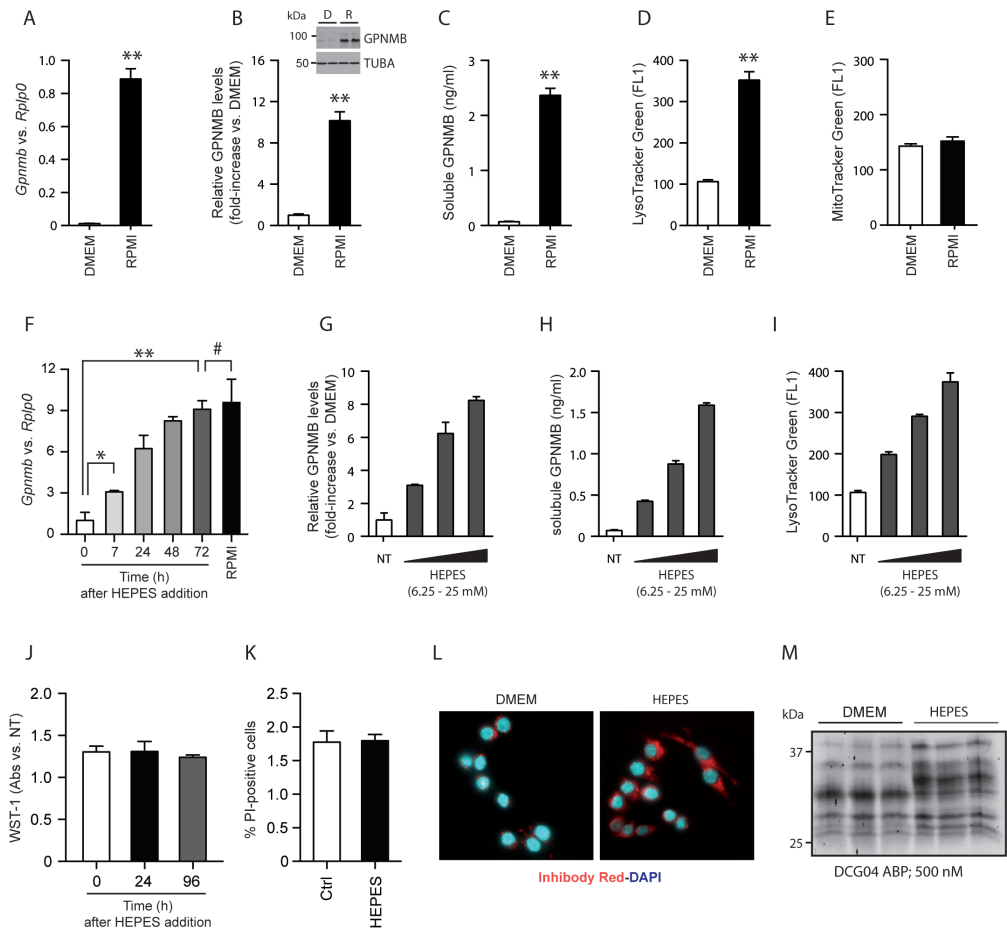
1. De Duve C, Pressman BC, Gianetto R, Wattiaux R, Appelmanns F. Tissue fractionation studies. 6. Intracellular distribution patterns of enzymes in rat-liver tissue. *Biochem J*. 60(4):604-17 (1955).
2. Settembre C, Fraldi A, Medina DL, Ballabio A. Signals from the lysosome: a control centre for cellular clearance and energy metabolism. *Nat Rev Mol Cell Biol*. 14(5):283-96 (2013).
3. Bar-Peled L, Sabatini DM. Regulation of mTORC1 by amino acids. *Trends Cell Biol*. 24(7):400-6 (2014).
4. Meijer AJ, Codogno P. Autophagy: regulation and role in disease. *Crit Rev Clin Lab Sci*. 46(4):210-40 (2009).
5. Aerts JM, Hollak C, Boot R, Groener A. Biochemistry of glycosphingolipid storage disorders: implications for therapeutic intervention. *Philos Trans R Soc Lond B Biol Sci*. 358(1433):905-14 (2003).
6. Platt FM. Sphingolipid lysosomal storage disorders. *Nature*. 510(7503):68-75 (2014).
7. Parenti G, Andria G, Ballabio A. Lysosomal storage diseases: from pathophysiology to therapy. *Annu Rev Med*. 66:471-86 (2015).
8. Folick A, Oakley HD, Yu Y, Armstrong EH, Kumari M, Sanor L, Moore DD, Ortlund EA, Zechner R, Wang MC. Aging. Lysosomal signaling molecules regulate longevity in *Caenorhabditis elegans*. *Science*. 347(6217):83-6 (2015).
9. Xu X, Grijalva A, Skowronski A, van Eijk M, Serlie MJ, Ferrante AW, Jr. Obesity activates a program of lysosomal-dependent lipid metabolism in adipose tissue macrophages independently of classic activation. *Cell Metab*. 18(6):816-30 (2013).
10. Bieghs V, Walenbergh SM, Hendriks T, van Gorp PJ, Verheyen F, Olde Damink SW, Masclee AA, Koek GH, Hofker MH, Binder CJ, et al. Trapping of oxidized LDL in lysosomes of Kupffer cells is a trigger for hepatic inflammation. *Liver Int*. 33(7):1056-61 (2013).
11. Perera RM, Stoykova S, Nicolay BN, Ross KN, Fitamant J, Boukhali M, Lengrand J, Deshpande V, Selig MK, Ferrone CR, et al. Transcriptional control of autophagy-lysosome function drives pancreatic cancer metabolism. *Nature*. 524(7565):361-5 (2015).
12. Sardiello M, Palmieri M, di Ronza A, Medina DL, Valenza M, Gennarino VA, Di Malta C, Donaudo F, Embrione V, Polishchuk RS, et al. A gene network regulating lysosomal biogenesis and function. *Science*. 325(5939):473-7 (2009).
13. Steingrimsson E, Copeland NG, Jenkins NA. Melanocytes and the microphthalmia transcription factor network. *Annu Rev Genet*. 38:365-411 (2004).
14. Settembre C, Di Malta C, Polito VA, Garcia Arencibia M, Vetrini F, Erdin S, Erdin SU, Huynh T, Medina D, Colella P, et al. TFEB links autophagy to lysosomal biogenesis. *Science*. 332(6036):1429-33 (2011).
15. Palmieri M, Impey S, Kang H, di Ronza A, Pelz C, Sardiello M, Ballabio A. Characterization of the CLEAR network reveals an integrated control of cellular clearance pathways. *Hum Mol Genet*. 20(19):3852-66 (2011).
16. Martina JA, Diab HI, Lishu L, Jeong AL, Patange S, Raben N, Puertollano R. The nutrient-responsive transcription factor TFE3 promotes autophagy, lysosomal biogenesis, and clearance of cellular debris. *Sci Signal*. 7(309):ra9 (2014).
17. Aksan I, Goding CR. Targeting the microphthalmia basic helix-loop-helix-leucine zipper transcription factor to a subset of E-box elements in vitro and in vivo. *Mol Cell Biol*. 18(12):6930-8 (1998).
18. Ploper D, Taelman VF, Robert L, Perez BS, Titz B, Chen HW, Graeber TG, von Eeuw E, Ribas A, De Robertis EM. MITF drives endolysosomal biogenesis and potentiates Wnt

- signaling in melanoma cells. *Proc Natl Acad Sci U S A*. 112(5):E420-9 (2015).
19. Sancak Y, Peterson TR, Shaul YD, Lindquist RA, Thoreen CC, Bar-Peled L, Sabatini DM. The Rag GTPases bind raptor and mediate amino acid signaling to mTORC1. *Science*. 320(5882):1496-501 (2008).
20. Sancak Y, Bar-Peled L, Zoncu R, Markhard AL, Nada S, Sabatini DM. Ragulator-Rag complex targets mTORC1 to the lysosomal surface and is necessary for its activation by amino acids. *Cell*. 141(2):290-303 (2010).
21. Zoncu R, Bar-Peled L, Efeyan A, Wang S, Sancak Y, Sabatini DM. mTORC1 senses lysosomal amino acids through an inside-out mechanism that requires the vacuolar H(+)-ATPase. *Science*. 334(6056):678-83 (2011).
22. Bar-Peled L, Schweitzer LD, Zoncu R, Sabatini DM. Ragulator is a GEF for the rag GTPases that signal amino acid levels to mTORC1. *Cell*. 150(6):1196-208 (2012).
23. Sarbassov DD, Ali SM, Sabatini DM. Growing roles for the mTOR pathway. *Curr Opin Cell Biol*. 17(6):596-603 (2005).
24. Wullschlegel S, Loewith R, Hall MN. TOR signaling in growth and metabolism. *Cell*. 124(3):471-484 (2006).
25. Laplante M, Sabatini DM. mTOR signaling in growth control and disease. *Cell*. 149(2):274-93 (2012).
26. Ganley IG, Lam du H, Wang J, Ding X, Chen S, Jiang X. ULK1-ATG13-FIP200 complex mediates mTOR signaling and is essential for autophagy. *J Biol Chem*. 284(18):12297-305 (2009).
27. Hosokawa N, Hara T, Kaizuka T, Kishi C, Takamura A, Miura Y, Iemura S, Natsume T, Takehana K, Yamada N, et al. Nutrient-dependent mTORC1 association with the ULK1-Atg13-FIP200 complex required for autophagy. *Mol Biol Cell*. 20(7):1981-91 (2009).
28. Jung CH, Jun CB, Ro SH, Kim YM, Otto NM, Cao J, Kundu M, Kim DH. ULK-Atg13-FIP200 complexes mediate mTOR signaling to the autophagy machinery. *Mol Biol Cell*. 20(7):1992-2003 (2009).
29. Settembre C, Zoncu R, Medina DL, Vetrini F, Erdin S, Erdin S, Huynh T, Ferron M, Karsenty G, Vellard MC, et al. A lysosome-to-nucleus signalling mechanism senses and regulates the lysosome via mTOR and TFEB. *EMBO J*. 31(5):1095-108 (2012).
30. Martina JA, Chen Y, Gucek M, Puertollano R. mTORC1 functions as a transcriptional regulator of autophagy by preventing nuclear transport of TFEB. *Autophagy*. 8(6):903-14 (2012).
31. Rocznik-Ferguson A, Petit CS, Froehlich F, Qian S, Ky J, Angarola B, Walther TC, Ferguson SM. The transcription factor TFEB links mTORC1 signaling to transcriptional control of lysosome homeostasis. *Sci Signal*. 5(228):ra42 (2012).
32. Martina JA, Puertollano R. Rag GTPases mediate amino acid-dependent recruitment of TFEB and MITF to lysosomes. *J Cell Biol*. 200(4):475-91 (2013).
33. Gabriel TL, Tol MJ, Ottenhof R, van Roomen C, Aten J, Claessen N, Hooibrink B, de Weijer B, Serlie MJ, Argmann C, et al. Lysosomal stress in obese adipose tissue macrophages contributes to MITF-dependent Gpnmb induction. *Diabetes*. 63(10):3310-23 (2014).
34. Witte MD, Kallemeyn WW, Aten J, Li KY, Strijland A, Donker-Koopman WE, van den Nieuwendijk AM, Bleijlevens B, Kramer G, Florea BI, et al. Ultrasensitive in situ visualization of active glucocerebrosidase molecules. *Nat Chem Biol*. 6(12):907-13 (2010).
35. Lennon-Dumenil AM, Bakker AH, Maehr R, Fiebigler E, Overkleeft HS, Roseblatt M, Ploegh HL, Lagaudriere-Gesbert C. Analysis of protease activity in live antigen-presenting cells shows regulation of the phagosomal proteolytic contents during dendritic cell activation. *J Exp Med*. 196(4):529-40 (2002).
36. Voss EW, Jr., Workman CJ, Mummert ME. Detection of protease activity using a

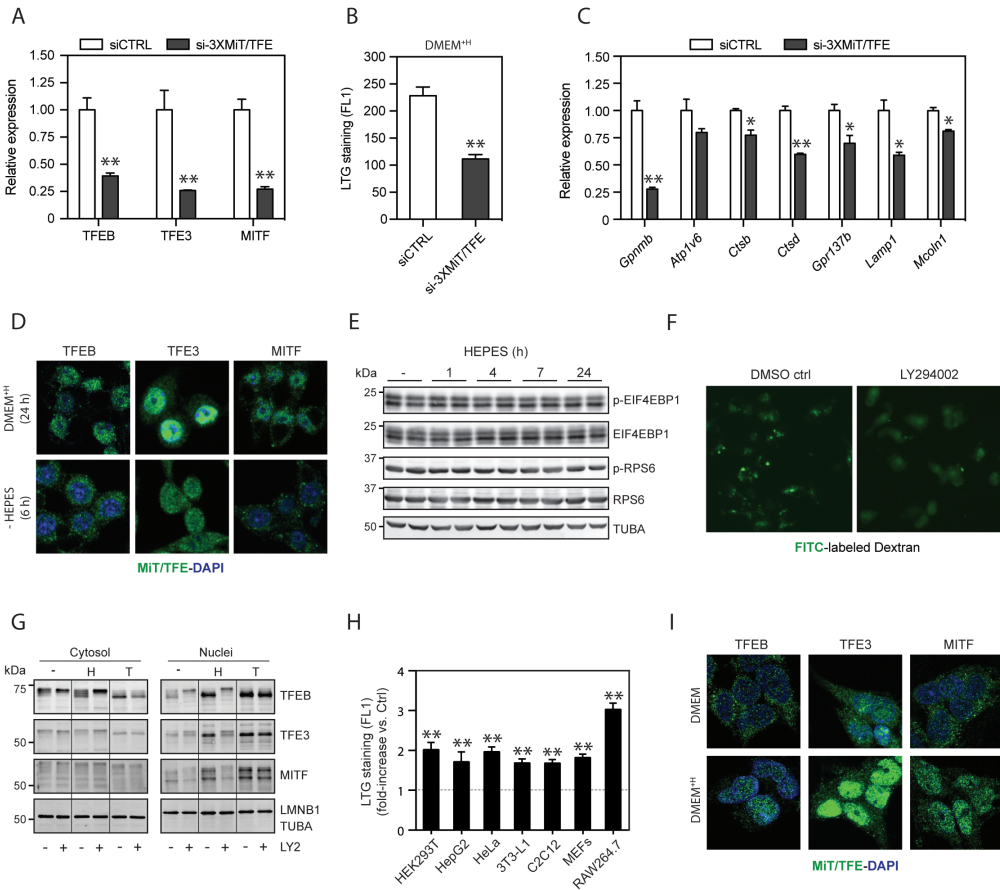
- fluorescence-enhancement globular substrate. *Biotechniques*. 20(2):286-91 (1996).
37. Klionsky DJ, Abdelmohsen K, Abe A, Abedin MJ, Abeliovich H, Acevedo Arozena A, Adachi H, Adams CM, Adams PD, Adeli K, et al. Guidelines for the use and interpretation of assays for monitoring autophagy (3rd edition). *Autophagy*. 12(1):1-222 (2016).
38. Cohn ZA, Ehrenreich BA. The uptake, storage, and intracellular hydrolysis of carbohydrates by macrophages. *J Exp Med*. 129(1):201-25 (1969).
39. Karageorgos LE, Isaac EL, Brooks DA, Ravenscroft EM, Davey R, Hopwood JJ, Meikle PJ. Lysosomal biogenesis in lysosomal storage disorders. *Exp Cell Res*. 234(1):85-97 (1997).
40. Helip-Wooley A, Thoene JG. Sucrose-induced vacuolation results in increased expression of cholesterol biosynthesis and lysosomal genes. *Exp Cell Res*. 292(1):89-100 (2004).
41. Araki N, Johnson MT, Swanson JA. A role for phosphoinositide 3-kinase in the completion of macropinocytosis and phagocytosis by macrophages. *J Cell Biol*. 135(5):1249-60 (1996).
42. Gekle M, Drumm K, Mildenerberger S, Freudinger R, Gassner B, Silbernagl S. Inhibition of Na⁺-H⁺ exchange impairs receptor-mediated albumin endocytosis in renal proximal tubule-derived epithelial cells from opossum. *J Physiol*. 520 Pt 3:709-21 (1999).
43. Diwu Z, Chen CS, Zhang C, Klaubert DH, Haugland RP. A novel acidotropic pH indicator and its potential application in labeling acidic organelles of live cells. *Chem Biol*. 6(7):411-8 (1999).
44. Amyere M, Payraastre B, Krause U, Van Der Smissen P, Veithen A, Courtoy PJ. Constitutive macropinocytosis in oncogene-transformed fibroblasts depends on sequential permanent activation of phosphoinositide 3-kinase and phospholipase C. *Mol Biol Cell*. 11(10):3453-67 (2000).
45. Canton J, Schlam D, Breuer C, Gutschow M, Glogauer M, Grinstein S. Calcium-sensing receptors signal constitutive macropinocytosis and facilitate the uptake of NOD2 ligands in macrophages. *Nat Commun*. 7:11284 (2016).
46. Pastore N, Brady OA, Diab HI, Martina JA, Sun L, Huynh T, Lim JA, Zare H, Raben N, Ballabio A, et al. TFEB and TFE3 Cooperate in the Regulation of the Innate Immune Response in Activated Macrophages. *Autophagy*. 12:0 (2016).
47. Huan C, Kelly ML, Steele R, Shapira I, Gottesman SR, Roman CA. Transcription factors TFE3 and TFEB are critical for CD40 ligand expression and thymus-dependent humoral immunity. *Nat Immunol*. 7(10):1082-91 (2006).
48. Visvikis O, Ihuegbu N, Labe SA, Luhachack LG, Alves AM, Wollenberg AC, Stuart LM, Stormo GD, Irazoqui JE. Innate host defense requires TFEB-mediated transcription of cytoprotective and antimicrobial genes. *Immunity*. 40(6):896-909 (2014).
49. Brignull LM, Czimmerer Z, Saidi H, Daniel B, Villela I, Bartlett NW, Johnston SL, Meira LB, Nagy L, Nohturfft A. Reprogramming of lysosomal gene expression by interleukin-4 and Stat6. *BMC Genomics*. 14:853 (2013).
50. Ferguson WJ, Braunschweiler KI, Braunschweiler WR, Smith JR, McCormick JJ, Wasmann CC, Jarvis NP, Bell DH, Good NE. Hydrogen ion buffers for biological research. *Anal Biochem*. 104(2):300-10 (1980).
51. Poole CA, Reilly HC, Flint MH. The adverse effects of HEPES, TES, and BES zwitterion buffers on the ultrastructure of cultured chick embryo epiphyseal chondrocytes. *In Vitro*. 18(9):755-65 (1982).
52. Medina DL, Di Paola S, Peluso I, Armani A, De Stefani D, Venditti R, Montefusco S, Scotto-Rosato A, Prezioso C, Forrester A, et al. Lysosomal calcium signalling regulates autophagy through calcineurin and TFEB. *Nat Cell Biol*. 17(3):288-99 (2015).
53. Li Y, Xu M, Ding X, Yan C, Song Z, Chen L, Huang X, Wang X, Jian Y, Tang G, et al.

- Protein kinase C controls lysosome biogenesis independently of mTORC1. *Nat Cell Biol.* 18(10):1065-77 (2016).
54. Sarkar S, Davies JE, Huang Z, Tunnacliffe A, Rubinsztein DC. Trehalose, a novel mTOR-independent autophagy enhancer, accelerates the clearance of mutant huntingtin and alpha-synuclein. *J Biol Chem.* 282(8):5641-52 (2007).
55. Aguib Y, Heiseke A, Gilch S, Riemer C, Baier M, Schatzl HM, Ertmer A. Autophagy induction by trehalose counteracts cellular prion infection. *Autophagy.* 5(3):361-9 (2009).
56. Delmouly K, Belondrade M, Casanova D, Milhavel O, Lehmann S. HEPES inhibits the conversion of prion protein in cell culture. *J Gen Virol.* 92(Pt 5):1244-50 (2011).
57. Dobrowolski R, Vick P, Ploper D, Gumper I, Snitkin H, Sabatini DD, De Robertis EM. Presenilin deficiency or lysosomal inhibition enhances Wnt signaling through relocalization of GSK3 to the late-endosomal compartment. *Cell Rep.* 2(5):1316-28 (2012).
58. Dobin A, Davis CA, Schlesinger F, Drenkow J, Zaleski C, Jha S, Batut P, Chaisson M, Gingeras TR. STAR: ultrafast universal RNA-seq aligner. *Bioinformatics.* 29(1):15-21 (2013).
59. Liao Y, Smyth GK, Shi W. featureCounts: an efficient general purpose program for assigning sequence reads to genomic features. *Bioinformatics.* 30(7):923-30 (2014).
60. Smyth GK. Linear models and empirical bayes methods for assessing differential expression in microarray experiments. *Stat Appl Genet Mol Biol.* 3:Article3 (2004).
61. Subramanian A, Kuehn H, Gould J, Tamayo P, Mesirov JP. GSEA-P: a desktop application for Gene Set Enrichment Analysis. *Bioinformatics.* 23(23):3251-3 (2007).
62. Plaisier SB, Taschereau R, Wong JA, Graeber TG. Rank-rank hypergeometric overlap: identification of statistically significant overlap between gene-expression signatures. *Nucleic Acids Res.* 38(17):e169 (2010).
63. Bindea G, Mlecnik B, Hackl H, Charoentong P, Tosolini M, Kirilovsky A, Fridman WH, Pages F, Trajanoski Z, Galon J. ClueGO: a Cytoscape plug-in to decipher functionally grouped gene ontology and pathway annotation networks. *Bioinformatics.* 25(8):1091-3 (2009).
64. Bindea G, Galon J, Mlecnik B. CluePedia Cytoscape plugin: pathway insights using integrated experimental and in silico data. *Bioinformatics.* 29(5):661-3 (2013).
65. Shannon P, Markiel A, Ozier O, Baliga NS, Wang JT, Ramage D, Amin N, Schwikowski B, Ideker T. Cytoscape: a software environment for integrated models of biomolecular interaction networks. *Genome Res.* 13(11):2498-504 (2003).

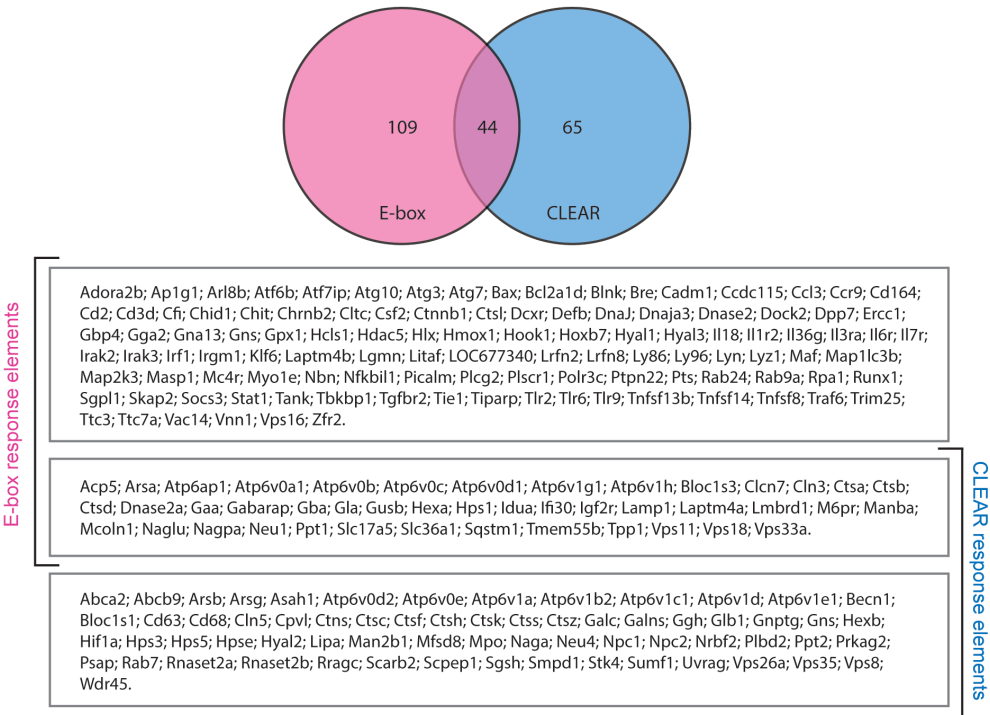
Supplemental figures



Supplemental figure 1. Identification of a HEPES-mediated lysosomal stress signature in cultured cells. (A-D) RAW cells were grown in DMEM (31966) and RPMI (22409; containing HEPES). (A) RT-PCR analysis of *Gpnmb* mRNA levels, normalized to *Rplp0*. (B) Western blot analysis and quantification of GPNMB protein levels, normalized to TUBA. (C) Secreted (s)GPNMB levels were probed by ELISA. (D) Flow cytometric analysis of LTG and (E) MTG staining (FL1). (F) Time-course analysis of *Gpnmb* mRNA levels in RAW cells cultured in DMEM supplemented with HEPES (25 mM) for 6-72 h, and normalized to *Rplp0*. RPMI-grown cells served as a positive control. (G-I) RAW cells were grown in DMEM supplemented with HEPES (6.25-25 mM) for 24 h. (G) Intracellular and (H) sGPNMB levels were quantified by immunoblotting and ELISA, respectively. (I) Lysosomal number was evaluated by flow cytometric analysis of LTG-stained RAW cells (FL1). (J-K) Cell viability was determined in DMEM or DMEM⁺ using (J) WST-1 and (K) propidium iodide (PI) exclusion assays, respectively. (L) Visualization of active GBA1 molecules using the activity-based probe MDW941/Inhibitory Red. RAW cells were grown in either DMEM or DMEM⁺ for 40 h, and incubated with Inhibitory Red (1 nM) for the last 16 h. (M) Western blot analysis of active lysosomal cysteine cathepsins in cells grown in either DMEM or DMEM⁺ for 24 h, and incubated with the ABP DCG04 (500 nM) for the last 2 h. Values are expressed as mean \pm SEM, $n=3-4$ in A-M. * $P < 0.05$, ** $P < 0.01$.



Supplemental figure 2. HEPES induces a MiT/TFE-mediated lysosomal stress pathway in cultured cells. (A-C) DMEM^H-grown RAW cells were exposed to either scrambled siRNA ctrl (siCTRL) or siRNA cocktail targeting MiT/TFE genes (si-3XMiT/TFE). (A) RT-PCR analysis of *Tfeb*, *Tfe3*, and *Mitf* mRNA levels, normalized to *Rplpo*. (B) Flow cytometric analysis of LTG-stained RAW cells (FL1). (C) RT-PCR analysis of various MiT/TFE-regulated lysosomal target genes, normalized to *Rplpo*. (D) RAW cells were grown in DMEM^H for 24 h (top) and subsequently deprived of HEPES for 6 h (bottom). RAW cells were stained for TFE3, TFE3, or MITF levels (in green) and counterstained with DAPI (in blue). (E) Western blot analysis on protein extracts isolated from RAW cells grown in the presence of HEPES for the indicated times. Membranes were probed with antibodies against p-EIF4EBP1 (Thr37/46) and p-RPS6 (Ser235/236) to evaluate MTORC1 activity. (F) Representative images of RAW cells pre-treated with LY2 for 30 min, followed by addition of FITC-labeled dextran for another 30 min. (G) LY2 does not inhibit Torin1-mediated MiT/TFE nuclear import. Western blot analysis on the cytosolic and nuclear fractions derived from RAW cells pretreated with LY2 (50 μM) for 30 min, and with the MTOR catalytic site inhibitor Torin1 (400 nM) for another 6 h. Membranes were probed with antibodies against MiT/TFE family members. TUBA and LMNB1 were used as internal controls for cytosolic and nuclear fractions, respectively. (H) LTG staining in a panel of broadly used cancerous and fibroblastic cell lines adapted to grow in DMEM (31966) or DMEM (32430; containing HEPES), and analyzed by flow cytometry. (I) Immunolocalization analysis of endogenous TFE3, TFE3, or MITF in HEK293T cells grown in DMEM or DMEM^H for 24 h. Values are expressed as mean ± SEM, n=3-4 in A-H. *P < 0.05, **P < 0.01.



Supplemental figure 3. Datasets used for the GSEA of lysosomal-autophagic and innate host-immune genes in DMEM^H-grown RAW cells. Venn diagram representation and a gene list containing CLEAR and/or E-box response elements within their promoters (see also **Figure 3C-D**).

Chapter 2

Glucocerebrosidase in cultured cells: extreme sensitivity for medium conditions

Contributing authors:

M.J.C. van der Lienden, J. Aten, R. Boot, M. van Eijk, J.M.F.G. Aerts & C.-L. Kuo. *To be submitted.*

Abstract

Glucocerebrosidase (GCase) is the lysosomal acid β -glucosidase encoded by the GBA gene that degrades the ubiquitous glycosphingolipid glucosylceramide. Inherited GCase deficiency causes the lysosomal storage disorder Gaucher disease. In addition, carriers of an abnormal GBA allele are markedly increased at risk for Parkinson's disease. Newly formed GCase is known to undergo extensive modifications in its four N-glycans en route to and inside the lysosome. These glycan modifications are reflected in changes in apparent molecular weight (MW) of GCase as detected with SDS-PAGE. Fluorescent activity-based probes (ABPs) have been generated that covalently label GCase in reaction-based manner in vivo and in vitro and thus allow sensitive visualization of GCase molecules. Using these ABPs, we studied the life cycle of GCase in cultured fibroblasts and macrophage-like RAW264.7 cells. Specific attention was paid to the impact of the medium. We here report that the pH of culture medium, buffered with compounds such as HEPES, markedly influences processing of GCase and the total cellular enzyme level. The implications of our findings for diagnosis of GD based on measurement of cellular enzyme activity in lysates of cultured cells are described and discussed.

Introduction

Glucocerebrosidase (GCase) is the lysosomal acid β -glucosidase that degrades glucosylceramide (GlcCer). Inherited defects in the *GBA* gene encoding GCase cause the lysosomal storage disorder Gaucher disease (GD).^{1,2} More recently, mutations in *GBA* have been shown to pose a marked risk factor for developing Parkinson's disease and Lewy-body dementia, even upon haploinsufficiency.^{3,4} A hallmark of GD is lysosomal accumulation of GlcCer in tissue macrophages.^{5,6} The lipid-laden macrophages (Gaucher cells) are viable cells and are thought to contribute to the characteristic visceral GD symptoms such as hepatosplenomegaly, thrombocytopenia and anemia.^{2,5} Most GD patients do not develop prominent complications in the central nervous system and are designated as type 1. More severe GD cases (type 2 and 3) may develop lethal neurological symptoms and skin abnormalities.¹ With respect to the non-neuronopathic type 1 GD, two types of therapy are currently available: enzyme replacement therapy (ERT), by means of a macrophage-targeted recombinant enzyme, and substrate reduction therapy (SRT), which utilizes inhibitors of GlcCer biosynthesis.⁷⁻¹² Both approaches lead to impressive corrections in organomegaly and pancytopenia, which is preceded by corrections in plasma biomarkers of Gaucher disease.¹³ The value of alternative therapy for GD is currently being studied, with a focus on gene therapy and a chaperone/activator mediated approach to augment mutant enzyme in patients.^{12,14-16}

The availability of effective therapies has boosted the interest in laboratory diagnosis of GD, including (newborn) screening programs.^{17,18} Nowadays, the first step in diagnosis is detection of abnormalities in the *GBA* gene by genome sequencing. Demonstration of impaired GCase activity is subsequently performed by enzyme activity measurement, often by use of the fluorescent substrate 4-methylumbelliferyl- β -glucoside (4MU- β -Glc).^{2,13} For this purpose, dried blood spots, white blood cells and fibroblasts are all used, depending on the laboratory. Specific inhibitors may help to discriminate GCase and that of other β -glucosidases (*GBA2* and *GBA3*) with respect to their contribution to the total activity.¹³ Unfortunately, neither genotyping nor the measurement of residual GCase activity in cell lysates accurately predicts onset and progression of GD in individual patients.¹⁹ Although heteroallelic presence of N370S *GBA* in GD patients is always associated with a non-neuropathic pathology, the disease course may vary markedly in severity, even among siblings.^{19,20} Moreover, monozygotic GD twins with different disease severity have been documented.^{21,22} It has been speculated that modifier genes and toxic secondary metabolites contribute to the variability in outcome of GCase abnormalities.¹² Onset of GD disease can be sensitively detected by demonstration of elevated Gaucher cell marker proteins in plasma, like chitotriosidase, CCL18 and GPNMB as well as the lipid glucosylsphingosine.²³⁻²⁵ However, accurate assessment of true residual GCase activity would greatly improve diagnosis and monitoring of GD. Novel cell permeable fluorogenic substrates for *in situ* measurement of GCase activity in cultured cells have recently been developed.^{26,27} Other recent tools to detect active GCase molecules *in situ* are fluorescent cyclophellitol-based activity bases probes (ABPs).^{28,29} These cell permeable cyclophellitol analogues act as suicide inhibitors that selectively react with GCase by covalent and irreversible binding to its catalytic nucleophile, E340. ABP-labeled GCase molecules can be visualized by microscopy and gel electrophoresis.^{28,29} These novel tools allow in depth study of GCase and of factors that could impact on its function.

GCase is synthesized as 497 aa polypeptide containing 4 N-linked glycans.² The initially formed enzyme has a molecular weight of 62kDa that subsequently increases to 66-69 kDa by modification of its glycans to sialylated complex type structures.³⁰ Inside the lysosomes, the local action of neuraminidase, β -galactosidase and β -hexosaminidase cause stepwise reduction to the 58 kDa ('mature') isoform (see also Figure 1C).³¹ Although the precise composition of the N-glycans does not impact catalytic activity, N-glycans are essential for correct folding of newly synthesized enzyme molecules in the endoplasmic reticulum.² Unlike most other lysosomal hydrolases, GCase in fibroblasts does not acquire mannose-6-phosphate moieties but is transported to lysosomes via binding to LIMP-2 (lysosomal integral membrane protein-2).³²⁻³⁴ The GCase/LIMP-2 complex is sorted to lysosomes and dissociates upon low luminal pH.³⁵ Early pulse-chase experiments in fibroblasts showed that [³⁵S]methionine-labeled GCase requires considerable time (several hours) to reach mature lysosomes, where it is degraded by leupeptin-sensitive proteases.³⁶ GCase is already folded into its active conformation in the ER, as can be detected with fluorogenic substrate and ABP labeling. Therefore, the measured GCase activity in cell lysates does not necessarily reflect actual enzyme capacity in lysosomes.

Recently, we reported how medium conditions impact on lysosomes by using HEPES to buffer the pH of the culture medium.³⁷ By exploiting the GCase-specific ABPs, we demonstrate that GCase is particularly influenced by medium conditions. The presence of HEPES in the culture medium impaired maturation and reduced proteolytic turnover of GCase in abnormal lysosomes. This eventually resulted in an increase in overall cellular enzyme levels. The implications for diagnosis of GD based on measurement of cellular enzyme activity in lysates of cultured cells are described and discussed.

Results

Impact of medium pH on cellular GCase glycoforms

Murine macrophage-like RAW264.7 cells and human skin fibroblasts were cultured in DMEM and DMEM/F12 medium respectively, at 7% CO₂. Different buffers were added to the medium at a final concentration of 50 mM: MES (2-(N-morpholino) ethanesulfonic acid) (pKa = 6.15) or HEPES (4-(2-hydroxyethyl)-1-piperazineethanesulfonic acid) (pKa=7.5). The final medium pH was 7.0, and 7.4 respectively. After a week of culture, cells were harvested and lysed in KPi-buffer supplemented with 0.1% Triton X-100. Active GCase molecules in cell lysates were labelled with fluorescent ABP ME569 and were analysed by SDS-PAGE (**Figure 1**). The cellular abundance of GCase and the GCase glycoform profile was found to be clearly influenced by the medium composition. In fibroblasts and RAW264.7 cells cultured at lower pH, less GCase was labelled with ABP (**Figure 1A**), and less GCase activity was detected (**Figure 1B**). In cells cultured at pH 7.4, in the presence of HEPES, GCase was more abundant, in particular glycoforms with MW of 62-66 kDa (**Figure 1A**). PNGase digestion resulted in the generation of a 52 kDa labelled protein in lysates of both MES and HEPES exposed cells, which confirms that all labelled enzyme is GCase and various MW forms stem from differences in glycans (**Figure 1C**). We also studied cells that were exposed to 50 mM MOPS (3-(N-morpholino) propanesulfonic acid; pKa = 7.15), which buffered the final medium pH at 7.15. As shown in **Supplemental figure 1**, cells cultured at pH 7.15 showed an intermediate GCase profile when compared to the glycan isoform profile of cells cultured at higher and lower medium pH.

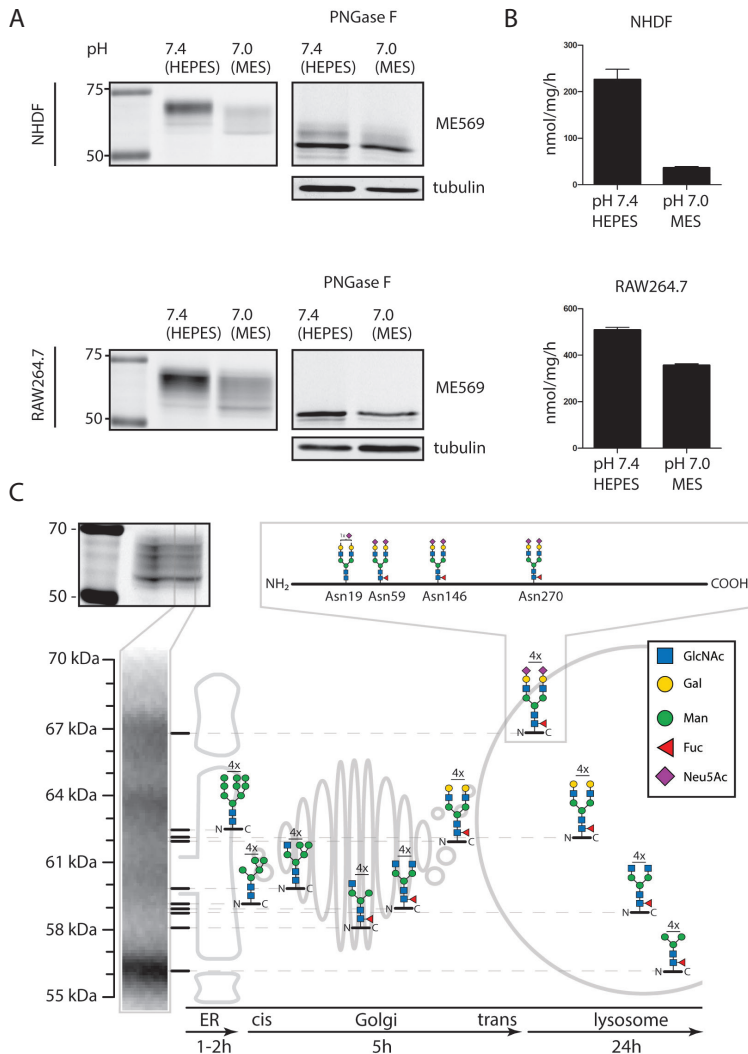


Figure 1. Impact of medium on cellular GCase glycoforms. (A) GCase in lysates of skin fibroblasts (NHDF) and RAW264.7 cells was labelled with GCase-specific ABP and subsequently visualized by fluorescence scanning after SDS-PAGE. Labeled GCase was digested with PNGase F to remove N-glycans, as described in M&M. (B) GCase of the same lysates of skin fibroblasts (NHDF) and RAW264.7 cells was measured with 4MU- β -Glc substrate as described in M&M. (C) Scheme depicting processing of GCase glycoforms (adapted from Aerts, thesis).

Dynamics of induced changes in GCase by medium pH

The induction and reversibility of changes in cellular GCase induced by culture medium composition was investigated more closely. For this, cells (fibroblasts and RAW264.7 cells) were exposed to culture medium containing 50 mM HEPES (medium pH 7.4). In both cell types, GCase with higher MW (reflecting enzyme species with more sialylated complex glycans) accumulated and an increase in overall GCase activity was detected over time (**Figure 2A**). Next, the reversibility of the induced changes in GCase was examined.

Cells were first exposed to medium containing 50 mM HEPES for 3 days. Subsequently, cells were washed and further cultured in the presence of 50 mM MES (medium pH 7.0). At different time points (0-96 hours), cells were harvested and cellular GCase was studied by ABP-labeling and SDS-PAGE, as well as by enzymatic activity measurements (**Figure 2B**). Exposure to a lower medium pH caused a reversal of GCase glycoform profile, which was accompanied by reduced total cellular enzymatic activity (**Figure 2B**). Of note, the correction of GCase in fibroblasts proceeded slower than that in RAW cells (**Figure 2B**). Brightfield microscopy analysis of RAW264.7 cells showed a prominent change in vacuolar morphology upon HEPES induction, which could be reversed through subsequent and prolonged replacement by MES (**Supplemental Figure 2**).

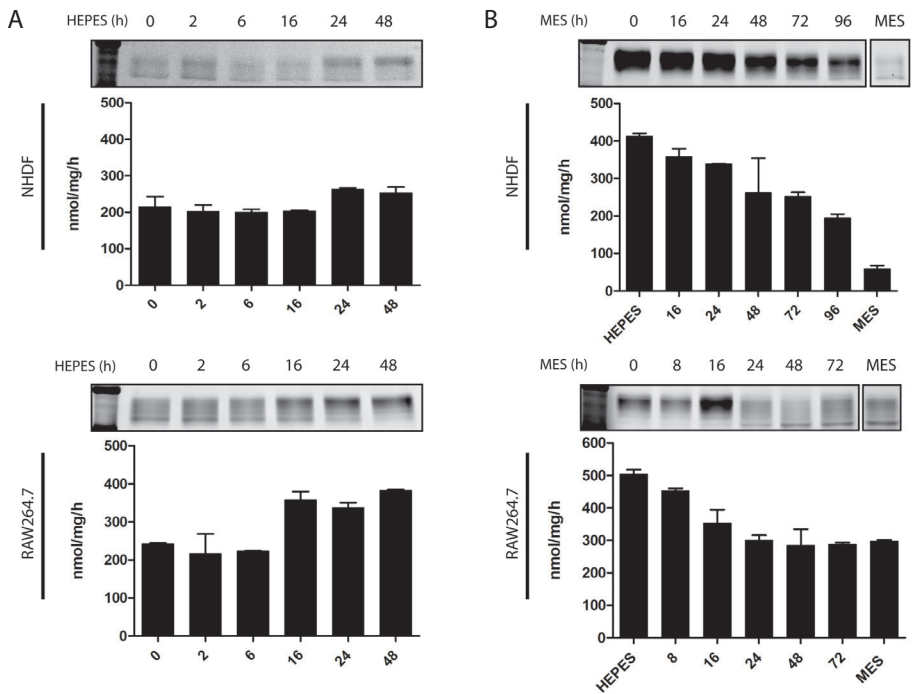


Figure 2. Induction and reversibility of GCase changes by HEPES-containing medium. (A) Induction. Skin fibroblasts (NHDF) and RAW264.7 cells were exposed to either 50 mM HEPES or MES, and cellular GCase was monitored in time (0-48 hours) by means of ABP labeling of enzyme in cell lysates and the measurement of enzymatic activity in lysates. (B) Reversibility. Skin fibroblasts (NHDF) and RAW264.7 cells were exposed for 3 days to 50 mM HEPES in the culture medium (pH 7.4). Following washing, cells were cultured in medium containing 50 mM MES (medium pH 7.0), and cellular GCase was monitored in time (0-96 hours) in cell lysates by means of ABP labeling of enzyme molecules and measurement of GCase activity. The last lane to the right represents cells chronically cultured in the presence of 50 mM MES.

Life cycle of GCase visualized with ABPs

Two earlier published GCase-specific ABPs conjugated with green and red boron dipyrromethene (BODIPY), MDW933 and MDW941 respectively²⁸, were used to perform a pulse-chase experiment. Cultured fibroblasts and RAW264.7 cells were first exposed to 100 nM cell permeable MDW933 overnight to irreversibly label all active GCase molecules. Next, cells were extensively washed and subsequently cultured in the presence of red fluorescent MDW941. Detection of MDW941-labeled enzyme allows selective monitoring of *de novo* synthesized GCase in time. The pulse-chase experiments were performed with fibroblasts and RAW264.7 cells cultured in medium containing either 50 mM HEPES or 50 mM MES. Cells were harvested at different time points during the chase period (0-96 h) and cellular GCase was analyzed by SDS-PAGE (**Figure 3**). Incubation of RAW264.7 cells with the red MDW941 probe for extended periods of time resulted in complete labeling of GCase and its inactivation as measured with 4MU-assay, whereas GCase activity was restored 96h after removal of green MDW933 without the MDW941 chase (**Supplemental figure 3**).

During the chase period, MDW941-labeled GCase increased in both types of cells cultured in both media, indicating sustained synthesis of GCase during the various chases (**Figure 3**). Cells cultured with HEPES did not show the transition of 66 kDa GCase to 58 kDa enzyme, a process known to depend on stepwise removal of external sugars from the N-glycans.³¹ In contrast, cells cultured with 50 mM MES at pH 7.0 did show detectable formation of 58 kDa GCase after one day of chase (**Figure 3**).

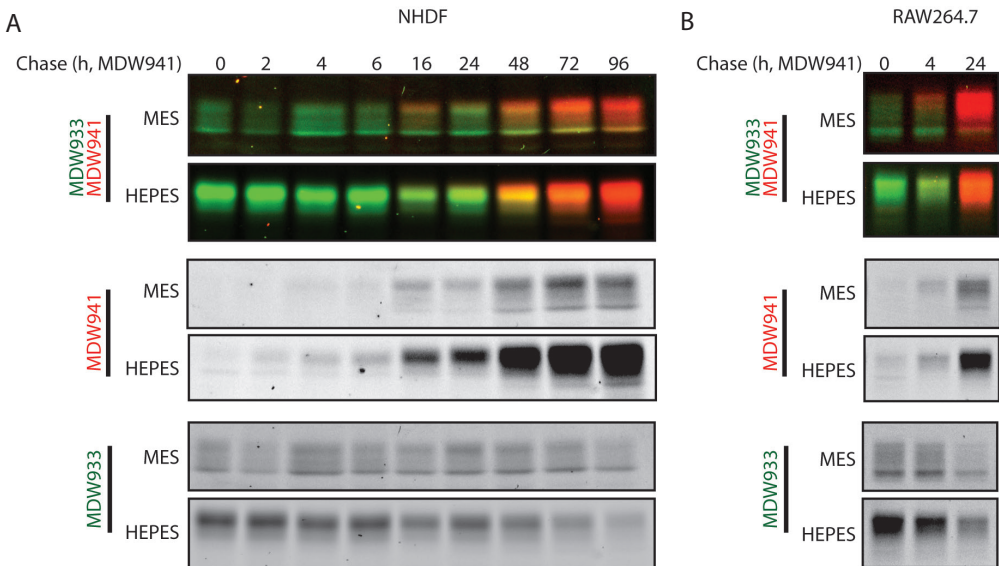


Figure 3. Visualization of GCase isoforms with two distinct ABPs: reduced glycan maturation in HEPES-containing medium. (A) Pulse-chase experiments with fibroblasts, performed as described in M&M. Following pre-labeling with MDW933 (green fluorescent, existing GCase), cells were incubated continuously with MDW941 (red fluorescent, newly synthesized GCase) for indicated time periods. Cells were harvested and labeled GCase was visualized following SDS-PAGE. (B) Same experimental set-up was used for GCase studies in RAW 264.7 cells.

Subcellular localization of GCase in cells cultured in the presence of different buffers.

Immunofluorescence analysis of fibroblasts revealed a punctate pattern for ABP-labeled GCase when cultured in presence of HEPES and MES, that similarly overlapped with immunocytochemically labelled LIMP2, the transporter of GCase (**Figure 4A**). No marked overlap was observed for GCase with the ER protein Calnexin, the Golgi marker Giantin and the early endosome marker EEA1 (Early Endosome Antigen 1) in cells cultured in HEPES-supplemented medium (**Figure 4B**). Localization of labelled GCase was however associated with that of the (endo)lysosome marker LAMP1 (**Figure 4B**). Of note, an increase in LAMP1 positive punctae was observed in fibroblasts cultured in the presence of HEPES, which suggests that more (endo)lysosomes exist upon exposure to HEPES-containing medium (**Supplemental figure 4**).

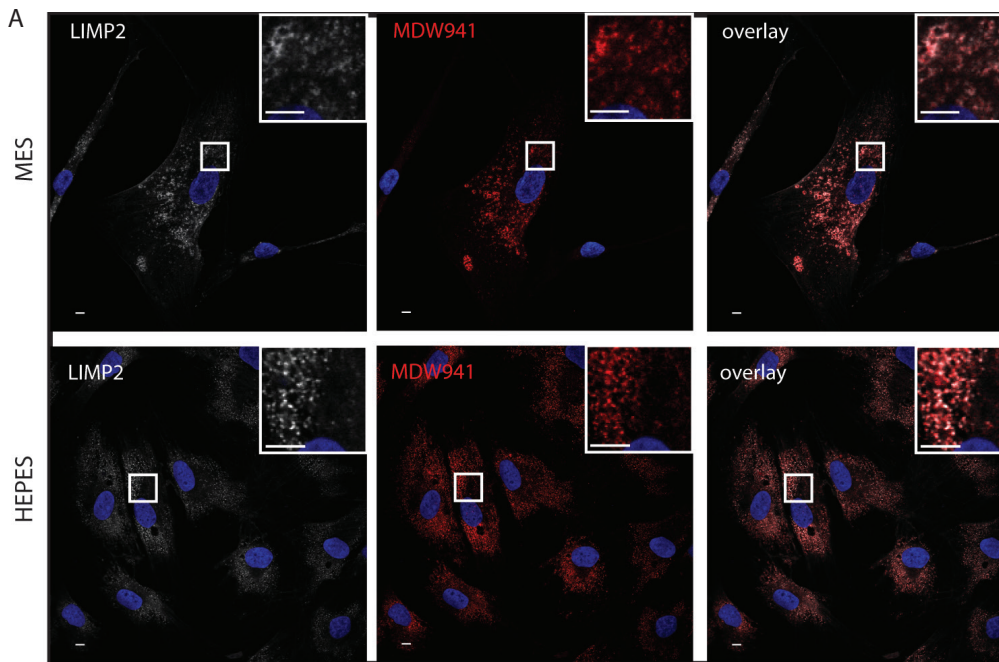
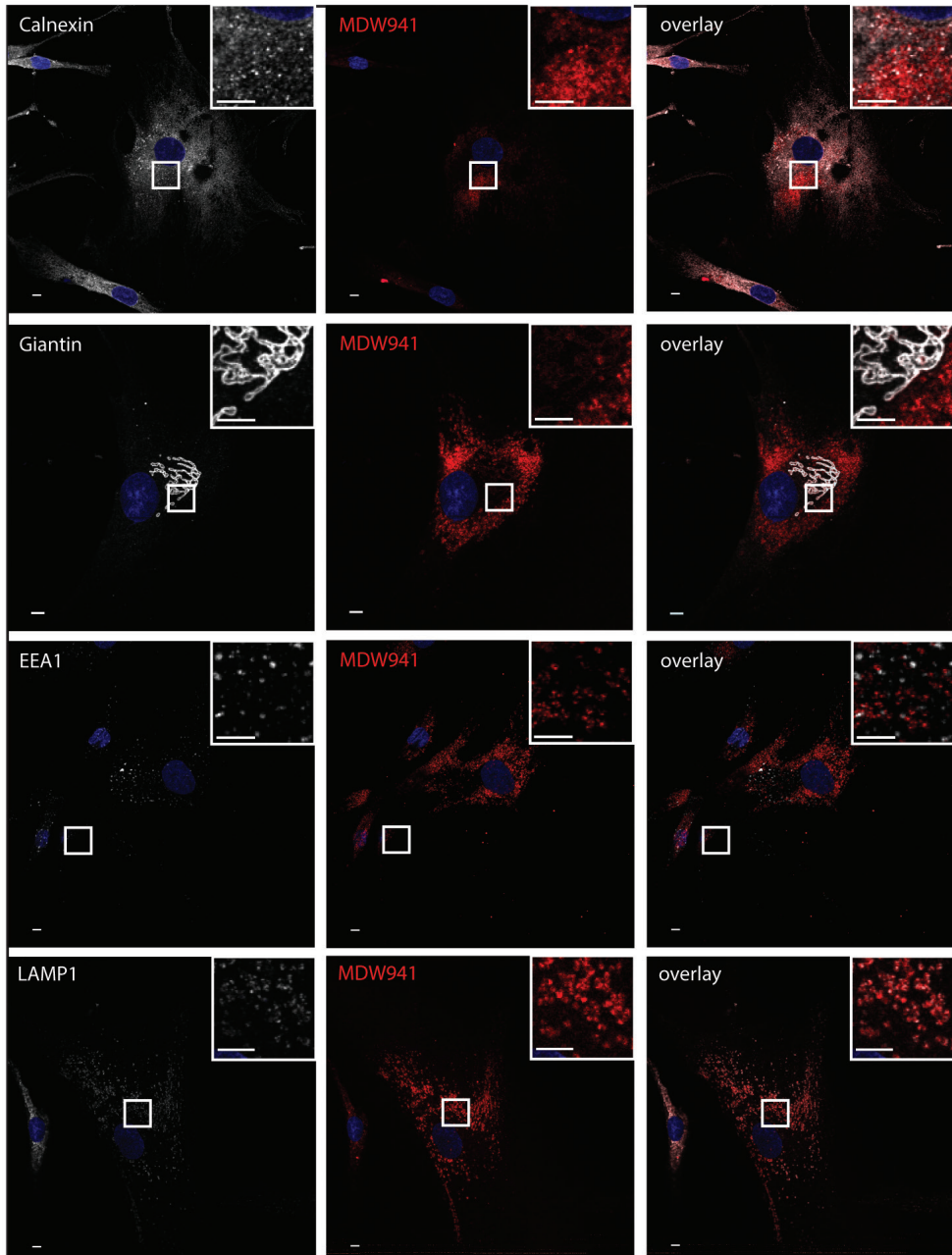


Figure 4. *GCase colocalizes with LAMP1- and LIMP2 in HEPES treated fibroblasts.* Cells were pretreated ABP MDW941 to label GCase and subsequently fixed and analyzed by immunohistochemistry to establish overlap of GCase with other marker proteins. (A) Visualization of GCase and LIMP2 in fibroblasts cultured in the presence of MES or HEPES. (B; next page ->) Visualization of GCase and Calnexin, Giantin, EEA1 and LAMP1 in fibroblasts cultured in the presence of HEPES. Scale bar: 10 μ m

Lysosomes are dense organelles and can be separated from ER and Golgi structures based on density difference. Subcellular fractionation was used to separate compartments by means of a continuous Percoll density gradient, as described in M&M. In gradient fractions, the enzyme activities of GCase and the lysosomal enzyme β -hexosaminidase were determined. In the case of MES-exposed RAW264.7 cells, GCase and β -hexosaminidase activities were detected in fractions with high density. These fractions are known to contain mature dense lysosomes (**Figure 5**). GCase β -hexosaminidase activity was virtually absent

in highly dense fractions of cells exposed to HEPES. The lysosomal enzyme activities in compartments with lower density reflect enzymes in pre-lysosomal compartments (ER, Golgi, endolysosomes and immature lysosomes). Similar observations were made for fibroblasts (**Supplemental figure 5**). These findings indicate that HEPES-exposed cells contain on average less dense lysosomes compared to MES-conditioned cells.

B



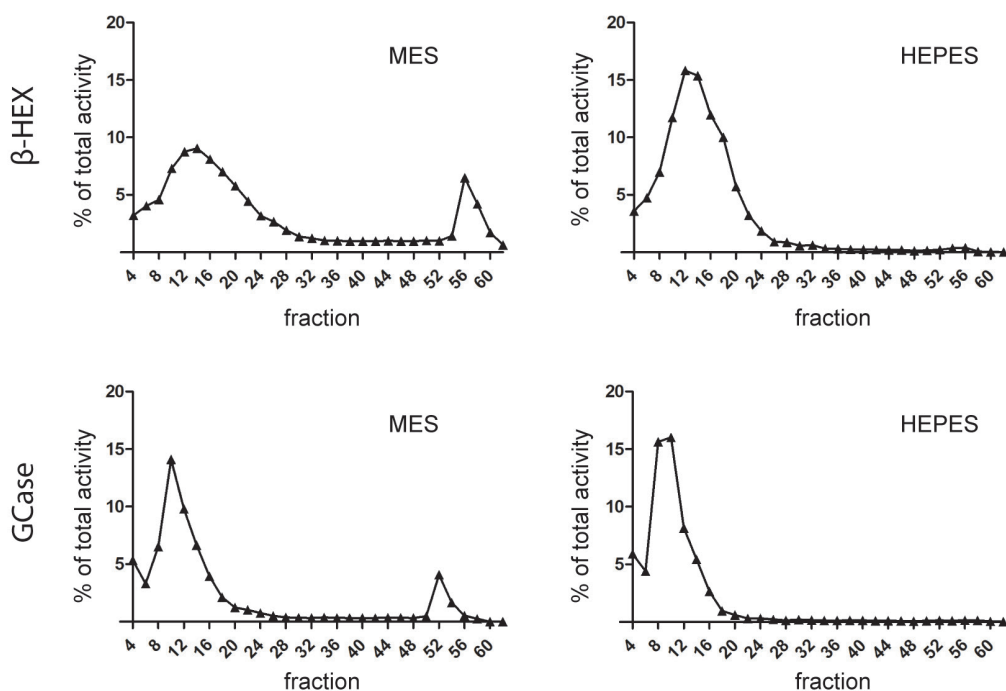


Figure 5. Subcellular fractionation of fibroblasts cultured in the presence of 50 mM HEPES or MES. Homogenates of RAW264.7 cells treated with HEPES or MES were fractionated and compartments were separated on the basis of density using 49% Percoll centrifugation to generate density gradients. In collected fractions enzymatic activities of GCase and β -hexosaminidase were measured as described in M&M.

Intralysosomal proteolytic degradation of GCase is known to be potently inhibited by leupeptin, a broad protease inhibitor.^{36,38} Consequently, leupeptin induces accumulation of mature 58 kDa GCase upon complete maturation of GCase. The impact of leupeptin on GCase in cells (fibroblasts and RAW264.7) cultured in the presence of MES, MOPS and HEPES was examined. The presence of leupeptin led to accumulation of 58 kDa GCase (**Figure 6A**) and overall GCase activity (**Figure 6B**) in cells cultured with MES and MOPS but not those with HEPES. Thus, even in the presence of leupeptin, HEPES-treated cells do not form the mature 58 kDa form of GCase. This suggests that the machinery leading to the formation of 58 kDa GCase, likely exo-glycosidase activity, is perturbed in these cells.

In summary, the microscopy analyses (**Figure 4**), the outcome of subcellular fractionation experiments (**Figure 5**), and the noted effects of leupeptin (**Figure 6**) all rendered data consistent with the hypothesis that the presence of HEPES in the culture medium affects normal maturation of lysosomes to dense structures, and instead promotes formation of compartments with lower density that contain altered activity of glycosidases and proteases.³⁷ GCase undergoes prominent trimming of its N-glycans by glycosidases and is degraded relatively rapidly by proteases in mature lysosomes.

Therefore, it is not surprising that GCase is highly sensitive to the presence of HEPES in the medium which causes cellular accumulation of the 66 kDa enzyme.

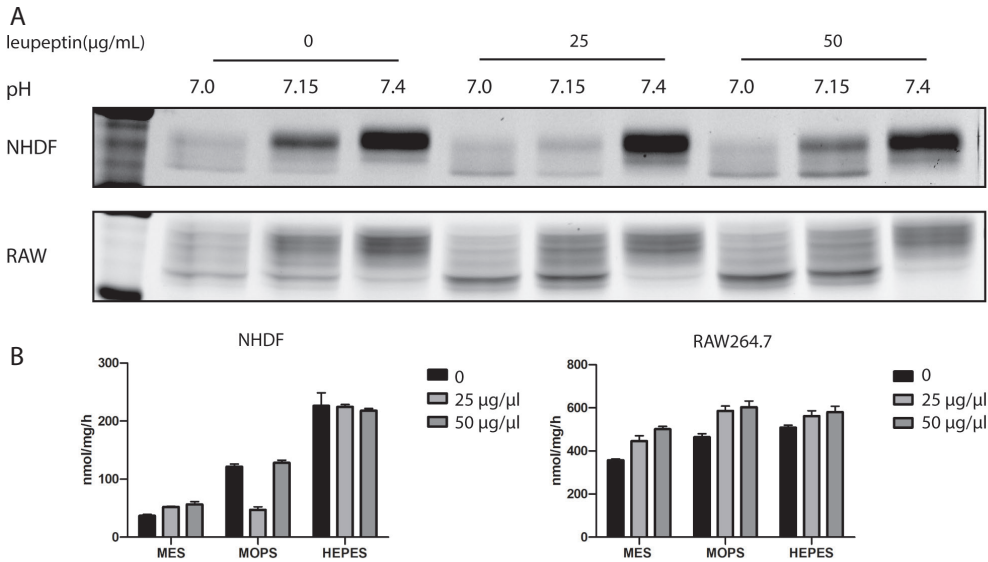


Figure 6. Inhibition of lysosomal cathepsins in increases GCase in cells exposed to MES and MOPS, but not those exposed to HEPES. Cells (fibroblasts and RAW264.7) were cultured in the presence of 50 mM buffer compound (MES, MOPS or HEPES) in the absence or presence of 0, 25 or 50 μ g/mL leupeptin for 48 hours. Cells were harvested and GCase in lysates was visualized by (A) ABP labeling, SDS-PAGE and fluorescence scanning, or (B) by enzymatic GCase activity measurements (as described in M&M).

Implications for diagnosis of GD using cultured cells.

The use of culture medium with added HEPES is increasingly popular because it allows stable buffering of medium for extended amount of days. Here we show that in cultured cells the enzyme GCase is particularly influenced by the use of this buffer. This has repercussions regarding measurement of enzyme activity levels for diagnostic purposes. **Figure 7** shows the GCase levels (nmol/mg protein/hour) in lysates of fibroblasts from type 1 Gaucher disease patients and normal individuals cultured in the presence of HEPES and MES. The levels for lysates of cells from some patients cultured in the presence of HEPES overlap with values in lysates of cells from normal individuals cultured in the presence of MES. Culturing patient and control cells at different conditions might result in false negatives in GD diagnosis. It also was observed that glucosylsphingosine levels in Gaucher patient-derived fibroblasts were increased when cells were cultured in the presence of 25 mM HEPES, a finding that again points to reduced lysosomal GCase activity under this condition (**Supplemental Table 1**).

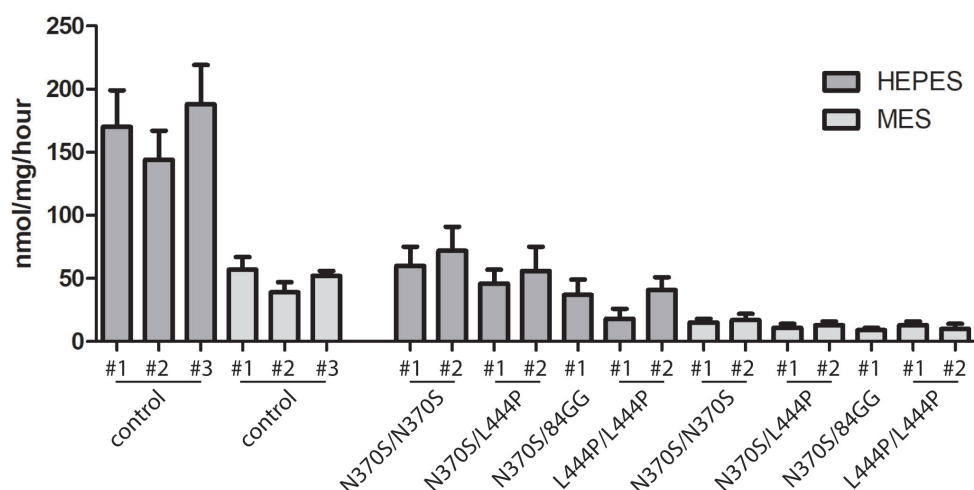


Figure 7. GCase activity level in control and Gaucher fibroblasts cultured in the presence of 25 mM MES or HEPES. Values expressed a mean \pm SD; measurements performed in triplicate.

Impact of medium on other lysosomal glycosidases

Selective ABPs are nowadays also available for a number of other lysosomal retaining glycosidases like the α -glucosidases (GAA) and β -glucuronidase (GUSB).^{39,40} We examined the impact of the culture medium buffers on these enzymes using corresponding ABPs for visualization. **Figure 8** shows that in fibroblasts cultured in the presence of HEPES at a medium pH of 7.4, the ratio of intermediate and mature GAA is altered, pointing to perturbed lysosomes. Likewise, an increase in the intermediate form of GUSB (75 kDa) and a decrease in the mature form (65 kDa) was noted in cells cultured in the presence of HEPES. Proteolytic processing of 95 and 76 kDa GAA and 75 kDa GUSB is thought to largely take place in lysosomes. The findings therefore suggest that the involved proteases in this processing are less active. This explanation was substantiated by the finding that leupeptin treatment did not cause an increase in mature 65 kDa GUSB in fibroblasts cultured in the presence of HEPES (**Supplemental figure 6**). Of note, the intermediate 75 kDa GUSB was increased in cells cultured in the presence of HEPES (**Supplemental figure 6**).

Discussion

In recent times, attractive new tools have become available for investigations on GCase in intact cells. For the purpose of GCase visualization, cell permeable fluorescent activity-based probes have been designed that covalently bind to the catalytic nucleophile E340 of active GCase molecules with extreme specificity, allowing their convenient visualization in intact cells.²⁸ Based on earlier observations with irreversible inhibitors, the attachment of a bulky group to the pseudo C6 position in substrates confers specificity for GCase over GBA2 and GBA3.^{28,29,41,42}

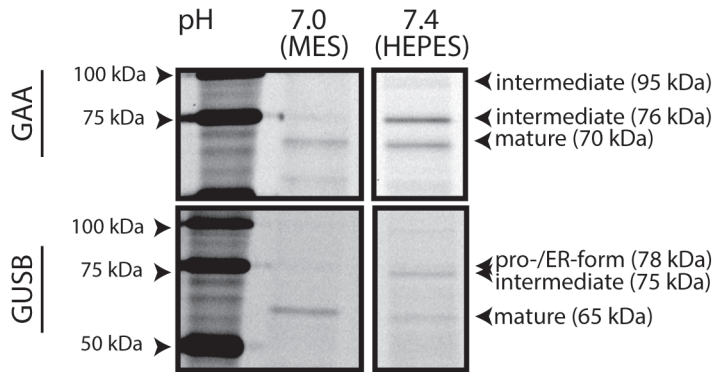


Figure 8. Impact of medium pH on alpha-galactosidase (GAA) and beta-glucuronidase (GUSB) isoforms. Fibroblasts were cultured in the presence of 50 mM buffer compound (MES or HEPES). Cells were harvested and GAA and GUSB in lysates was visualized by ABP labeling, SDS-PAGE and fluorescence scanning.

Additional novel GCase-specific substrates have been designed based on this principle, including the cell-permeable fluorescence-quenched substrates for *in situ* measurement of GCase activity²⁶, or the resorufin substrates for *in vitro* GCase activity and kinetic analysis.²⁷ Many investigations on GCase make use of cultured cells. Earlier work in our lab revealed that culture conditions may impact on GCase in cells, in particular the addition of the increasingly popular buffer HEPES to culture medium. HEPES maintains the medium at the relative high pH of 7.4.³⁷ Our present investigation illustrates the marked impact on cellular GCase of the presence of HEPES in the culture medium, both qualitatively and quantitatively.⁴³ In cells, fibroblasts and macrophage-like RAW264.7 cells alike, exposure to HEPES containing medium causes GCase to steadily accumulate. The accumulating enzyme shows a MW of about 66 kDa, which suggests an abundance of complex-type sialylated glycans. The subsequent intralysosomal conversion to a 58 kDa glycoform by trimming of N-glycans does not seem to occur in cells that are exposed to HEPES. Also, an overall increase in the 66 kDa isoform of GCase is observed in these cells. The observed reduction in lysosomal glycan processing increased abundance of GCase could theoretically be caused by an arrest of the enzyme in the trans-Golgi region. However, microscopy revealed that GCase in HEPES-exposed cells is present in LAMP1-positive compartments and does not overlap in location with Giantin, a Golgi marker and the early endosome marker EEA1. This suggests that the enzyme has passed the Golgi apparatus and does not accumulate in early endosomes. The subcellular distribution of LIMP2 and GCase were also found to overlap in cells cultured in the presence of HEPES. At present, it seems most attractive to assume that mature lysosomes acquire a higher pH upon uptake of HEPES, consequently exhibit lower density and have reduced hydrolase capacities. These include the activities of glycosidases and proteases involved in GCase N-glycan trimming and proteolytic degradation. However, additional explanations cannot be entirely excluded yet. The relatively high medium pH might impact on cytosolic pH, which could in turn impact on lysosome acidification. Indeed, it has been recently reported that STAT3 can promote lysosome acidification via direct interaction with the v-ATPase. The cytosolic pH was found to play a key role in the association of STAT3 with lysosomes.⁴⁴ In light of this, recent work by Grinstein and colleagues has

revealed the existence of two pools of lysosomes in cells: highly acid and lytic, perinuclear ones, and less acidic peripheral ones.⁴⁵ The two types of lysosomes are similar in v-ATPase composition but nevertheless fundamentally differ in luminal pH.⁴⁵ Cytosolic pH has earlier been reported to impact on location of lysosomes in cultured macrophages.⁴⁶ Acidification of the cytosol by the presence of acetate in medium was found to cause movement of lysosomes to the cell periphery.⁴⁶ At present, we have no indications for a marked difference in distribution of lysosomes in cells cultured in the presence of HEPES compared to those cultured in the presence of MES. It may nevertheless be of relevance to study to which extent medium pH impacts on retrograde and anterograde transport of lysosomes along microtubules.⁴⁷

The change in GCase glycan isoforms in cells exposed to HEPES reveals a striking sensitivity of this glycan composition to lysosomal perturbations. Of note, the mild lysosomal stressor sucrose (80 mM) induced a similar enrichment of the high MW variant of GCase (**Supplemental figure 7**). Sucrose induced vacuolation might negatively impact on lysosomal pH homeostasis and thereby impair GCase maturation in a similar fashion as HEPES. The perturbed vacuolar processing of GCase to the mature 58 kDa isoform was not accompanied by an impaired catalytic function as measured by 4MU-assay. This is in line with previous reports, suggesting that whereas conformational folding of GCase requires occupation of reported glycan sites, the hydrolytic capacity is not dependent on the precise glycan composition.³¹ Moreover, buffering medium pH at 7.4 by HEPES induces a prominent increase in total cellular GCase content, as measured in lysates. The majority of GCase in these cells is not present in physiologically mature lysosomes and might therefore be relatively inactive towards substrate. Indeed, we noted that formation of glucosylsphingosine in lysosomes, a measure for impaired degradation of GlcCer, is significantly higher in type 1 GD fibroblasts cultured in the presence of HEPES (**Supplemental Table 1**).⁴⁸ It might therefore be prudent to use culture medium with a measured, predefined pH as well as to assess the molecular weight and abundance of cellular GCase when using cultured cells in fundamental research on GCase and related disorders such as GD and PD. This could facilitate comparable and reproducible assessment of cellular GCase functions. Importantly, as pointed out in the results section, during diagnostic demonstration of reduced GCase activity in lysates of cultured cells, special care should be taken that tentative patient cells and normal cells are cultured in identical media.

In conclusion, GCase is remarkably sensitive to presence of HEPES in the culture medium. In view of the major effect of this buffer compound, investigations concerning GCase should better refrain from the use of this medium addition.

Material and Methods

Cell Culture Experiments

RAW264.7 cells (American Type Culture Collection #TIB-71) were cultured in DMEM and normal human dermal fibroblasts cells (NHDFs, Lonza #CC-2511) were cultured in DMEM/F12. Both mediums contained 10% (v/v) fetal calf serum, 1% (w/v) glutamax and 0.2% (w/v) antibiotics (penicillin-streptomycin; all purchased from Thermo Fisher Scientific) at 37°C at 7% CO₂ at controlled humidity. For modulation of medium pH, MES (Sigma, M3671), MOPS (Sigma, M1254) and HEPES (Sigma, H3375) were dissolved and filtered to obtain culture grade stock buffers (1 M). Where mentioned, culture medium was supplemented with culture grade HEPES, MES or MOPS to a final concentration of 50 mM for at least 72h, if not stated otherwise. Stock solutions were titrated so that final pH in medium was 7.0 for MES, 7.20 for MOPS and 7.5 for HEPES. Leupeptin (Sigma, L9783) was added in 25 or 50 µg/mL concentration to medium of cells pre-treated with MES, MOPS or HEPES for 72h and incubated along with the respective buffers for 48 h. Sucrose (Sigma, S7903) was incubated for 24h at a concentration of 80 mM. Gaucher fibroblasts were obtained for fundamental investigations with consent of patients and their GBA genotype was confirmed by sequencing.

Activity-based probe analysis

Cultured cells were lysed in KPi lysis buffer (25 mM K₂HPO₄/KH₂PO₄, pH 6.5, 0.1% (v/v) Triton X-100) supplemented with protease inhibitors (Roche) and sonicated 5x 1 second with 9 minutes interval (amplitude 25%). Protein concentration was assessed by bicinchoninic acid assay (Thermo Fisher Scientific, 23225) and absorbance measurements (EMax Plus microplate reader, Molecular Devices). Equal protein amounts were labelled with excess of activity-based probe (ABP) conjugated to a fluorescent dye. Labelling of all active GCase molecules in cell homogenates and recombinant GCase (Cerezyme) was performed using 100 nM ABP-ME569 (Cy5).⁴² Incubation was performed at 100 nM for 1 h (0.5-1% (v/v) DMSO) on ice. Labelling of acid alpha-glucosidase (GAA) and beta-glucuronidase (GUSB) was performed as described earlier.⁴¹ Shortly, homogenates were prelabelled with 200 nM of β-glc aziridine ABP JJB70 for 30 min at 37 °C, pH 4.0 and 5.0 resp. GAA was subsequently labeled by incubation of 500 nM JJB383 for 30 min at 37 °C, pH 4.0. GUSB labelling was performed through incubation with 200 nM JJB392 for 30 min at 37 °C, pH 5.0. After labelling, 5x Laemlli buffer (50% (v/v) 1 M Tris-HCl, pH 6.8, 50% (v/v) 100% glycerol, 10% (w/v) DTT, 10% (w/v) SDS, 0.01 % (w/v) bromophenol blue) was added and samples were denatured at 95°C. Proteins were resolved by 10% polyacrylamide gel through SDS-PAGE.

PNGase F treatment

Buffer-exchange was performed on GCase-labelled protein homogenate by spin desalting column (Pierce, 89849) and incubated with PNGase F according to the manufacturer's instructions (NEB, P0705S). Shortly, denaturation of protein was performed in denaturing buffer at 100°C for 10 minutes. Subsequent digestion by PNGase F was performed at 37°C for 1h.

Pulse-chase experiment

For *In situ* labelling of GCase in living cells, RAW264.7 cells and NHDFs were cultured overnight in the presence of 100 nM green fluorescent cyclophellitol based ABP (MDW933). Next, cells were thoroughly washed and incubated with 100 nM red fluorescent ABP (MDW941) for different amount of times. Thus, existing GCase is labeled green and newly synthesized GCase is red. Cells were extensively washed, lysed in KPi lysis buffer and equal amounts of protein were analyzed by SDS-PAGE.

In-gel visualization of probes

Detection of fluorescence in wet gel slabs was performed using a Typhoon FLA 9500 fluorescence scanner (GE Healthcare). Green fluorescence (MDW931 and JJB70) was detected using λ_{EX} 473 nm and $\lambda_{\text{EM}} \geq 510$ nm, red fluorescence (MDW941) using λ_{EX} 532 nm and $\lambda_{\text{EM}} \geq 575$ nm and far red fluorescence (ABP-ME569, JJB383, JJB392) using λ_{EX} 635 nm and $\lambda_{\text{EM}} \geq 665$ nm. After imaging, gels were either stained by Coomassie G250 for total protein and scanned on ChemiDoc MP imager (Bio-Rad) or used for western blotting.

Western Blot Analysis

Samples resolved on 10% polyacrylamide gels were transferred to 0.2 μm nitrocellulose membrane (#1704159, Biorad). Blocking of membranes occurred in 5% (w/v) bovine serum albumin (Sigma, A1906) solution in PBS/0.1% Tween-20 (Sigma, P1379) for 1 h at room temperature (RT). Primary antibodies used target GCase (clone 8E4, manufactured in Aerts lab) and tubulin (Cedarlane, CLT 9002). Proteins were detected by using specific secondary conjugated antibodies (Alexa Fluor™ 488/647) (Molecular Probes). Detection of immunoblots was performed using a Typhoon FLA 9500 fluorescence scanner (GE Healthcare).

Labeling of GCase in situ

Functionalized glass coverslips were seeded with NHDF at a confluency of 70% as described and treated with MES or HEPES.⁴⁹ Active GCase was labelled by 2 h medium supplementation of 5 nM MDW941. Next, the cells were washed 3x with PBS and fixed with 4% (w/v) formaldehyde (Sigma) in PBS for 20 min at room temperature while kept in the dark. Fixed cells were then washed with PBS and blocked in 5% normal donkey serum (NDS, Jackson Laboratory, 145-017-000-121) for 60 min. Cells were either stained for immunofluorescence microscopy or mounted directly on a microscope slide with ProLong Diamond antifade reagent containing DAPI (Molecular Probes, P36962). Immunofluorescence staining was performed in 2% NDS. Antibodies used were rabbit anti-LAMP-1 (Abcam, AB24170), rabbit-anti-LIMP2 (Novus Biologicals, NB400-129), rabbit-anti-Calnexin (Sigma, C4731), rabbit-anti Giantin (Abcam, AB24586), all at a dilution of 1:400 and rabbit-anti-EEA1 (Cell Signaling, 2411S) at a concentration of 1:200. Secondary antibodies used was Alexa Fluor conjugated IgGs (H + L) donkey anti-rabbit Alexa 488 (Invitrogen). Fluorescence microscopy was performed using a Leica TCS SP8 confocal microscope with a 63x/1.40 numerical aperture (NA) HC Plan Apo CS2 oil immersion objective and equipped with a hybrid detector (HyD).

Enzyme activity assays

Equal protein amounts as assessed by bicinchoninic acid assay were used for enzyme activity assays. GCase activity was assayed using 3.75 mM 4-methylumbelliferyl (4-MU) substrate beta-D-glucopyranoside (44059, Glycosynth) in McIlvaine buffer, pH 5.2, with 0.1% (w/v) BSA, 0.2% (w/v) sodium taurocholate and 0.1% (v/v) Triton X-100. For activity measurements of β -hexosaminidases HexA/B, 5 mM 4MU- β -N-acetyl-glucosaminide at pH 4.5 was used.

Density gradient fractionation

Cultured cells were harvested and washed 2x in PBS and 2x MME buffer (250 mM mannitol, 2 mM EGTA, 5 mM MOPS/Tris pH 7.0) through centrifugation at 1000 g for 5 min. Cells were resuspended in MME buffer and homogenized by 30 strokes using a Dounce homogenizer (B. Braun). The suspension was centrifuged for 2 min at 1000 rpm. The post-nuclear fraction (PSN, supernatant) was transferred to a percoll column (49% percoll (Sigma, P1644), 250 mM mannitol, 2.5 mM MOPS-Tris, HCl titrated to pH 7.0) on top of a cushion of 2.5 M Sucrose (Sigma). Ultracentrifugation of the column was performed at 30,000 g in a SW 41 Ti swinging bucket rotor (Beckman). Optimal density-based fractionation was verified by Density Marker Beads (Pharmacia, 17-0459-01). After centrifugation, fractions of 250 μ l were obtained, weighed, and used for enzyme activity measurements.

Measurement of glucosylsphingosine

Levels of glucosylsphingosine in cultured fibroblasts were determined as earlier described.^{50,51} Briefly, samples were analyzed by mass spectrometry (ESI-LC-MS/MS), along with a ¹³C-isotope encoded internal standard.⁵⁰

References

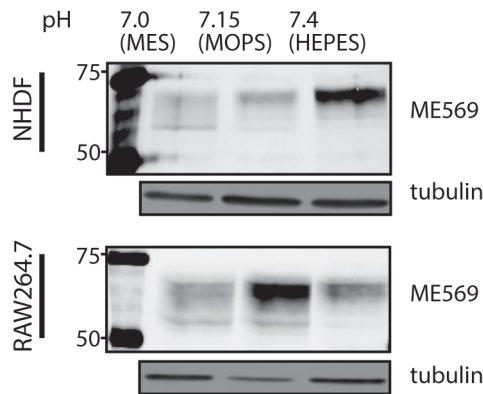
1. Beutler, E. & Grabowski, G. Gaucher Disease. In Scriver CR, Valle D, Beaudet A, Sly WS, eds. *The Metabolic and Molecular Bases of Inherited Diseases* **8** 3635–3668 (2001).
2. Ferraz, M. J., Kallemijn, W. W., Mirzaian, M., Herrera Moro, D., Marques, A., Wisse, P., Boot, R. G., Willems, L. I., Overkleeft, H. S. & Aerts, J. M. Gaucher disease and Fabry disease: New markers and insights in pathophysiology for two distinct glycosphingolipidoses. *Biochim. Biophys. Acta - Mol. Cell Biol. Lipids* **1841**, 811–825 (2014).
3. Sidransky, E., Nalls, M. A., Aasly, J. O., Aharon-Peretz, J., Annesi, G., *et al.* Multicenter analysis of glucocerebrosidase mutations in Parkinson's disease. *N. Engl. J. Med.* **361**, 1651–1661 (2009).
4. Nalls, M. A., Duran, R., Lopez, G., Kurzawa-Akanbi, M., McKeith, I. G., *et al.* A multicenter study of glucocerebrosidase mutations in dementia with Lewy bodies. *JAMA Neurol.* **70**, 727–735 (2013).
5. Boven, L. A., van Meurs, M., Boot, R. G., Mehta, A., Boon, L., Aerts, J. M. & Laman, J. D. Gaucher cells demonstrate a distinct macrophage phenotype and resemble alternatively activated macrophages. *Am. J. Clin. Pathol.* **122**, 359–369 (2004).
6. Bussink, A. P., van Eijk, M., Renkema, G. H., Aerts, J. M. & Boot, R. G. The biology of the Gaucher cell: the cradle of human chitinases. *Int. Rev. Cytol.* **252**, 71–128 (2006).
7. Brady, R. O. Enzyme replacement therapy: conception, chaos and culmination. *Philos. Trans. R. Soc. Lond. B. Biol. Sci.* **358**, 915–9 (2003).
8. De Fost, M., Hollak, C. E. M., Groener, J. E. M., Aerts, J. M. F. G., Maas, M., Poll, L. W., Wiersma, M. G., Häussinger, D., Brett, S., Brill, N. & Vom Dahl, S. Superior effects of high-dose enzyme replacement therapy in type 1 Gaucher disease on bone marrow involvement and chitotriosidase levels: A 2-center retrospective analysis. *Blood* **108**, 830–835 (2006).
9. Platt, F. M., Jeyakumar, M., Andersson, U., Priestman, D. A., Dwek, R. A., Butters, T. D., Cox, T. M., Lachmann, R. H., Hollak, C., Aerts, J. M. F. G., Van Weely, S., Hrebíček, M., Moyses, C., Gow, I., Elstein, D. & Zimran, A. Inhibition of substrate synthesis as a strategy for glycolipid lysosomal storage disease therapy. *J. Inherit. Metab. Dis.* **24**, 275–290 (2001).
10. Heitner, R., Elstein, D., Aerts, J. & Zimran, A. Low-dose N-butyldeoxynojirimycin (OGT 918) for type I Gaucher disease. *Blood Cells, Mol. Dis.* **28**, 127–133 (2002).
11. Mistry, P. K., Balwani, M., Baris, H. N., Turkia, H. Ben, Burrow, T. A., *et al.* Safety, efficacy, and authorization of eliglustat as a first-line therapy in Gaucher disease type 1. *Blood Cells Mol. Dis.* **71** 71–74 (2018).
12. Aerts, J. M. F. G., Kuo, C. L., Lelieveld, L. T., Boer, D. E. C., van der Lienden, M. J. C., Overkleeft, H. S. & Artola, M. Glycosphingolipids and lysosomal storage disorders as illustrated by gaucher disease. *Curr. Opin. Chem. Biol.* **53** 204–215 (2019).
13. Aerts, J. M. F. G., Kallemijn, W. W., Wegdam, W., Joao Ferraz, M., van Breemen, M. J., Dekker, N., Kramer, G., Poorthuis, B. J., Groener, J. E. M., Cox-Brinkman, J., Rombach, S. M., Hollak, C. E. M., Linthorst, G. E., Witte, M. D., Gold, H., van der Marel, G. A., Overkleeft, H. S. & Boot, R. G. Biomarkers in the diagnosis of lysosomal storage disorders: proteins, lipids, and inhibobodies. *J. Inherit. Metab. Dis.* **34**, 605–19 (2011).
14. Dahl, M., Doyle, A., Olsson, K., Månsson, J. E., Marques, A. R. A., Mirzaian, M., Aerts, J. M., Ehinger, M., Rothe, M., Modlich, U., Schambach, A. & Karlsson, S. Lentiviral gene therapy using cellular promoters cures type 1 gaucher disease in mice. *Mol. Ther.* **23**, 835–844 (2015).
15. Narita, A., Shirai, K., Itamura, S., Matsuda, A., Ishihara, A., *et al.* Ambroxol chaperone therapy for neuronopathic Gaucher disease: A pilot study. *Ann. Clin. Transl. Neurol.* **3**, 200–215 (2016).
16. Fog, C. K., Zago, P., Malini, E., Solanko, L. M., Peruzzo, P., Bornaes, C., Magnoni, R.,

- Mehmedbasic, A., Petersen, N. H. T., Bembi, B., Aerts, J. F. M. G., Dardis, A. & Kirkegaard, T. The heat shock protein amplifier arimoclomol improves refolding, maturation and lysosomal activity of glucocerebrosidase. *EBioMedicine* **38**, 142–153 (2018).
17. Mechtler, T. P., Stary, S., Metz, T. F., De Jesús, V. R., Greber-Platzer, S., Pollak, A., Herkner, K. R., Streubel, B. & Kasper, D. C. Neonatal screening for lysosomal storage disorders: Feasibility and incidence from a nationwide study in Austria. *Lancet* **379**, 335–341 (2012).
18. Wittmann, J., Karg, E., Turi, S., Legnini, E., Wittmann, G., Giese, A. K., Lukas, J., Gölnitz, U., Klingenhäger, M., Bodamer, O., Mühl, A. & Rolfs, A. Newborn screening for lysosomal storage disorders in Hungary. *JIMD Rep.* **6** 117–125 (2012).
19. Boot, R. G., Hollak, C. E. M., Verhoek, M., Sloof, P., Poorthuis, B. J. H. M., Kleijer, W. J., Wevers, R. A., Van Oers, M. H. J., Mannens, M. M. A. M., Aerts, J. M. F. G. & van Weely, S. Glucocerebrosidase genotype of Gaucher patients in the Netherlands: Limitations in prognostic value. *Hum. Mutat.* **10**, 348–358 (1997).
20. Ohashi, T., Hong, C. M., Weiler, S., Tomich, J. M., Aerts, J. M. F. G., Tager, J. M. & Barranger, J. A. Characterization of human glucocerebrosidase from different mutant alleles. *J. Biol. Chem.* **266**, 3661–3667 (1991).
21. Lachmann, R. H., Grant, I. R., Halsall, D. & Cox, T. M. Twin pairs showing discordance of phenotype in adult Gaucher's disease. *QJM* **97**, 199–204 (2004).
22. Biegstraaten, M., van Schaik, I. N., Aerts, J. M. F. G., Langeveld, M., Mannens, M. M. A. M., Bour, L. J., Sidransky, E., Tayebi, N., Fitzgibbon, E. & Hollak, C. E. M. A monozygotic twin pair with highly discordant Gaucher phenotypes. *Blood Cells, Mol. Dis.* **46**, 39–41 (2011).
23. Hollak, C. E. M., van Weely, S., van Oers, M. H. J. & Aerts, J. M. F. G. Marked elevation of plasma chitotriosidase activity. A novel hallmark of Gaucher disease. *J. Clin. Invest.* **93**, 1288–1292 (1994).
24. Boot, R. G., Verhoek, M., de Fost, M., Hollak, C. E. M., Maas, M., Bleijlevens, B., van Breemen, M. J., van Meurs, M., Boven, L. A., Laman, J. D., Moran, M. T., Cox, T. M. & Aerts, J. M. F. G. Marked elevation of the chemokine CCL18/PARC in Gaucher disease: a novel surrogate marker for assessing therapeutic intervention. *Blood* **103**, 33–9 (2004).
25. Kramer, G., Wegdam, W., Donker-Koopman, W., Ottenhoff, R., Gaspar, P., Verhoek, M., Nelson, J., Gabriel, T., Kallemeijn, W., Boot, R. G., Laman, J. D., Vissers, J. P. C., Cox, T., Pavlova, E., Moran, M. T., Aerts, J. M. & van Eijk, M. Elevation of glycoprotein nonmetastatic melanoma protein B in type 1 Gaucher disease patients and mouse models. *FEBS Open Bio* **6**, 902–913 (2016).
26. Yadav, A. K., Shen, D. L., Shan, X., He, X., Kermode, A. R. & Vocadlo, D. J. Fluorescence-quenched substrates for live cell imaging of human glucocerebrosidase activity. *J. Am. Chem. Soc.* **137**, 1181–1189 (2015).
27. Deen, M. C., Proceviat, C., Shan, X., Wu, L., Shen, D. L., Davies, G. J. & Vocadlo, D. J. Selective fluorogenic β -glucocerebrosidase substrates for convenient analysis of enzyme activity in cell and tissue homogenates. *ACS Chem. Biol.* **15**, 824–829 (2020).
28. Witte, M. D., Kallemeijn, W. W., Aten, J., Li, K.-Y., Strijland, A., Donker-Koopman, W. E., van den Nieuwendijk, A. M. C. H., Bleijlevens, B., Kramer, G., Florea, B. I., Hooibrink, B., Hollak, C. E. M., Ottenhoff, R., Boot, R. G., van der Marel, G. A., Overkleeft, H. S. & Aerts, J. M. F. G. Ultrasensitive in situ visualization of active glucocerebrosidase molecules. *Nat. Chem. Biol.* **6**, 907–13 (2010).
29. Kallemeijn, W. W., Li, K. Y., Witte, M. D., Marques, A. R. A., Aten, J., *et al.* Novel activity-based probes for broad-spectrum profiling of retaining β -exoglucosidases in situ and in vivo. *Angew. Chemie - Int. Ed.* **51**, 12529–12533 (2012).
30. Aerts, J. M., Hollak, C., Boot, R. & Groener, A. Biochemistry of glycosphingolipid storage disorders: implications for therapeutic intervention. *Philos. Trans. R. Soc. Lond. B. Biol.*

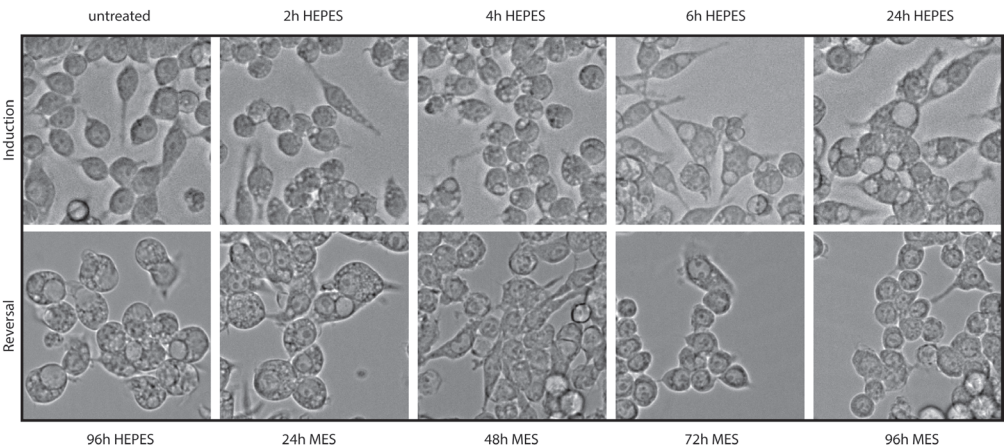
- Sci.* **358**, 905–14 (2003).
31. Weely, S. Van, Aerts, J. M. F. G., Leeuwen, M. B., Heikoop, J. C., Donker-Koopman, W. E., *et al.* Function of oligosaccharide modification in glucocerebrosidase, a membrane-associated lysosomal hydrolase. *Eur. J. Biochem.* **191**, 669–677 (1990).
 32. Aerts, J. M. F. G., Schram, A. W., Strijland, A., van Weely, S., Jonsson, L. M. V., Tager, J. M., Sorrell, S. H., Ginns, E. I., Barranger, J. A. & Murray, G. J. Glucocerebrosidase, a lysosomal enzyme that does not undergo oligosaccharide phosphorylation. *Biochim. Biophys. Acta - Gen. Subj.* **964**, 303–308 (1988).
 33. Reczek, D., Schwake, M., Schröder, J., Hughes, H., Blanz, J., Jin, X., Brondyk, W., Van Patten, S., Edmunds, T., Saftig, P., Schröder, J., Hughes, H., Blanz, J., Jin, X., Brondyk, W., Van Patten, S., Edmunds, T. & Saftig, P. LIMP-2 is a receptor for lysosomal mannose-6-phosphate-independent targeting of β -glucocerebrosidase. *Cell* **131**, 770–783 (2007).
 34. Gaspar, P., Kallemeyjn, W. W., Strijland, A., Scheij, S., Van Eijk, M., Aten, J., Overkleeft, H. S., Balreira, A., Zunke, F., Schwake, M., Sá Miranda, C. & Aerts, J. M. F. G. Action myoclonus-renal failure syndrome: diagnostic applications of activity-based probes and lipid analysis. *J. Lipid Res.* **55**, 138–45 (2014).
 35. Zunke, F., Andresen, L., Wessler, S., Groth, J., Arnold, P., Rothaug, M., Mazzulli, J. R., Krainc, D., Blanz, J., Saftig, P. & Schwake, M. Characterization of the complex formed by β -glucocerebrosidase and the lysosomal integral membrane protein type-2. *Proc. Natl. Acad. Sci. U. S. A.* **113**, 3791–6 (2016).
 36. Jonsson, L. M. V., Murray, G. J., Sorrell, S. H., Strijland, A., Aerts, J. F. G. M., Ginns, E. I., Barranger, J. A., Tager, J. M. & Schram, A. W. Biosynthesis and maturation of glucocerebrosidase in Gaucher fibroblasts. *Eur. J. Biochem.* **164**, 171–179 (1987).
 37. Tol, M. J., van der Lienden, M. J. C. C., Gabriel, T. L., Hagen, J. J., Scheij, S., *et al.* HEPES activates a MiT/TFE-dependent lysosomal-autophagic gene network in cultured cells: a call for caution. *Autophagy* **14**, 1–13 (2018).
 38. Ben Bdira, F., Kallemeyjn, W. W., Oussoren, S. V., Scheij, S., Bleijlevens, B., Florea, B. I., Van Roomen, C. P. A. A., Ottenhoff, R., Van Kooten, M. J. F. M., Walvoort, M. T. C., Witte, M. D., Boot, R. G., Ubbink, M., Overkleeft, H. S. & Aerts, J. M. F. G. Stabilization of glucocerebrosidase by active site occupancy. *ACS Chem. Biol.* **12**, 1830–1841 (2017).
 39. Jiang, J., Kuo, C. L., Wu, L., Franke, C., Kallemeyjn, W. W., Florea, B. I., Van Meel, E., Van Der Marel, G. A., Codée, J. D. C., Boot, R. G., Davies, G. J., Overkleeft, H. S. & Aerts, J. M. F. G. Detection of active mammalian GH31 α -glucosidases in health and disease using in-class, broad-spectrum activity-based probes. *ACS Cent. Sci.* **2**, 351–358 (2016).
 40. Wu, L., Jiang, J., Jin, Y., Kallemeyjn, W. W., Kuo, C. L., Artola, M., Dai, W., Van Elk, C., Van Eijk, M., Van Der Marel, G. A., Codée, J. D. C., Florea, B. I., Aerts, J. M. F. G., Overkleeft, H. S. & Davies, G. J. Activity-based probes for functional interrogation of retaining β -glucuronidases. *Nat. Chem. Biol.* **13**, 867–873 (2017).
 41. Kuo, C., Kallemeyjn, W. W., Lelieveld, L. T., Mirzaian, M., Zoutendijk, I., Vardi, A., Futerman, A. H., Meijer, A. H., Spaink, H. P., Overkleeft, H. S., Aerts, J. M. F. G. & Artola, M. *In vivo* inactivation of glycosidases by conduritol B epoxide and cyclophellitol as revealed by activity-based protein profiling. *FEBS J.* **286**, 584–600 (2019).
 42. Artola, M., Kuo, C. L., Lelieveld, L. T., Rowland, R. J., Van Der Marel, G. A., Codée, J. D. C., Boot, R. G., Davies, G. J., Aerts, J. M. F. G. & Overkleeft, H. S. Functionalized cyclophellitols are selective glucocerebrosidase inhibitors and induce a bona fide neuropathic Gaucher model in zebrafish. *J. Am. Chem. Soc.* **141**, 4214–4218 (2019).
 43. Cook, S. R., Badell-Grau, R. A., Kirkham, E. D., Jones, K. M., Kelly, B. P., Winston, J., Waller-Evans, H., Allen, N. D. & Lloyd-Evans, E. Detrimental effect of zwitterionic buffers on lysosomal homeostasis in cell lines and iPSC-derived neurons. *AMRC Open Res.* **2**, 21 (2020).
 44. Liu, B., Palmfeldt, J., Lin, L., Colaço, A., Clemmensen, K. K. B. B., Huang, J., Xu, F., Liu,

- X., Maeda, K., Luo, Y. & Jäättelä, M. STAT3 associates with vacuolar H⁺-ATPase and regulates cytosolic and lysosomal pH. *Cell Res.* **28**, 996–1012 (2018).
45. Johnson, D. E., Ostrowski, P., Jaumouillé, V. & Grinstein, S. The position of lysosomes within the cell determines their luminal pH. *J. Cell Biol.* **212**, 677–692 (2016).
46. Heuser, J. Changes in lysosome shape and distribution correlated with changes in cytoplasmic pH. *J. Cell Biol.* **108**, 855–864 (1989).
47. Cabukusta, B. & Neefjes, J. Mechanisms of lysosomal positioning and movement. *Traffic* **19** 761–769 (2018).
48. Dekker, N., van Dussen, L., Hollak, C. E. M., Overkleeft, H., Scheij, S., Ghauharali, K., van Breemen, M. J., Ferraz, M. J., Groener, J. E. M., Maas, M., Wijburg, F. A., Speijer, D., Tylki-Szymanska, A., Mistry, P. K., Boot, R. G. & Aerts, J. M. Elevated plasma glucosylsphingosine in Gaucher disease: relation to phenotype, storage cell markers, and therapeutic response. *Blood* **118**, e118–27 (2011).
49. Kuo, C.-L., van Meel, E., Kytidou, K., Kallemeijn, W. W., Witte, M., Overkleeft, H. S., Artola, M. E. & Aerts, J. M. Activity-based probes for glycosidases: profiling and other applications. *Methods Enzymol.* **598**, 217–235 (2018).
50. Groener, J. E. M., Poorthuis, B. J. H. M., Kuiper, S., Helmond, M. T. J., Hollak, C. E. M. & Aerts, J. M. F. G. HPLC for simultaneous quantification of total ceramide, glucosylceramide, and ceramide trihexoside concentrations in plasma. *Clin. Chem.* **53**, 742–747 (2007).
51. Mirzaian, M., Wisse, P., Ferraz, M. J., Gold, H., Donker-Koopman, W. E., Verhoek, M., Overkleeft, H. S., Boot, R. G., Kramer, G., Dekker, N. & Aerts, J. M. F. G. Mass spectrometric quantification of glucosylsphingosine in plasma and urine of type 1 Gaucher patients using an isotope standard. *Blood Cells, Mol. Dis.* **54**, 307–314 (2015).

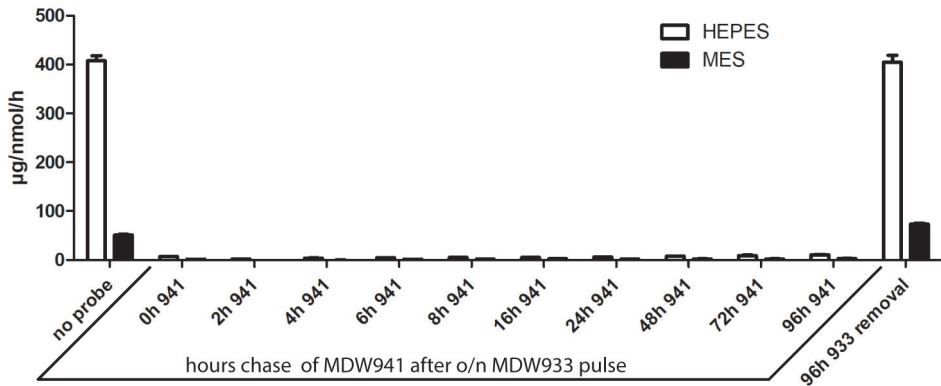
Supplemental Figures



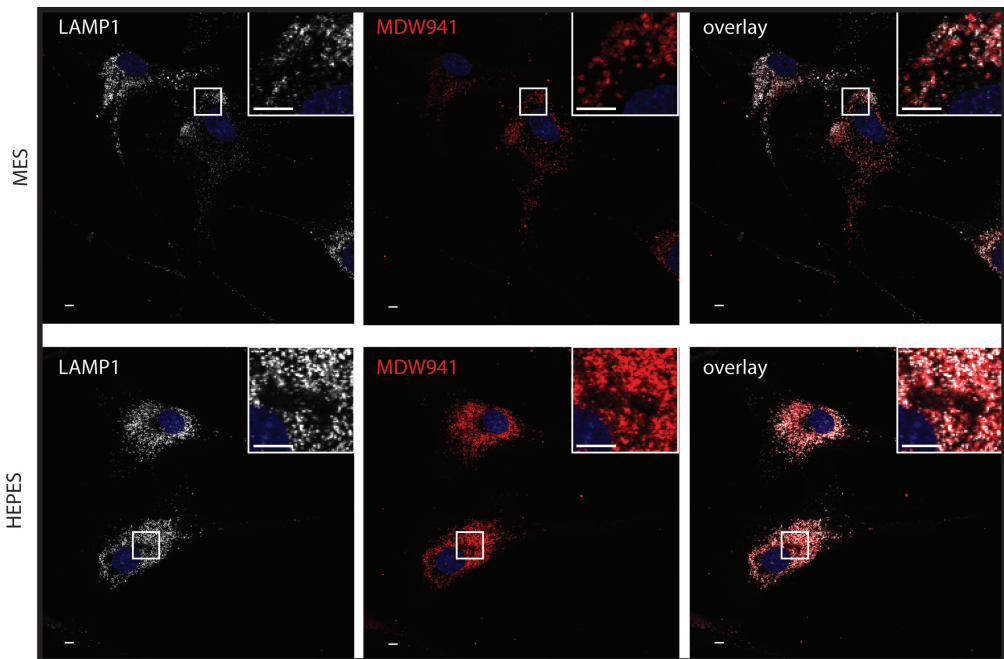
Supplemental figure 1. Impact of the presence of 50 mM MES, MOPS and HEPES in medium on GCase in cultured fibroblasts and RAW264.7 cells. GCase in aliquots of the same lysates was labelled with GCase-specific ABP and subsequently visualized by fluorescence scanning after SDS-PAGE.



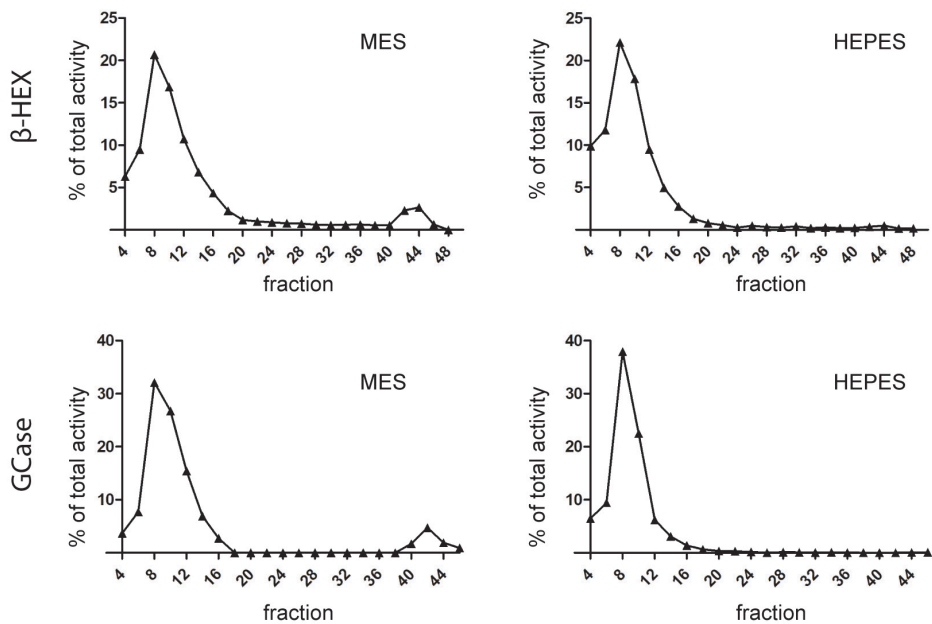
Supplemental figure 2. Reversible vacuolization upon HEPES exposure of RAW264.7 cells over time. RAW264.7 cells were cultured in the presence of HEPES (50mM) for 0-96h and visualized over time by phase contrast microscopy. Cells were subsequently washed, and medium was replaced by MES (50mM) containing medium for 96h and captured by phase contrast microscopy.



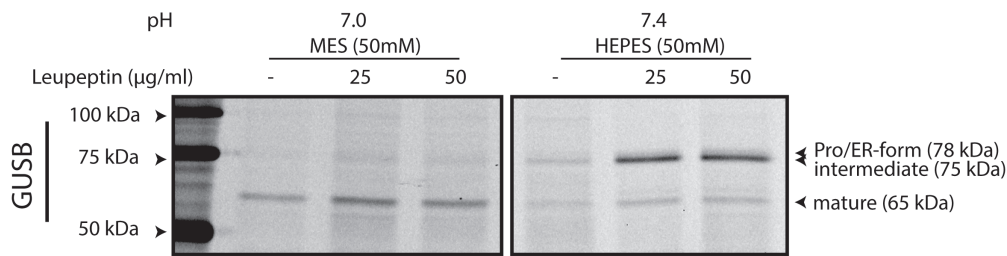
Supplemental figure 3. Inhibition of GCase in pulse (MDW933)-chase (MDW941) experiments as measured by 4 MU-assay. Pulse-chase experiments with HEPES and MES treated RAW264.7 cells, performed as described in M&M. Following pre-labeling with MDW933 (green fluorescent), cells were incubated continuously with MDW941 (red fluorescent) for indicated time periods. Basal GCase activity was assessed in samples left untreated with probes. Recovery of GCase after block was assessed by applying pulse (MDW933) and subsequent culturing without probe for 96h. Cells were harvested and lysed for enzyme activity measurements using fluorogenic substrate for GCase as described in M&M.



Supplemental figure 4. Immunofluorescence analysis of LAMP1 in fibroblasts exposed to MES or HEPES. Cells were pretreated ABP MDW941 to label GCase and subsequently fixed and analyzed by immunohistochemistry to establish overlap of GCase with other marker proteins. Scale bar: 10µm



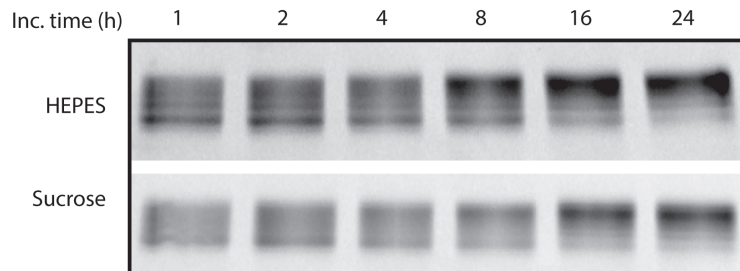
Supplemental figure 5. Subcellular fractionation of fibroblasts cultured in the presence of 50 mM HEPES or MES. Normal human derived fibroblasts (NHDFs) were fractionated and compartments were separated on the basis of density using 49% Percoll centrifugation to generate density gradients. In collected fractions enzymatic activities of GCase and β -hexosaminidase were measured as described in M&M.



Supplemental figure 6. Impact of leupeptin and medium pH on β -glucuronidase (GUSB). Fibroblasts were cultured in the presence of 50 mM buffer compound (MES or HEPES) simultaneously with 72h hour incubation with different concentrations leupeptin. Cells were harvested and GAA and GUSB in lysates was visualized by ABP labeling, SDS-PAGE and fluorescence scanning.

Supplemental Table 1. Glucosylsphingosine (GlcSph) content of fibroblasts cultured in the absence or presence of 25 mM HEPES. Values expressed as mean \pm SD on three independent cell cultures and triplicate measurements.

Fibroblasts	GlcSph (pmol/mg total protein of cell lysate)	
	no HEPES	+ 25 mM HEPES (pH 7.4)
Control wt GBA	<0.3	<0.3
Control wt GBA	<0.3	<0.3
N370S/L444P GBA	1.3 \pm 0.4	4.2 \pm 1.2
N370S/L444P GBA	0.9 \pm 0.3	3.3 \pm 0.6
N370 S/N370S GBA	0.7 \pm 0.3	1.4 \pm 0.5
L444P/L444P GBA	2.5 \pm 0.4	2.4 \pm 0.8



Supplemental figure 7. Sucrose induced changes in GCase glycan isoform profile. RAW264.7 cells were cultured in the presence of 80 mM Sucrose for different amounts of time. Cells were harvested and GCase in lysates was visualized by ABP labeling, SDS-PAGE and fluorescence scanning.

Chapter 3

Localization of active endogenous and exogenous GBA by correlative light-electron microscopy in human fibroblasts

Manuscript published as:

Van Meel, E., Bos, E., **van der Lienden, M. J. C.**, Overkleeft, H. S., van Kasteren, S. I., Koster, A. J. & Aerts, J. M. F. G. Localization of active endogenous and exogenous β -glucocerebrosidase by correlative light-electron microscopy in human fibroblasts. *Traffic* **20**, 346–356 (2019).

Abstract

β -Glucocerebrosidase (GBA) is the enzyme that degrades glucosylceramide in lysosomes. Defects in GBA that result in overall loss of enzymatic activity give rise to the lysosomal storage disorder Gaucher disease, which is characterized by the accumulation of glucosylceramide in tissue macrophages. Gaucher disease is currently treated by infusion of mannose receptor-targeted recombinant GBA. The recombinant GBA is thought to reach the lysosomes of macrophages, based on the impressive clinical response that is observed in Gaucher patients (type 1) receiving this enzyme replacement therapy. In this study, we used cyclophellitol-derived activity-based probes with a fluorescent reporter that irreversibly bind to the catalytic pocket of GBA, to visualize the active enzymes in a correlative microscopy approach. The uptake of pre-labeled recombinant enzyme was monitored by fluorescence and electron microscopy in human fibroblasts that stably expressed the mannose receptor. The endogenous active enzyme was simultaneously visualized by *in situ* labeling with the activity-based probe containing an orthogonal fluorophore. This method revealed the efficient delivery of recombinant GBA to lysosomal target compartments that contained endogenous active enzyme.

Introduction

The lysosomal acid β -glucosidase, β -glucocerebrosidase (GBA, EC 3.2.1.45), is essential to the catabolism of glycosphingolipids in lysosomes as it removes the β -D-glucopyranose group from glucosylceramide. The enzyme encoded by the *GBA* gene is synthesized as a 497 amino acid protein in the endoplasmic reticulum. While the majority of the lysosomal enzymes are modified with the mannose 6-phosphate recognition marker to mediate their transport from the biosynthetic pathway to the lysosomes, GBA does not contain phosphomannosyl residues.¹⁻³ Instead, GBA is routed via a mannose 6-phosphate independent targeting pathway, by binding to the lysosomal membrane protein, LIMP II.⁴ LIMP II interacts with newly synthesized GBA at the site of the endoplasmic reticulum. After passage through the Golgi complex, the LIMP II-GBA complex is directed to endosomes and lysosomes, likely through a dileucine-based sorting motif in its C-terminal cytosolic tail.^{5,6} The importance of LIMP II is evident as individuals with LIMP II deficiency develop progressive myoclonic epilepsy with glomerulosclerosis and neurological manifestations, named action myoclonus-renal failure syndrome (AMRF).^{7,8} In AMRF, mutations in the *SCARB2* gene encoding LIMP II cause the failure of normally synthesized GBA to interact with LIMP II. As a result, GBA is secreted from the cells, leading to reduced lysosomal levels of the enzyme in various cell types.^{4,7,9,10}

Mutations in *GBA* result in a prominent loss of GBA in lysosomes and cause the autosomal recessive lysosomal storage disorder Gaucher disease.¹¹ Gaucher disease is characterized by the accumulation of the substrate glucosylceramide in tissue macrophages.¹² The clinical manifestations of the disease are remarkably variable, but usually include enlargement of the liver and spleen, infiltration of the bone marrow by storage macrophages, thrombocytopenia, anemia and bone disease, and can include neurological symptoms. Currently approved treatments are substrate reduction therapy aiming to reduce substrate buildup in macrophages and enzyme replacement therapy (ERT), in which human recombinant GBA (hrGBA) is administered intravenously. To mediate uptake by macrophages, hrGBA is modified to expose its mannose moieties, which bind to the mannose receptor (Man-R) present at the surface of these cells. Endocytosis of the Man-R delivers hrGBA to the endo-lysosomal system.

The development of activity-based probes (ABPs) that covalently and irreversibly tag GBA with high sensitivity and almost complete selectivity has allowed the ultra-sensitive visualization of active GBA molecules *in vitro* and *in vivo* in cells and organisms.¹³ These cyclophellitol-derived ABPs react with the catalytic nucleophile Glu340 of GBA to form an enzyme-substrate complex, linked through an ester bond that is stable under native physiological conditions. When applied to the cell culture medium, the ABPs rapidly enter the cells, a process that appears independent of endocytosis¹³, and bind to the intracellular pools of GBA. The presence of a fluorescent reporter allows the detection by light microscopy.¹³ As fluorescence microscopy does not provide information about the underlying ultrastructure, in this study a correlative light and electron microscopy (CLEM) approach was employed to allow the more detailed localization of active GBA. Moreover, the cellular fate of hrGBA following binding to the Man-R was investigated. The uptake of ABP-prelabeled hrGBA was monitored while simultaneously visualizing the endogenous enzyme by using ABPs with different fluorescent reporters. Light microscopy showed co-localization of endocytosed and endogenous GBA, but also distinct punctae

for either endocytosed or endogenous enzyme. By CLEM, the endogenous GBA was localized to lysosomes, where it showed substantial overlap with endocytosed hrGBA. Of note, some lysosomes did not appear to be reached by hrGBA during the course of the experiment. In addition, the endocytosed enzyme was detected in earlier compartments of the endo-lysosomal system that showed no detectable endogenous GBA. This method will be valuable in determining the efficiency of ERT for Gaucher disease and potentially other lysosomal storage diseases.

Results

GBA was readily detected in normal human dermal fibroblasts (NHDFs) by fluorescence microscopy upon *in situ* labeling with the ABP, MDW941 (**Figure 1**), consistent with previous observations by our lab.¹³ Under these conditions, approximately 50% of total GBA was labeled, as determined by GBA activity assays. Pre-incubation with conduritol B epoxide (CBE) for 16h prior to the *in situ* labeling with MDW941, which should block the active site of all available GBA molecules¹⁴, resulted in no detectable signal (**Supplemental figure 1**), neither was any signal detected upon DMSO or CBE incubation in the absence of probe (**Supplemental figure 1**). These data indicate that the fluorescent signal does not represent unbound, endocytosed probe and is specific to active GBA. Importantly, *in situ* labeled GBA showed clear overlap with total GBA as detected by confocal immunofluorescence microscopy after staining with antibodies to GBA (**Figure 1**, upper panels, **Supplemental figure 2**). Significant overlap was also detected with the late endosomal/lysosomal marker LAMP-1, although not all LAMP-1-containing compartments appeared positive for GBA (**Figure 1**, lower panels, **Supplemental figure 2**). Loading of the late compartments of the endo-lysosomal system with the endocytic tracer dextran-FITC (3h pulse, 6h chase), resulted in substantial co-localization with MDW941, although not all MDW941 positive punctae contained dextran (**Supplemental figure 3**).

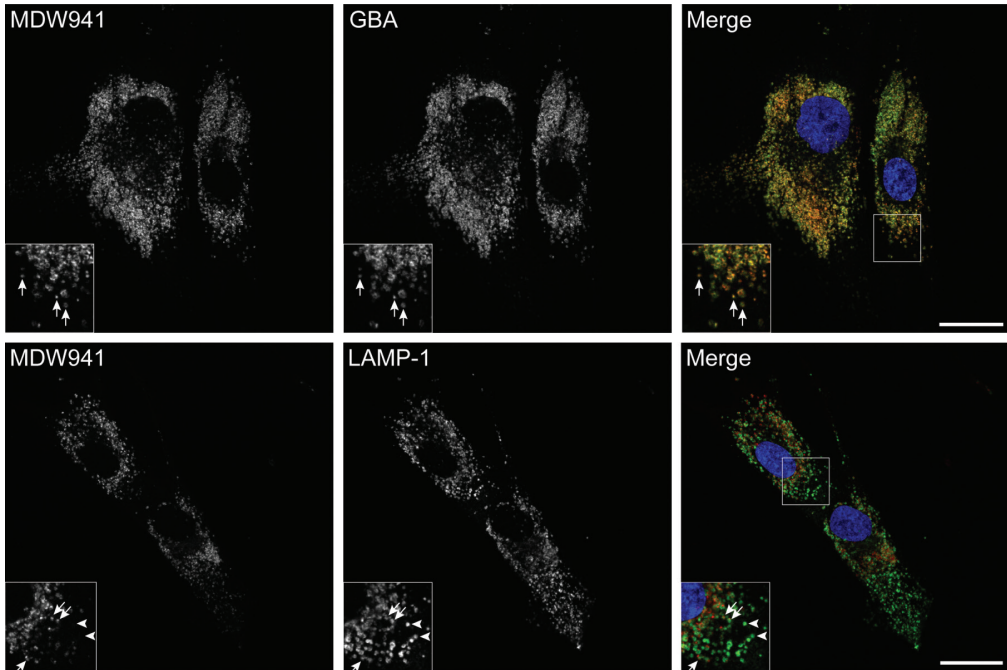


Figure 1: Active GBA accumulates in late endosomes and lysosomes. *In situ* labeling of active GBA in NHDFs with 5 nM MDW941 for 2h shows a punctate staining pattern (red) by confocal fluorescence microscopy. Significant overlap is observed with total GBA (see arrows in insets upper panels, green) and the late endosomal/lysosomal marker LAMP-1 (see arrows in insets lower panels, green) upon immunostaining with specific antibodies. The arrowheads show LAMP-1 positive compartments that contain no detectable levels of MDW941. Nuclei were stained with DAPI (blue). Scale bars, 25 μ m.

To identify the endo-lysosomal compartments that accumulated active GBA, a correlative microscopy approach was applied. First, GBA was *in situ* labeled as in the previous experiments, after which the cells were fixed, gelatin embedded and prepared for electron microscopy according to the Tokuyasu technique.¹⁵ The ultrathin cryosections on grids were first mounted on glass slides with 50% glycerol to allow their imaging by confocal microscopy. This revealed the presence of numerous fluorescent punctae per cell profile (**Figure 2A**). Subsequently, the sections were contrasted and embedded with uranyl acetate/methylcellulose and imaged with an electron microscope. Overlay of the fluorescent images and electron micrographs showed that most of the fluorescent signal localized to membrane-bound compartments (**Figure 2B, C**), while the CBE-pre-treated and DMSO-treated sections showed no fluorescent signal. The membrane-bound compartments mainly represented lysosomes, as identified by the presence of the characteristic internal membrane sheets and their electron dense appearance (**Figure 2D, E**). The earlier compartments of the endo-lysosomal system, the endosomes, characterized by their more electron lucent appearance and intraluminal vesicles and the absence of internal membrane sheets, occasionally showed low levels of active GBA, but in most cases the signal was below the detection limit (**Figure 2D, E**). These data indicate that the majority of the active GBA molecules in fibroblasts reside in the lysosomes.

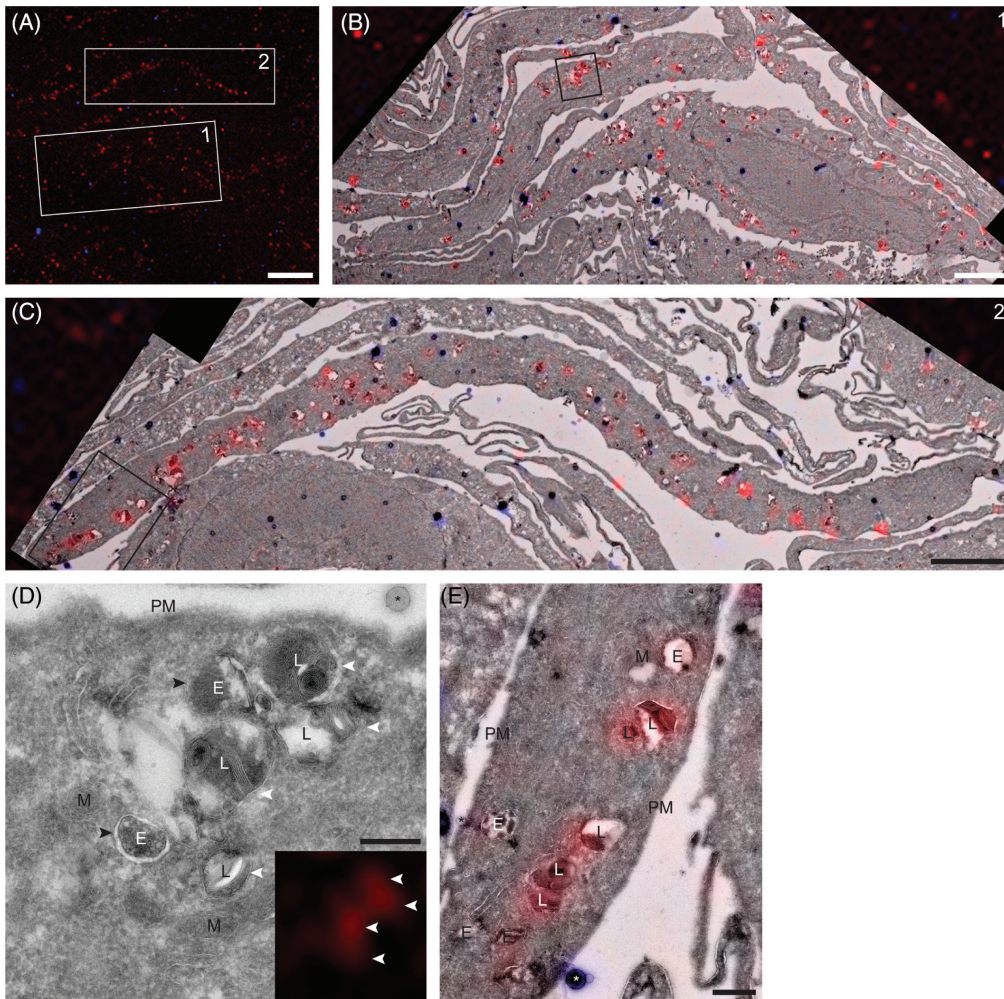


Figure 2: Correlative microscopy shows the accumulation of active GBA in lysosomes of NHDFs. (A) Confocal fluorescence image of an ultrathin cryosection of NHDFs in situ labeled with MDW941 for 2h at 5 nM. The red punctae represent active GBA (MDW941), while the blue dots represent fluorescent electron dense beads used for correlation of the images. Scale bar, 10 μ m. Merged fluorescence and electron microscopy images of boxed areas 1 and 2 are shown in (B) and (C), respectively. Scale bars, 3 μ m. (D, E). Magnifications of boxed areas in (B) and (C), respectively. MDW941 (red), which labels active GBA, is present in lysosomes. E, endosome; L, lysosome; M, mitochondrion; PM, plasma membrane; *, bead used for correlation. The white arrowheads indicate lysosomes positive for MDW941, recognized by the internal membrane sheets, while the black arrowheads indicate endosomes negative for the ABP. Scale bars, D, 250 nm; E, 500 nm.

To allow the efficient internalization of hrGBA by human fibroblasts, cell lines were generated that stably express the mannose receptor (Man-R) with a C-terminal V5 tag. In this way, the uptake of hrGBA by the modified fibroblasts mimics the mode of uptake by tissue macrophages, which express Man-R at their surface. Fibroblasts that were obtained from a patient homozygous for the nonsense mutation p.W178X⁷ contained no detectable levels of LIMP II by Western blotting (Figure 3A). As a result, the intracellular level of

GBA was significantly reduced. In control fibroblasts, three bands were detected for GBA by Western blotting (**Figure 3A**), i.e. the complex glycosylated form, the ER form and the late endosomal/lysosomal form.¹⁶ In the LIMP II^{-/-} cells low levels of the ER form were detected (**Figure 3A**) and the intracellular GBA activity was reduced to approximately $5 \pm 0.9\%$ of the level in control fibroblasts (**Figure 3B**). These findings are consistent with the absence of the lysosomal targeting receptor LIMP II, which results in the increased secretion of GBA by these cells. Lentiviral transduction of both NHDFs and LIMP II^{-/-} fibroblasts with *MRC1* resulted in the expression of the Man-R as determined by anti-V5 immunoblotting (**Figure 3A**) and immunofluorescence microscopy (**Supplemental figure 4**), with the LIMP II^{-/-} cells containing slightly higher expression levels of Man-R than the NHDFs.

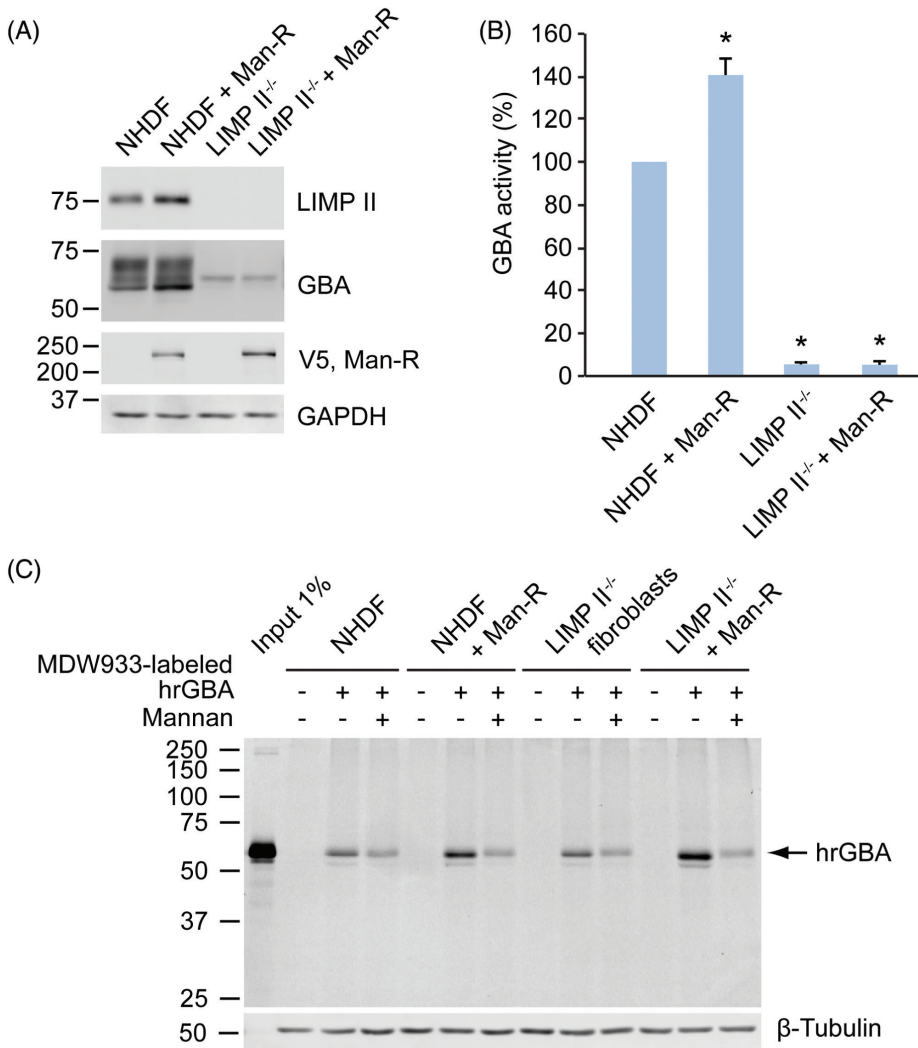


Figure 3: Man-R expressing fibroblasts endocytose increased amounts of MDW933-labeled hrGBA. A. NHDFs and LIMP II^{-/-} fibroblast lysates with or without Man-R with a V5-tag were subjected to SDS-PAGE and immunoblotting. No detectable levels of LIMP II are present in the LIMP

II^{-/-} cells, while the levels of GBA are significantly reduced (lane 3 and 4). The Man-R is expressed in the control and LIMP *II^{-/-}* fibroblast lines (lane 2 and 4), as detected with an antibody to the V5 tag. GAPDH shows equal protein loading. **B.** GBA activity in the various cell lines as determined with 4-methylumbelliferyl-coupled specific substrate. The values are averages of 3 independent experiments \pm standard deviations, with the activity in NHDFs set to 100%. The activity in LIMP *II^{-/-}* fibroblast lines is ~5% of NHDFs, while the Man-R expressing NHDFs show a somewhat increased activity. * $p < 0.01$. **C.** Representative wet slab gel of at least 3 independent experiments shows the increased uptake of hrGBA by Man-R expressing NHDFs and LIMP *II^{-/-}* fibroblasts, as compared to the Man-R negative fibroblasts. The addition of mannan reduces the hrGBA uptake to the same levels in all four cell lines, likely representing the uptake by non-specific, fluid-phase endocytosis. 1% of total MDW933-hrGBA that was added to the culture medium (input) was loaded for comparison. β -tubulin shows equal protein loading.

Subsequently, hrGBA was *in vitro* labeled with MDW933 (an ABP functionalized with a green fluorescent BODIPY dye ¹³) and, after the removal of unreacted ABP (**Supplemental figure 5**), added to the culture medium to follow its uptake in the various cell lines. A 6h-incubation with MDW933-hrGBA resulted in the enhanced internalization of hrGBA by fibroblasts that expressed the Man-R, both NHDFs and LIMP *II^{-/-}*, as compared to those that did not express the receptor (**Figure 3C**). Somewhat higher levels of hrGBA were observed in the LIMP *II^{-/-}* cells as compared to the NHDFs, which is likely due to the higher levels of Man-R present in the former, resulting in increased uptake. Competition with mannan, to block the Man-R, reduced the uptake to the same level in all cell lines. This level likely reflects the uptake by fluid-phase endocytosis. The effect of mannan that was observed in NHDFs and LIMP *II^{-/-}* fibroblasts that did not overexpress the Man-R might be caused by the block of another lectin responsible for hrGBA internalization, as these cells are unlikely to express the Man-R endogenously.

To visualize the delivery of hrGBA to the intracellular target compartments and find out whether it reaches the lysosomes that contain active GBA, MDW933-labeled hrGBA was applied to the culture medium of the four different cell lines, while endogenous GBA was labeled simultaneously with MDW941. Analysis by SDS-PAGE showed labeling of the endogenous enzyme with the red probe in NHDFs, identified as two bands representing the complex glycosylated and lysosomal forms of GBA (**Figure 4**). In LIMP *II^{-/-}* fibroblasts the GBA levels were in most instances too low to be detected by this method (**Figure 4**). Importantly, uptake of MDW933-labeled hrGBA did not result in significant cross-labeling of the endogenous enzyme due to unreacted MDW933, as only a single band was labeled with MDW933, representing hrGBA. In addition, the signal for MDW941 had a similar intensity in the lanes with or without MDW933-hrGBA. Likewise, no cross-labeling of internalized hrGBA with MDW941 appeared to occur.

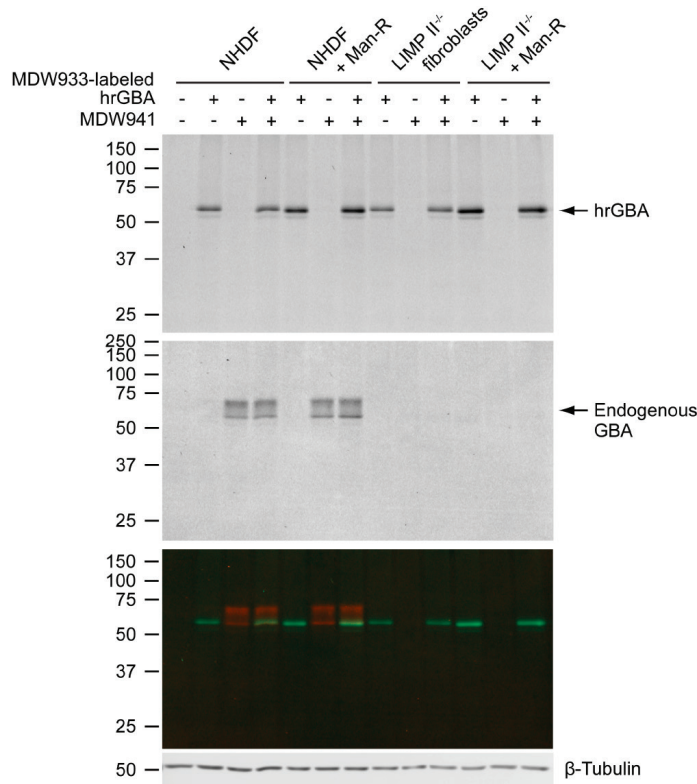


Figure 4. Simultaneous uptake of ABP-labeled hrGBA and labeling of the active endogenous enzyme. The four different fibroblast cell lines were allowed to take up 2 $\mu\text{g/mL}$ MDW933-hrGBA for 6h, while endogenous GBA was in situ labeled during the final 2h with MDW941. A representative wet slab gel shows endocytosed hrGBA (upper panel, scanned green channel MDW933) and labeled endogenous GBA (middle panel, scanned red channel MDW941). The lower panel shows the overlay of the two channels. While endogenous GBA is readily detected in NHDFs, the signal is too low in LIMP II^{-/-} fibroblasts. β -tubulin shows equal protein loading.

Subsequently, the same experimental set-up was used in confocal fluorescence microscopy. The Man-R expressing cells represented a heterogeneous population, as they expressed varying levels of receptor. While the signal for MDW933-labeled hrGBA was below the detection level in all cells without Man-R, a punctate staining pattern was observed in NHDFs that expressed sufficient levels of Man-R (**Figure 5**, upper panels). These punctae significantly overlapped with endogenous GBA as visualized with MDW941, suggesting the delivery of hrGBA to lysosomes. However, some punctae were mainly positive for either hrGBA or endogenous GBA (see insets **Figure 5**, **Supplemental figure 2**). A similar result was observed in NHDFs that were immunostained for LAMP-1 after the 6h-uptake with hrGBA (**Supplemental figure 6**). There was a significant overlap of hrGBA and LAMP-1, in addition to LAMP-1-positive compartments that did not contain detectable levels of hrGBA. Importantly, no signal for MDW933-hrGBA could be visualized after uptake in the presence of mannan, which further suggests that no cross-labeling of endogenous GBA occurred with MDW933. As expected, endogenous GBA failed to be detected in the LIMP II^{-/-} fibroblasts (**Figure 5**, middle panels). However,

uptake of MDW933-labeled hrGBA resulted in a punctate pattern that showed partial overlap with LAMP-1 (**Figure 5**, lower panels, see insets, **Supplemental figure 2**). These data suggest that hrGBA is delivered to late endosomes/lysosomes in the absence of LIMP II.

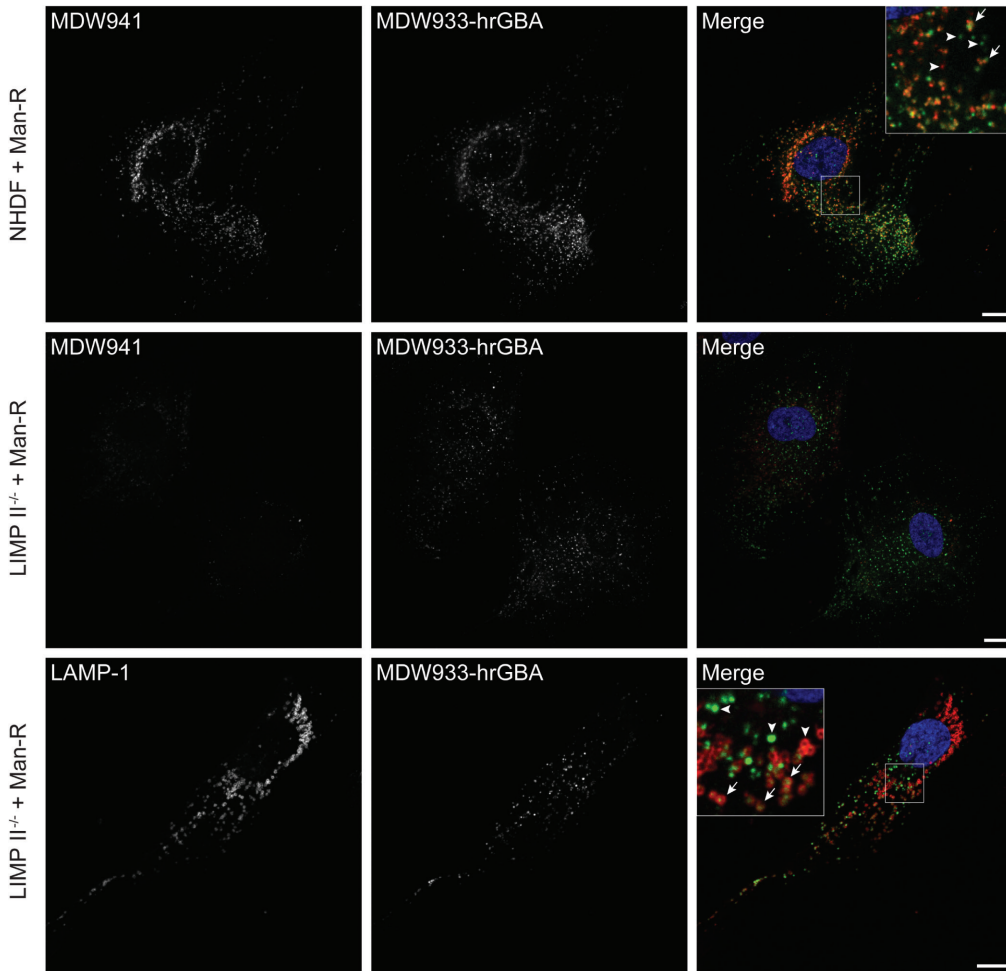


Figure 5: Endocytosed hrGBA partially co-localizes with active GBA and LAMP-1. Confocal fluorescence microscopy of NHDFs and LIMP II^{-/-} fibroblasts expressing the Man-R after a 6h uptake of 2 μg/mL MDW933-hrGBA (green) and 2h in situ labeling of endogenous GBA (red) with 5 nM MDW941 (upper and middle panels) or immunofluorescent staining of LAMP-1 (red, lower panels; see also Supplemental figure 4 for LAMP-1 staining in NHDFs). Substantial co-localization was observed in NHDFs between endocytosed hrGBA and endogenous GBA (see arrows in inset upper panels). In LIMP II^{-/-} fibroblasts, the endocytosed enzyme reached a portion of the LAMP-1 positive compartments (arrows in inset lower panels). The arrowheads indicate compartments positive for either endocytosed hrGBA or endogenous GBA/LAMP-1. Scale bars, 10 μm.

With CLEM the nature of the various fluorescent punctae could be identified. As the uptake of labeled hrGBA was continuous for 6h, we anticipated that the hrGBA-containing punctae would represent both early and late compartments of the endo-lysosomal system. Consistent with this prediction, hrGBA was present in endosomes, as well as in lysosomes

(Figure 6A-D). Significant overlap was observed between endocytosed and endogenous GBA in lysosomes (Figure 6E). Interestingly, some lysosomes appeared to be negative for endocytosed hrGBA (Figure 6E). In agreement with the previous data, no endogenous GBA was detected by CLEM in the LIMP II^{-/-} fibroblasts. However, endocytosed hrGBA was delivered to the endosomes and lysosomes (Figure 7), suggesting that the absence of LIMP II does not have a major effect on the lysosomal delivery of GBA upon endocytosis.

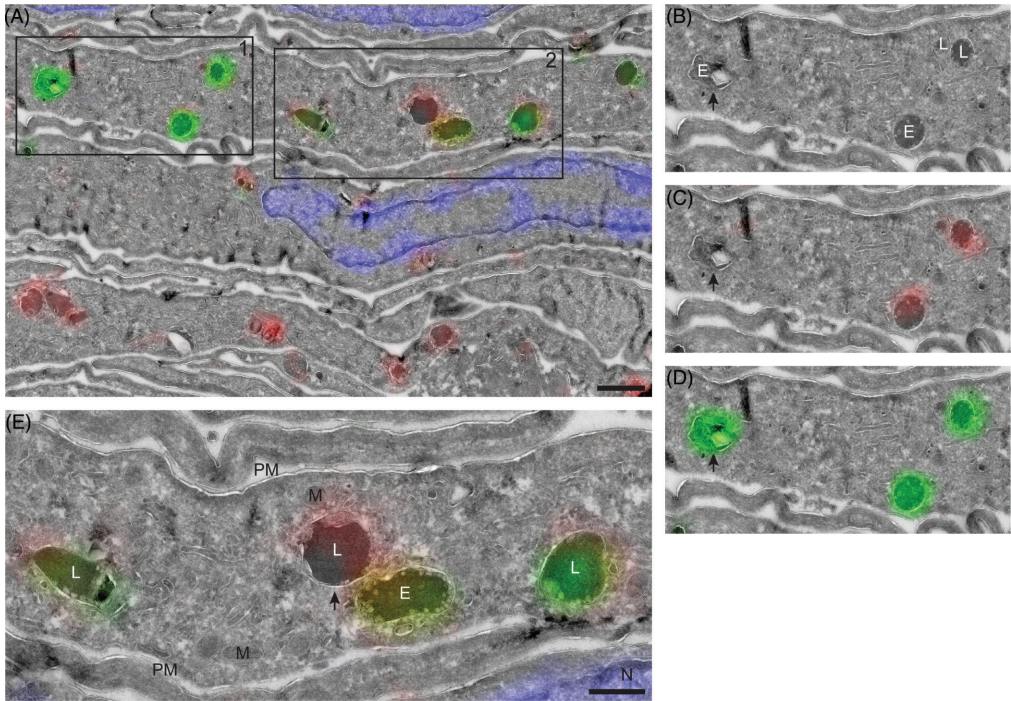


Figure 6: hrGBA is delivered to GBA-containing lysosomes in NHDFs as determined by CLEM. (A-E). Overlay of electron micrograph and confocal fluorescence image of an ultrathin cryosection of NHDFs expressing the Man-R. The cells were allowed to take up MDW933-labeled hrGBA (green) for 6h, while endogenous GBA was labeled by adding MDW941 to the culture medium at a concentration of 5 nM for 2h (red). Nuclei were stained with DAPI (blue). Scale bar in A, 1 μ m. (B-D). Magnification of boxed area 1 from A. E, endosome; L, lysosome. The arrow indicates an endosome that contains endocytosed hrGBA (green). The lysosomes contain both endocytosed hrGBA and endogenous enzyme (red). (E). Magnification of boxed area 2 from A showing lysosomes with both endocytosed hrGBA (green) and endogenous GBA (red). One lysosome (arrow) contains mainly the endogenous enzyme. M, mitochondrion; PM, plasma membrane. Scale bar, 500 nm.

Discussion

In this study we have presented a correlative microscopy technique that combines the use of ABPs, for the detection of active lysosomal enzyme by fluorescence microscopy, with electron microscopy. This allows the visualization of the positive structures at high resolution. The cyclophellitol-derived ABPs that irreversibly bind to the active site of the lysosomal β -glucosidase GBA, readily penetrate through the cellular membranes, which provides the great benefit that they can be applied to living cells.¹³ In our approach, *in situ*

labeling of human fibroblasts with ABP, equipped with a fluorescent tag, was followed by fixation and sample preparation according to the Tokuyasu technique.^{15,17} The ultrathin cryosections were directly imaged for their fluorescent signal by confocal microscopy, without the need of on-section labeling reactions that could increase background signals or influence the sensitivity of detection. The subsequent imaging by electron microscopy provides a relatively straightforward technique to localize the active enzyme to distinct subcellular compartments.

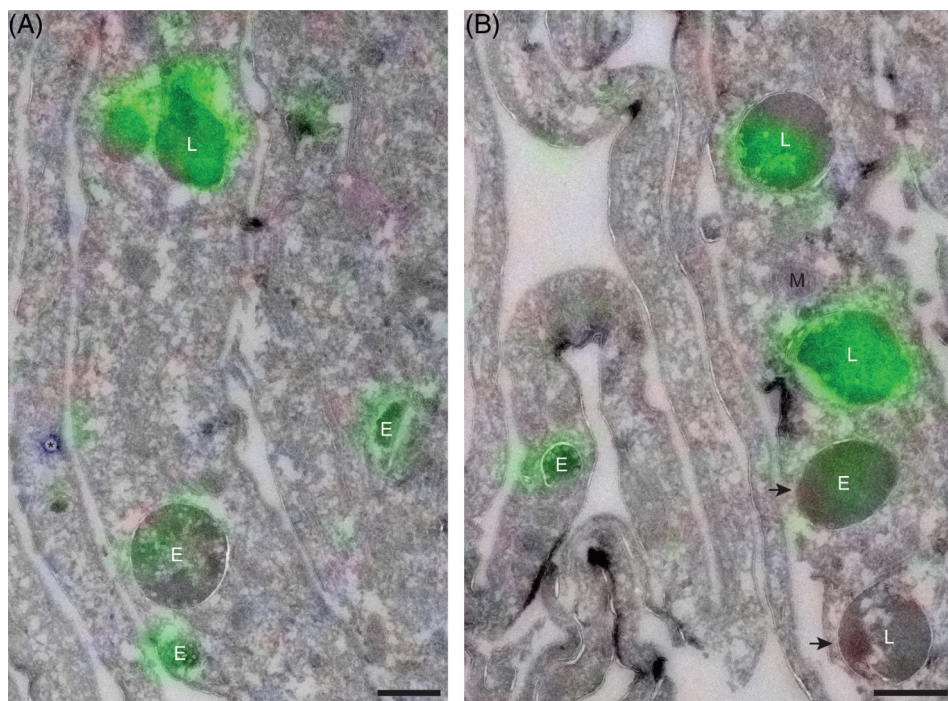


Figure 7: hrGBA is delivered to lysosomes in *LIMP II^{-/-}* fibroblasts as determined by CLEM. (A, B). Overlay of electron micrograph and confocal fluorescent image of an ultrathin cryosection showing *LIMP II^{-/-}* fibroblasts + Man-R, after a 6h-uptake of MDW933-labeled hrGBA (green) and in situ labeling of endogenous GBA (red, not detected). Nuclei were stained with DAPI (blue). Both endosomes (E) and lysosomes (L) are positive for hrGBA, however, not all of them are reached (arrows). M, mitochondrion; *, bead used for correlation. Scale bars, 500 nm.

This correlative approach to localize GBA resulted in the detection of active enzyme mainly in lysosomes. By confocal fluorescence microscopy, the ABP co-localized well with our antibody to GBA and was blocked by pre-incubation with the inhibitor CBE, showing the specificity of GBA labeling. In addition, the ABP co-localized significantly with the lysosomal membrane protein LAMP-1, which is present in late endosomes and lysosomes.^{18,19} By CLEM we were able to determine that the highest levels of active GBA were present in lysosomes, based on the morphological characteristics of these compartments, while endosomes appeared negative. Thus the LAMP-1-containing, ABP-negative compartments most likely represent late endosomes with GBA levels below the detection limit.

Subsequently, we aimed to follow the uptake of recombinant GBA and relate it to the localization of the endogenous enzyme using two-color CLEM. To this end, hrGBA was *in vitro* labeled with ABP containing a green fluorophore, while the endogenous pool of GBA was *in situ* labeled with a red ABP. By confocal fluorescence microscopy we observed a significant overlap of green and red fluorescent signals, while there were also punctae positive for either fluorophore. Correlative microscopy showed that the overlapping green/red signals localized to lysosomes, while the green dots represented early and late endosomes containing hrGBA and the red dots lysosomes that had not been reached by endocytosed hrGBA. The observation that many, but not all lysosomes were reached by endocytosed hrGBA could be a technicality due to the imaging of sections instead of intact cells, or other factors such as the duration of uptake. Alternatively, an interesting possibility could be that there are different populations of lysosomes, some more and others less accessible by endocytosis.

Altogether, the imaging of GBA with ABPs in this correlative microscopy approach resulted in the localization of the enzyme to specific subcellular compartments, without the need for additional labeling.^{20,21} This method could be applied to model organisms as well, as these ABPs can be delivered to various tissues upon intravenous or intracerebroventricular injection in rodents.^{13,22} Moreover, correction of lysosomal enzyme deficiency by ERT is presently pursued for several other lysosomal storage disorders, such as Fabry disease and Pompe disease, which are caused by deficiency of lysosomal α -galactosidase A (GLA) and lysosomal α -glucosidase (GAA), respectively.²³⁻²⁵ As ABPs have already been designed for GLA and GAA^{26,27}, this method might be applied to analyze the targeting of these expensive drugs. Finally, mutations in *GBA* have recently been recognized as a risk factor for multiple myeloma and carriers of one mutant *GBA* allele are more likely to develop Parkinsonism and Lewy body dementia.^{28,29} Extending our knowledge of this enzyme could be instrumental to the understanding of these, and possibly other, pathologies.

Material and Methods

Cell lines

Normal human dermal fibroblasts (NHDFs) were obtained from Lonza and LIMP II^{-/-} fibroblasts from a patient homozygous for the mutation c.533G>A, resulting in an early stop codon at W178.⁷ All cell lines were maintained in Dulbecco's Modified Eagle's Medium with 4.5 g/L glucose, sodium pyruvate and sodium bicarbonate (D6546, Sigma), supplemented with 10% (v/v) fetal bovine serum, 100,000 units/L penicillin, 100 mg/L streptomycin and 2 mM glutamax (Thermo Fisher Scientific Inc.) at 37°C in a 5% CO₂ humidified incubator.

NHDFs or LIMP II^{-/-} fibroblasts stably expressing the mannose receptor (Man-R) were generated by lentiviral transduction. Human spleen mRNA was used to amplify the human *MRC1* (*MRC1*, NM_002438.3) coding sequence by PCR using the following oligonucleotides: sense 5'-GGG GAC AAG TTT GTA CAA AAA AGC AGG CTT CGG TAC CAC CAT GAG GCT ACC CCT GC -3' and antisense 5'-GGG GAC CAC TTT GTA CAA GAA AGC TGG GTC GAT GAC CGA GTG TTC ATT CTG -3'. The fragment was cloned into pDNOR-221, and subsequently sub-cloned into pLenti6.3/TO/V5-DEST using the Gateway system (Invitrogen), generating a C-terminal V5 fusion protein. Due to toxicity of the construct in *E. coli* CopyCutter™ EPI400™ chemically competent *E. coli* cells were used according to the manufacturer's protocol (Epicentre). The full sequence was verified by DNA sequencing.

To produce lentiviral particles, HEK293T cells in 6-well plates were transfected at ~70% confluency with the envelope and packaging plasmids pMD2.G, pRSV, pMDL-RRE and pLenti6.3-MRC1 at a 1:1 ratio, 3 µg DNA in total, and 9 µg polyethylenimine (PEI 25K, Polysciences Inc.). The culture medium was replaced 16h after transfection with culture medium containing 20 mM HEPES and collected twice after a 24h incubation period. The culture medium containing viral particles was passed over a 0.45 µm filter and applied to the control and LIMP II^{-/-} fibroblast lines for 8-24h. Transduced cells were selected for by incubation with 2.5 µg/mL blasticidin (Sigma) containing culture medium for several weeks.

In situ labeling of GBA and fluorescence microscopy

Cells were grown to ~70% confluency on glass coverslips in 12-well plates. GBA was *in situ* labeled by adding MDW941 ('red', BODIPY 573/612) to the culture medium at a concentration of 5 nM. The cells were incubated for 2h in a humidified incubator at 37°C with 5% CO₂. Pre-incubation with CBE (Enzo Life Sciences Inc.) was performed at a concentration of 0.3 mM for 16h. Unlabeled cells were incubated with similar percentages (v/v) of DMSO. Uptake with FITC-CM-dextran (MW 70,000, Sigma) was performed at a concentration of 1 mg/mL for 3h (pulse). Subsequently, the cells were washed 5 times with PBS and incubated in culture medium for 6h (chase). *In situ* labeling with 5 nM MDW941 was performed during the last 2h of the chase.

At the end of the incubations, the cells were washed 3 times with PBS and fixed with 4% (w/v) formaldehyde (Sigma)/PBS for 30 minutes at RT. After the fixation, the cells were washed with PBS and distilled H₂O, after which they were either stained for immunofluorescence microscopy or mounted directly on a microscope slide with ProLong Diamond antifade reagent containing DAPI (Molecular Probes). Immunofluorescence

staining was performed as described.³⁰ Antibodies used were mouse anti-GBA monoclonal (8E4, generated in the Aerts lab) at dilution 1:500, rabbit anti-LAMP-1 (Abcam) at dilution 1:400, mouse anti-V5 (Invitrogen) at dilution 1:250 and Alexa Fluor conjugated IgGs (H+L) donkey anti-mouse Alexa 488 and donkey anti-rabbit Alexa 488 (Invitrogen). The cells were imaged under a Leica TCS SP8 confocal microscope with a 63x/1.40 NA HC Plan Apo CS2 oil immersion objective and equipped with a hybrid detector (HyD).

In vitro labeling of hrGBA with MDW933

hrGBA (Cerezyme) was a kind gift from Genzyme (Boston, MA). 5 μ L hrGBA at a concentration of 1 μ g/ μ L was incubated for 16h at 37°C with 40 μ L of 150 mM McIlvaine buffer pH=5.2, 0.2% (w/v) sodium taurocholate (Calbiochem), 0.1% (v/v) Triton X-100 and 2 μ M MDW933 ('green', BODIPY 493/503), while protected from the light. After the incubation, an aliquot was kept to confirm that the residual hrGBA activity was reduced >99% (see below). The remainder was passed over a protein desalting spin column, MWCO 7K (Thermo Scientific) according to the manufacturer's protocol, to remove any unreacted probe (see also **Supplemental figure 3**).

GBA activity assay

The enzymatic activity of hrGBA preparations or GBA in cell lysates was measured by incubating 10-20 μ L sample with 100 μ L substrate mix, which consisted of 3.75 mM 4-methylumbelliferyl β -D-glucopyranoside (Glycosynth Limited), 0.2% (w/v) sodium taurocholate (Calbiochem), 0.1% (w/v) BSA, 0.1% (v/v) Triton X-100 in 150 mM McIlvaine buffer pH=5.2, in a 96-well plate at 37°C. The reactions were stopped with 200 μ L 1 M glycine-NaOH pH=10.3 and read in an LS55 fluorescence spectrometer (PerkinElmer) at λ_{ex} 366 nm, λ_{em} 445 nm.

Uptake of MDW933-labeled hrGBA and in situ labeling of endogenous GBA

All uptake experiments were performed with 2 μ g/mL MDW933-labeled hrGBA for 6h. When indicated, MDW941 was added during the last 2h of the incubation at a concentration of 5 nM. To block uptake of hrGBA by the Man-R, mannan from *Saccharomyces cerevisiae* (Sigma) was added simultaneously at 3 mg/mL. At the end of the incubations, the cells were washed 3 times with PBS and either lysed (for the GBA activity assay/SDS-PAGE) or fixed for microscopy.

SDS-PAGE and Western blotting

Cells were lysed by the addition of ice-cold lysis buffer, i.e. 25 mM potassium phosphate buffer pH=6.5, 0.1% Triton X-100 and a protease inhibitor cocktail (cOmplete, Roche Diagnostics GmbH). Total protein concentration in the lysates was determined by the BCA protein assay (Pierce BCA protein assay kit, Thermo Fisher Scientific Inc.) in a 96-well plate format, according to the manufacturer's protocol. The samples were read in an EMax Plus microplate reader (Molecular Devices). Equal protein amounts (5 μ g) were resolved on 10% polyacrylamide gels and transferred onto 0.2 μ m nitrocellulose membranes (Amersham, GE Healthcare). Antibodies used were rabbit anti-LIMP II (Novus Biologicals), mouse anti-GBA (8E4, generated in the Aerts lab), rabbit anti-GAPDH (Cell Signaling), mouse anti-V5 (Invitrogen) and rabbit anti- β -tubulin (Cell

Signaling) and secondary antibodies used were donkey anti-rabbit Alexa Fluor 647 IgG (H+L) (Invitrogen), goat anti-mouse IgG (H+L)-HRP conjugate and goat anti-rabbit IgG (H+L)-HRP conjugate (BioRad). HRP-conjugated antibodies were visualized by chemiluminescence (Pierce ECL Plus Western blotting substrate, Thermo Fisher Scientific Inc.). The wet slab gels and immunoblots were scanned on a Typhoon FLA 9500 scanner (GE Healthcare).

Correlative microscopy

NHDFs were grown in 100 mm culture dishes to ~70% confluency. GBA was *in situ* labeled with 5 nM MDW941 for 2h at 37°C, either with or without pre-incubation with 0.3 mM CBE for 16h as a control for the specificity of the signal. To check for autofluorescence, one dish was incubated for 2h with a similar percentage (v/v) of DMSO. The uptake experiments were performed with NHDFs + Man-R and LIMP II^{-/-} fibroblasts + Man-R, with 2 µg/mL MDW933-labeled hrGBA for 6h. During the last 2h endogenous GBA was *in situ* labeled with 5 nM MDW941. As a control for the Man-R-specific uptake of MDW933-hrGBA, the uptake in NHDFs + Man-R, followed by the *in situ* labeling was performed in the presence of 3 mg/mL mannan.

At the end of the incubations, the culture medium was removed and the cells were washed 3 times quickly with culture medium at 37°C. Subsequently, the cells were fixed with 2% (w/v) formaldehyde + 0.2% glutaraldehyde (Electron Microscopy Sciences) in 0.1 M PHEM buffer for 2h at RT, while protected from the light. Embedding of the samples and cryosectioning was performed as described.¹⁵ For correlation purposes, fluospheresTM carboxylate-modified microspheres blue (350/440) with a diameter of 100 nm (Thermo Fisher Scientific Inc.) were added to the grids, which were coated with a formvar film, either before or after collection of the sections by incubating the grids for 2 minutes on the beads (1:2000 dilution of 2% solids). Subsequently, the sections were incubated on 2% gelatin for 30 minutes at 37°C and on 15 mM glycine/PBS for 10 minutes at RT. The nuclei were stained with 50 ng/mL DAPI (Sigma)/PBS for 5 minutes. After a quick wash with distilled H₂O, the ultrathin cryosections on titanium grids (Agar Scientific) were mounted on microscope glass slides in 50% glycerol/H₂O and imaged under a Leica TCS SP8 confocal microscope with a 63x/1.40 NA HC Plan Apo CS2 oil immersion objective. Immediately after imaging, the glycerol was removed from the grids by washing in distilled H₂O. The sections were contrasted with 1.8% methylcellulose/0.6% uranyl acetate/H₂O at pH=4.8 and analyzed in a FEI Tecnai 12 BioTwin electron microscope at 120 kV. Correlation of the images was performed using Adobe Photoshop CC 2015.5.

Labeling specificity in correlative microscopy

The specificity of the green and red fluorescent signals for hrGBA and endogenous GBA, respectively, was determined in the following way. First of all, the *in vitro* labeling reaction was optimized to label over 99% of hrGBA, which was confirmed by an enzymatic activity assay to result in near absence of hrGBA activity. In this way, cross-labeling of hrGBA with red ABP was prevented during the *in situ* labeling. Consistent herewith, no red ABP signal was detected in fibroblasts that lack GBA, due to a mutation in the receptor LIMP II, upon endocytosis of labeled hrGBA. Secondly, any unreacted green ABP was removed from the preparation before addition to the culture medium. SDS-PAGE analysis showed substantial reduction of unreacted ABP. Any remaining unreacted probe was not sufficient

to result in detectable cross-labeling of endogenous GBA as determined by SDS-PAGE of the cell lysates. Finally, the uptake of ABP-labeled hrGBA in the presence of mannan did not result in a detectable green fluorescent signal in the cells by microscopy, indicating that the endogenous enzyme was not labeled with green probe.

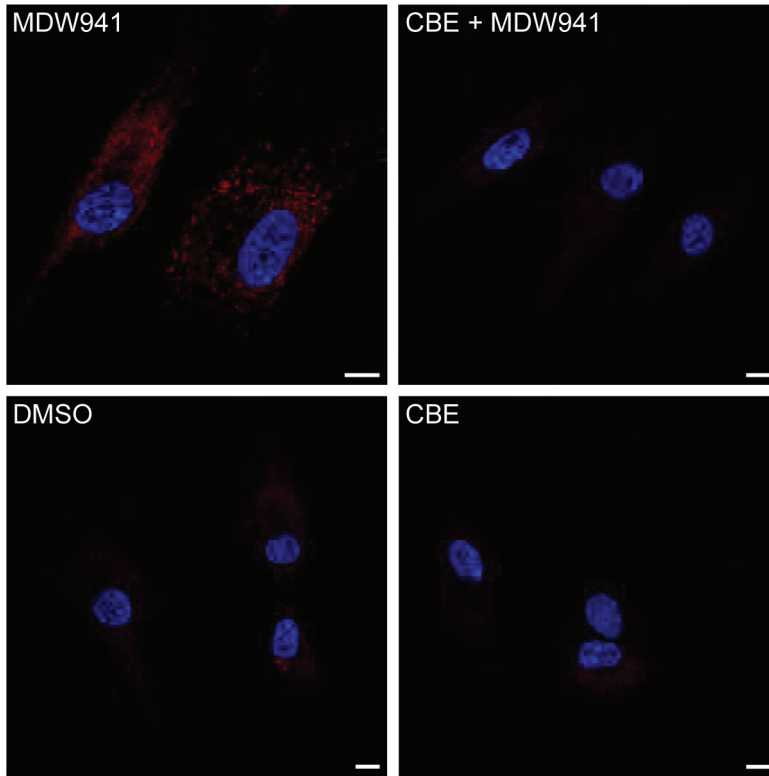
References

1. Aerts, J. M., Schram, A. W., Strijland, A., van Weely, S., Jonsson, L. M., Tager, J. M., Sorrell, S. H., Ginns, E. I., Barranger, J. A., Murray, G. J. Glucocerebrosidase, a lysosomal enzyme that does not undergo oligosaccharide phosphorylation. *Biochim Biophys. Acta.*, **964**, 303-308 (1988).
2. Rijnboutt, S., Aerts, H. M., Geuze, H. J., Tager, J. M., Strous, G. J. Mannose 6-phosphate-independent membrane association of cathepsin D, glucocerebrosidase, and sphingolipid-activating protein in HepG2 cells. *J. Biol. Chem.*, **266**, 4862-4868 (1991).
3. Rijnboutt, S., Kal, A. J., Geuze, H. J., Aerts, H., Strous, G. J. Mannose 6-phosphate-independent targeting of cathepsin D to lysosomes in HepG2 cells. *J. Biol. Chem.*, **266**, 23586-23592 (1991).
4. Reczek, D., Schwake, M., Schroder, J., Hughes, H., Blanz, J., Jin, X., Brondyk, W., Van Patten, S., Edmunds, T., Saftig, P. LIMP-2 is a receptor for lysosomal mannose-6-phosphate-independent targeting of beta-glucocerebrosidase. *Cell*, **131**, 770-783 (2007).
5. Ogata, S., Fukuda, M. Lysosomal targeting of Limp II membrane glycoprotein requires a novel Leu-Ile motif at a particular position in its cytoplasmic tail. *J. Biol. Chem.*, **269**, 5210-5217 (1994).
6. Sandoval, I. V., Arredondo, J. J., Alcalde, J., Gonzalez Noriega, A., Vandekerckhove, J., Jimenez, M. A., Rico, M. The residues Leu(Ile)₄₇₅-Ile(Leu, Val, Ala)₄₇₆, contained in the extended carboxyl cytoplasmic tail, are critical for targeting of the resident lysosomal membrane protein LIMP II to lysosomes. *J. Biol. Chem.*, **269**, 6622-6631 (1994).
7. Balreira, A., Gaspar, P., Caiola, D., Chaves, J., Beirao, I., Lima, J. L., Azevedo, J. E., Miranda, M. C. A nonsense mutation in the LIMP-2 gene associated with progressive myoclonic epilepsy and nephrotic syndrome. *Hum. Mol. Genet.*, **17**, 2238-2243 (2008).
8. Berkovic, S. F., Dibbens, L. M., Oshlack, A., Silver, J. D., Katerelos, M., Vears, D. F., Lullmann-Rauch, R., Blanz, J., Zhang, K. W., Stankovich, J., Kalnins, R. M., Dowling, J. P., Andermann, E., Andermann, F., Faldini, E., D'Hooge, R., Vadlamudi, L., Macdonell, R. A., Hodgson, B. L., Bayly, M. A., Savige, J., Mulley, J. C., Smyth, G. K., Power, D. A., Saftig, P., Bahlo, M. Array-based gene discovery with three unrelated subjects shows SCARB2/LIMP-2 deficiency causes myoclonus epilepsy and glomerulosclerosis. *Am. J. Hum. Genet.*, **82**, 673-684 (2008).
9. Gaspar, P., Kallemeijn, W. W., Strijland, A., Scheij, S., Van Eijk, M., Aten, J., Overkleeft, H. S., Balreira, A., Zunke, F., Schwake, M., Sa Miranda, C., Aerts, J. M. Action myoclonus-renal failure syndrome: diagnostic applications of activity-based probes and lipid analysis. *J. Lipid Res.*, **55**, 138-145 (2014).
10. Malini, E., Zampieri, S., Deganuto, M., Romanello, M., Sechi, A., Bembi, B., Dardis, A. Role of LIMP-2 in the intracellular trafficking of beta-glucosidase in different human cellular models. *FASEB J.*, **29**, 3839-3852 (2015).
11. Brady, R. O., Kanfer, J. N., Bradley, R. M., Shapiro, D. Demonstration of a deficiency of glucocerebrosidase-cleaving enzyme in Gaucher's disease. *J. Clin. Invest.*, **45**, 1112-1115 (1966).
12. Grabowski, G. A., Petsko, G. A., Kolodny, E. H. Gaucher disease. In: D. Valle, A. L. Beaudet, B. Vogelstein, K. W. Kinzler, S. E. Antonarakis, A. Ballabio, K. M. Gibson, and G. Mitchell (Eds.), *The Online Metabolic and Molecular Bases of Inherited Disease*. New York: McGraw-Hill (2014).
13. Witte, M. D., Kallemeijn, W. W., Aten, J., Li, K. Y., Strijland, A., Donker-Koopman, W. E., van den Nieuwendijk, A. M., Bleijlevens, B., Kramer, G., Florea, B. I., Hooibrink, B., Hollak, C. E., Ottenhoff, R., Boot, R. G., van der Marel, G. A., Overkleeft, H. S., Aerts, J.

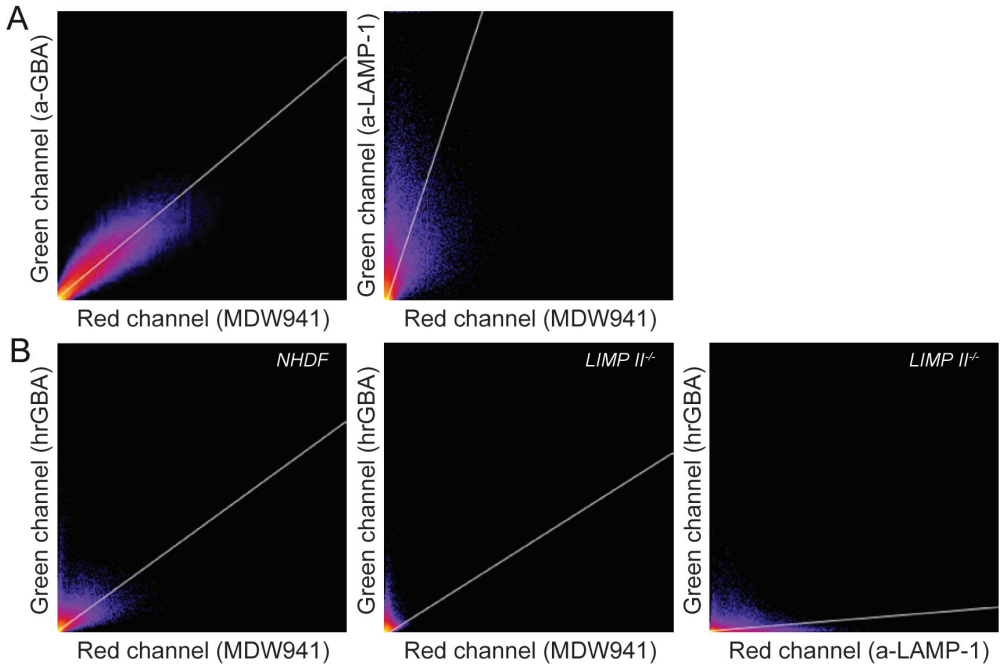
- M. Ultrasensitive in situ visualization of active glucocerebrosidase molecules. *Nat. Chem. Biol.*, **6**, 907-913 (2010).
14. Daniels, L. B., Glew, R. H., Radin, N. S., Vunnam, R. R. A revised fluorometric assay for Gaucher's disease using conduritol-beta-epoxide with liver as the source of Beta-glucosidase. *Clin. Chim Acta.*, **106**, 155-163 (1980).
15. Slot, J. W., Geuze, H. J. Cryosectioning and immunolabeling. *Nat Protoc.*, **2**, 2480-2491 (2007).
16. Van Weely, S., Aerts, J. M., Van Leeuwen, M. B., Heikoop, J. C., Donker-Koopman, W. E., Barranger, J. A., Tager, J. M., Schram, A. W. Function of oligosaccharide modification in glucocerebrosidase, a membrane-associated lysosomal hydrolase. *Eur. J. Biochem.*, **191**, 669-677 (1990).
17. Tokuyasu, K. T. A technique for ultracryotomy of cell suspensions and tissues. *J. Cell. Biol.*, **57**, 551-565 (1973).
18. Barriocanal, J. G., Bonifacino, J. S., Yuan, L., Sandoval, I. V. Biosynthesis, glycosylation, movement through the Golgi system, and transport to lysosomes by an N-linked carbohydrate-independent mechanism of three lysosomal integral membrane proteins. *J. Biol. Chem.*, **261**, 16755-16763 (1986).
19. Marsh, M., Schmid, S., Kern, H., Harms, E., Male, P., Mellman, I., Helenius, A. Rapid analytical and preparative isolation of functional endosomes by free flow electrophoresis. *J. Cell. Biol.*, **104**, 875-886 (1987).
20. Ngo, J. T., Adams, S. R., Deerinck, T. J., Boassa, D., Rodriguez-Rivera, F., Palida, S. F., Bertozzi, C. R., Ellisman, M. H., Tsien, R. Y. Click-EM for imaging metabolically tagged nonprotein biomolecules. *Nat. Chem. Biol.*, **12**, 459-465 (2016).
21. van Elsland, D. M., Bos, E., de Boer, W., Overkleeft, H. S., Koster, A. J., van Kasteren, S. I. Detection of bioorthogonal groups by correlative light and electron microscopy allows imaging of degraded bacteria in phagocytes. *Chem Sci*, **7**, 752-758 (2016).
22. Herrera Moro Chao, D., Kallemeijn, W. W., Marques, A. R., Orre, M., Ottenhoff, R., van Roomen, C., Foppen, E., Renner, M. C., Moeton, M., van Eijk, M., Boot, R. G., Kamphuis, W., Hol, E. M., Aten, J., Overkleeft, H. S., Kalsbeek, A., Aerts, J. M. Visualization of Active Glucocerebrosidase in Rodent Brain with High Spatial Resolution following In Situ Labeling with Fluorescent Activity Based Probes. *PLoS One*, **10**, e0138107 (2015).
23. Eng, C. M., Guffon, N., Wilcox, W. R., Germain, D. P., Lee, P., Waldek, S., Caplan, L., Linthorst, G. E., Desnick, R. J., International Collaborative Fabry Disease Study Group Safety and efficacy of recombinant human alpha-galactosidase A replacement therapy in Fabry's disease. *N. Engl. J. Med.*, **345**, 9-16 (2001).
24. Schiffmann, R., Kopp, J. B., Austin, H. A., 3rd, Sabnis, S., Moore, D. F., Weibel, T., Balow, J. E., Brady, R. O. Enzyme replacement therapy in Fabry disease: a randomized controlled trial. *JAMA*, **285**, 2743-2749 (2001).
25. Van den Hout, J. M., Reuser, A. J., de Klerk, J. B., Arts, W. F., Smeitink, J. A., Van der Ploeg, A. T. Enzyme therapy for pompe disease with recombinant human alpha-glucosidase from rabbit milk. *J. Inherit Metab. Dis.*, **24**, 266-274 (2001).
26. Jiang, J., Kuo, C. L., Wu, L., Franke, C., Kallemeijn, W. W., Florea, B. I., van Meel, E., van der Marel, G. A., Codee, J. D., Boot, R. G., Davies, G. J., Overkleeft, H. S., Aerts, J. M. Detection of Active Mammalian GH31 alpha-Glucosidases in Health and Disease Using In-Class, Broad-Spectrum Activity-Based Probes. *ACS Cent. Sci.*, **2**, 351-358 (2016).
27. Willems, L. I., Beenakker, T. J., Murray, B., Scheij, S., Kallemeijn, W. W., Boot, R. G., Verhoek, M., Donker-Koopman, W. E., Ferraz, M. J., van Rijssel, E. R., Florea, B. I., Codee,

- J. D., van der Marel, G. A., Aerts, J. M., Overkleeft, H. S. Potent and selective activity-based probes for GH27 human retaining alpha-galactosidases. *J. Am. Chem. Soc.*, **136**, 11622-11625 (2014).
28. Aflaki, E., Westbroek, W., Sidransky, E. The Complicated Relationship between Gaucher Disease and Parkinsonism: Insights from a Rare Disease. *Neuron*, **93**, 737-746 (2017).
29. Nair, S., Branagan, A. R., Liu, J., Boddupalli, C. S., Mistry, P. K., Dhodapkar, M. V. Clonal Immunoglobulin against Lysolipids in the Origin of Myeloma. *N. Engl. J. Med.*, **374**, 555-561 (2016).
30. Qian, Y., Flanagan-Steet, H., van Meel, E., Steet, R., Kornfeld, S. A. The DMAP interaction domain of UDP-GlcNAc:lysosomal enzyme N-acetylglucosamine-1-phosphotransferase is a substrate recognition module. *Proc. Natl. Acad. Sci. USA.*, **110**, 10246-10251 (2013).

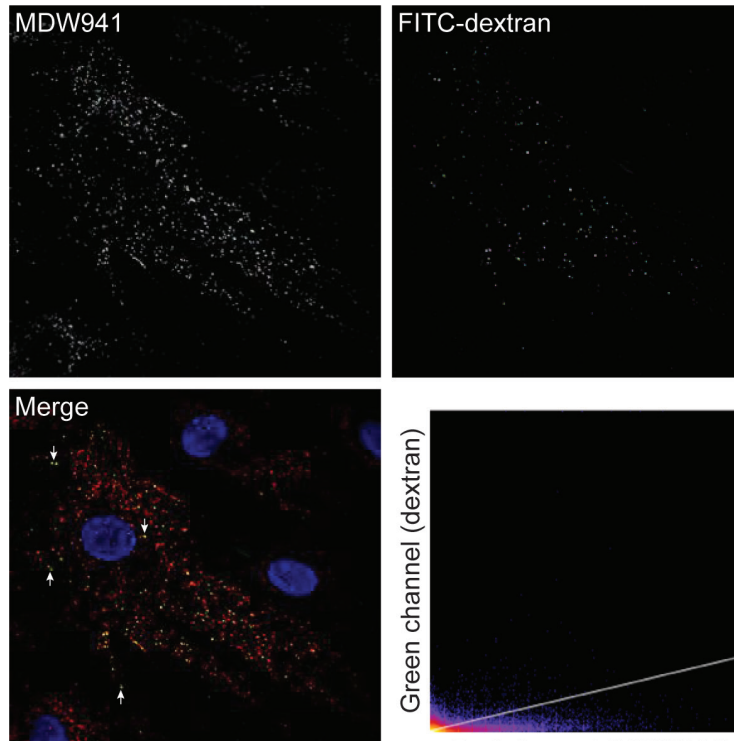
Supplemental Figures



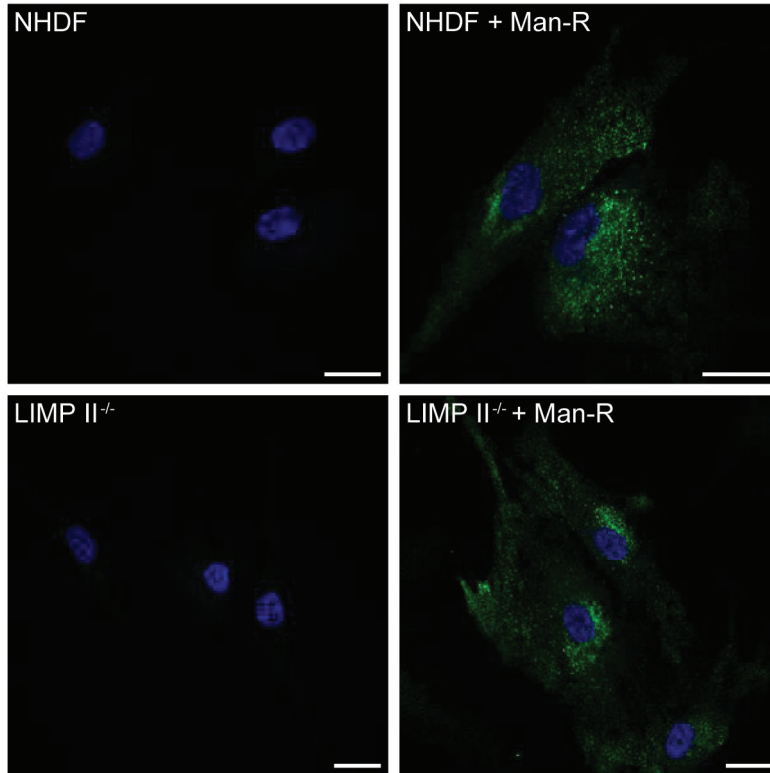
Supplemental figure 1: In situ labeling of NHDFs with MDW941 specifically visualizes active GBA. While in situ labeling of active GBA with MDW941 shows a punctate staining pattern in NHDFs (left upper panel), pre-incubation with CBE followed by in situ labeling with MDW941 results in loss of the fluorescent signal (right upper panel). Incubation with DMSO or CBE shows no detectable autofluorescence in lysosomes with the same imaging settings (lower panels). Nuclei were stained with DAPI. Scale bars, 10 μ m.



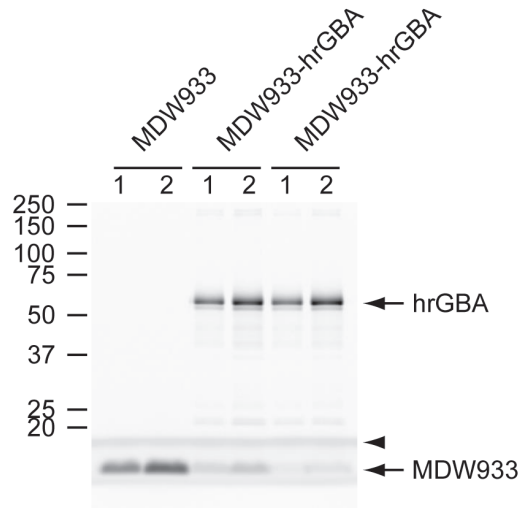
Supplemental figure 2: 2D intensity histograms of confocal fluorescence microscopy images. The 2D intensity histograms of the merged fluorescence microscopy images from figure 1 (A) and figure 5 (B) are shown. The histograms were generated with the ImageJ plugin 'Coloc 2', using Costes threshold regression and 30 Costes randomizations.



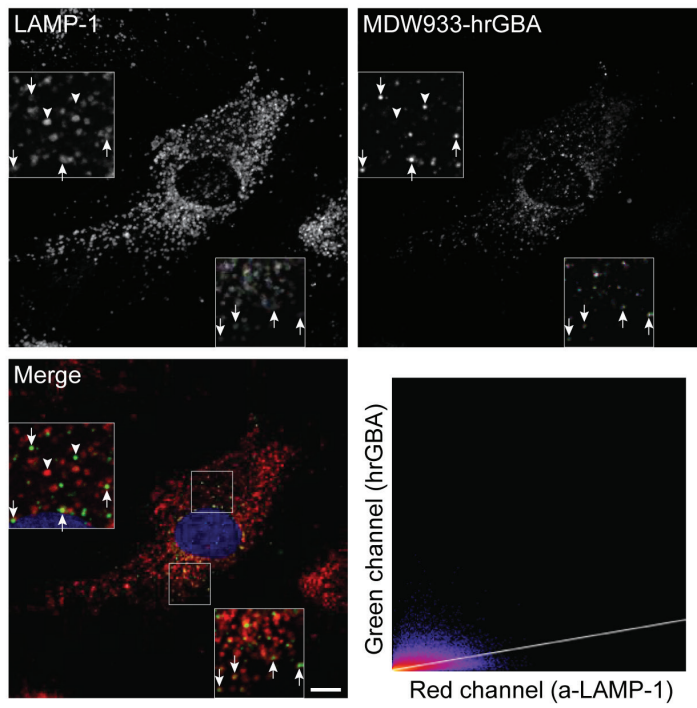
Supplemental figure 3: MDW941 reaches lysosomes marked with the endocytic tracer dextran. Confocal fluorescence images of NHDFs after uptake of FITC-dextran (green) and in situ labeling of endogenous GBA with 5 nM MDW941 (red) for 2h. The 3h-uptake with 1 mg/mL dextran-FITC was followed by a 6h-chase to mark lysosomes. The arrows show examples of co-localization of dextran with MDW941. Not all MDW941 positive compartments were reached by dextran. Nuclei were stained with DAPI (blue). The 2D intensity histogram of the merged image is shown. Scale bar, 10 μ m.



Supplemental figure 4: Expression of the Man-R is detected by immunofluorescence microscopy. NHDFs and LIMP II^{-/-} fibroblasts + or - Man-R were stained with anti-V5 antibodies (green) to detect the presence of the Man-R with a C-terminal V5 tag. As the cells were permeabilized, the signal is detected in intracellular compartments by confocal fluorescence microscopy. Nuclei were stained with DAPI. Note that no signal is detected in the Man-R negative cells. Scale bars, 25 μ m.



Supplemental figure 5. In vitro labeling of hrGBA with MDW933 and removal of unbound ABP. Representative wet slab gel showing equivalent amounts (lanes '2' contain the double amounts of lanes '1') of MDW933 used in the in vitro reaction (lane 1 and 2), MDW933-labeled hrGBA at the end of the reaction with residual free ABP (lane 3 and 4) and MDW933-labeled GBA after passage over a protein desalting column to remove unreacted MDW933 (lane 5 and 6). Note that MDW933 runs ahead of the dye front (indicated with the arrowhead) and is greatly reduced in lanes 5 and 6.



Supplemental figure 6: Endocytosed hrGBA partially co-localizes with the late endosomal/lysosomal marker LAMP-1 in NHDFs. Confocal fluorescence images of NHDFs expressing the Man-R, after a 6h uptake of MDW933-hrGBA (green) and immunostaining of LAMP-1 (red). The arrows in the insets show co-localization of endocytosed GBA and LAMP-1, while the arrowheads show punctae that are positive for either MDW933-hrGBA or LAMP-1. Nuclei were stained with DAPI (blue). The 2D intensity histogram of the merged image is shown. Scale bar, 10 μ m.

Chapter 4

Glycoprotein non metastatic protein B: An Emerging Biomarker for Lysosomal Dysfunction in Macrophages

Manuscript published as:

Van Der Lienden, M. J. C., Gaspar, P., Boot, R., Aerts, J. M. F. G. & Van Eijk, M. Glycoprotein non-metastatic protein B: An emerging biomarker for lysosomal dysfunction in macrophages. *International Journal of Molecular Sciences* vol. 20 66 (2019).

Abstract

Several diseases are caused by inherited defects in lysosomes, the so-called lysosomal storage disorders (LSDs). In some of these LSDs, tissue macrophages transform into prominent storage cells, as is the case in Gaucher disease. Here, macrophages become the characteristic Gaucher cells filled with lysosomes laden with glucosylceramide, because of its impaired enzymatic degradation. Biomarkers of Gaucher cells have been actively searched, particularly after the development of costly therapies based on enzyme supplementation and substrate reduction. Proteins selectively expressed by storage macrophages and secreted into the circulation have been identified, among which glycoprotein non metastatic protein B (GPNMB). This review focusses on the emerging potential of GPNMB as biomarker of stressed macrophages in LSDs as well as in acquired pathologies accompanied by excessive lysosomal substrate load in macrophages.

Inherited lysosomal storage disorders

LSDs comprise at least fifty distinct disorders, each caused by specific defects in the function of the lysosomal apparatus.^{1,2} In LSDs, primary and secondary metabolites accumulate within lysosomes of specific cells, which in turn gives rise to progressive multi-organ pathologies. In many LSDs, tissue macrophages are among the prominent storage cells. Of note, with each particular LSD the clinical manifestation is heterogeneous, resulting in neonatal, infantile, juvenile and adult variants. This heterogeneity is thought to stem from different primary genetic defects impacting differently on residual activity of a lysosomal enzyme. However, complex interplay between the genetic defect, modifier genes, epigenetics and environmental factors seems to further contribute to variable clinical manifestation. This is exemplified by Gaucher disease (GD), a relatively common LSD.³ GD is caused by an inherited deficiency in the lysosomal β -glucosidase glucocerebrosidase (GBA), causing accumulation of its substrate glucosylceramide (GlcCer).⁴ GlcCer is the most simple glycosphingolipid consisting of a glucose linked to the lipid moiety ceramide.⁵ Lysosomal GlcCer storage occurs in GD patients almost exclusively in tissue macrophages, thus transforming into Gaucher cells.⁶ Accumulation of viable Gaucher cells in tissues is thought to contribute to characteristic symptoms of adult GD patients such as enlargement of liver and spleen, anemia and skeletal deterioration.^{3,7} The overall severity of GD may vary considerably among patients and consequently different phenotypic variants are historically distinguished: the colloidon baby with impaired skin permeability features incompatible with life outside the womb, the acute (infantile, type 3) and sub-acute (juvenile, type 2) variants with fatal neurological symptoms and the non-neuronopathic (adult, type 1) variant most common in Caucasian populations.^{3,7} There is no strict correlation between mutations in *GBA* and disease manifestation in GD patients.^{8,9} The most striking illustration of this comes from reports on monozygotic GD twins with marked discordance in symptoms.^{10,11} The remarkable poor predictive value of *GBA* genotype for GD phenotype complicates confirmation of diagnosis. Currently, clinical assessment of Gaucher patients includes analysis of blood parameters (platelet count), examination of enlarged liver and spleen (MRI)/computed tomography (CT), skeletal status (MRI/X-ray) and a quality-of-life survey.^{3,12,13} As described below, the demonstration in plasma of biomarkers, i.e. metabolites or proteins specifically secreted by the lipid laden macrophages (Gaucher cells), provides an additional tool to confirm the diagnosis of GD and may assist the monitoring of progression of disease.¹⁴ Such biomarkers are also increasingly exploited to assess responses to costly therapies based on chronic intravenous supplementation with macrophage-targeted recombinant GBA or pharmacological reduction of endogenous GlcCer by oral administration of inhibitors of glucosylceramide synthase.^{7,15}

Gaucher cell biomarkers: lipids

Since the Gaucher cells primarily accumulate GlcCer, plasma glycosphingolipid abnormalities in GD patients have received considerable interest. Plasma of symptomatic GD-patients was found to show only moderately elevated levels of GlcCer, being associated with lipoproteins.¹⁶ Likely, the excessive GlcCer in the patient's plasma does not stem from Gaucher cells but rather from hepatocytes. The same may hold for the elevated ganglioside

GM₃ observed in plasma of GD patients.¹⁷ There is consensus that plasma GlcCer has no value as GD biomarker. More relevant in this connection is the occurrence of more than hundred-fold increased glucosylsphingosine (GlcSph) in plasma of GD patients and animal models of GBA deficiency.^{18,19} GlcSph is de-acylated GlcCer lacking the fatty acyl moiety. This sphingoid base was demonstrated to be actively formed inside lysosomes by the enzyme acid ceramidase acting on accumulating GlcCer.²⁰ Intralysosomally formed GlcSph may partly leave cells, and even leave the body via bile and urine. The prominent cellular producers of plasma GlcSph in GD patients seem to be visceral Gaucher cells¹⁸, however many cell types produce GlcSph during marked GBA deficiency. Indeed, about ten-fold increased plasma GlcSph has been observed in plasma of patients with Action Myoclonus Renal Failure syndrome (AMRF).²¹ This disorder is caused by genetic deficiency of lysosome membrane protein 2 (LIMP-2; also called Scavenger Receptor Class B Member 2 (SCARB2)), the membrane protein involved in transport of newly formed GBA to lysosomes.²² GBA is markedly reduced in many cell types of AMRF patients, but actually not in their macrophages likely due to some alternative transport mechanism in these cells or their ability of re-uptake of faulty secreted GBA by other cells.²³ At present plasma GlcSph is considered as useful GD biomarker and its measurement is already broadly used.^{18,19,24,25} Of note, sphingoid bases, rather than the corresponding primary storage lipids, are also used as markers in other sphingolipid storage disorders.^{7,26} Examples are galactosylsphingosine in Krabbe Disease, globotriaosylsphingosine in Fabry Disease, a phosphorylcholinesphingosine (lyso-sphingomyelin 509) in Niemann-Pick type C (NPC) and B (NPB).^{27–29} Convenient and sensitive multiplex measurements of several sphingoid bases have been developed and their use may assist in confirmation of diagnosis of several sphingolipid storage disorders.^{30–32} A role of the sphingoid bases in pathophysiology has also been hypothesized. For example, it has been proposed that excessive GlcSph may play a role in abnormal osteoblast differentiation and thus contribute to osteoporosis in GD patients.³³ A role of GlcSph as auto-antigen has been identified, promoting B-cell proliferation and the associated risk for multiple myeloma, a common cancer in GD patients.^{34,35} Recently it was reported that chronic administration of GlcSph to mice induces organomegalies and hematological abnormalities characteristic of GD.³⁶ Furthermore, excessive GlcSph has been proposed to promote alpha-synuclein aggregation.³⁷ This may provide an explanation for the increased risk of individuals with abnormal GBA to develop Parkinson's disease.³⁸ Likewise, excessive globotriaosylsphingosine (lyso-Gb₃) in Fabry patients is thought to contribute to neuropathic pain and loss of podocytes.^{39,40} It is of interest to point out that apparently a dysfunction in lysosomal catabolism of glycosphingolipids leads to metabolic adaptations generating secondary metabolites that ultimately may cause specific symptoms beyond the storage cells.⁴¹ A recently recognized glycolipid abnormality in GD patients concerns glucosylcholesterol (GlcChol).⁴² It appears that glucosylcholesterol is formed in cells by sequential action of the enzymes glucosylceramide synthase (GCS) and the transglucosylating non-lysosomal GBA variant GBA2.⁴² Lysosomal glucocerebrosidase (GBA) normally degrades GlcChol, but during lysosomal cholesterol accumulation the enzyme forms via transglucosylation of cholesterol GlcChol, using GlcCer as glucose donor.^{42,43} This pathway explains the massive increase in GlcChol in liver of mice with NPC, a condition caused by defects in either *Npc1* or *Npc2*, proteins involved in the normal efflux of cholesterol from lysosomes.⁴²

Currently, biochemical confirmation of the diagnosis of NPC relies on identification of cholesterol accumulation in patient derived fibroblasts and measurement of excessive plasma oxysterols by advanced mass spectrometry.^{44,45} Oxysterols are formed in the body through enzymatic, and non-enzymatic reactions involving reactive oxygen species (ROS). The latter reaction seems to be driving the enhanced levels of oxysterols in NPC.⁴⁵⁻⁴⁹ Moderate elevation of oxysterol levels is also observed in other cholesterol related storage diseases such as atherosclerosis, obesity and diabetes.⁵⁰⁻⁵² The role of GlcChol in pathophysiology of NPC still warrants investigation. Of note in this connection, pharmacological inhibition or genetic deletion of GBA2 causing marked reduction of GlcChol has been found to ameliorate disease manifestations in NPC mice.⁵³ Furthermore, N-butyl-1-deoxynojirimycin (Zavesca or Miglustat), an inhibitor of GCS and GBA2, is an approved drug to treat the neurological symptoms of NPC.⁵⁴⁻⁵⁷

Gaucher cell biomarkers: proteins

Discovery of protein markers of Gaucher cells was prompted by the development of enzyme replacement therapy (ERT) for non-neuropathic GD some three decades ago by researchers at the National Institutes of Health.⁵⁸ Brady and colleagues used GBA isolated from human placentas being modified in its N-glycans to favor mannose-receptor mediated uptake by macrophages following intravenous administration.⁵⁹ This macrophage-targeted ERT was found to result in prominent corrections in organomegaly and hematological symptoms of GD patients.⁶⁰ The high costs associated with ERT of GD patients limited its application and stimulated research on personalized ERT, i.e. the minimal effective dose of recombinant enzyme for each patient.^{61,62} Novel tools to sensitively monitor corrections in Gaucher cell burden of GD patients following ERT became urgently needed. Already reported were a number of plasma protein abnormalities in Gaucher patients, for example elevated levels of lysozyme, beta-hexosaminidase, ferritin, tartrate-resistant acid phosphatase (TRAP) and angiotensin-converting enzyme (ACE), see for a review.⁶³ However, for none of these abnormalities it was clear that they are uniquely related to Gaucher cells and not also released by other cell types, as for example TRAP by pro-inflammatory macrophages, osteoclasts and dendritic cells.⁶⁴ Subsequent research led to the discovery that Gaucher cells massively produce and secrete the enzyme chitotriosidase (CHIT1), causing a stunning average 1000-fold elevated plasma level in type 1 GD patients.⁶⁵ CHIT1 has been subsequently studied in great detail.⁶⁵⁻⁷⁴ Importantly, it was found that the enzyme is specifically produced in tissue macrophages and neutrophils. In particular Gaucher cells are producers of CHIT1 that is partly routed to lysosomes and partly secreted.^{68,71} Improved substrates were next developed to accurately monitor CHIT1 levels in plasma of patients.^{75,76} Plasma CHIT1 has been extensively investigated in relation to GD in clinical centers applying ERT. From these studies it has become apparent that the reductions in plasma CHIT1 of GD patients following ERT have a prognostic value for corrections in organomegaly and the risk for long-term complications.⁷⁷ Of note, elevated plasma CHIT1 is not unique for GD.⁷³ The enzyme levels may be increased during various disease conditions, albeit to a much lesser extent as in type 1 GD patients.⁷⁸⁻⁸⁰ Many LSDs show modest elevations in plasma CHIT1, most notably Fabry Disease and NPC⁸¹⁻⁸³. Likely, accumulation of materials in lysosomes of macrophages induces expression of CHIT1. A major drawback regarding CHIT1 as

marker stems from the common occurrence of a duplication in the CHIT1 gene causing absence active CHIT1.⁶⁷ Homozygosity for this mutation occurs relatively frequently, being present in about 1 in 20 individuals in most ethnic groups. CHIT1 deficiency also occurs with the same frequency among GD patients.⁶⁷ This stimulated a search for additional protein markers of Gaucher cells. It was subsequently discovered that chemokine (C-C motif) ligand 18 (CCL18), also called pulmonary and activation- regulated chemokine (PARC) is also massively produced and secreted by Gaucher cells, resulting in twenty to forty-fold elevated plasma levels.^{84–86} Corrections in plasma CCL18 and CHIT1 during ERT mimic each other closely, illustrating the common source of these markers being the Gaucher cell.⁸⁵ Like CHIT1, CCL18 is also elevated in NPC patients.^{87–89} Monitoring of corrections in plasma CHIT1 and/or CCL18 is not only performed in patients receiving ERT for which presently multiple recombinant enzymes are registered.^{90,91} Corrections of Gaucher cell markers are also monitored in GD patients treated by means of substrate reduction therapy (SRT). In this alternative therapeutic approach an inhibitor of GCS is orally administered to GD patients to reduce the endogenous synthesis of GlcCer and thus balance the impaired capacity of lysosomal degradation of the lipid.⁴¹ Registered for SRT of type 1 GD are at present two GCS inhibitors Miglustat and Eliglustat.^{92–94}; responses in CHIT1, CCL18 and GlcSph to the SRT therapies have been analyzed.⁹⁵

Emerging marker: GPNMB

In recent years, the impact of deficiency of GBA is increasingly studied in mouse models, either generated by genetic modification or pharmacologically induced with GBA inhibitors. The two existing protein biomarkers of storage macrophages in GD patients are unfortunately of no use for these murine GD models. In the mouse, CHIT1 is not expressed by phagocytes due to a different promotor.⁷³ In addition, no rodent homologue of CCL18 exists.⁸⁵ Moran et al. studied differentially expressed transcripts in type 1 GD spleen.⁸⁴ Among the observed overexpressed mRNAs was the one coding for glycoprotein non metastatic protein B (GPNMB). GPNMB, was previously shown to be induced upon stimulation of monocytes with granulocyte-macrophage colony stimulating factor (GM-CSF) as well as with M-CSF.⁹⁶ Much later, Kramer and colleagues observed in their analysis of the proteome of normal and GD spleens marked increases in GPNMB in patients tissues.⁹⁷ Isolation of Gaucher cells by laser-capture revealed the massive presence of the protein in Gaucher cells. Moreover, release of a soluble fragment of GPNMB was observed, explaining the up to several hundred fold elevated levels in plasma of GD patients as can be detected by ELISA.⁹⁷ Furthermore, it became apparent that also GBA-deficient mice in the hematopoietic lineage that form Gaucher cells show elevated GPNMB.⁹⁸ Treatment of such mice by substrate reduction therapy as well as lentiviral gene therapy leads to prominent corrections in GPNMB in key organs.^{97–99} Independently, other researchers noted in other non-neuronopathic GD mouse models increased expression of GPNMB.^{33,100} Zigdon and co-workers reported elevated GPNMB in cerebrospinal fluid (CSF) of type 3 GD patients and a pharmacological neuronopathic GD mouse model.¹⁰¹ In a larger GD cohort, the applicability of GPNMB as biomarker was carefully examined.¹⁰² This study revealed a correlation between serum GPNMB levels and disease severity.¹⁰²

Macrophage storage, reflected by a foamy cell appearance, is also observed in NPC.

Interestingly, in NPC mouse models it was demonstrated that these macrophages (Iba1⁺ cells) showed high GPNMB protein levels in spleen, liver and brain.¹⁰³ These observations extend on the earlier reported gene expression elevations in the same tissues in NPC mouse models.^{104,105} Furthermore, GPNMB was found to be elevated in human NPC plasma samples, correlating with CHIT1 levels.¹⁰³ In summary, like CHIT1, GPNMB is strongly associated with lipid laden macrophages. Unlike CHIT1, GPNMB, is also elevated in mouse models of GD and NPC and can thus be used as a cross-species foam cell marker that could be instrumental in monitoring disease burden in LSD.^{33,103}

GPNMB: properties

Human GPNMB is a type 1 transmembrane glycoprotein that, as the result of alternative splicing, occurs as two polypeptide isoforms, one of 572 amino acids and a shorter of 560 amino acids.^{106,107} The protein is encoded by the GPNMB gene at locus 7p15. Murine GPNMB shares 71% sequence homology with the human orthologue and is slightly smaller (574 amino acids).^{108,109} GPNMB is highly glycosylated: there are twelve putative glycosylation sites in the predicted extracellular part of human protein and eleven in that of the murine orthologue. Several domains in the GPNMB protein have been identified, including an integrin-recognition (RGD) motif and a polycystic kidney disease (PKD)/Chitinase domain in the extracellular part and an immunoreceptor tyrosine-based activation-like motif (ITAM-like; YxxI) and a lysosomal targeting (dileucine) motif in the intracellular part (**Figure 1**). Extensive N-glycosylation of GPNMB increases its molecular mass to about 120 kDa.¹¹⁰ After traversing the Golgi apparatus, GPNMB is directed to the cell membrane. At the cell surface, a soluble fragment may be proteolytically released by ADAM-10. Alternatively, GPNMB may be internalized to intracellular vesicles through phagocytosis/endocytosis.^{111–114}

GPNMB was originally discovered in a melanoma cell line.¹¹⁵ and occurs in various tissues and cell types. It has relatively high expression in retina and skin, followed by adipose tissue, bone marrow, lung, cervix and immune system, and to lesser extent liver and muscle.¹¹⁶ Several cell types are reported to express GPNMB: these include phagocytes (dendritic cells and macrophages), osteoclasts and melanocytes.^{109,117–119} In addition, well documented is expression of GPNM in melanoma cells as well as other types of cancer cells (reviewed in ¹¹¹).

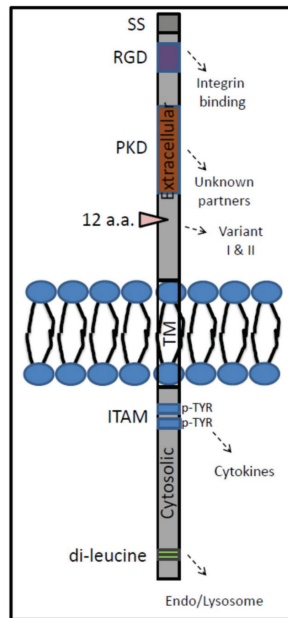


Figure 1. Schematic overview of *Gpnmb* protein. SS, signal sequence; RGD, RGD tripeptide; PKD, Polycystic kidney disease domain; a.a., amino acid; ADAM, a disintegrin and metalloproteinase; ITAM, immunoreceptor tyrosine-based activation like motif; TM, transmembrane domain.

As addressed in more detail below, GPNMB has been associated with endosomal/lysosomal structures in phagocytes overexpressing the protein during specific stress conditions.^{113,117,119} In melanocytes, GPNMB is also targeted to a lysosome-like organelle, the membrane of melanosomes. This particular targeting in melanocytes relies on C-terminal motives in the cytoplasmic tail, shared with the homologous protein premelanosome protein 17 (PMEL17).^{114,121} GPNMB is important in melanosome formation as is reflected by defective formation of pigment by iris pigment epithelium in a mouse strain (DBA/2J (D2)) with a truncated version of *Gpnmb*.^{122–124} In humans, a truncated version of GPNMB is associated with hyper- and hypopigmentation of the skin in an autosomal recessive variant of Amyloidosis cutis dyschromica (ACD).¹²⁵ Unlike its homologue PMEL17, GPNMB expression is not restricted to melanocytes. GPNMB has received multiple names. Within the context of bone marrow cells, human GPNMB was initially called Hematopoietic growth factor inducible neurokinin-1 type (HGFIN).¹²⁶ In mouse, GPNMB was independently identified in dendritic (Langerhans) cells and was named DC-associated, HSPG-dependent integrin ligand (DC-HIL).¹⁰⁹ This variant shared 88.3% homology to its rat homologue, named osteoactivin.¹²⁷ GPNMB was found to be upregulated upon differentiation of monocytes into dendritic cells (DCs), macrophages and osteoclasts.^{109,117–119}

An established regulator of GPNMB expression is melanogenesis associated transcription factor (MITF).^{119,128–132} Of note, MITF is a member of the MiT/TFE subfamily of transcription factors known to regulate expression of proteins involved in autophagy and lysosome biogenesis.^{133–135} Other members of the Mi/TF subfamily are transcription factor EB (TFEB), transcription factor E3 (TFE3) and transcription factor EC (TFEC).

Homozygosity for many mutations in *Mitf* alleles gives rise to dysfunctional melanocyte differentiation and defective development of retinal pigment epithelium.¹³⁶ Following activation, MITF translocates into the nucleus and binds preferentially to the conserved M-box sequence TCATGTG.^{129,137,138} Recent advances in the field of lysosomes have placed the Mi/TFE subfamily at the center of lysosomal homeostasis.^{133,135,139,140} The transcriptional activity of TFEB, MITF and TFE3 can be induced upon pharmacological disruption of lysosomal integrity in cultured cells.

Function of GPNMB in myeloid cells

Many studies on the function of GPNMB in myeloid cells have been performed with DCs. Upon stimulation with interleukin 10 (IL-10), GPNMB expression is found to be induced in DCs through inhibition of phosphoinositide 3-kinase (PI3K)/ RAC- α serine/threonine-protein kinase (AKT) and subsequent activation of glycogen synthase kinase-3- β (GSK3 β). GSK3 β in turn activates MITF to promote expression of GPNMB.^{131,141} DC-expressed, membrane bound GPNMB is found to bind to T-cells, thereby inhibiting proliferation of CD4⁺ and CD8⁺ T-cells and secretion of IL-2.¹⁴² Syndecan-4, an heparan sulfate proteoglycan (HSPG) containing membrane protein on activated T-cells, has been identified as primary ligand for GPNMB.^{143–145} Binding of GPNMB to syndecan-4 is thought to take place in two steps: initial binding via the extracellular arginylglycylaspartic acid (RGD-) domain facilitates PKD-dependent binding.¹⁰⁹ Since the RGD-domain is known to interact with integrin, GPNMB possibly exerts its adhesive action through activation of integrin interactions.^{109,146–148} Similarly, DC expressed GPNMB has been reported to bind to dermatophytic fungi in a heparan sulfate dependent manner.¹⁴⁹ Another identified binding partner of GPNMB is CD44. Macrophages with anti-inflammatory characteristics (M2) show a marked upregulation of GPNMB.¹⁵⁰ Upon skin wounding, GPNMB derived from infiltrating macrophages was found to promote recruitment of MCSs and subsequent wound repair.¹⁵¹ Given the fact that MSCs can differentiate into osteoblasts, these studies are in line with findings correlating GPNMB with osteogenesis and osteoblast maturation.^{33,152,153} Lastly, GPNMB was found to bind to calnexin, which was suggested to reduce oxidative stress.¹⁵⁴

In several studies on tissue damage, an increase in GPNMB has been reported.^{155–164} Upon renal and liver tissue damage, upregulation of GPNMB is associated with infiltration of macrophages into the damaged tissue.^{161–164} Interestingly, in a model of reversible liver fibrosis, a subset of profibrotic macrophages (Ly6C^{hi}) undergoes a phenotypic switch into macrophages associated with resolution of fibrosis (Ly6C^{low}) and concomitantly with increased expression of GPNMB.¹⁵⁹ The phenotypic switch gives rise to macrophages with pro-inflammatory (M1) as well as M2 characteristics and can be triggered by phagocytosis. Of note, a study revealed that GPNMB is crucial for clearance of cellular debris by F4/80⁺ macrophages upon repair of ischemia reperfusion injury (IRI) in the murine kidney.¹¹³ Li et al. showed that GPNMB is associated with LC-3 positive phagocytic vesicles formed upon engulfment of apoptotic cells by macrophages.¹¹³ Monocyte expressed GPNMB seems associated with formation of intracellular vesicles such as (auto-) phagosomes and lysosomes.^{113,117,119}

An M2-phenotype nature of GPNMB positive macrophages is in line with earlier work on splenic Gaucher cells.⁷¹ Morphologically, the Gaucher cell exhibits a foamy

appearance due to dramatic enlargement of the lysosomal compartment, in which lipids accumulate in tubular deposits.¹⁶⁵ Gaucher cells are M2-like cells,⁷¹ and are surrounded in tissue lesions by macrophages expressing proinflammatory molecules such as IL-1 β or monocyte chemoattractant protein 1 (MCP-1).⁷¹ Possibly, the latter cells are responsible for the elevated levels of the chemokines MIP-1 α and MIP-1 β in plasma of symptomatic Gaucher patients.¹⁶⁶

GPNMB and foam cells in acquired ‘metabolic’ disorders

As indicated earlier, defects in the lysosomal catabolic machinery trigger massive induction of GPNMB in macrophages in spleen, liver and brain in GD and NPC.^{33,97,101,103,104} Interestingly, when the amount of lipid substrate exceeds the lysosomal capacity in macrophages, a foamy appearance and clear induction of GPNMB is observed.^{132,154,167,168} Examples are: cholesterol accumulation in atherosclerosis, lipid accumulation in macrophages during obesity and myelin accumulation in brain macrophages during MS. In a proteome analysis of ascending aortic extracts of rabbits fed a high cholesterol diet (HCD), 15-fold elevated GPNMB was detected.¹⁶⁹ In LDLR^{-/-} mice fed a HCD a 300-fold induction of *Gpnmb* was found in liver, most likely in Kupffer cells.¹⁶⁷ Interestingly, GPNMB was also found to be increased in human subjects with fatty liver disease. In subjects with non-alcoholic steatohepatitis plasma GPNMB levels were significantly elevated compared to simple steatosis.¹⁵⁴ Studies on rodent models of obesity, leptin-deficient and high fat diet fed mice, revealed striking induction of GPNMB in obese adipose tissue macrophages.¹³² Again, a high lipid load derived from phagocytosis of dysfunctional/apoptotic adipocytes is the likely trigger. In liver, a less pronounced induction of GPNMB was detected in Kupffer cells. Consistently, increased lysosomal volume occurs in obese adipose macrophages.¹⁷⁰ Also in human obese adipose tissue, *GPNMB* expression was found to be increased.¹³² In post-mortem analyzed human brain tissue of MS patients, it was found that *GPNMB* is increased around the rim of chronic active lesions. This rim is characterized by the abundant presence of foamy, lipid-laden, macrophages.¹⁶⁸ The *GPNMB* increase was accompanied by an increase in macrophage restricted *CD68* expression, as well as *CHIT* and *CCL18*. Together these data point to a role of accumulating lipids like (glyco) sphingolipids and cholesterol as inducers of GPNMB. During an LSD flaws in the catabolic machinery in macrophages drive lipid accumulation, whereas in acquired metabolic diseases such as atherosclerosis and obesity, as well as MS, the lysosomal load of lipids exceeds the catabolic capacity.

In vitro studies support a connection between GPNMB and lysosomal function. A variety of lysosomal stressors, including sucrose, chloroquine, bafilomycin, concanamycin A, palmitate (but not oleate), induce GPNMB expression in cultured RAW264.7 cells.^{132,171} Upregulation of *Gpnmb* occurs also in RAW264.7 macrophages upon blocking cholesterol efflux from the lysosome by U18666A, thereby mimicking aspects of NPC pathology.¹⁰³ Impairing lysosomal function in different ways (increasing luminal pH, swelling by accumulation of non-degradable material, excessive lipid load and impaired lipid efflux) all induces upregulation of GPNMB. mTORC1 is known to mediate regulation of lysosome biogenesis and autophagy via the Mi/TFE transcription factors.^{132,172} Consistently, inhibition of mTORC1 activity with torin 1 induces markedly GPNMB.[150] Recently, the buffer HEPES was found to also potently induce GPNMB

expression through Mi/TFE members in cultured RAW264.7 cells.¹⁷¹ In this manner the presence of HEPES impacts on cellular lysosomal enzyme levels. Therefore, the finding highlights the importance of culture conditions (such as presence of HEPES) for diagnosis of LSDs with cultured cells.

Besides being highly expressed in macrophages in LSDs and acquired metabolic disorders, GPNMB is also increasingly linked to neuroinflammation.^{173–175} For example, elevated GPNMB in glioma tissue stems largely from reactive glioma-associated phagocytosing microglia and macrophages (GAMs).^{176–179} Data also link GPNMB to neurodegeneration, including cerebral ischemia, amyotrophic lateral sclerosis (ALS), Alzheimers Disease (AD), Multiple Sclerosis (MS) and Parkinson Disease (PD).^{180–185} Increased GPNMB expression has been associated with a particular microglial state called the ‘microglial neurodegenerative phenotype’ (MGnD), observed in mouse models for AD, MS and ALS.¹⁸⁶ This phenotype was shown to markedly differ from M1-differentiated microglia and cells with this phenotype were associated with amyloid- β deposits in a murine AD-model.^{183,186} Strikingly, upon injection of apoptotic neurons in the hippocampus and cortex of healthy mice, the MGnD-phenotype could be induced through TREM2, a phosphatidylserine sensing protein, and upregulation of apolipoprotein E (APOE). Upregulated expression of GPNMB was also found in the substantia nigra (SN) of PD-patients.^{184,185} Moloney et al. could recapitulate this GPNMB-increase in mice by blocking GBA activity through systemic conduritol-beta-epoxide administration, which suggests a connection between neuronopathic glycosphingolipidoses and PD.^{38,97,103,185,187} In a chemically induced mouse model of PD, CD44 has been proposed to function as binding partner of GPNMB in the SN.¹⁸⁴ The dopamine-producing neurons in the SN produce neuromelanin, causing their pigmentation. Neuromelanin increases upon ageing and has been associated with PD. Neuromelanin accumulation may occur along with defective trafficking and degradation by the endolysosomal apparatus.^{188,189} It is conceivable that GPNMB is upregulated as response to lysosomal stress caused by accumulating, undegradable neuromelanin.

It is of interest to consider the advantages and disadvantages of the use of GPNMB as marker of lipid laden macrophages, instead of chitotriosidase or CCL18. Firstly, GPNMB can be conveniently quantified by ELISA, a methodology accessible to most laboratories. Secondly, GPNMB is expressed also by lipid laden macrophages in mice; this is not the case for either chitriosidase or CCL18.^{73,85} A potential disadvantage is the present lack of knowledge on possible genetic heterogeneity in (expression of) GPNMB. This may not be irrelevant: for example, the CHIT1 gene has common mutations, resulting in no protein or enzyme with abnormal catalytic features.^{67,73} This limits the value of CHIT1 as marker of lipid laden macrophages. The selectivity of GPNMB as marker warrants further research. It is still unclear to which extent other cell types than lipid-laden macrophages may also express and secrete GPNMB during pathological conditions. It seems likely that in disease characterized by the presence of lipid laden macrophages abnormalities in GPNMB will occur: such candidate diseases include Wolman disease and the more benign mature variant, cholesteryl ester storage disorder, both caused by a deficiency in lysosomal acid lipase.¹⁹⁰ In this disorder chitotriosidase is also markedly elevated.¹⁹¹

Conclusion

Lipid laden macrophages may orchestrate pathology, an accepted notion in the field of inborn lysosomal storage disorders and more recently also in the field of the metabolic syndrome (**Figure 2**). The development of ERT for specific LSDs has led in the last decades to identification of markers of lipid laden macrophages. In LSDs characterized by foamy macrophages as storage cells, plasma GPNMB has been shown to accurately reflect disease burden. Moreover, GPNMB is also applicable in mouse models of LSDs like GD and NPC. GPNMB is also increased in several acquired diseases, such as the metabolic syndrome and neurodegeneration. It therefore might be that specific LSDs and the latter disease conditions share elements in pathophysiology, in particular the involvement of accumulating foamy, lysosomal stressed, macrophages, see **Figure 2**.

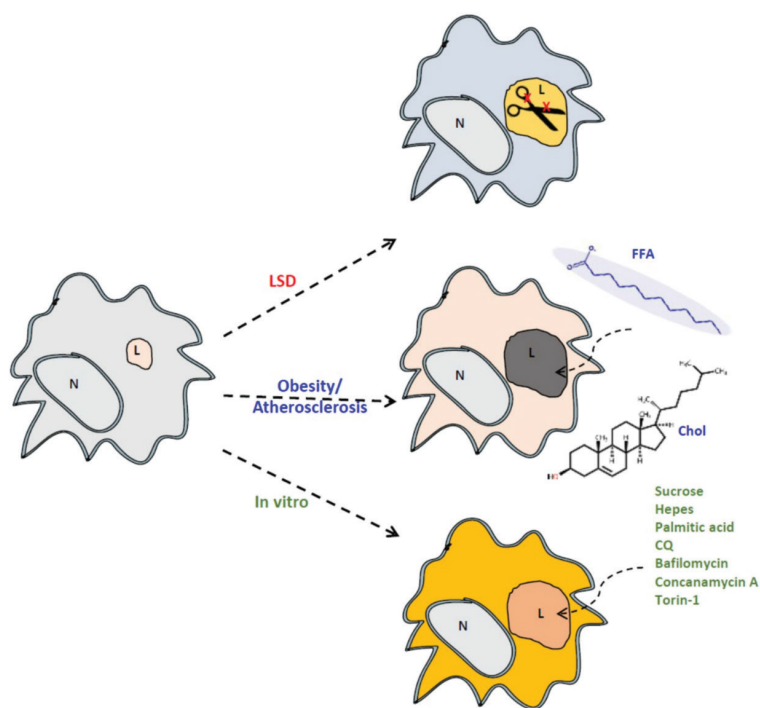


Figure 2. Model for lysosomal dysfunction in LSD, metabolic syndrome, and cultured cells. Lysosomal dysfunction could be caused in vivo by deficiencies in lysosomal hydrolases (LSD) or chronic excess of nutritional intake (metabolic syndrome). In vitro, lysosomal dysfunction can be recapitulated by several compounds that model in vivo systems.

GPNMB is among the highest upregulated proteins in lipid laden macrophages. Nevertheless, at present its exact function in the foamy macrophage remains largely enigmatic. Important unanswered questions concern the function(s) served by GPNMB, either the cellular membrane-bound or (extracellular) soluble isoforms, in lipid laden macrophages and beyond.

References

1. Neufeld, E. F. Lysosomal storage diseases. *Annu. Rev. Biochem.* **60**, 257–280 (1991).
2. Platt, F. M. Sphingolipid lysosomal storage disorders. *Nature* (2014).
3. Beutler, E. & Grabowski, G. Glucosylceramide lipidosis-Gaucher disease. In *The Metabolic and Molecular Bases of Inherited Diseases* **8** (2001).
4. Brady, R. O., Kanfer, J. N., Bradley, R. M. & Shapiro, D. Demonstration of a deficiency of glucocerebrosidase-cleaving enzyme in Gaucher's disease. *J. Clin. Invest.* **45**, (1966).
5. Wennekes, T., van den Berg, R. J. B. H. N., Boot, R. G., van der Marel, G. A., Overkleeft, H. S. & Aerts, J. M. F. G. Glycosphingolipids--nature, function, and pharmacological modulation. *Angew. Chem. Int. Ed. Engl.* **48**, 8848–8869 (2009).
6. Boot, R. G., van Breemen, M. J., Wegdam, W., Sprenger, R. R., de Jong, S., Speijer, D., Hollak, C. E., Van Dussen, L., Hoefsloot, H. C., Smilde, A. K., De Koster, C. G., Vissers, J. P. & Aerts, J. M. Gaucher disease: a model disorder for biomarker discovery. *Expert Rev. Proteomics* **6**, 411–419 (2009).
7. Ferraz, M. J., Kallemijn, W. W., Mirzaian, M., Herrera Moro, D., Marques, A., Wisse, P., Boot, R. G., Willems, L. I., Overkleeft, H. S. & Aerts, J. M. Gaucher disease and Fabry disease: New markers and insights in pathophysiology for two distinct glycosphingolipidoses. *Biochim. Biophys. Acta - Mol. Cell Biol. Lipids* **1841**, 811–825 (2014).
8. Aerts, J. M., Hollak, C., Boot, R. & Groener, A. Biochemistry of glycosphingolipid storage disorders: implications for therapeutic intervention. *Philos. Trans. R. Soc. Lond. B. Biol. Sci.* **358**, 905–14 (2003).
9. Boot, R. G., Hollak, C. E. M., Verhoek, M., Sloof, P., Poorthuis, B. J. H. M., Kleijer, W. J., Wevers, R. A., Van Oers, M. H. J., Mannens, M. M. A. M., Aerts, J. M. F. G. & van Weely, S. Glucocerebrosidase genotype of Gaucher patients in the Netherlands: limitations in prognostic value. *Hum. Mutat.* **10**, 348–358 (1997).
10. Lachmann, R. H., Grant, I. R., Halsall, D. & Cox, T. M. Twin pairs showing discordance of phenotype in adult Gaucher's disease. *QJM* **97**, 199–204 (2004).
11. Biegstraaten, M., van Schaik, I. N., Aerts, J. M. F. G., Langeveld, M., Mannens, M. M. A. M., Bour, L. J., Sidransky, E., Tayebi, N., Fitzgibbon, E. & Hollak, C. E. M. A monozygotic twin pair with highly discordant Gaucher phenotypes. *Blood Cells, Mol. Dis.* **46**, 39–41 (2011).
12. Pastores, G. M., Weinreb, N. J., Aerts, H., Andria, G., Cox, T. M., Giral, M., Grabowski, G. A., Mistry, P. K. & Tylki-Szymańska, A. Therapeutic goals in the treatment of Gaucher disease. *Semin. Hematol.* **41**, 4–14 (2004).
13. Weinreb, N. J., Aggio, M. C., Andersson, H. C., Andria, G., Charrow, J., *et al.* Gaucher disease type 1: revised recommendations on evaluations and monitoring for adult patients. *Semin. Hematol.* **41**, 15–22 (2004).
14. Cox, T. M., Aerts, J. M. F. G., Belmatoug, N., Cappellini, M. D., vom Dahl, S., Goldblatt, J., Grabowski, G. A., Hollak, C. E. M., Hwu, P., Maas, M., Martins, A. M., Mistry, P. K., Pastores, G. M., Tylki-Szymanska, A., Yee, J. & Weinreb, N. Management of non-neuronopathic Gaucher disease with special reference to pregnancy, splenectomy, bisphosphonate therapy, use of biomarkers and bone disease monitoring. *J. Inher. Metab. Dis.* **31**, 319–336 (2008).
15. Aerts, J. M. F. G., Kallemijn, W. W., Wegdam, W., Joao Ferraz, M., van Breemen, M. J., Dekker, N., Kramer, G., Poorthuis, B. J., Groener, J. E. M., Cox-Brinkman, J., Rombach, S. M., Hollak, C. E. M., Linthorst, G. E., Witte, M. D., Gold, H., van der Marel, G. A.,

- Overkleeft, H. S. & Boot, R. G. Biomarkers in the diagnosis of lysosomal storage disorders: proteins, lipids, and inhibodies. *J. Inherit. Metab. Dis.* **34**, 605–19 (2011).
16. Groener, J. E. M., Poorthuis, B. J. H. M., Kuiper, S., Hollak, C. E. M. & Aerts, J. M. F. G. Plasma glucosylceramide and ceramide in type 1 Gaucher disease patients: Correlations with disease severity and response to therapeutic intervention. *Biochim. Biophys. Acta - Mol. Cell Biol. Lipids* **1781**, 72–78 (2008).
 17. Ghauharali-van der Vlugt, K., Langeveld, M., Poppema, A., Kuiper, S., Hollak, C. E. M., Aerts, J. M. & Groener, J. E. M. Prominent increase in plasma ganglioside GM3 is associated with clinical manifestations of type I Gaucher disease. *Clin. Chim. Acta* **389**, 109–113 (2008).
 18. Dekker, N., van Dussen, L., Hollak, C. E. M., Overkleeft, H., Scheij, S., Ghauharali, K., van Breemen, M. J., Ferraz, M. J., Groener, J. E. M., Maas, M., Wijburg, F. A., Speijer, D., Tytki-Szymanska, A., Mistry, P. K., Boot, R. G. & Aerts, J. M. Elevated plasma glucosylsphingosine in Gaucher disease: relation to phenotype, storage cell markers, and therapeutic response. *Blood* **118**, e118–27 (2011).
 19. Murugesan, V., Chuang, W.-L., Liu, J., Lischuk, A., Kacena, K., Lin, H., Pastores, G. M., Yang, R., Keutzer, J., Zhang, K. & Mistry, P. K. Glucosylsphingosine is a key biomarker of Gaucher disease. *Am. J. Hematol.* **91**, 1082–1089 (2016).
 20. Ferraz, M. J., Marques, A. R. A., Appelman, M. D., Verhoek, M., Strijland, A., Mirzaian, M., Scheij, S., Ouairy, C. M., Lahav, D., Wisse, P., Overkleeft, H. S., Boot, R. G. & Aerts, J. M. Lysosomal glycosphingolipid catabolism by acid ceramidase: formation of glycosphingoid bases during deficiency of glycosidases. *FEBS Lett.* **590**, 716–725 (2016).
 21. Gaspar, P., Kallemeyjn, W. W., Strijland, A., Scheij, S., Van Eijk, M., Aten, J., Overkleeft, H. S., Balreira, A., Zunke, F., Schwake, M., Sá Miranda, C. & Aerts, J. M. F. G. Action myoclonus-renal failure syndrome: diagnostic applications of activity-based probes and lipid analysis. *J. Lipid Res.* **55**, 138–45 (2014).
 22. Reczek, D., Schwake, M., Schröder, J., Hughes, H., Blanz, J., Jin, X., Brondyk, W., Van Patten, S., Edmunds, T. & Saftig, P. LIMP-2 is a receptor for lysosomal mannose-6-phosphate-independent targeting of β -glucocerebrosidase. *Cell* **131**, 770–783 (2007).
 23. Balreira, A., Gaspar, P., Caiola, D., Chaves, J., Beirão, I., Lima, J. L., Azevedo, J. E. & Miranda, M. C. S. A nonsense mutation in the LIMP-2 gene associated with progressive myoclonic epilepsy and nephrotic syndrome. *Hum. Mol. Genet.* **17**, 2238–2243 (2008).
 24. Mirzaian, M., Wisse, P., Ferraz, M. J., Gold, H., Donker-Koopman, W. E., Verhoek, M., Overkleeft, H. S., Boot, R. G., Kramer, G., Dekker, N. & Aerts, J. M. F. G. Mass spectrometric quantification of glucosylsphingosine in plasma and urine of type 1 Gaucher patients using an isotope standard. *Blood Cells, Mol. Dis.* **54**, 307–314 (2015).
 25. Elstein, D., Mellgard, B., Dinh, Q., Lan, L., Qiu, Y., Cozma, C., Eichler, S., Böttcher, T. & Zimran, A. Reductions in glucosylsphingosine (lyso-Gb1) in treatment-naïve and previously treated patients receiving velaglucerase alfa for type 1 Gaucher disease: data from phase 3 clinical trials. *Mol. Genet. Metab.* **122**, 113–120 (2017).
 26. Ferraz, M. J., Marques, A. R. A. A., Gaspar, P., Mirzaian, M., van Roomen, C., Ottenhoff, R., Alfonso, P., Irún, P., Giraldo, P., Wisse, P., Sá Miranda, C., Overkleeft, H. S. & Aerts, J. M. Lyso-glycosphingolipid abnormalities in different murine models of lysosomal storage disorders. *Mol. Genet. Metab.* **117**, 186–93 (2016).
 27. Suzuki, K. Twenty five years of the “psychosine hypothesis”: a personal perspective of its history and present status. *Neurochem. Res.* **23**, 251–259 (1998).
 28. Aerts, J. M., Groener, J. E., Kuiper, S., Donker-Koopman, W. E., Strijland, A., Ottenhoff, R., van Roomen, C., Mirzaian, M., Wijburg, F. A., Linthorst, G. E., Vedder, A. C., Rombach, S. M., Cox-Brinkman, J., Somerharju, P., Boot, R. G., Hollak, C. E., Brady, R. O. & Poorthuis,

- B. J. Elevated globotriaosylsphingosine is a hallmark of Fabry disease. *Proc. Natl. Acad. Sci. USA*. **105**, 2812–7 (2008).
29. Kuchar, L., Sikora, J., Gulinello, M. E., Poupetova, H., Lugowska, A., Malinova, V., Jahnova, H., Asfaw, B. & Ledvinova, J. Quantitation of plasmatic lysosphingomyelin and lysosphingomyelin-509 for differential screening of Niemann-Pick A/B and C diseases. *Anal. Biochem.* **525**, 73–77 (2017).
30. Mirzaian, M., Wisse, P., Ferraz, M. J., Marques, A. R. A., Gaspar, P., Oussoren, S. V., Kytidou, K., Codée, J. D. C., van der Marel, G., Overkleeft, H. S. & Aerts, J. M. Simultaneous quantitation of sphingoid bases by UPLC-ESI-MS/MS with identical ¹³C-encoded internal standards. *Clin. Chim. Acta* **466**, 178–184 (2017).
31. Pettazzoni, M., Froissart, R., Pagan, C., Vanier, M. T., Ruet, S., Latour, P., Guffon, N., Fouilhous, A., Germain, D. P., Levade, T., Vianey-Saban, C., Piraud, M. & Cheillan, D. LC-MS/MS multiplex analysis of lysosphingolipids in plasma and amniotic fluid: a novel tool for the screening of sphingolipidoses and Niemann-Pick type C disease. *PLoS One* **12**, e0181700 (2017).
32. Polo, G., Burlina, A. P. A. B., Kolamunnage, T. B., Zampieri, M., Dionisi-Vici, C., Strisciuglio, P., Zaninotto, M., Plebani, M. & Burlina, A. P. A. B. Diagnosis of sphingolipidoses: a new simultaneous measurement of lysosphingolipids by LC-MS/MS. *Clin. Chem. Lab. Med.* **55**, 403–414 (2017).
33. Mistry, P. K., Liu, J., Yang, M., Nottoli, T., McGrath, J., *et al.* Glucocerebrosidase gene-deficient mouse recapitulates Gaucher disease displaying cellular and molecular dysregulation beyond the macrophage. *Proc. Natl. Acad. Sci. USA*. **107**, 19473–8 (2010).
34. Nair, S., Branagan, A. R., Liu, J., Boddupalli, C. S., Mistry, P. K. & Dhodapkar, M. V. Clonal immunoglobulin against lysolipids in the origin of myeloma. *N. Engl. J. Med.* **374**, 555–561 (2016).
35. Pavlova, E., Wang, S., Archer, J., Dekker, N., Aerts, J., Karlsson, S. & Cox, T. B cell lymphoma and myeloma in murine Gaucher's disease. *J. Pathol.* **231**, 88–97 (2013).
36. Lukas, J., Cozma, C., Yang, F., Kramp, G., Meyer, A., Neßlauer, A.-M., Eichler, S., Böttcher, T., Witt, M., Bräuer, A. U., Kropp, P. & Rolfs, A. Glucosylsphingosine causes hematological and visceral changes in mice-evidence for a pathophysiological role in Gaucher disease. *Int. J. Mol. Sci.* **18**, (2017).
37. Taguchi, Y. V., Liu, J., Ruan, J., Pacheco, J., Zhang, X., Abbasi, J., Keutzer, J., Mistry, P. K. & Chandra, S. S. Glucosylsphingosine promotes α -synuclein pathology in mutant GBA-associated Parkinson's disease. *J. Neurosci.* **37**, 9617–9631 (2017).
38. Sidransky, E., Nalls, M. A., Aasly, J. O., Aharon-Peretz, J., Annesi, G., *et al.* Multicenter analysis of glucocerebrosidase mutations in Parkinson's disease. *N. Engl. J. Med.* **361**, 1651–1661 (2009).
39. Choi, L., Vernon, J., Kopach, O., Minett, M. S., Mills, K., Clayton, P. T., Meert, T. & Wood, J. N. The Fabry disease-associated lipid Lyso-Gb₃ enhances voltage-gated calcium currents in sensory neurons and causes pain. *Neurosci. Lett.* **594**, 163–168 (2015).
40. Sanchez-Niño, M. D., Carpio, D., Sanz, A. B., Ruiz-Ortega, M., Mezzano, S. & Ortiz, A. Lyso-Gb₃ activates Notch1 in human podocytes. *Hum. Mol. Genet.* **24**, 5720–5732 (2015).
41. Aerts, J. M., Ferraz, M. J., Mirzaian, M., Gaspar, P., Oussoren, S. V., *et al.* Lysosomal storage diseases. For better or worse: adapting to defective lysosomal glycosphingolipid breakdown. *eLS* 1–13 (2017).
42. Marques, A. R. A., Mirzaian, M., Akiyama, H., Wisse, P., Ferraz, M. J., *et al.* Glucosylated cholesterol in mammalian cells and tissues: Formation and degradation by multiple

- cellular β -glucosidases. *J. Lipid Res.* **57**, 451–463 (2016).
43. Akiyama, H., Kobayashi, S., Hirabayashi, Y. & Murakami-Murofushi, K. Cholesterol glucosylation is catalyzed by transglucosylation reaction of β -glucosidase 1. *Biochem. Biophys. Res. Commun.* **441**, 838–843 (2013).
 44. Wraith, J. E., Baumgartner, M. R., Bembi, B., Covanis, A., Levade, T., Mengel, E., Pineda, M., Sedel, F., Topçu, M., Vanier, M. T., Widner, H., Wijburg, F. A. & Patterson, M. C. Recommendations on the diagnosis and management of Niemann-Pick disease type C. *Mol. Genet. Metab.* **98** 152–165 (2009).
 45. Porter, F. D., Scherrer, D. E., Lanier, M. H., Langmade, S. J., Molugu, V., Gale, S. E., Olzeski, D., Sidhu, R., Dietzen, D. J., Fu, R., Wassif, C. A., Yanjanin, N. M., Marso, S. P., House, J., Vite, C., Schaffer, J. E. & Ory, D. S. Cholesterol oxidation products are sensitive and specific blood-based biomarkers for Niemann-Pick C1 disease. *Sci. Transl. Med.* **2**, 56ra81–56ra81 (2010).
 46. Tint, G. S., Pentchev, P., Xu, G., Batta, A. K., Shefer, S., Salen, G. & Honda, A. Cholesterol and oxygenated cholesterol concentrations are markedly elevated in peripheral tissue but not in brain from mice with the Niemann-Pick type C phenotype. *J. Inher. Metab. Dis.* **21**, 853–863 (1998).
 47. Jiang, X., Sidhu, R., Porter, F. D., Yanjanin, N. M., Speak, A. O., te Vrugte, D. T., Platt, F. M., Fujiwara, H., Scherrer, D. E., Zhang, J., Dietzen, D. J., Schaffer, J. E. & Ory, D. S. A sensitive and specific LC-MS/MS method for rapid diagnosis of Niemann-Pick C1 disease from human plasma. *J. Lipid Res.* **52**, 1435–45 (2011).
 48. Hammerschmidt, T. G., de Oliveira Schmitt Ribas, G., Saraiva-Pereira, M. L., Bonatto, M. P., Kessler, R. G., Souza, F. T. S., Trapp, F., Michelin-Tirelli, K., Burin, M. G., Giugliani, R. & Vargas, C. R. Molecular and biochemical biomarkers for diagnosis and therapy monitorization of Niemann-Pick type C patients. *Int. J. Dev. Neurosci.* **66**, 18–23 (2018).
 49. Polo, G., Burlina, A., Furlan, F., Kolamunnage, T., Cananzi, M., Giordano, L., Zaninotto, M., Plebani, M. & Burlina, A. High level of oxysterols in neonatal cholestasis: a pitfall in analysis of biochemical markers for Niemann-Pick type C disease. *Clin. Chem. Lab. Med.* **54**, 1221–1229 (2016).
 50. Prunet, C., Petit, J. M., Ecartot-Laubriet, A., Athias, A., Miguet-Alfonsi, C., Rohmer, J. F., Steinmetz, E., Néel, D., Gambert, P. & Lizard, G. High circulating levels of 7β - and 7α -hydroxycholesterol and presence of apoptotic and oxidative markers in arterial lesions of normocholesterolemic atherosclerotic patients undergoing endarterectomy. *Pathol. Biol.* **54**, 22–32 (2006).
 51. Ferderbar, S., Pereira, E. C., Apolinário, E., Bertolami, M. C., Faludi, A., Monte, O., Calliari, L. E., Sales, J. E., Gagliardi, A. R., Xavier, H. T. & Abdalla, D. S. P. Cholesterol oxides as biomarkers of oxidative stress in type 1 and type 2 diabetes mellitus. *Diabetes. Metab. Res. Rev.* **23**, 35–42 (2007).
 52. Alkazemi, D., Egeland, G., Vaya, J., Meltzer, S. & Kubow, S. Oxysterol as a marker of atherogenic dyslipidemia in adolescence. *J. Clin. Endocrinol. Metab.* **93**, 4282–4289 (2008).
 53. Marques, A. R. A., Aten, J., Ottenhoff, R., van Roomen, C. P. A. A., Herrera Moro, D., Claessen, N., Vinueza Veloz, M. F., Zhou, K., Lin, Z., Mirzaian, M., Boot, R. G., De Zeeuw, C. I., Overkleeft, H. S., Yildiz, Y. & Aerts, J. M. F. G. Reducing GBA2 activity ameliorates neuropathology in Niemann-Pick Type C mice. *PLoS One* **10**, e0135889 (2015).
 54. Cox, T., Lachmann, R., Hollak, C., Aerts, J., van Weely, S., Hrebíček, M., Platt, F., Butters, T., Dwek, R., Moyes, C., Gow, I., Elstein, D. & Zimran, A. Novel oral treatment of Gaucher's disease with N-butyldeoxynojirimycin (OGT 918) to decrease substrate biosynthesis. *Lancet* **355**, 1481–1485 (2000).

55. Platt, F. M., Jeyakumar, M., Andersson, U., Priestman, D. A., Dwek, R. A., Butters, T. D., Cox, T. M., Lachmann, R. H., Hollak, C., Aerts, J. M. F. G., Van Weely, S., Hrebíček, M., Moyses, C., Gow, I., Elstein, D. & Zimran, A. Inhibition of substrate synthesis as a strategy for glycolipid lysosomal storage disease therapy. *J. Inherit. Metab. Dis.* **24**, 275–290 (2001).
56. Aerts, J. M. F. G., Hollak, C. E. M., Boot, R. G., Groener, J. E. M. & Maas, M. Substrate reduction therapy of glycosphingolipid storage disorders. *J. Inherit. Metab. Dis.* **29**, 449–456 (2006).
57. Patterson, M. C., Vecchio, D., Prady, H., Abel, L. & Wraith, J. E. Miglustat for treatment of Niemann-Pick C disease: a randomised controlled study. *Lancet Neurol.* **6**, 765–772 (2007).
58. Aerts, J. M. F. G., Hollak, C. E. M., Breemen, M., Maas, M., Groener, J. E. M. & Boot, R. Identification and use of biomarkers in Gaucher disease and other lysosomal storage diseases. *Acta Paediatr.* **94**, 43–46 (2007).
59. Brady, R. O. Enzyme replacement therapy: conception, chaos and culmination. *Philos. Trans. R. Soc. Lond. B. Biol. Sci.* **358**, 915–9 (2003).
60. Barton, N. W., Furbish, F. S., Murray, G. J., Garfield, M. & Brady, R. O. Therapeutic response to intravenous infusions of glucocerebrosidase in a patient with Gaucher disease. *Proc. Natl. Acad. Sci. USA.* **87**, (1990).
61. McCabe, E. R. B., Fine, B. A., Golbus, M. S., Greenhouse, J. B., McGrath, G. L., *et al.* Gaucher disease. *JAMA* **275**, 548 (1996).
62. Hollak, C., Aerts, J. & van Oers, H. Treatment of Gaucher's disease. *N. Engl. J. Med.* **328**, 1564–1568 (1993).
63. Aerts, J. M. F. G., Hollak, C. E. M., E G Aerts, J. M. & M Hollak, C. E. 4 Plasma and metabolic abnormalities in Gaucher's disease. *Baillieres Clin. Haematol.* **10** 691–709 (1997).
64. Hayman, A. R. & Cox, T. M. Tartrate-resistant acid phosphatase: a potential target for therapeutic gold. *Cell Biochem. Funct.* **22**, 275–280 (2004).
65. Hollak, C. E. M., van Weely, S., van Oers, M. H. J. & Aerts, J. M. F. G. Marked elevation of plasma chitotriosidase activity. A novel hallmark of Gaucher disease. *J. Clin. Invest.* **93**, 1288–1292 (1994).
66. Renkema, G. H., Boot, R. G., Muijsers, A. O., Donker-Koopman, W. E. & Aerts, J. M. Purification and characterization of human chitotriosidase, a novel member of the chitinase family of proteins. *J. Biol. Chem.* **270**, 2198–202 (1995).
67. Boot, R. G., Renkema, G. H., Strijland, A., van Zonneveld, A. J. & Aerts, J. M. Cloning of a cDNA encoding chitotriosidase, a human chitinase produced by macrophages. *J. Biol. Chem.* **270**, 26252–6 (1995).
68. Renkema, G. H., Boot, R. G., Strijland, A., Donker-Koopman, W. E., Berg, M., Muijsers, A. O. & Aerts, J. M. F. G. Synthesis, sorting, and processing into distinct isoforms of human macrophage chitotriosidase. *Eur. J. Biochem.* **244**, 279–285 (1997).
69. Boot, R. G., Renkema, G. H., Verhoek, M., Strijland, A., Blik, J., de Meulemeester, T. M., Mannens, M. M. & Aerts, J. M. The human chitotriosidase gene. Nature of inherited enzyme deficiency. *J. Biol. Chem.* **273**, 25680–5 (1998).
70. Fusetti, F., von Moeller, H., Houston, D., Rozeboom, H. J., Dijkstra, B. W., Boot, R. G., Aerts, J. M. F. G. & van Aalten, D. M. F. Structure of human chitotriosidase. Implications for specific inhibitor design and function of mammalian chitinase-like lectins. *J. Biol. Chem.* **277**, 25537–44 (2002).
71. Boven, L. A., van Meurs, M., Boot, R. G., Mehta, A., Boon, L., Aerts, J. M. & Laman, J. D. Gaucher cells demonstrate a distinct macrophage phenotype and resemble alternatively

- activated macrophages. *Am. J. Clin. Pathol.* **122**, 359–369 (2004).
72. van Eijk, M., van Roomen, C. P. A. A., Renkema, G. H., Bussink, A. P., Andrews, L., Blommaart, E. F. C., Sugar, A., Verhoeven, A. J., Boot, R. G. & Aerts, J. M. F. G. Characterization of human phagocyte-derived chitotriosidase, a component of innate immunity. *Int. Immunol.* **17**, 1505–1512 (2005).
 73. Bussink, A. P., van Eijk, M., Renkema, G. H., Aerts, J. M. & Boot, R. G. The biology of the Gaucher cell: the cradle of human chitinases. *Int. Rev. Cytol.* **252**, 71–128 (2006).
 74. Bussink, A. P., Speijer, D., Aerts, J. M. F. G. & Boot, R. G. Evolution of mammalian chitinase(-like) members of family 18 glycosyl hydrolases. *Genetics* **177**, 959–70 (2007).
 75. Aguilera, B., Ghauharali-van der Vlugt, K., Helmond, M. T. J., Out, J. M. M., Donker-Koopman, W. E., Groener, J. E. M., Boot, R. G., Renkema, G. H., van der Marel, G. A., van Boom, J. H., Overkleef, H. S. & Aerts, J. M. F. G. Transglycosidase activity of chitotriosidase: improved enzymatic assay for the human macrophage chitinase. *J. Biol. Chem.* **278**, 40911–6 (2003).
 76. Schoonhoven, A., Rudensky, B., Elstein, D., Zimran, A., Hollak, C. E. M., Groener, J. E. & Aerts, J. M. F. G. Monitoring of Gaucher patients with a novel chitotriosidase assay. *Clin. Chim. Acta* **381**, 136–139 (2007).
 77. van Dussen, L., Hendriks, E. J., Groener, J. E. M., Boot, R. G., Hollak, C. E. M. & Aerts, J. M. F. G. Value of plasma chitotriosidase to assess non-neuronopathic Gaucher disease severity and progression in the era of enzyme replacement therapy. *J. Inherit. Metab. Dis.* **37**, 991–1001 (2014).
 78. Boot, R. G., van Achterberg, T. A. E., van Aken, B. E., Renkema, G. H., Jacobs, M. J. H. M., Aerts, J. M. F. G. & de Vries, C. J. M. Strong induction of members of the chitinase family of proteins in atherosclerosis. *Arterioscler. Thromb. Vasc. Biol.* **19**, 687–694 (1999).
 79. Iyer, A., van Eijk, M., Silva, E., Hatt, M., Faber, W., Aerts, J. M. F. G. & Das, P. K. Increased chitotriosidase activity in serum of leprosy patients: association with bacillary leprosy. *Clin. Immunol.* **131**, 501–509 (2009).
 80. Boot, R. G., Hollak, C. E. M., Verhoek, M., Alberts, C., Jonkers, R. E. & Aerts, J. M. Plasma chitotriosidase and CCL18 as surrogate markers for granulomatous macrophages in sarcoidosis. *Clin. Chim. Acta* **411**, 31–36 (2010).
 81. Guo, Y., He, W., Boer, A. M., Wevers, R. A., de Bruijn, A. M., Groener, J. E. M., Hollak, C. E. M., Aerts, J. M. F. G., Galjaard, H. & van Diggelen, O. P. Elevated plasma chitotriosidase activity in various lysosomal storage disorders. *J. Inherit. Metab. Dis.* **18**, 717–722 (1995).
 82. Vedder, A. C., Cox-Brinkman, J., Hollak, C. E. M., Linthorst, G. E., Groener, J. E. M., Helmond, M. T. J., Scheij, S. & Aerts, J. M. F. G. Plasma chitotriosidase in male Fabry patients: A marker for monitoring lipid-laden macrophages and their correction by enzyme replacement therapy. *Mol. Genet. Metab.* **89**, 239–244 (2006).
 83. Ries, M., Schaefer, E., Lührs, T., Mani, L., Kuhn, J., Vanier, M. T., Krummenauer, F., Gal, A., Beck, M. & Mengel, E. Critical assessment of chitotriosidase analysis in the rational laboratory diagnosis of children with Gaucher disease and Niemann–Pick disease type A/B and C. *J. Inherit. Metab. Dis.* **29**, 647–652 (2006).
 84. Moran, M. T., Schofield, J. P., Hayman, A. R., Shi, G. P., Young, E. & Cox, T. M. Pathologic gene expression in Gaucher disease: up-regulation of cysteine proteinases including osteoclastic cathepsin K. *Blood* **96**, 1969–78 (2000).
 85. Boot, R. G., Verhoek, M., de Fost, M., Hollak, C. E. M., Maas, M., Bleijlevens, B., van Breemen, M. J., van Meurs, M., Boven, L. A., Laman, J. D., Moran, M. T., Cox, T. M. & Aerts, J. M. F. G. Marked elevation of the chemokine CCL18/PARC in Gaucher disease: a novel

- surrogate marker for assessing therapeutic intervention. *Blood* **103**, 33–9 (2004).
86. Deegan, P. B., Moran, M. T., McFarlane, I., Schofield, J. P., Boot, R. G., Aerts, J. M. F. G. & Cox, T. M. Clinical evaluation of chemokine and enzymatic biomarkers of Gaucher disease. *Blood Cells, Mol. Dis.* **35**, 259–267 (2005).
87. Chang, K.-L., Hwu, W.-L., Yeh, H.-Y., Lee, N.-C. & Chien, Y.-H. CCL18 as an alternative marker in Gaucher and Niemann-Pick disease with chitotriosidase deficiency. *Blood Cells, Mol. Dis.* **44**, 38–40 (2010).
88. Pineda, M., Perez-Poyato, M. S., O'Callaghan, M., Vilaseca, M. A., Pocovi, M., Domingo, R., Portal, L. R., Pérez, A. V., Temudo, T., Gaspar, A., Peñas, J. J. G., Roldán, S., Fumero, L. M., de la Barca, O. B., Silva, M. T. G., Macías-Vidal, J. & Coll, M. J. Clinical experience with miglustat therapy in pediatric patients with Niemann-Pick disease type C: a case series. *Mol. Genet. Metab.* **99**, 358–66 (2010).
89. De Castro-Orós, I., Irún, P., Cebolla, J. J., Rodriguez-Sureda, V., Mallén, M., Pueyo, M. J., Mozas, P., Dominguez, C. & Pocoví, M. Assessment of plasma chitotriosidase activity, CCL18/PARC concentration and NP-C suspicion index in the diagnosis of Niemann-Pick disease type C: a prospective observational study. *J. Transl. Med.* **15**, 43 (2017).
90. Aerts, J. M. F. G., Yasothan, U. & Kirkpatrick, P. Velaglucerase alfa. *Nat. Rev. Drug Discov.* **9**, 837–838 (2010).
91. Zimran, A., Brill-Almon, E., Chertkoff, R., Petakov, M., Blanco-Favela, F., *et al.* Pivotal trial with plant cell-expressed recombinant glucocerebrosidase, taliglucerase alfa, a novel enzyme replacement therapy for Gaucher disease. *Blood* **118**, 5767–73 (2011).
92. Elstein, D., Hollak, C., Aerts, J. M. F. G., van Weely, S., Maas, M., Cox, T. M., Lachmann, R. H., Hrebicek, M., Platt, F. M., Butters, T. D., Dwek, R. A. & Zimran, A. Sustained therapeutic effects of oral miglustat (Zavesca, N-butyldeoxynojirimycin, OGT 918) in type I Gaucher disease. *J. Inher. Metab. Dis.* **27**, 757–766 (2004).
93. Cox, T. M., Drelichman, G., Cravo, R., Balwani, M., Burrow, T. A., Martins, A. M., Lukina, E., Rosenbloom, B., Ross, L., Angell, J. & Puga, A. C. Eliglustat compared with imiglucerase in patients with Gaucher's disease type 1 stabilised on enzyme replacement therapy: a phase 3, randomised, open-label, non-inferiority trial. *Lancet* **385**, 2355–2362 (2015).
94. Mistry, P. K., Lukina, E., Ben Turkia, H., Amato, D., Baris, H., *et al.* Effect of Oral Eliglustat on Splenomegaly in patients with Gaucher disease type 1. *JAMA* **313**, 695 (2015).
95. Smid, B. E., Ferraz, M. J., Verhoek, M., Mirzaian, M., Wisse, P., Overkleeft, H. S., Hollak, C. E. & Aerts, J. M. Biochemical response to substrate reduction therapy versus enzyme replacement therapy in Gaucher disease type 1 patients. *Orphanet J. Rare Dis.* **11**, 28 (2016).
96. Hashimoto, S., Yamada, M., Motoyoshi, K., Akagawa, K. S. & Matsushima, K. Enhancement of macrophage colony-stimulating factor-induced growth and differentiation of human monocytes by interleukin-10. *Blood* **89**, 315–21 (1997).
97. Kramer, G., Wegdam, W., Donker-Koopman, W., Ottenhoff, R., Gaspar, P., Verhoek, M., Nelson, J., Gabriel, T., Kallemeijn, W., Boot, R. G., Laman, J. D., Vissers, J. P. C., Cox, T., Pavlova, E., Moran, M. T., Aerts, J. M. & van Eijk, M. Elevation of glycoprotein nonmetastatic melanoma protein B in type 1 Gaucher disease patients and mouse models. *FEBS Open Bio.* **6**, 902–913 (2016).
98. Dahl, M., Doyle, A., Olsson, K., Månsson, J. E., Marques, A. R. A., Mirzaian, M., Aerts, J. M., Ehinger, M., Rothe, M., Modlich, U., Schambach, A. & Karlsson, S. Lentiviral gene therapy using cellular promoters cures type 1 gaucher disease in mice. *Mol. Ther.* **23**, 835–844 (2015).
99. Pavlova, E. V., Archer, J., Z Wang, S., Dekker, N., Aerts, J. M., Karlsson, S. & Cox, T. M.

- Inhibition of UDP-glucosylceramide synthase in mice prevents Gaucher disease-associated B-cell malignancy. *J. Pathol.* **235**, 113–124 (2015).
100. Xu, Y.-H., Jia, L., Quinn, B., Zamzow, M., Stringer, K., Aronow, B., Sun, Y., Zhang, W., Setchell, K. D. & Grabowski, G. A. Global gene expression profile progression in Gaucher disease mouse models. *BMC Genomics* **12**, 20 (2011).
 101. Zigdon, H., Savidor, A., Levin, Y., Meshcheriakova, A., Schiffmann, R. & Futerman, A. H. Identification of a biomarker in cerebrospinal fluid for neuronopathic forms of Gaucher disease. *PLoS One* **10**, e0120194 (2015).
 102. Murugesan, V., Liu, J., Yang, R., Lin, H., Lischuk, A., Pastores, G., Zhang, X., Chuang, W.-L. & Mistry, P. K. Validating glycoprotein non-metastatic melanoma B (gpNMB, osteoactivin), a new biomarker of Gaucher disease. *Blood Cells, Mol. Dis.* **68**, 47–53 (2018).
 103. Marques, A. R. A., Gabriel, T. L., Aten, J., Van Roomen, C. P. A. A., Ottenhoff, R., Claessen, N., Alfonso, P., Irún, P., Giraldo, P., Aerts, J. M. F. G. & Van Eijk, M. Gpnmb is a potential marker for the visceral pathology in Niemann-Pick type C disease. *PLoS One* **11**, e0147208 (2016).
 104. Alam, M. S., Getz, M., Safeukui, I., Yi, S., Tamez, P., Shin, J., Velázquez, P. & Haldar, K. Genomic expression analyses reveal lysosomal, innate immunity proteins, as disease correlates in murine models of a lysosomal storage disorder. *PLoS One* **7**, e48273 (2012).
 105. Cluzeau, C. V. M., Watkins-Chow, D. E., Fu, R., Borate, B., Yanjanin, N., Dail, M. K., Davidson, C. D., Walkley, S. U., Ory, D. S., Wassif, C. A., Pavan, W. J. & Porter, F. D. Microarray expression analysis and identification of serum biomarkers for Niemann-Pick disease, type C1. *Hum. Mol. Genet.* **21**, 3632–3646 (2012).
 106. UniProtKB - Q14956. <https://www.uniprot.org/uniprot/Q14956> (accessed 4-4-2020).
 107. Strausberg, R. L., Feingold, E. A., Grouse, L. H., Derge, J. G., Klausner, R. D., *et al.* Generation and initial analysis of more than 15,000 full-length human and mouse cDNA sequences. *Proc. Natl. Acad. Sci. U. S. A.* **99**, 16899–903 (2002).
 108. UniProtKB - Q99P91. <https://www.uniprot.org/uniprot/Q99P91> (accessed 4-4-2020).
 109. Shikano, S., Bonkobara, M., Zukas, P. K. & Ariizumi, K. Molecular cloning of a dendritic cell-associated transmembrane protein, DC-HIL, that promotes RGD-dependent adhesion of endothelial cells through recognition of heparan sulfate proteoglycans. *J. Biol. Chem.* **276**, 8125–34 (2001).
 110. Hoashi, T., Sato, S., Yamaguchi, Y., Passeron, T., Tamaki, K. & Hearing, V. J. Glycoprotein nonmetastatic melanoma protein b, a melanocytic cell marker, is a melanosome-specific and proteolytically released protein. *FASEB J.* **24**, 1616–1629 (2010).
 111. Furochi, H., Tamura, S., Mameoka, M., Yamada, C., Ogawa, T., Hirasaka, K., Okumura, Y., Imagawa, T., Oguri, S., Ishidoh, K., Kishi, K., Higashiyama, S. & Nikawa, T. Osteoactivin fragments produced by ectodomain shedding induce MMP-3 expression via ERK pathway in mouse NIH-3T3 fibroblasts. *FEBS Lett.* **581**, 5743–5750 (2007).
 112. Rose, A. A. N., Annis, M. G., Dong, Z., Pepin, F., Hallett, M., Park, M. & Siegel, P. M. ADAM10 releases a soluble form of the GPNMB/Osteoactivin extracellular domain with angiogenic properties. *PLoS One* **5**, e12093 (2010).
 113. Li, B., Castano, A. P., Hudson, T. E., Nowlin, B. T., Lin, S.-L., Bonventre, J. V., Swanson, K. D. & Duffield, J. S. The melanoma-associated transmembrane glycoprotein Gpnmb controls trafficking of cellular debris for degradation and is essential for tissue repair. *FASEB J.* **24**, 4767–4781 (2010).
 114. Theos, A. C., Watt, B., Harper, D. C., Janczura, K. J., Theos, S. C., Herman, K. E. & Marks, M. S. The PKD domain distinguishes the trafficking and amyloidogenic properties of the

- pigment cell protein PMEL and its homologue GPNMB. *Pigment Cell Melanoma Res.* **26**, 470–486 (2013).
115. Weterman, M. A. J., Ajubi, N., van Dinter, I. M. R., Degen, W. G. J., van Muijen, G. N. P., Ruiter, D. J. & Bloemers, H. P. J. Nmb, a novel gene, is expressed in low-metastatic human melanoma cell lines and xenografts. *Int. J. Cancer* **60**, 73–81 (1995).
116. Tissue expression of GPNMB - Summary - The Human Protein Atlas. <https://www.proteinatlas.org/ENSG00000136235-GPNMB/tissue> (accessed 4-4-2020).
117. Ripoll, V. M., Irvine, K. M., Ravasi, T., Sweet, M. J., Hume, D. A., Ripoll, V. M., Irvine, K. M., Ravasi, T., Sweet, M. J. & Hume, D. A. Gpnmb Is Induced in Macrophages by IFN- γ and Lipopolysaccharide and Acts as a Feedback Regulator of Proinflammatory Responses. *J. Immunol. Ref. J. Immunol.* **178**, 6557–6566 (2018).
118. Sheng, M. H.-C., Wergedal, J. E., Mohan, S. & Lau, K.-H. W. Osteoactivin is a novel osteoclastic protein and plays a key role in osteoclast differentiation and activity. *FEBS Lett.* **582**, 1451–1458 (2008).
119. Ripoll, V. M., Meadows, N. A., Raggatt, L.-J., Chang, M. K., Pettit, A. R., Cassady, A. I. & Hume, D. A. Microphthalmia transcription factor regulates the expression of the novel osteoclast factor GPNMB. *Gene* **413**, 32–41 (2008).
120. Maric, G., Rose, A. A., Annis, M. G. & Siegel, P. M. Glycoprotein non-metastatic b (GPNMB): a metastatic mediator and emerging therapeutic target in cancer. *Onco. Targets. Ther.* **6**, 839–52 (2013).
121. Le Borgne, R., Planque, N., Martin, P., Dewitte, F., Saule, S. & Hoflack, B. The AP-3-dependent targeting of the melanosomal glycoprotein QNR-71 requires a di-leucine-based sorting signal. *J. Cell Sci.* **114**, 2831–41 (2001).
122. Zhang, P., Liu, W., Zhu, C., Yuan, X., Li, D., Gu, W., Ma, H., Xie, X. & Gao, T. Silencing of GPNMB by siRNA inhibits the formation of melanosomes in melanocytes in a MITF-independent fashion. *PLoS One* **7**, e42955 (2012).
123. Anderson, M. G., Libby, R. T., Mao, M., Cosma, I. M., Wilson, L. A., Smith, R. S. & John, S. W. Genetic context determines susceptibility to intraocular pressure elevation in a mouse pigmentary glaucoma. *BMC Biol.* **4**, 20 (2006).
124. Anderson, M. G., Smith, R. S., Hawes, N. L., Zabaleta, A., Chang, B., Wiggs, J. L. & John, S. W. M. Mutations in genes encoding melanosomal proteins cause pigmentary glaucoma in DBA/2J mice. *Nat. Genet.* **30**, 81–85 (2001).
125. Yang, C.-F., Lin, S.-P., Chiang, C.-P., Wu, Y.-H., H'ng, W. S., Chang, C.-P., Chen, Y.-T. & Wu, J.-Y. Loss of GPNMB causes autosomal-recessive amyloidosis cutis dyschromica in humans. *Am. J. Hum. Genet.* **102**, 219–232 (2018).
126. Bandari, P. S., Qian, J., Yehia, G., Joshi, D. D., Maloof, P. B., Potian, J., Oh, H. S., Gascon, P., Harrison, J. S. & Rameshwar, P. Hematopoietic growth factor inducible neurokinin-1 type: a transmembrane protein that is similar to neurokinin 1 interacts with substance P. *Regul. Pept.* **111**, 169–178 (2003).
127. Safadi, F. F., Xu, J., Smock, S. L., Rico, M. C., Owen, T. A. & Popoff, S. N. Cloning and Characterization of Osteoactivin, A Novel cDNA Expressed in Osteoblasts. *J. Cell. Biochem.* **84**, 12–26 (2002).
128. Turque, N., Denhez, F., Martin, P., Planque, N., Bailly, M., Bègue, A., Stéhelin, D. & Saule, S. Characterization of a new melanocyte-specific gene (QNR-71) expressed in v-myc-transformed quail neuroretina. *EMBO J.* **15**, 3338–50 (1996).
129. Aksan, I. & Goding, C. R. Targeting the microphthalmia basic helix-loop-helix-leucine zipper transcription factor to a subset of E-box elements in vitro and in vivo. *Mol. Cell. Biol.*

18, 6930–8 (1998).

130. Du, J., Miller, A. J., Widlund, H. R., Horstmann, M. A., Ramaswamy, S. & Fisher, D. E. MLANA/MART1 and SILV/PMEL17/GP100 are transcriptionally regulated by MITF in melanocytes and melanoma. *Am. J. Pathol.* **163**, 333–343 (2003).
131. Gutknecht, M., Geiger, J., Joas, S., Dörfel, D., Salih, H. R., Müller, M. R., Grünebach, F. & Rittig, S. M. The transcription factor MITF is a critical regulator of GPNMB expression in dendritic cells. *Cell Commun. Signal.* **13**, 19 (2015).
132. Gabriel, T. L., Tol, M. J., Ottenhof, R., van Roomen, C., Aten, J., *et al.* Lysosomal stress in obese adipose tissue macrophages contributes to MITF-dependent Gpnmb induction. *Diabetes* **63**, 3310–3323 (2014).
133. Martina, J. A., Diab, H. I., Li, H. & Puertollano, R. Novel roles for the Mitf/TFE family of transcription factors in organelle biogenesis, nutrient sensing, and energy homeostasis. *Cell. Mol. life Sci. C.* **71**, 2483–2497 (2014).
134. Klionsky, D. J., Abdelmohsen, K., Abe, A., Abedin, M. J., Abeliovich, H., *et al.* *Guidelines for the use and interpretation of assays for monitoring autophagy* (3rd edition). **12** 1–222 (2016).
135. Settembre, C., Di Malta, C., Polito, V. A., Arencibia, M. G., Vetrini, F., Erdin, S., Erdin, S. U., Huynh, T., Medina, D., Colella, P., Sardiello, M., Rubinsztein, D. C. & Ballabio, A. TFEB links autophagy to lysosomal biogenesis. *Science* **332**, 1429–1433 (2011).
136. Moore, K. J. Insight into the microphthalmia gene. *Trends Genet.* **11**, 442–448 (1995).
137. Hemesath, T. J., Steingrímsson, E., McGill, G., Hansen, M. J., Vaught, J., Hodgkinson, C. A., Arnheiter, H., Copeland, N. G., Jenkins, N. A. & Fisher, D. E. Microphthalmia, a critical factor in melanocyte development, defines a discrete transcription factor family. *Genes Dev.* **8**, 2770–80 (1994).
138. Pogenberg, V., Ögmundsdóttir, M. H., Bergsteinsdóttir, K., Schepsky, A., Phung, B., *et al.* Restricted leucine zipper dimerization and specificity of DNA recognition of the melanocyte master regulator MITF. *Genes Dev.* **26**, 2647–2658 (2012).
139. Martina, J. A. & Puertollano, R. Rag GTPases mediate amino acid-dependent recruitment of TFEB and MITF to lysosomes. *J. Cell Biol.* **200**, 475–491 (2013).
140. Palmieri, M., Pal, R., Nelvagal, H. R., Lotfi, P., Stinnett, G. R., *et al.* mTORC1-independent TFEB activation via Akt inhibition promotes cellular clearance in neurodegenerative storage diseases. *Nat. Commun.* **8**, 14338 (2017).
141. Takeda, K., Takemoto, C., Kobayashi, I., Watanabe, A., Nobukuni, Y., Fisher, D. E. & Tachibana, M. Ser298 of MITF, a mutation site in Waardenburg syndrome type 2, is a phosphorylation site with functional significance. *Hum. Mol. Genet.* **9**, 125–132 (2000).
142. Chung, J.-S., Sato, K., Dougherty, I. I., Cruz, P. D. & Ariizumi, K. DC-HIL is a negative regulator of T lymphocyte activation. *Blood* **109**, 4320–7 (2007).
143. Chung, J.-S., Dougherty, I., Cruz, P. D. & Ariizumi, K. Syndecan-4 mediates the coinhibitory function of DC-HIL on T cell activation. *J. Immunol.* **179**, 5778–84 (2007).
144. Chung, J.-S., Bonkobara, M., Tomihari, M., Cruz, P. D. & Ariizumi, K. The DC-HIL/syndecan-4 pathway inhibits human allogeneic T-cell responses. *Eur. J. Immunol.* **39**, 965–974 (2009).
145. Chung, J.-S., Tamura, K., Akiyoshi, H., Cruz, P. D. & Ariizumi, K. The DC-HIL/syndecan-4 pathway regulates autoimmune responses through myeloid-derived suppressor cells. *J. Immunol.* **192**, 2576–84 (2014).
146. Smith, L. L. & Giachelli, C. M. Structural requirements for $\alpha 9\beta 1$ -mediated adhesion and migration to thrombin-cleaved Osteopontin. *Exp. Cell Res.* **242**, 351–360 (1998).

147. Redick, S. D., Settles, D. L., Briscoe, G. & Erickson, H. P. Defining fibronectin's cell adhesion synergy site by site-directed mutagenesis. *J. Cell Biol.* **149**, 521–7 (2000).
148. Tomihari, M., Hwang, S.-H., Chung, J.-S., Cruz, P. D., Ariizumi, K. & Ariizumi, K. Gpnmb is a melanosome-associated glycoprotein that contributes to melanocyte/keratinocyte adhesion in a RGD-dependent fashion. *Exp. Dermatol.* **18**, 586–95 (2009).
149. Chung, J.-S., Yudate, T., Tomihari, M., Akiyoshi, H., Cruz, P. D. & Ariizumi, K. Binding of DC-HIL to dermatophytic fungi induces tyrosine phosphorylation and potentiates antigen presenting cell function. *J. Immunol.* **183**, 5190–8 (2009).
150. Yu, B., Sondag, G. R., Malcuit, C., Kim, M.-H. & Safadi, F. F. Macrophage-associated Osteoactivin/GPNMB mediates mesenchymal stem cell survival, proliferation, and migration via a CD44-dependent mechanism. *J. Cell. Biochem.* **117**, 1511–1521 (2016).
151. Yu, B., Alboslemy, T., Safadi, F. & Kim, M.-H. Glycoprotein nonmelanoma clone B regulates the crosstalk between macrophages and mesenchymal stem cells toward wound repair. *J. Invest. Dermatol.* **138**, 219–227 (2018).
152. Hu, X., Zhang, P., Xu, Z., Chen, H. & Xie, X. GPNMB enhances bone regeneration by promoting angiogenesis and osteogenesis: Potential role for tissue engineering bone. *J. Cell. Biochem.* **114**, 2729–2737 (2013).
153. Abdelmagid, S. M., Barbe, M. F., Rico, M. C., Salihoglu, S., Arango-Hisijara, I., Selim, A. H., Anderson, M. G., Owen, T. A., Popoff, S. N. & Safadi, F. F. Osteoactivin, an anabolic factor that regulates osteoblast differentiation and function. *Exp. Cell Res.* **314**, 2334–2351 (2008).
154. Katayama, A., Nakatsuka, A., Eguchi, J., Murakami, K., Teshigawara, S., Kanzaki, M., Nunoue, T., Hida, K., Wada, N., Yasunaka, T., Ikeda, F., Takaki, A., Yamamoto, K., Kiyonari, H., Makino, H. & Wada, J. Beneficial impact of Gpnmb and its significance as a biomarker in nonalcoholic steatohepatitis. *Sci. Rep.* **5**, 16920 (2015).
155. Onaga, M., Ido, A., Hasuike, S., Uto, H., Moriuchi, A., Nagata, K., Hori, T., Hayash, K. & Tsubouchi, H. Osteoactivin expressed during cirrhosis development in rats fed a choline-deficient, l-amino acid-defined diet, accelerates motility of hepatoma cells. *J. Hepatol.* **39**, 779–785 (2003).
156. Haralanova-Ilieva, B., Ramadori, G. & Armbrust, T. Expression of osteoactivin in rat and human liver and isolated rat liver cells. *J. Hepatol.* **42**, 565–572 (2005).
157. Sasaki, T., Ishikawa, T., Abe, R., Nakayama, R., Asada, A., Matsuki, N. & Ikegaya, Y. Astrocyte calcium signaling orchestrates neuronal synchronization in organotypic hippocampal slices. *J. Physiol.* **592**, 2771–2783 (2014).
158. Patel-Chamberlin, M., Wang, Y., Satirapoj, B., Phillips, L. M., Nast, C. C., Dai, T., Watkins, R. A., Wu, X., Natarajan, R., Leng, A., Ulanday, K., Hirschberg, R. R., Lapage, J., Nam, E. J., Haq, T. & Adler, S. G. Hematopoietic growth factor inducible neurokinin-1 (Gpnmb/Osteoactivin) is a biomarker of progressive renal injury across species. *Kidney Int.* **79**, 1138–48 (2011).
159. Ramachandran, P., Pellicoro, A., Vernon, M. A., Boulter, L., Aucott, R. L., Ali, A., Hartland, S. N., Snowdon, V. K., Cappon, A., Gordon-Walker, T. T., Williams, M. J., Dunbar, D. R., Manning, J. R., van Rooijen, N., Fallowfield, J. A., Forbes, S. J. & Iredale, J. P. Differential Ly-6C expression identifies the recruited macrophage phenotype, which orchestrates the regression of murine liver fibrosis. *Proc. Natl. Acad. Sci. USA.* **109**, E3186–95 (2012).
160. Abe, H., Uto, H., Takami, Y., Takahama, Y., Hasuike, S., Kodama, M., Nagata, K., Moriuchi, A., Numata, M., Ido, A. & Tsubouchi, H. Transgenic expression of osteoactivin in the liver attenuates hepatic fibrosis in rats. *Biochem. Biophys. Res. Commun.* **356**, 610–615 (2007).
161. Kumagai, K., Tabu, K., Sasaki, F., Takami, Y., Morinaga, Y., Mawatari, S., Hashimoto,

- S., Tanoue, S., Kanmura, S., Tamai, T., Moriuchi, A., Uto, H., Tsubouchi, H. & Ido, A. Glycoprotein nonmetastatic melanoma B (Gpnmb)-positive macrophages contribute to the balance between fibrosis and fibrolysis during the repair of acute liver injury in mice. *PLoS One* **10**, e0143413 (2015).
162. Pahl, M. V, Vaziri, N. D., Yuan, J. & Adler, S. G. Upregulation of monocyte/macrophage HGFIN (Gpnmb/Osteoactivin) expression in end-stage renal disease. *Clin. J. Am. Soc. Nephrol.* **5**, 56–61 (2010).
 163. Sasaki, F., Kumagai, K., Uto, H., Takami, Y., Kure, T., Tabu, K., Nasu, Y., Hashimoto, S., Kanmura, S., Numata, M., Moriuchi, A., Sakiyama, T., Tsubouchi, H. & Ido, A. Expression of Glycoprotein nonmetastatic melanoma protein B in macrophages infiltrating injured mucosa is associated with the severity of experimental colitis in mice. *Mol. Med. Rep.* **12**, 7503–7511 (2015).
 164. Bhattacharyya, S., Feferman, L., Sharma, G. & Tobacman, J. K. Increased GPNMB, phospho-ERK1/2, and MMP-9 in cystic fibrosis in association with reduced arylsulfatase B. *Mol. Genet. Metab.* **124**, 168–175 (2018).
 165. Naito, M., Takahashi, K. & Hojo, H. An ultrastructural and experimental study on the development of tubular structures in the lysosomes of Gaucher cells. *Lab. Invest.* **58**, 590–8 (1988).
 166. van Breemen, M. J., de Fost, M., Voerman, J. S. A., Laman, J. D., Boot, R. G., Maas, M., Hollak, C. E. M., Aerts, J. M. & Rezaee, F. Increased plasma macrophage inflammatory protein (MIP)-1 α and MIP-1 β levels in type 1 Gaucher disease. *Biochim. Biophys. Acta - Mol. Basis Dis.* **1772**, 788–796 (2007).
 167. Lombardo, E., van Roomen, C. P. A. A., van Puijvelde, G. H., Ottenhoff, R., van Eijk, M., Aten, J., Kuiper, J., Overkleeft, H. S., Groen, A. K., Verhoeven, A. J., Aerts, J. M. F. G. & Bietrix, F. Correction of liver steatosis by a hydrophobic iminosugar modulating glycosphingolipids metabolism. *PLoS One* **7**, e38520 (2012).
 168. Hendrickx, D. A. E., van Scheppingen, J., van der Poel, M., Bossers, K., Schuurman, K. G., van Eden, C. G., Hol, E. M., Hamann, J. & Huitinga, I. Gene expression profiling of multiple sclerosis pathology identifies early patterns of demyelination surrounding chronic active lesions. *Front. Immunol.* **8**, 1810 (2017).
 169. Xu, J., Jüllig, M., Middleditch, M. J. & Cooper, G. J. S. Modelling atherosclerosis by proteomics: Molecular changes in the ascending aortas of cholesterol-fed rabbits. *Atherosclerosis* **242**, 268–76 (2015).
 170. Xu, X., Grijalva, A., Skowronski, A., van Eijk, M., Serlie, M. J. J., Ferrante, A. W. W., van Eijk, M., Serlie, M. J. J. & Ferrante, A. W. W. Obesity activates a program of lysosomal-dependent lipid metabolism in adipose tissue macrophages independently of classic activation. *Cell Metab.* **18**, 816–830 (2013).
 171. Tol, M. J., van der Lienden, M. J. C. C., Gabriel, T. L., Hagen, J. J., Scheij, S., *et al.* HEPES activates a MiT/TFE-dependent lysosomal-autophagic gene network in cultured cells: A call for caution. *Autophagy* **14**, 1–13 (2018).
 172. Settembre, C., Zoncu, R., Medina, D. L., Vetrini, F., Erdin, S. S. S., Erdin, S. S. S., Huynh, T., Ferron, M., Karsenty, G., Vellard, M. C., Facchinetti, V., Sabatini, D. M. & Ballabio, A. A lysosome-to-nucleus signalling mechanism senses and regulates the lysosome via mTOR and TFEB. *EMBO J.* **31**, 1095–1108 (2012).
 173. Kawahara, K., Hirata, H., Ohbuchi, K., Nishi, K., Maeda, A., Kuniyasu, A., Yamada, D., Maeda, T., Tsuji, A., Sawada, M. & Nakayama, H. The novel monoclonal antibody 9F5 reveals expression of a fragment of GPNMB/osteactivin processed by furin-like protease(s) in a subpopulation of microglia in neonatal rat brain. *Glia* **64**, 1938–1961 (2016).

174. Huang, J.-J., Ma, W.-J. & Yokoyama, S. Expression and immunolocalization of Gpnmb, a glioma-associated glycoprotein, in normal and inflamed central nervous systems of adult rats. *Brain Behav.* **2**, 85–96 (2012).
175. Shi, F., Duan, S., Cui, J., Yan, X., Li, H., Wang, Y., Chen, F., Zhang, L., Liu, J. & Xie, X. Induction of Matrix metalloproteinase-3 (MMP-3) expression in the microglia by lipopolysaccharide (LPS) via upregulation of Glycoprotein nonmetastatic melanoma B (GPnMB) expression. *J. Mol. Neurosci.* **54**, 234–242 (2014).
176. Tyburczy, M. E., Kotulska, K., Pokarowski, P., Mieczkowski, J., Kucharska, J., Grajkowska, W., Roszkowski, M., Jozwiak, S. & Kaminska, B. Novel proteins regulated by mTOR in subependymal giant cell astrocytomas of patients with Tuberous sclerosis complex and new therapeutic implications. *Am. J. Pathol.* **176**, 1878–1890 (2010).
177. Szulzewsky, F., Pelz, A., Feng, X., Synowitz, M., Markovic, D., Langmann, T., Holtman, I. R., Wang, X., Eggen, B. J. L., Boddeke, H. W. G. M., Hambardzumyan, D., Wolf, S. A. & Kettenmann, H. Glioma-associated microglia/macrophages display an expression profile different from M1 and M2 polarization and highly express Gpnmb and Spp1. *PLoS One* **10**, e0116644 (2015).
178. Hudson, A. L., Parker, N. R., Khong, P., Parkinson, J. F., Dwight, T., Ikin, R. J., Zhu, Y., Chen, J., Wheeler, H. R. & Howell, V. M. Glioblastoma recurrence correlates with increased APE1 and polarization toward an immuno-suppressive microenvironment. *Front. Oncol.* **8**, 314 (2018).
179. Kuan, C.-T., Wakiya, K., Dowell, J. M., Herndon, J. E., Reardon, D. A., Graner, M. W., Riggins, G. J., Wikstrand, C. J., Bigner, D. D., Herndon, J. E., Reardon, D. A., Graner, M. W., Riggins, G. J., Wikstrand, C. J. & Bigner, D. D. Glycoprotein nonmetastatic melanoma protein B, a potential molecular therapeutic target in patients with glioblastoma multiforme. *Clin. Cancer Res.* **12**, 1970–1982 (2006).
180. Tanaka, H., Shimazawa, M., Kimura, M., Takata, M., Tsuruma, K., Yamada, M., Takahashi, H., Hozumi, I., Niwa, J., Iguchi, Y., Nikawa, T., Sobue, G., Inuzuka, T. & Hara, H. The potential of GPnMB as novel neuroprotective factor in amyotrophic lateral sclerosis. *Sci. Rep.* **2**, 573 (2012).
181. Nakano, Y., Suzuki, Y., Takagi, T., Kitashoji, A., Ono, Y., Tsuruma, K., Yoshimura, S., Shimazawa, M., Iwama, T. & Hara, H. Glycoprotein nonmetastatic melanoma protein B (GPnMB) as a novel neuroprotective factor in cerebral ischemia-reperfusion injury. *Neuroscience* **277**, 123–131 (2014).
182. Budge, K. M., Neal, M. L., Richardson, J. R. & Safadi, F. F. Glycoprotein NMB: an emerging role in neurodegenerative disease. *Mol. Neurobiol.* **55**, 5167–5176 (2018).
183. Hüttenrauch, M., Ogorek, I., Klafki, H., Otto, M., Stadelmann, C., Weggen, S., Wiltfang, J. & Wirths, O. Glycoprotein NMB: a novel Alzheimer's disease associated marker expressed in a subset of activated microglia. *Acta Neuropathol. Commun.* **6**, 108 (2018).
184. Neal, M. L., Boyle, A. M., Budge, K. M., Safadi, F. F. & Richardson, J. R. The glycoprotein GPnMB attenuates astrocyte inflammatory responses through the CD44 receptor. *J. Neuroinflammation* **15**, 73 (2018).
185. Moloney, E. B., Moskites, A., Ferrari, E. J., Isacson, O. & Hallett, P. J. The glycoprotein GPnMB is selectively elevated in the substantia nigra of Parkinson's disease patients and increases after lysosomal stress. *Neurobiol. Dis.* **120**, 1–11 (2018).
186. Krasemann, S., Madore, C., Cialic, R., Baufeld, C., Calcagno, N., *et al.* The TREM2-APOE pathway drives the transcriptional phenotype of dysfunctional microglia in neurodegenerative diseases. *Immunity* **47**, 566–581.e9 (2017).
187. Sidransky, E. & Lopez, G. The link between the GBA gene and parkinsonism. *Lancet*.

Neurol. **11**, 986–98 (2012).

188. Sulzer, D., Mosharov, E., Talloczy, Z., Zucca, F. A., Simon, J. D. & Zecca, L. Neuronal pigmented autophagic vacuoles: lipofuscin, neuromelanin, and ceroid as macroautophagic responses during aging and disease. *J. Neurochem.* **106**, 24–36 (2008).
189. Perrett, R. M., Alexopoulou, Z. & Tofaris, G. K. The endosomal pathway in Parkinson's disease. *Mol. Cell. Neurosci.* **66**, 21–28 (2015).
190. Pericleous, M., Kelly, C., Wang, T., Livingstone, C. & Ala, A. Wolman's disease and cholesteryl ester storage disorder: the phenotypic spectrum of lysosomal acid lipase deficiency. *Lancet Gastroenterol. Hepatol.* **2**, 670–679 (2017).
191. Dahl, S. vom, Harzer, K., Rolfs, A., Albrecht, B., Niederau, C., Vogt, C., Weely, S. van, Aerts, J., Müller, G. & Häussinger, D. Hepatosplenomegalic lipidosis: what unless Gaucher? Adult cholesteryl ester storage disease (CESD) with anemia, mesenteric lipodystrophy, increased plasma chitotriosidase activity and a homozygous lysosomal acid lipase –1 exon 8 splice junction mutation. *J. Hepatol.* **31**, 741–746 (1999).

Chapter 5

GCase and LIMP2 abnormalities in the liver of Niemann Pick type C mice

Contributing authors:

M.J.C. van der Lienden, M. van Eijk, J. Aten & J.M.F.G. Aerts. *To be submitted.*

Abstract

The lysosomal storage disease Niemann Pick type C (NPC) is caused by impaired cholesterol efflux from lysosomes which is accompanied by secondary lysosomal accumulation of sphingomyelin and glucosylceramide (GlcCer). Similar to Gaucher disease (GD) patients deficient in glucocerebrosidase (GCase) degrading GlcCer, NPC patients show an elevation in glucosylsphingosine and glucosylated cholesterol. In livers of mice lacking the lysosomal cholesterol efflux transporter NPC1, we investigated the expression of established biomarkers of lipid-laden macrophages in GD patients, their GCase status, and the presence of the cytosol facing glucosylceramidase GBA2 and LIMP2, the transporter of newly formed GCase to lysosomes. Livers of 80-week-old *Npc1*^{-/-} mice showed a partial reduction in level of GCase protein and enzymatic activity. In contrast, GBA2 levels tended to be reciprocally increased compared to GCase deficiency. In *Npc1*^{-/-} liver, increased expression of lysosomal enzymes (cathepsin D, acid ceramidase) was observed as well as an increase in markers of lipid-stressed macrophages (GPNMB and galectin-3). Immunohistochemistry showed that the latter markers are expressed by lipid laden Kupffer cells. An elevation of LIMP2 in *Npc1*^{-/-} liver was detected by western blotting. Unexpectedly, immunohistochemistry revealed a marked overexpression of LIMP2 specifically in hepatocytes of the *Npc1*^{-/-} liver. The subcellular distribution of LIMP2 and LAMP1 in NPC1-deficient hepatocytes differed, suggesting that LIMP2 not only localizes to (endo)lysosomes. The recent recognition that LIMP2 harbours a cholesterol channel prompts the speculation that LIMP2 in *Npc1*^{-/-} hepatocytes mediates export of cholesterol into the bile and thus protects the hepatocytes.

Introduction

The liver plays a key role in maintaining bodily cholesterol homeostasis. It produces, metabolizes, secretes, and endocytoses cholesterol. Following the endocytic uptake by hepatocytes and Kupffer cells, cholesterol is exported from their (endo)lysosomes to the cytosol. This process is carried out by the lysosomal proteins NPC1 and NPC2.¹ The latter protein transfers cholesterol from (endo)lysosomal luminal membrane vesicles to the lysosomal membrane protein NPC1 that next mediates its efflux from the lysosome. Deficiencies in either NPC1 or NPC2 cause Niemann Pick disease type C (NPC), a lysosomal storage disorder characterized by lysosomal accumulation of cholesterol that is accompanied by increases in other lipids including sphingomyelin and glucosylceramide (GlcCer).² In NPC liver, lysosomal lipid accumulation is more prominent in Kupffer cells than hepatocytes.³

The secondary accumulation of GlcCer in NPC liver suggests interaction between cholesterol and GlcCer metabolism. Several other findings point to this. For example, the activity of glucocerebrosidase (GCase), the lysosomal β -glucosidase degrading GlcCer to ceramide, is found to be reduced in NPC.^{4–6} Indeed, like GCase-deficient GD patients, NPC patients show an elevation in glucosylsphingosine (GlcSph).⁷ GlcSph is also increased in tissues and plasma of *Npc1*^{-/-} mice. GlcSph is formed from excessive lysosomal GlcCer by acid ceramidase.⁸ GCase is also known to act as transglucosidase, generating glucosylated cholesterol (GlcChol) during lysosomal cholesterol accumulation.⁹ Consequently, GlcChol is more than fifty-fold elevated in liver of *Npc1*^{-/-} mice and significantly increased in plasma of NPC1-deficient mice and patients.⁹ Under normal conditions, GlcChol is synthesized by the cytosol-facing enzyme GBA2 and is degraded to glucose and cholesterol by GCase in lysosomes.¹⁰

The enzyme GCase is transported to lysosomes being bound to the membrane protein LIMP2.¹¹ Following folding in the endoplasmic reticulum, GCase associates to LIMP2 and the complex is routed to lysosomes where dissociation is favored by the locally low pH.^{12,13} Recently it has become apparent that LIMP2 contains a putative channel allowing transport of cholesterol molecules.¹⁴ During deficiency of NPC1, LIMP2 appears to be involved in cholesterol efflux from lysosomes.¹⁴ This is substantiated by the observation that a dual deficiency in NPC1 and LIMP2 results in a more prominent SREBP2-driven induction of HMGCoA reductase transcription, a classic readout for impaired cholesterol efflux from lysosomes.¹⁴ Of note, LIMP2-deficient mice show no marked abnormalities in cholesterol homeostasis, suggesting that NPC1 is normally sufficient to govern cholesterol efflux from lysosomes.⁹

A striking similarity between NPC and GCase-deficiency (GD) is the overexpression of specific proteins by lipid-laden macrophages. In GD, GlcCer-laden macrophages excessively produce the chitinase chitotriosidase, the chemokine CCL18 and GPNMB.^{15–19} In plasma of symptomatic Gaucher patients, chitotriosidase, CCL18 and a soluble fragment of GPNMB are spectacularly increased and these abnormalities are exploited as biomarkers.²⁰ Increased plasma levels of these biomarkers also occur in NPC.^{21,22} Finally, increased metabolism of GlcCer by the cytosol-facing glucosylceramidase GBA2, which is observed during GCase deficiency, has also been noted in brain of *Npc1*^{-/-} mice.¹⁰ Pharmacological inhibition of GBA2 activity with a hydrophobic iminosugar, or GBA2 gene ablation, remarkably ameliorates neuropathology in *Npc1*^{-/-} mice and increases their

life span.^{10,23}

We examined the status of GCase in the liver of mice lacking the NPC1 protein and determined the expression of biomarkers of lipid-laden macrophages. Furthermore, we investigated the status of GBA2 and LIMP2. Our study revealed an expected increased expression of biomarkers of lipid-stressed macrophages, but it also disclosed remarkable upregulation of LIMP2 in hepatocytes.

Results

Structural analysis of *Npcr*^{-/-} liver

The livers of 80-days-old *Npcr*^{-/-} mice showed clusters of enlarged macrophages as visualized by toluidine blue staining (**Figure 1A**). Ultrastructural analysis of the tissue by transmission electron microscopy (TEM) confirmed the presence in *Npcr*^{-/-} liver of characteristic, vacuole containing storage cells of macrophage origin (**Figure 1B**). Altered ultrastructure was also observed in the case of hepatocytes in the *Npcr*^{-/-} liver (**Figure 1B**). Of note, the *Npcr*^{-/-} hepatocytes contained clefts suggestive for deposition of cholesterol crystals (**Figure 1A & B**).^{24–26}

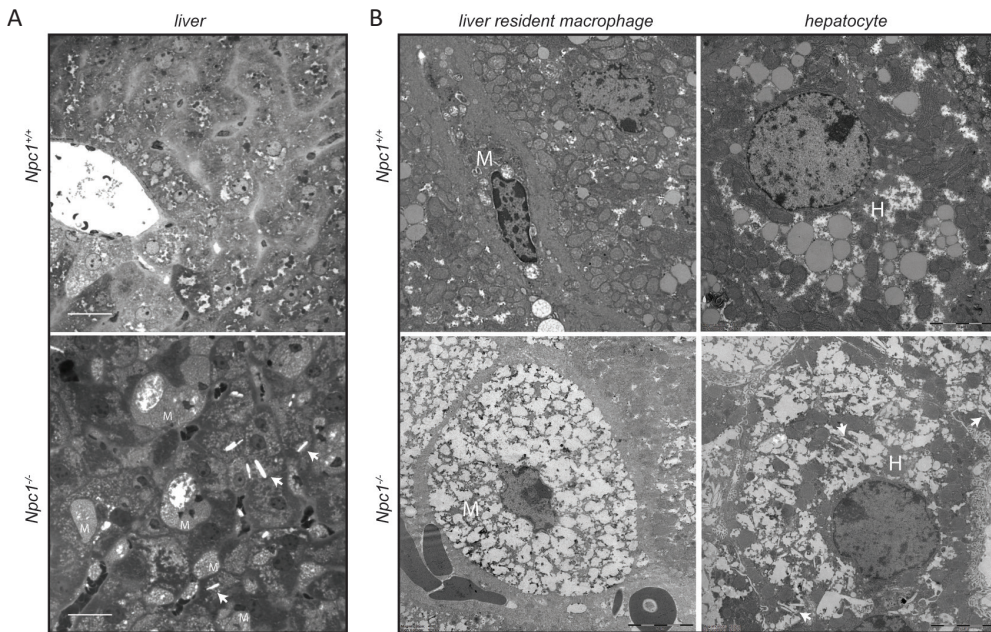


Figure 1. Structural analysis of liver of 80-days-old *Npcr*^{+/+} and *Npcr*^{-/-} mice. (A) Micrographs of toluidine blue-stained sections. Scale bar=25μm; M: liver resident macrophage(clusters). **(B)** Transmission electron microscopy (TEM) micrographs of liver resident macrophages (M) and hepatocytes (H). Scale bar=5μm. Arrows indicate clefts in hepatocytes of *NPCr*^{-/-} liver.

Lysosomal GCase and cytosol facing GBA2 in *Npcr*^{-/-} liver

The enzymatic activity of GCase in total *Npcr*^{-/-} liver extract was on average 60% reduced (**Figure 2A**). This reduction is similar to earlier observations made with *Npcr*^{-/-} brain.¹⁰ Of note, the expression of the *Gba1* gene tended to be upregulated in the *Npcr*^{-/-} liver (**Figure 2B**), which indicates that GCase in the *Npcr*^{-/-} liver is post-transcriptionally

reduced. An activity-based probe, covalently binding to the catalytic nucleophile of retaining β -glucosidases, was used to simultaneously visualize active GCase (59-66 kDa) and GBA2 (110 kDa) enzyme molecules in extracts of the various livers. Although considerable interindividual variation was noted for levels of GCase and GBA2 activities in livers (**Figure 2C**), a reduction in GCase was found to correlate with an elevation of GBA2 (**Figure 2D**).

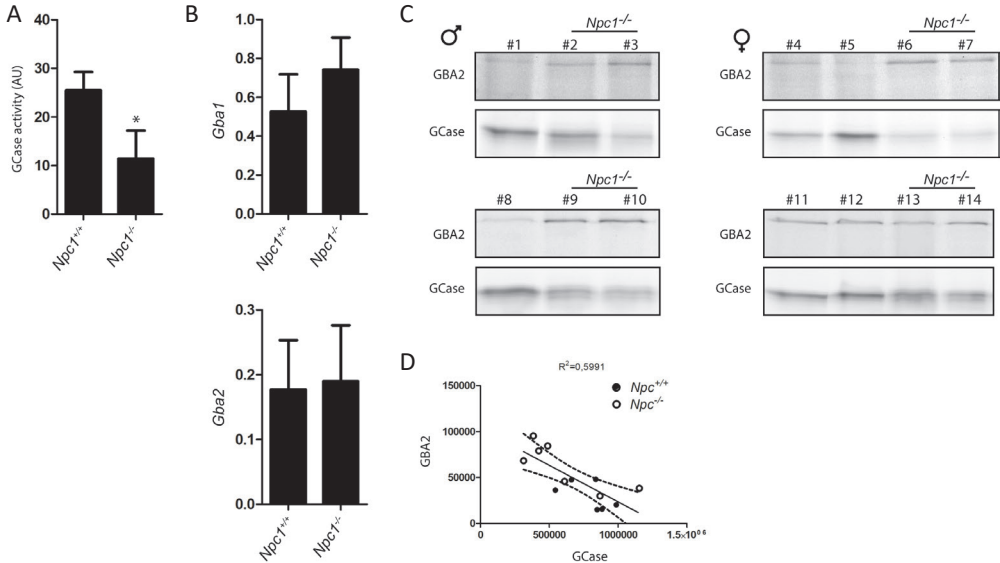


Figure 2. Lysosomal GCase and cytosol facing GBA2 in *NPC*^{+/+}- and *Npc1*^{-/-} mouse liver. (A) GCase activity was measured in liver lysates of *NPC*^{+/+}- and *NPC*^{-/-}-mice with 4MU- β -Glc substrate as described in M&M. (B) Real-time (Rt) qPCR RNA analysis on *Gba1* and *Gba2* gene expression in lysates of the same livers. Values represent relative numbers compared to ribosomal gene *Rplpo*. (C) GCase and GBA2 in aliquots of the same lysates were labelled with GCase-specific ABP and subsequently visualized by fluorescence scanning after SDS-PAGE. # *Npc1*^{+/+}: 1, 4, 5, 8, 11, 12; # *Npc1*^{-/-}: 2, 3, 6, 7, 9, 10, 13, 14. (D) Reciprocal correlation between overall active GCase and GBA2 molecules in liver lysates of *Npc1*^{+/+}- and *Npc1*^{-/-} mice based on quantification of labelled bands in C.

Response to lysosomal storage in NPC liver

Npc1^{-/-} mice exhibit a striking degree of storage that is particularly confined to macrophages. Lysosome perturbation by storage is usually accompanied by increased lysosomal biogenesis and expression of particular markers such as GPNMB.^{22,27} Employing western blotting, a clear increase in GPNMB in *Npc1*^{-/-} livers was demonstrable (**Figure 3A**). Likewise, the lysosomal membrane protein LAMP1 and galectin-3, a protein associated with lysosome stress, were found to be increased as visualized by western blotting. Next, the expression of illustrative genes encoding lysosomal proteins was analysed (**Figure 3B**). We noted markedly increased expression of the *Gpnmb* and *Lgals3* genes, coding for GPNMB and galectin-3. No significant upregulation of expression of the genes *Lamp1*, encoding the lysosomal membrane protein LAMP1 and *Atp6via*, encoding the ATPase H⁺ transporting V1 subunit A, was detected. However, an increased expression of *Asah1*, encoding acid ceramidase, and *Ctsd*, encoding cathepsin D was observed in the

NPC1-deficient mouse livers. Furthermore, the *Npc1*^{-/-} mouse livers showed increased expression of genes coding for proteins implicated in inflammation (TNFα, CCL2; **Figure 3C**). No clear changes were observed in expression of the *Iba1* gene, which encodes for a commonly used marker of macrophages (**Figure 3C**).

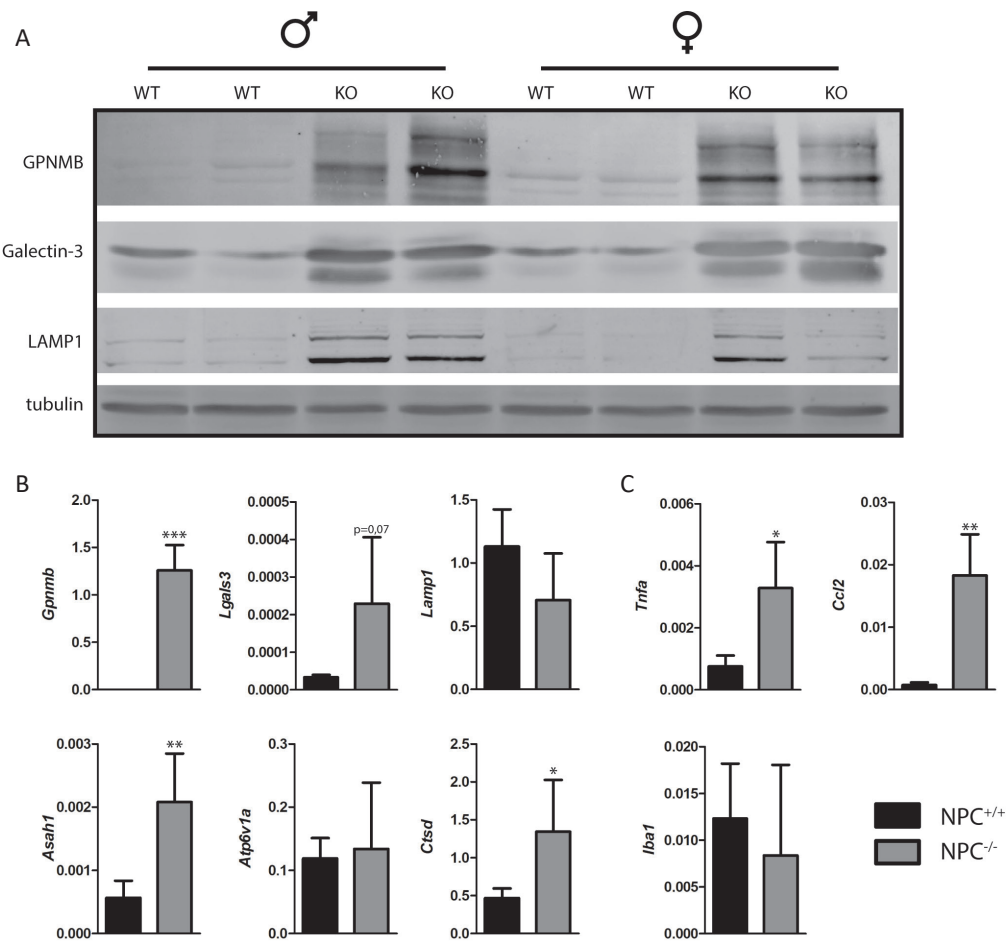


Figure 3. Response to lysosomal storage in NPC liver. (A) Western blot analysis of lysosome storage associated proteins in lysates of *Npc1*^{+/+} and *Npc1*^{-/-} mouse liver; Real-time (Rt) qPCR RNA analysis of the same livers regarding lysosomal storage associated genes (B) and inflammatory genes (C). Values represent relative numbers compared to ribosomal gene *Rplp0*.

*LIMP2 upregulation in *Npc1*^{-/-} liver but not in cultured cells with pharmacologically induced lysosomal cholesterol accumulation*

Analysis of LIMP2 by Western blotting revealed a clear increase in the membrane protein in the *Npc1*^{-/-} livers (**Figure 4A**). Next, we employed U18666A, an agent causing lysosomal cholesterol accumulation. No change in morphology was detected in HEPG2 cells treated with U18666A (**Figure 4B**). Treatment of HepG2 cells with U18666A caused a reduction in GCase as detected with activity-probe labelling but no change in LIMP2 as detected by western blotting (**Figure 4C**). In other words, the findings with NPC1-deficient liver for

LIMP2 were not recapitulated in cultured cells.

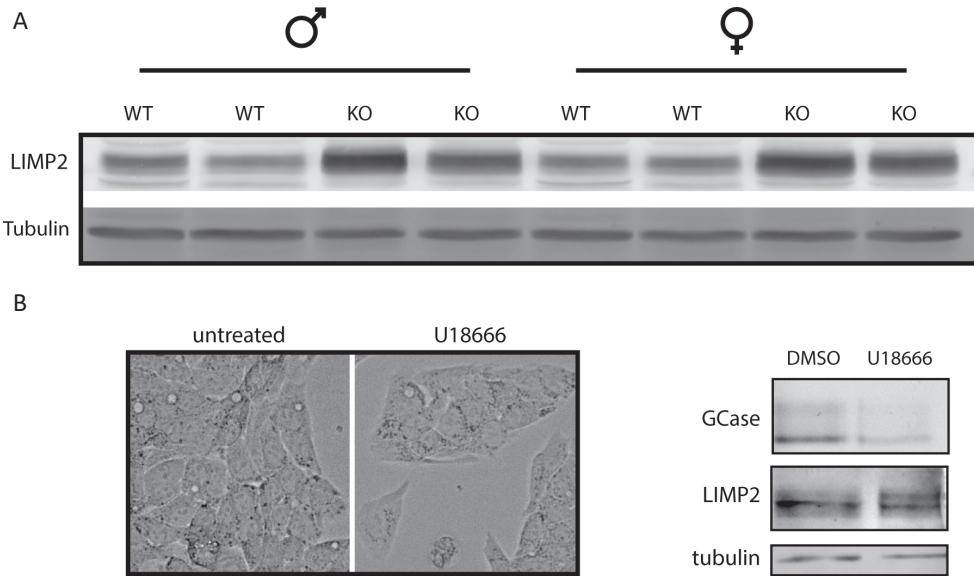


Figure 4. LIMP2 in NPC liver and U18666A treated HEPG2 cells. (A) Western blot analysis of LIMP2/SCARB2 in lysates of *Npc1*^{+/+} and *Npc1*^{-/-} mouse liver. (B) Phase contrast microscopy pictures of HEPG2 cells treated with NPC1-inhibitor U18666A. (C) GCase (GBA) in HEPG2 lysates was labelled with GCase-specific ABP and subsequently visualized by fluorescence scanning after SDS-PAGE. LIMP2/SCARB2 was analysed by western blotting of the same wet gel slab as described in M&M.

Immunohistochemical analysis of *Npc1*^{-/-} liver

To visualize the cellular source of the excessive macrophage marker galectin-3 as well as that of the lysosomal protease cathepsin D and LIMP2 in liver of 80 days old *Npc1*^{-/-} mice, immunohistochemistry was applied. Contrary to matched control liver, the *Npc1*^{-/-} tissue showed the presence of lipid-laden macrophages (Kupffer cells, positive for Iba1), previously reported to markedly express GPNMB (Figure 5A).²² Galectin-3 and cathepsin D staining were found to be also prominent for these storage cells (Figure 5A and B). Unexpectedly, the analysis of LIMP2 revealed predominant labelling of hepatocytes in the *Npc1*^{-/-} liver (Figure 5A). The location of LIMP2 in a peribiliary zone in wildtype hepatocytes was expanded to a more widespread peripheral distribution in *Npc1*^{-/-} hepatocytes (Figure 5B). The altered distribution of LIMP2 in *Npc1*^{-/-} liver was confirmed by fluorescence microscopy (Figure 5C). Again, LIMP2 staining was prominent in the hepatocytes. In contrast, GPNMB and galectin-3 staining was abundant in storage macrophages of the *Npc1*^{-/-} liver (Figure 5C). Of note, the staining pattern for LIMP2 in hepatocytes differed from that of LAMP1, an integral lysosomal membrane protein (Figure 5C).

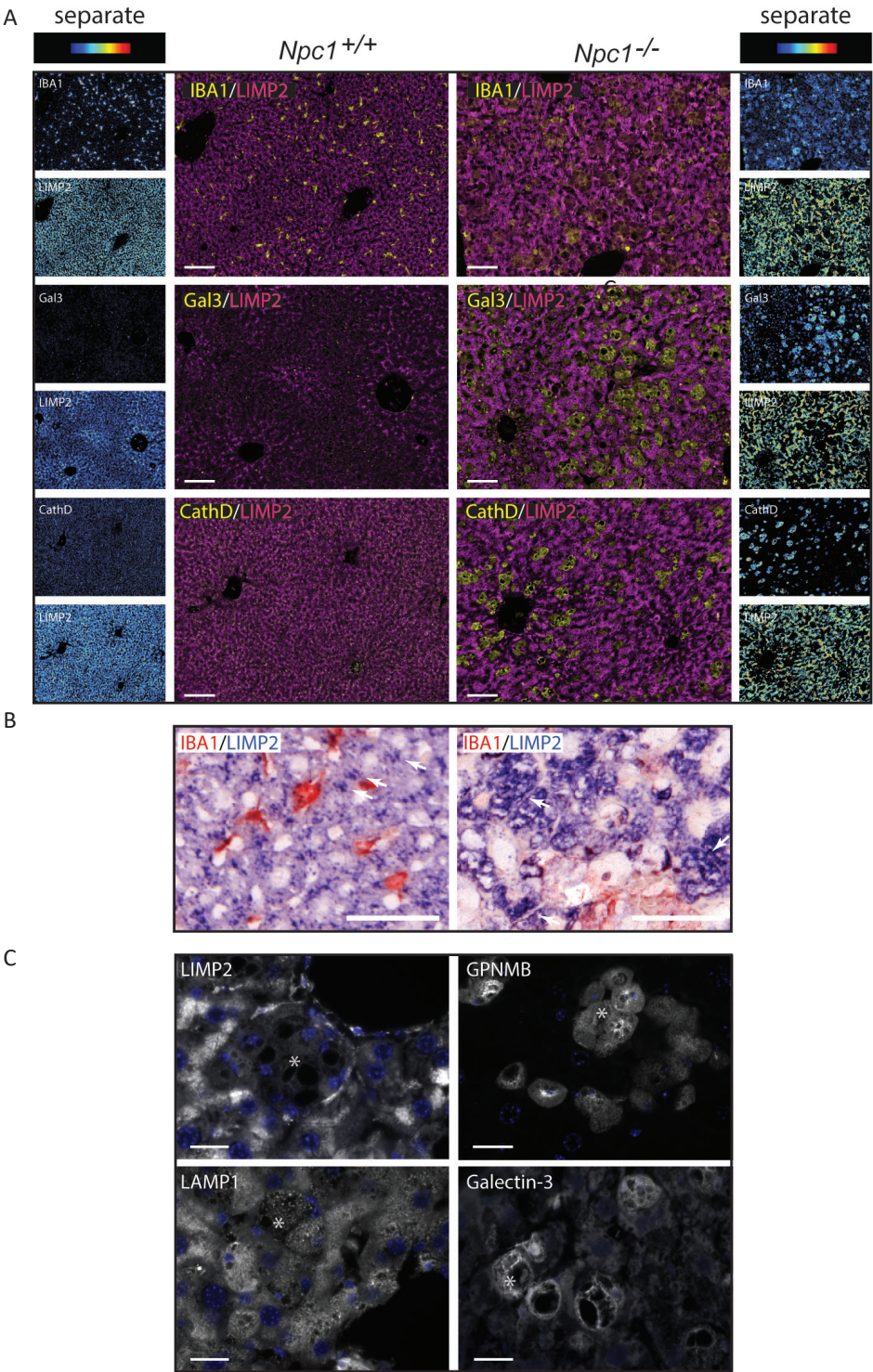


Figure 5. Immunohistochemistry *Npc1*^{-/-} liver. (A) ‘Composite’ panels of immunostaining of *Npc1*^{+/+} and *Npc1*^{-/-} liver of 80-days-old mice: LIMP2 is depicted in magenta and IBA1, galectin-3 and

cathepsin D in yellow. Brightfield scans were analysed using spectral imaging; separate images are displayed in heat-map intensity scale. Scale bar = 50 μm ; (B) Higher magnification of livers from (A): LIMP2 is depicted in blue and IBA1 in red. Arrows indicate peribiliary LIMP2 localization in *Npcr*^{+/+}-hepatocytes and widespread location along apical and lateral membranes in *Npcr*^{-/-} hepatocytes. Scale bar = 10 μm . (C) Immunofluorescence microscopy of the same livers (images taken with 63x magnification): LIMP2, GPNMB, LAMP1 and galectin-3. Nucleus is depicted in blue. Scale bar = 20 μm ; asterisk indicates (clusters of) storage cells.

Discussion

Our present study concerns abnormalities in GCase levels in the liver of mice that lack the lysosomal transmembrane protein NPC1 and consequently develop Niemann Pick disease type C. Earlier investigations already showed that the livers of *Npcr*^{-/-} mice contain increased levels of GlcCer along with cholesterol.⁷ In parallel, GlcSph is increased in the *Npcr*^{-/-} liver. These studies indicate that local degradation of GlcCer by lysosomal GCase is impaired, which is followed by increased de-acylation through lysosomal acid ceramidase.⁸ Moreover, livers of *Npcr*^{-/-} mice accumulate GlcChol, which points to an increased transglucosylation activity of GCase.⁹ Earlier work also described accumulation of GPNMB positive foamy cells in the liver of *Npcr*^{-/-} mice, resembling Gaucher cells during a primary GCase deficiency (Gaucher disease).²² We studied GCase in more detail in liver of *Npcr*^{-/-} mice using activity-based probes that selectively label active enzyme molecules. In addition, we employed western blotting, qPCR and immunohistochemistry to examine other proteins known to be changed by GCase deficiency. ABP labelling confirmed reduction in active GCase content of liver of *Npcr*^{-/-} mice. Reduction in GCase was accompanied by reciprocal increase of active GBA2 molecules in liver lysates of *Npcr*^{-/-} mice. Of note, in brain of *Npcr*^{-/-} mice, an increase in GBA2/GCase ratio was already observed previously¹⁰ and genetic ablation or pharmacological inhibition of GBA2 in *Npcr*^{-/-} mice significantly increases life span.¹⁰ The reduction of GCase following lysosomal cholesterol accumulation was recapitulated *in vitro* with cultured HEPG2 cells treated with a known NPC1 inhibitor, U18666A. Our immunohistochemical investigation of liver of *Npcr*^{-/-} mice confirmed the presence of characteristic storage cells that were positive for the macrophage marker Iba1. An increase in GPNMB in livers of 80 weeks old *Npcr*^{-/-} mice was observed on RNA level, and by western blot. The foamy storage cells were found to overexpress GPNMB, galectin-3 and cathepsin D.

Immunohistochemical analysis of the NPC livers unexpectedly revealed a very prominent expression of LIMP2 in hepatocytes and not in the lipid-laden storage cells. The pattern of LIMP2 staining differed from that of lysosome marker LAMP1 regarding subcellular localization. Interestingly, inducing lysosomal cholesterol accumulation in HEPG2 cells with U18666A caused no overexpression of LIMP2. These findings show that cultured cells do not provide a phenocopy of the polarized hepatocytes in the *Npcr*^{-/-} liver. The striking upregulation of LIMP2 in hepatocytes of the *Npcr*^{-/-} liver and apparent partial non-lysosomal localization is intriguing and warrants further discussion. The morphology of NPC1-deficient hepatocytes is not considered to undergo prominent lysosomal storage associated changes.³ It could be speculated that the upregulation of LIMP2 is instrumental to this. Heybrock et al. recently provided evidence that LIMP2 can assist efflux of cholesterol from lysosomes in an NPC1-independent manner. In NPC1-deficient cells, SREBP2 (Sterol regulatory element-binding protein 2) mediated transcription is

upregulated in response to the reduced cholesterol level in the endoplasmic reticulum that results from impaired sterol efflux from lysosomes. The transcription factor SREBP2 controls cholesterol homeostasis by stimulating transcription of genes encoding proteins involved in the biosynthesis of cholesterol.²⁸ A combined deficiency of NPC1 and LIMP2 was found to increase SREBP2-mediated *de novo* synthesis of cholesterol, which points to LIMP2-mediated cholesterol efflux from lysosomes during NPC1 deficiency.¹⁴ Clearly, the efflux of cholesterol from lysosomes is primarily mediated by the NPC2/NPC1 pathway since individuals deficient in LIMP2 (ko mice and patients suffering from acute myoclonus renal failure syndrome, AMRF) show no signs of disturbed cholesterol metabolism.²⁹ If overexpression of LIMP2 serves as a compensatory mechanism to NPC1 deficiency, the question arises why such response does not seem to take place in the macrophage-like cells that transform into lipid storage macrophages. These cells seem to change instead by increasing storage capacity through upregulation of their lysosomes.

The apparent partial non-lysosomal location of LIMP2 in *Npcr*^{-/-} hepatocytes prompts the hypothesis that LIMP2 could be additionally involved in the export of cholesterol to the bile. In view of this hypothesis, examination of *Npcr*^{-/-} enterocytes may be of interest. It has been recognized for some time that cholesterol is exported from enterocytes into the intestinal lumen via so-called TICE (trans-intestinal cholesterol export).³⁰ Possibly, LIMP2 could also be a player in this physiologically relevant process of cholesterol export.

In conclusion, the present study on liver of *Npcr*^{-/-} mice has led to the discovery of a prominent upregulation of LIMP2 in hepatocytes. These findings could give impetus to studies on compensatory mechanisms in lysosomal storage disorders and the beneficial value of these processes. Specifically, characterization of human NPC1-deficient liver and the putative role of LIMP2 in cholesterol efflux to the bile warrants further testing.

Materials & Methods

Cell Culture Experiments

RAW264.7 cells and HEPG2 cells (American Type Culture Collection, TIB-71 and HB-8065 resp.) were cultured in DMEM containing 10% fetal calf serum, 1% glutamax and 0,2% antibiotics (penicillin-streptomycin; all purchased from Thermo Fisher Scientific) at 37°C at 5% CO₂. NPC1 inhibition was performed using 10 µM U18666 (Sigma-Aldrich).⁹

Animals

Mice heterozygous for a spontaneous truncation of the *Npc1* gene, BALB/c Nctr-Npc1m1N/J mice (#003092) were obtained from The Jackson Laboratory (Bar Harbor, USA). Males and females of the two strains were crossed in-house to generate *Npc1*^{-/-} and wild-type littermates (*Npc1*^{+/+}). Mice received a normal chow diet and water *ad libitum* and were housed in a temperature and humidity controlled room with a 12h light/dark cycle. National and local ethical committee approval was obtained for conducting animal experiments and laboratory animal welfare rules were enforced (DBC101698 and DBC17AC). In order to anesthetize mice, Hypnorm (0.315 mg/mL phenyl citrate and 10 mg/mL fluanisone) and Dormicum (5 mg/mL midazolam) was administered according to their weight (80 µL per 10g body weight) and subsequent cervical dislocation was performed. Organs were dissected and fixed in 4% formalin for immunohistochemical analysis or snap-frozen for protein and mRNA analysis.

Electron microscopy and toluidine blue staining

For transmission electron microscopy (TEM) and toluidine blue staining, fresh liver was fixed in paraformaldehyde/glutaraldehyde (Karnovsky's fixative) and post-fixed with 1% osmium tetroxide. The fixed tissue samples were block-stained with 1% uranyl acetate, dehydrated in dimethoxypropane, and embedded in epoxyresin LX-112. 0.5 µm-thick sections were stained with toluidine blue and imaged by brightfield microscopy (Leica DM5500B) with an HCX PL APO 63x/1.40-0.60 Oil immersion objective. For TEM, ultrathin sections were stained with tannic acid, uranyl acetate, and lead citrate. Examination was performed using a Philips CM10 transmission electron microscope (Eindhoven, The Netherlands). Images were acquired using a digital transmission EM camera (Morada 10-12, Soft Imaging System, RvC, Soest, The Netherlands).

Immunohistochemistry and immunofluorescence

Dissected tissue was fixed in 4% formalin (pH 7.0 by phosphate buffer), and embedded in paraffin. Embedded tissue was cut in 4 µm-thick sections, washed in 100% xylene to remove paraffin, and washed in 100% ethanol. Rehydration occurred through incubation in 96% ethanol, 70% ethanol and milliQ water respectively and heat induced epitope retrieval (HIER) was performed at 98°C for 10 minutes in 10 mM citric acid (pH 6). Tissues were washed and permeabilized in PBS/0,01% Tween-20 (CAS 9005-64-5, Sigma) and incubated with primary antibodies goat-anti-GPNMB (AF2330; R&D Systems, Abingdon, UK), rat-anti-galectin-3 clone M3/38 (MABT51, Millipore; pre-blocked with 5% mouse serum and centrifuged), rabbit-anti-LAMP1 (ab24170, Abcam) or rabbit-anti-SCARB2 (NB400-129, Novus Biologicals). Antibodies were diluted in PBS/5% antibody diluent (ScyTek Laboratories). In order to prepare immunohistochemistry for spectral imaging,

slides stained for SCARB2 were washed and incubated with alkaline phosphatase-conjugated poly-AP goat anti-rabbit IgG (BrightVision; ImmunoLogic, Klinipath, Duiven, The Netherlands). Bound AP was visualized through incubation with AP substrate VectorBlue (SK-5300; Vector Laboratories, Burlingame, CA, USA) in presence of 0.2 mM levamisole to inhibit endogenous alkaline phosphatase activity. For double staining, slides were washed and subjected to a second HIER to inactivate and remove existing antibody-antigen bonds while leaving the precipitated chromogen unchanged.³¹ Sections were incubated with rabbit anti-IBA1 (019-19741, WAKO Chemicals), rat anti-galectin-3 clone M3/38 (MABT51) or rabbit anti-cathepsin D (antiserum was prepared in our laboratory) and subsequently washed, and incubated with poly-AP goat anti-rabbit IgG or goat anti-rat IgG according to their respective primary antibody. Development of signal was performed through incubation with VectorRed AP substrate (SK-5100; Vector Laboratories) in presence of 0.2 mM levamisole. Sections were mounted with VectaMount (Vector Laboratories). Images were obtained by brightfield microscopy (Leica DM5500B) with an HC PLAN APO 20x/0.70 or HCX PL APO 63x/1.40-0.60 Oil objective. Nuance imaging system (Perkin Elmer, Hopkinton, MA, USA) allowed acquisition of multispectral data sets from 420 to 720 nm with 10nm intervals. Single-stained sections were used to define the spectral properties of each colour in order to unmix the double staining patterns. Construction of composite images was done by Nuance 3.0.2 software, which rendered display intensity heat maps for single channels and subsequently allowing a colour universal design. With respect to immunofluorescence analysis, aforementioned primary antibodies were visualized by secondary donkey antibodies against rabbit or goat IgG, conjugated to Alexa Fluor™ 647 (Molecular Probes, A31573 and A21447 resp.). For detection of galectin-3, goat-anti-rat IgG conjugated to TxR was used (Southern Biotech, 3052-07). Images were obtained by fluorescence microscopy (Leica DM5500B) with an HCX PL APO 63x/1.40-0.60 Oil objective.

Enzyme activity assays

Protein quantification of cell and tissue homogenates was assessed by bicinchoninic acid assay (Thermo Fisher Scientific, 23225). Equal protein amounts were used for enzyme activity assays. GCase activity was assayed using 4-methylumbelliferyl (4-MU) substrate beta-D-glucopyranoside (44059, Glycosynth) in McIlvaine buffer, pH 5.2, with 0.1% (w/v) BSA.³²

Activity-based probe analysis

Where stated, homogenates of tissue and cells were labelled with excess of activity-based probe (ABP) conjugated to a fluorescent dye as earlier described.³³ When GCase was labelled in lysates of cultured cells (Figure 4), ultrasensitive labeling of all active GCase molecules was performed using 100 nM ABP-ME569 (Cy5, in 0.5-1% DMSO).³³ Incubation was performed for 1h at 37°C. In homogenates of tissue (Figure 2), GCase and GBA2 were labelled using a broad specificity ABP for retaining β -exoglucosidases, ABP-JJB367 (containing Cy5).³⁴ Labelling occurred at 200 nM ABP-JJB367 at pH 5.8 (0.5-1% DMSO) for 1h on ice. Samples were denatured and separated by SDS-PAGE. Detection of fluorescence in wet gel slabs was performed using a Typhoon FLA 9500 fluorescence scanner (GE Healthcare). Far red fluorescence (ME569 and JJB367) was detected using λ EX 635 nm and λ EM \geq 665 nm. After imaging, gels were either stained by Coomassie

G250 for total protein and scanned on ChemiDoc MP imager (Bio-Rad) or used for western blotting.³³

Western Blot Analysis

Frozen tissue samples and cultured cells were lysed in KPi lysis buffer (25 mM K_2HPO_4 / KH_2PO_4 , pH 6.5, 0.1% [v:v] Triton X-100) supplemented with protease inhibitors (Roche) and sonicated 5x 1 second with 9 minutes interval (amplitude 25%). Equal quantities of protein as assessed by bicinchoninic acid assay (Thermo Fisher Scientific, 23225) were resuspended in Laemmli buffer and denatured at 95°C. Proteins were subsequently separated by SDS-PAGE using a 10% acrylamide gel and transferred to 0.2 µm nitrocellulose membrane (#1704159, Biorad). Blocking of membranes occurred in 5% (w:v) bovine serum albumin (Sigma, A1906) solution in PBS/0.1% Tween-20 (Sigma, P1379) for 1 h at room temperature (RT). Primary antibodies used were targeted against GPNMB (AF2330; R&D Systems), LIMP2 (NB400-129, Novus Biologicals), LAMP1 (ab24170, Abcam) and galectin-3 (MABT51, Millipore). Furthermore, mouse-anti-tubulin (Cedarlane, CLT 9002) was used as loading control. Proteins were detected by using specific secondary conjugated antibodies (Alexa Fluor™ 488/647) (Molecular Probes). Detection of immunoblots was performed using a Typhoon FLA 9500 fluorescence scanner (GE Healthcare).

RNA Extraction and Real-time PCR

Total RNA from liver or cell culture was extracted by means of the NucleoSpin II extraction kit (Macherey Nagel) according to manufacturer's protocol. RNA concentrations were measured (DeNovix DS-1) and equal amounts of RNA were used for cDNA synthesis according to the manufacturer's protocol (Invitrogen). Real time qPCR was performed using Bio-Rad CFX96 Touch™ real-time PCR detection system (Bio-Rad Laboratories). Acidic ribosomal phosphoprotein 36B4 expression (*Rplp0*) was used as reference.

References

1. Infante, R. E., Wang, M. L., Radhakrishnan, A., Hyock, J. K., Brown, M. S. & Goldstein, J. L. NPC2 facilitates bidirectional transfer of cholesterol between NPC1 and lipid bilayers, a step in cholesterol egress from lysosomes. *Proc. Natl. Acad. Sci. USA*. **105**, 15287–15292 (2008).
2. Vanier, M. T. Niemann-Pick disease type C. *Orphanet J. Rare Dis.* **5**, 16 (2010).
3. Elleder, M., Smíd, F., Hyniová, H., Čihula, J., Zeman, J. & Macek, M. Liver findings in Niemann-Pic disease type C. *Histochem. J.* **16**, 1147–1170 (1984).
4. Pentchev, P. G., Gal, A. E., Booth, A. D., Omodeo-Sale, F., Fours, J., Neumeyer, B. A., Quirk, J. M., Dawson, G. & Brady, R. O. A lysosomal storage disorder in mice characterized by a dual deficiency of sphingomyelinase and glucocerebrosidase. *Biochim. Biophys. Acta - Lipids Lipid Metab.* **619**, 669–679 (1980).
5. Vanier, M. T. Biochemical studies in niemann-pick disease I. Major sphingolipids of liver and spleen. *Biochim. Biophys. Acta - Lipids Lipid Metab.* **750**, 178–184 (1983).
6. Salvoli, R., Scarpa, S., Ciaffoni, F., Tatti, M., Ramoni, C., Vanier, M. T. & Vaccaro, A. M. Glucosylceramidase mass and subcellular localization are modulated by cholesterol in Niemann-Pick disease type C. *J. Biol. Chem.* **279**, 17674–17680 (2004).
7. Ferraz, M. J., Marques, A. R. A. A., Gaspar, P., Mirzaian, M., van Roomen, C., Ottenhoff, R., Alfonso, P., Irún, P., Giraldo, P., Wisse, P., Sá Miranda, C., Overkleeft, H. S. & Aerts, J. M. Lyso-glycosphingolipid abnormalities in different murine models of lysosomal storage disorders. *Mol. Genet. Metab.* **117**, 186–93 (2016).
8. Ferraz, M. J., Marques, A. R. A., Appelman, M. D., Verhoek, M., Strijland, A., Mirzaian, M., Scheij, S., Ouairy, C. M., Lahav, D., Wisse, P., Overkleeft, H. S., Boot, R. G. & Aerts, J. M. Lysosomal glycosphingolipid catabolism by acid ceramidase: formation of glycosphingoid bases during deficiency of glycosidases. *FEBS Lett.* **590**, 716–725 (2016).
9. Marques, A. R. A., Mirzaian, M., Akiyama, H., Wisse, P., Ferraz, M. J., *et al.* Glucosylated cholesterol in mammalian cells and tissues: formation and degradation by multiple cellular β -glucosidases. *J. Lipid Res.* **57**, 451–63 (2016).
10. Marques, A. R. A., Aten, J., Ottenhoff, R., van Roomen, C. P. A. A., Herrera Moro, D., Claessen, N., Vinueza Veloz, M. F., Zhou, K., Lin, Z., Mirzaian, M., Boot, R. G., De Zeeuw, C. I., Overkleeft, H. S., Yildiz, Y. & Aerts, J. M. F. G. Reducing GBA2 activity ameliorates neuropathology in Niemann-Pick type C mice. *PLoS One* **10**, e0135889 (2015).
11. Reczek, D., Schwake, M., Schröder, J., Hughes, H., Blanz, J., Jin, X., Brondyk, W., Van Patten, S., Edmunds, T., Saftig, P. LIMP-2 Is a receptor for lysosomal mannose-6-phosphate-independent targeting of β -glucocerebrosidase. *Cell* **131**, 770–783 (2007).
12. Zachos, C., Blanz, J., Saftig, P. & Schwake, M. A critical histidine residue within LIMP-2 mediates pH sensitive binding to its ligand β -glucocerebrosidase. *Traffic* **13**, 1113–1123 (2012).
13. Schwake, M., Schröder, B. & Saftig, P. lysosomal membrane proteins and their central role in physiology. *Traffic* vol. 14 739–748 (2013).
14. Heybrock, S., Kanerva, K., Meng, Y., Ing, C., Liang, A., *et al.* Lysosomal integral membrane protein-2 (LIMP-2/SCARB2) is involved in lysosomal cholesterol export. *Nat. Commun.* **10**, 3521 (2019).
15. Hollak, C. E. M., van Weely, S., van Oers, M. H. J. & Aerts, J. M. F. G. Marked elevation of plasma chitotriosidase activity. A novel hallmark of Gaucher disease. *J. Clin. Invest.* **93**, 1288–1292 (1994).
16. Boot, R. G., Verhoek, M., de Fost, M., Hollak, C. E. M., Maas, M., Bleijlevens, B., van

- Breemen, M. J., van Meurs, M., Boven, L. A., Laman, J. D., Moran, M. T., Cox, T. M. & Aerts, J. M. F. G. Marked elevation of the chemokine CCL18/PARC in Gaucher disease: a novel surrogate marker for assessing therapeutic intervention. *Blood* **103**, 33–39 (2004).
17. Ferraz, M. J., Kallemijn, W. W., Mirzaian, M., Herrera Moro, D., Marques, A., Wisse, P., Boot, R. G., Willems, L. I., Overkleeft, H. S. & Aerts, J. M. Gaucher disease and Fabry disease: new markers and insights in pathophysiology for two distinct glycosphingolipidoses. *Biochim. Biophys. Acta - Mol. Cell Biol. Lipids* **1841**, 811–825 (2014).
18. Kramer, G., Wegdam, W., Donker-Koopman, W., Ottenhoff, R., Gaspar, P., Verhoek, M., Nelson, J., Gabriel, T., Kallemijn, W., Boot, R. G., Laman, J. D., Vissers, J. P. C., Cox, T., Pavlova, E., Moran, M. T., Aerts, J. M. & van Eijk, M. Elevation of glycoprotein nonmetastatic melanoma protein B in type 1 Gaucher disease patients and mouse models. *FEBS Open Bio* **6**, 902–913 (2016).
19. Van Der Lienden, M. J. C., Gaspar, P., Boot, R., Aerts, J. M. F. G. & Van Eijk, M. Glycoprotein non-metastatic protein B: an emerging biomarker for lysosomal dysfunction in macrophages. *Int. J. Mol. Sci.* **20** 66 (2019).
20. Aerts, J. M. F. G., Kuo, C. L., Lelieveld, L. T., Boer, D. E. C., van der Lienden, M. J. C., Overkleeft, H. S. & Artola, M. Glycosphingolipids and lysosomal storage disorders as illustrated by Gaucher disease. *Curr. Opin. Chem. Biol.* **53** 204–215 (2019).
21. Guo, Y., He, W., Boer, A. M., Wevers, R. A., de Bruijn, A. M., Groener, J. E. M., Hollak, C. E. M., Aerts, J. M. F. G., Galjaard, H. & van Diggelen, O. P. Elevated plasma chitotriosidase activity in various lysosomal storage disorders. *J. Inherit. Metab. Dis.* **18**, 717–722 (1995).
22. Marques, A. R. A., Gabriel, T. L., Aten, J., Van Roomen, C. P. A. A., Ottenhoff, R., Claessen, N., Alfonso, P., Irún, P., Giraldo, P., Aerts, J. M. F. G. & Van Eijk, M. Gpnmb is a potential marker for the visceral pathology in Niemann-Pick type C disease. *PLoS One* **11**, e0147208 (2016).
23. Overkleeft, H. S., Renkema, G. H., Neele, J., Vianello, P., Hung, I. O., Strijland, A., Van Der Burg, A. M., Koomen, G. J., Pandit, U. K. & Aerts, J. M. F. G. Generation of specific deoxynojirimycin-type inhibitors of the non-lysosomal glucosylceramidase. *J. Biol. Chem.* **273**, 26522–26527 (1998).
24. Abela, G. S., Aziz, K., Vedre, A., Pathak, D. R., Talbott, J. D. & DeJong, J. Effect of cholesterol crystals on plaques and intima in arteries of patients with acute coronary and cerebrovascular syndromes. *Am. J. Cardiol.* **103**, 959–968 (2009).
25. Ioannou, G. N., Landis, C. S., Jin, G., Haigh, W. G., Farrell, G. C., Kuver, R., Lee, S. P. & Savard, C. Cholesterol crystals in hepatocyte lipid droplets are strongly associated with human nonalcoholic steatohepatitis. *Hepatology* **3**, 776–791 (2019).
26. Bocan, T. M., Schifani, T. A. & Guyton, J. R. Ultrastructure of the human aortic fibrolipid lesion. Formation of the atherosclerotic lipid-rich core. *Am. J. Pathol.* **123**, 413–24 (1986).
27. Gabriel, T. L., Tol, M. J., Ottenhof, R., van Roomen, C., Aten, J., *et al.* Lysosomal stress in obese adipose tissue macrophages contributes to MITF-dependent Gpnmb induction. *Diabetes* **63**, 3310–3323 (2014).
28. Sakai, J., Duncan, E. A., Rawson, R. B., Hua, X., Brown, M. S. & Goldstein, J. L. Sterol-regulated release of SREBP-2 from cell membranes requires two sequential cleavages, one within a transmembrane segment. *Cell* **85**, 1037–1046 (1996).
29. Gaspar, P., Kallemijn, W. W., Strijland, A., Scheij, S., Van Eijk, M., Aten, J., Overkleeft, H. S., Balreira, A., Zunke, F., Schwake, M., Sá Miranda, C. & Aerts, J. M. F. G. Action myoclonus-renal failure syndrome: diagnostic applications of activity-based probes and lipid analysis. *J. Lipid Res.* **55**, 138–45 (2014).
30. de Boer, J. F., Kuipers, F. & Groen, A. K. Cholesterol Transport Revisited: A new turbo mechanism to drive cholesterol excretion. *Trends Endocrinol. Metab.* **29** 123–133 (2018).

31. de Boer, O. J., van der Meer, J. J., Teeling, P., van der Loos, C. M., Idu, M. M., van Maldegem, F., Aten, J. & van der Wal, A. C. Differential expression of interleukin-17 family cytokines in intact and complicated human atherosclerotic plaques. *J. Pathol.* **220**, 499–508 (2010).
32. Aerts, J. M. F. G., Donker-Koopman, W. E., Vliet, M. K., Jonsson, L. M. V., Ginns, E. I., Murray, G. J., Barranger, J. A., Tager, J. M. & Schram, A. W. The occurrence of two immunologically distinguishable beta-glucocerebrosidases in human spleen. *Eur. J. Biochem.* **150**, 565–574 (1985).
33. Witte, M. D., Kallemeijn, W. W., Aten, J., Li, K.-Y., Strijland, A., Donker-Koopman, W. E., van den Nieuwendijk, A. M. C. H., Bleijlevens, B., Kramer, G., Florea, B. I., Hooibrink, B., Hollak, C. E. M., Ottenhoff, R., Boot, R. G., van der Marel, G. A., Overkleeft, H. S. & Aerts, J. M. F. G. Ultrasensitive in situ visualization of active glucocerebrosidase molecules. *Nat. Chem. Biol.* **6**, 907–13 (2010).
34. Kallemeijn, W. W., Li, K. Y., Witte, M. D., Marques, A. R. A., Aten, J., *et al.* Novel activity-based probes for broad-spectrum profiling of retaining β -exoglucosidases in situ and in vivo. *Angew. Chemie - Int. Ed.* **51**, 12529–12533 (2012).

Chapter 6

Transcriptional regulation of macrophage lysosome biogenesis in vitro and in the obese adipose tissue

Contributing authors:

M.J.C. van der Lienden¹, H.J.P. van der Zande², F. Otto², C. Oses³, N. Claessen⁴, M. Verhoek¹, J. Aten⁴, J.M.F.G. Aerts¹, B. Guigas², M. Aouadi³ & M. van Eijk⁵. *To be submitted.*

¹Department of Medical Biochemistry, Leiden Institute of Chemistry, Leiden University, The Netherlands.

²Department of Parasitology, Leiden University Medical Centre, Leiden, The Netherlands.

³Department of Medicine, Integrated Cardio Metabolic Centre, Karolinska Institutet, Huddinge, Sweden.

⁴Department of Pathology, Academic Medical Centre, University of Amsterdam, Amsterdam, the Netherlands.

⁵Department of Medical Biochemistry, Leiden Institute of Chemistry, Leiden University, The Netherlands. m.c.van.eijk@LIC.leidenuniv.nl

Abstract

Recent studies suggest an important role for the lysosome in acquired metabolic disorders such as obesity. Obese adipose tissue macrophages (ATMs) scavenge lipid-rich debris and exhibit marked lysosomal storage and increased lysosomal mass. In line, GPNMB, a marker for lysosomal perturbation, is highly elevated in obese ATMs. In this study, the role of transcription factors that drive lysosomal biogenesis in macrophages was characterized. Interference with lysosomal integrity triggers a cellular response through three transcription factors that belong to the microphthalmia-transcription factor E (MiT/TFE) family. In cultured RAW264.7 cells TFEB, TFE3 and MITF all contribute to lysosomal biogenesis. Ablation of these TFs in ATMs of leptin deficient obese mice lowered adiponectin and worsened glucose metabolism. Altogether, we report a complex transcriptional regulation of the lysosome in macrophages. Our data suggest an adaptive role of lysosomal apparatus in ATMs that reduces the burden of sustained metabolic overload.

Introduction

The lysosome is an acidic, membrane enclosed organelle that is involved in the degradation of macromolecules derived from endocytosis, macropinocytosis and phagocytosis. Intracellular cargo enters the lysosome via (macro-) autophagy, a process that facilitates removal of dysfunctional organelles and misfolded protein.¹

The identification of a transcriptional machinery that drives lysosomal biogenesis upon high catabolic demand has put the lysosome at the forefront of metabolic regulation. Predominant in this cellular response is considered to be the microphthalmia-transcription factor E (MiT/TFE) subfamily of basic helix-loop-helix (bHLH) transcription factors (TFs).² This subfamily of leucine zipper regulatory proteins consists of transcription factor EB (TFEB), transcription factor E3 (TFE3), melanogenesis associated transcription factor (MITF) and transcription factor EC (TFEC).³ The MiT/TFE subfamily was associated with lysosomal biogenesis upon identification of TFEB as primary binding protein to a common sequence upstream of lysosomal genes, the so called Coordinated Lysosomal Expression and Regulation (CLEAR) element.⁴ These factors homo- or heterodimerize to bind DNA sequences involved in cellular metabolism.⁵ TFEB and TFE3 are ubiquitously expressed, whereas MITF is largely restricted to pigmented cells such as melanocytes and retinal epithelium cells, as well as to myeloid cells of the immune system, osteoclasts, and stem cells of the hair follicle.^{3,6}

TFEB, TFE3 and MITF are subjected to phosphorylation by Mammalian target of rapamycin complex 1 (mTORC1), an established master regulator of cell growth that resides at the cytosolic side of the lysosomal membrane.⁷⁻¹⁰ At this position, mTORC1 functions as a key signaling hub for nutrients and hormonal pathways.¹¹ Under basal, nutrient rich conditions, RAG GTPases facilitate lysosomal localization of mTORC1 that allows proximity with its activator protein Ras homologue enriched in brain (RHEB). Likewise, RAG GTPases and 14-3-3 proteins associate with phosphorylated MITF, TEB and TFE3 and sequester them in the cytosol.¹²⁻¹⁵ With respect to TFEB, a serine residue is phosphorylated by active mTORC1.^{13,16} A homologous serine residue can be found on MITF and its phosphorylation was previously shown to be important for cytosolic retention by 14-3-3 proteins.¹⁷ Inhibition of mTORC1 results in dephosphorylation of TFEB and its nuclear localization. This was initially achieved artificially through selective inhibition of mTORC1 by a commonly used drug Torin 1, as well as through lysosomal amino acid starvation.^{4,13,18,19} Treatment with conventional lysosomal stressors such as the undegradable sugar sucrose or elevation of lysosomal pH by the lysosomotropic compound chloroquine, induced a similar nuclear translocation of TFEB, MITF and TFE3. Moreover, evidence suggests that TFEB and other TFs exhibit enhanced transcriptional activity in diseases that are characterized by a lysosomal defect.^{4,15,20-22}

Perturbed lysosomal function is also implicated in other biological processes such as longevity, and in pathologies like cancer and neurodegeneration.²³⁻²⁶ Among the most common acquired metabolic disorders in which lysosomal function has been suggested to play an important role is obesity and its associated pathologies classified as the metabolic syndrome.^{27,28} Xu et al. discovered a lysosome driven program of lipid degradation in adipose tissue macrophages (ATMs) upon obesity and ultrastructural analysis revealed a foamy appearance of obese ATMs.²⁹ In line with this, glycoprotein non metastatic protein B (GPNMB), a marker for lysosomal problems in macrophages, is dramatically increased

in obese mice and, to a lesser extent, in men.^{30,31} It was furthermore shown in RAW264.7 cells that GPNMB expression was induced upon palmitate feeding (not oleate) and upon exposure to the lysosomotropic agent chloroquine, an induction that was driven by MITF. Moreover, GPNMB was shown to potentiate arginase-1 production upon IL-4 stimulation, thereby associating GPNMB with an immunomodulatory phenotype.³⁰ The immunological status of the adipose tissue is largely influenced by the bidirectional communication between adipocytes and macrophages. Macrophages react to adipocyte derived factors hormones such as adiponectin, which sensitizes tissues for insulin and alleviate toxic lipid accumulation (lipotoxicity) and inflammation.³² This balance is disturbed upon obesity.

Despite the increased understanding of the machinery that orchestrates lysosomal adaptation, it remains largely unclear to what extent adaptive lysosomal biogenesis contributes to pathology. Here, we test the contribution of MITF, TFEB and TFE3 in regulating increased lysosomal demand. Significance of these TFs in obese ATMs was characterized through recently developed ATM specific siRNA delivery molecules called glucan encapsulated particles (Gerps).^{33,34} A combinatorial approach was employed, targeting the TFs in ATMs simultaneously to highlight the importance of lysosomal adaptation within ATMs.

Results

In vitro analysis of MiT/TFE knockdown in cultured RAW264.7 cells

TFs belonging to the MiT/TFE subfamily are established regulators of lysosomal gene transcription, but redundancy and mutual exclusivity are incompletely understood. Macrophages express Tfeb, Tfe3 as well as Mitf. To impair lysosomal regulation macrophage-like cells, an siRNA-based approach was applied to specifically knock-down either MITF, TFEB or TFE3 in cultured RAW264.7 cells. Transfection with siRNA targeting *Mitf* in RAW264.7 cells resulted in knock down of *Mitf*, along with an increase in expression of *Tfeb* and *Tfe3* (**Figure 1A**). In contrast, successful knock down of *Tfeb* did not alter expression of *Mitf* and *Tfe3*. Knock-down of *Tfe3* resulted in a concomitant increase in *Mitf*, but not *Tfeb*. At the level of protein, knock-down could be verified by western blot (**Figure 1B**). The use of different oligonucleotide sequences for one of the respective targets confirmed a specific effect of the siRNA oligonucleotides used (**Supplemental figure 1A**). Immunohistochemistry provided additional proof for reduced protein abundance of respective target genes (**Figure 1C**). Of note, knock down of either MITF, TFEB or TFE3 with or without sucrose supplementation did not markedly affect nuclear translocation of the other TFs, suggesting that reduced presence of one MiT/TFE-member did not lead to changes in localization of subfamily members (**Supplemental figure 1B**). Subtle changes in MiT/TFE nuclear localization upon knock down of homologous TFs however, cannot be ruled out.

In the presence of the mild lysosomal stressor HEPES, a similar pattern with respect to *Mitf*, *Tfeb* and *Tfe3* RNA expression was observed upon each respective knock down (**Figure 1D**). Expression of lysosomal genes *Gpnmb*, *CtsD*, *Lamp1* and *Atp6via* and inflammatory genes *Ccl2* and *Tnfa* were elevated upon HEPES supplementation (**Supplemental figure 2A**) and were unaltered or further increased upon knock down of either *Mitf*, *Tfeb* or *Tfe3* (**Figure 1D**). This unanticipated increase could be explained by

cross regulation. It was therefore decided to use a combinatorial knockdown approach, in which two or three transcription factors are knocked down simultaneously. In DMEM cultured (basal conditions) RAW264.7 cells, *Tfeb* showed a more than two-fold induction upon simultaneous knock-down of *Mitf* and *Tfe3*, whereas *Mitf* exhibited increased expression upon combined knock-down of *Tfeb* and *Tfe3* (**Figure 1E**). *Tfe3* did not seem to be subjected to a regulatory feedback in the experimental set up. The changes in expression levels of *Mitf*, *Tfeb* and *Tfe3* remained the same in the presence of HEPES (**Figure 1F**). Next, we analysed the impact of the various knockdown combinations on lysosomal genes in the presence of HEPES. A combination of either reduced *Mitf* or *Tfe3* with reduced *Tfeb* showed reduction in the expression of *Gpnmb* in HEPES stimulated cells (**Figure 1F**). Surprisingly, knock-down of all three transcription factors was necessary to induce a significant reduction in *CtsD* and *Atp6v1a*. Of note, lysosomal and inflammatory genes were altered only to a limited extend under basal conditions (**Supplemental figure 2B**)

Analysis of inflammatory gene expression revealed that simultaneous knock-down of *Tfeb* and *Tfe3* induced an increase in *Ccl2* expression, but not *Tnfa* expression (**Supplemental figure 2C**). Additional knock-down of *Mitf* abolished this increase. In conclusion, simultaneous knock-down of *Mitf*, *Tfeb* and *Tfe3* resulted in the most potent reduction in target gene expression as measured by *Gpnmb*, *Cathepsin D* and *Lamp1*, without triggering upregulation of *Ccl2*.

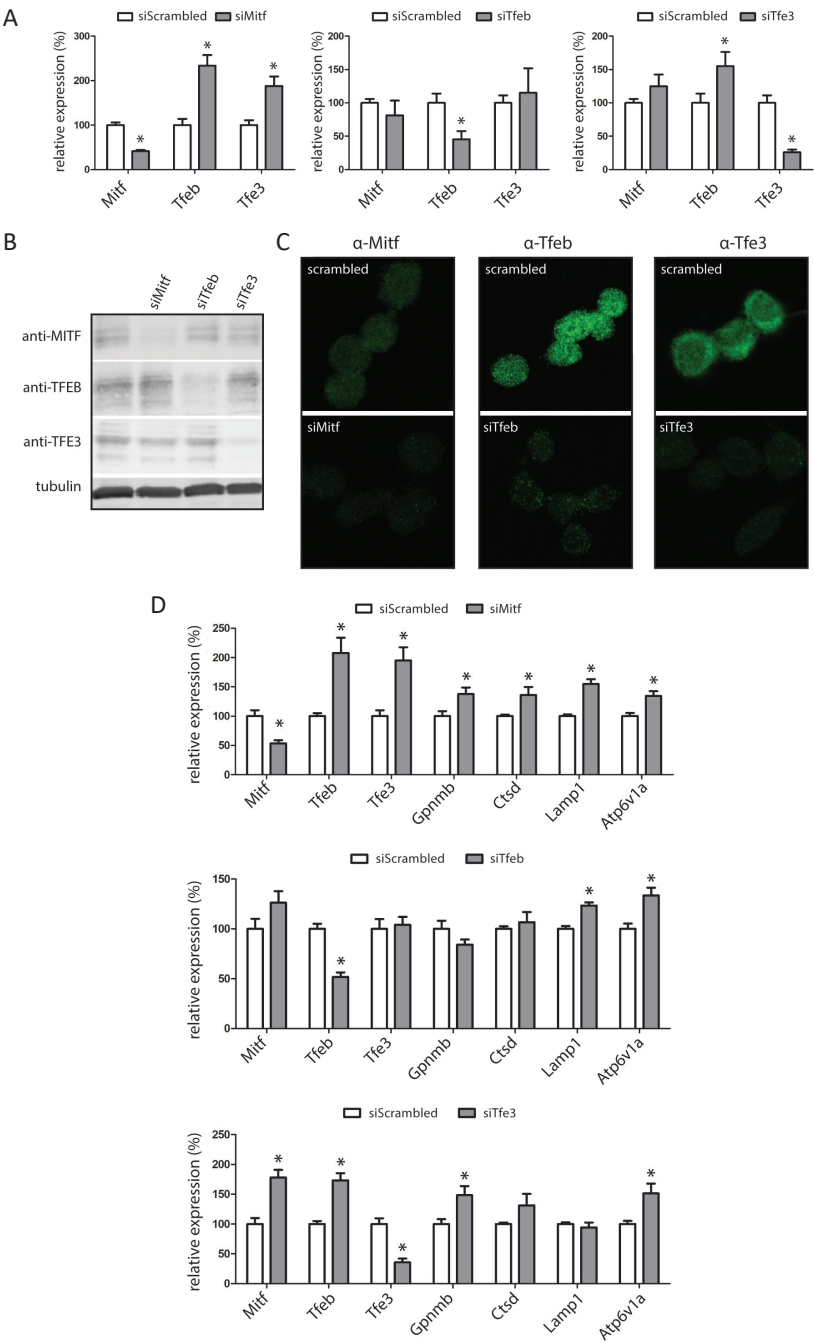
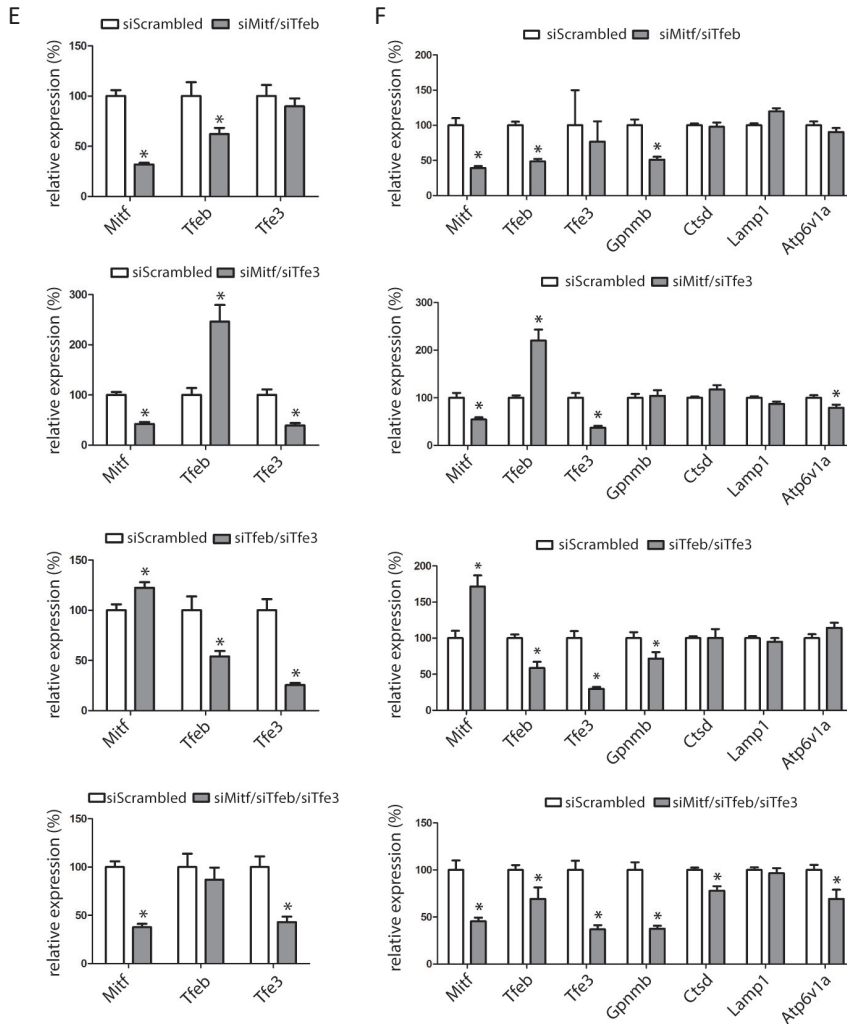


Figure 1. In vitro analysis of MiT/TFE knockdown in cultured RAW264.7 cells; (A) Real-time (Rt) qPCR RNA analysis on Mitf, Tfeb and Tfe3 gene expression in RAW264.7 macrophages subjected to siRNA mediated knock down under basal conditions; (B) Western blot analysis of siRNA treated RAW264.7 macrophages; (C) Immunohistochemical analysis of siRNA mediated knock down of Mitf, Tfeb and Tfe3 in RAW264.7 cells cultured in DMEM and in DMEM supplemented with 80mM Sucrose; (D) Rt qPCR expression analysis on Mi/TEF and lysosomal gene expression of HEPES

treated RAW264.7 cells upon single MiT/TFE knock-down; **Below** -> **(E)** Rt qPCR on target genes of *Mitf*, *Tfeb* and *Tfe3* through combined knock down of *Mitf*/*Tfeb*, *Mitf*/*Tfe3*, *Tfeb*/*Tfe3* or *Mitf*/*Tfeb*/*Tfe3* resp under basal conditions; **(F)** MiT/TFE and lysosomal gene expression of HEPES treated RAW264.7 cells upon combinatorial MiT/TFE knock-down.



Validation Gerp particles in RAW264.7 cells

To investigate the impact of MITF, TFEB and TFE3 *in vivo*, we optimized a macrophage specific siRNA delivery method through yeast derived glucan shells called glucan encapsulated particles (Gerps). Through this method we aimed to simultaneously knock down *Mitf*, *Tfeb* and *Tfe3*. Firstly, functionalized yeast derived glucan shells were prepared to deliver siRNA in RAW264.7 cells according to the described protocol.^{33,34} In cultured RAW264.7 cells, addition of Gerp-siRNA complexes resulted in internalization and accumulation of these Gerps inside the macrophage (**Figure 2A**). RNA expression analysis revealed knock-down of all three TFs (**Figure 2B**).

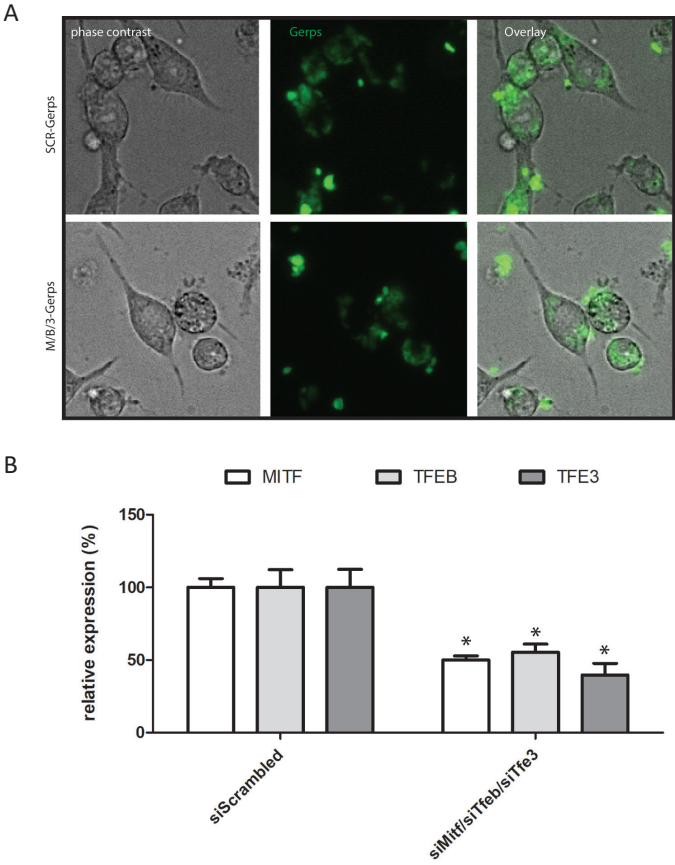
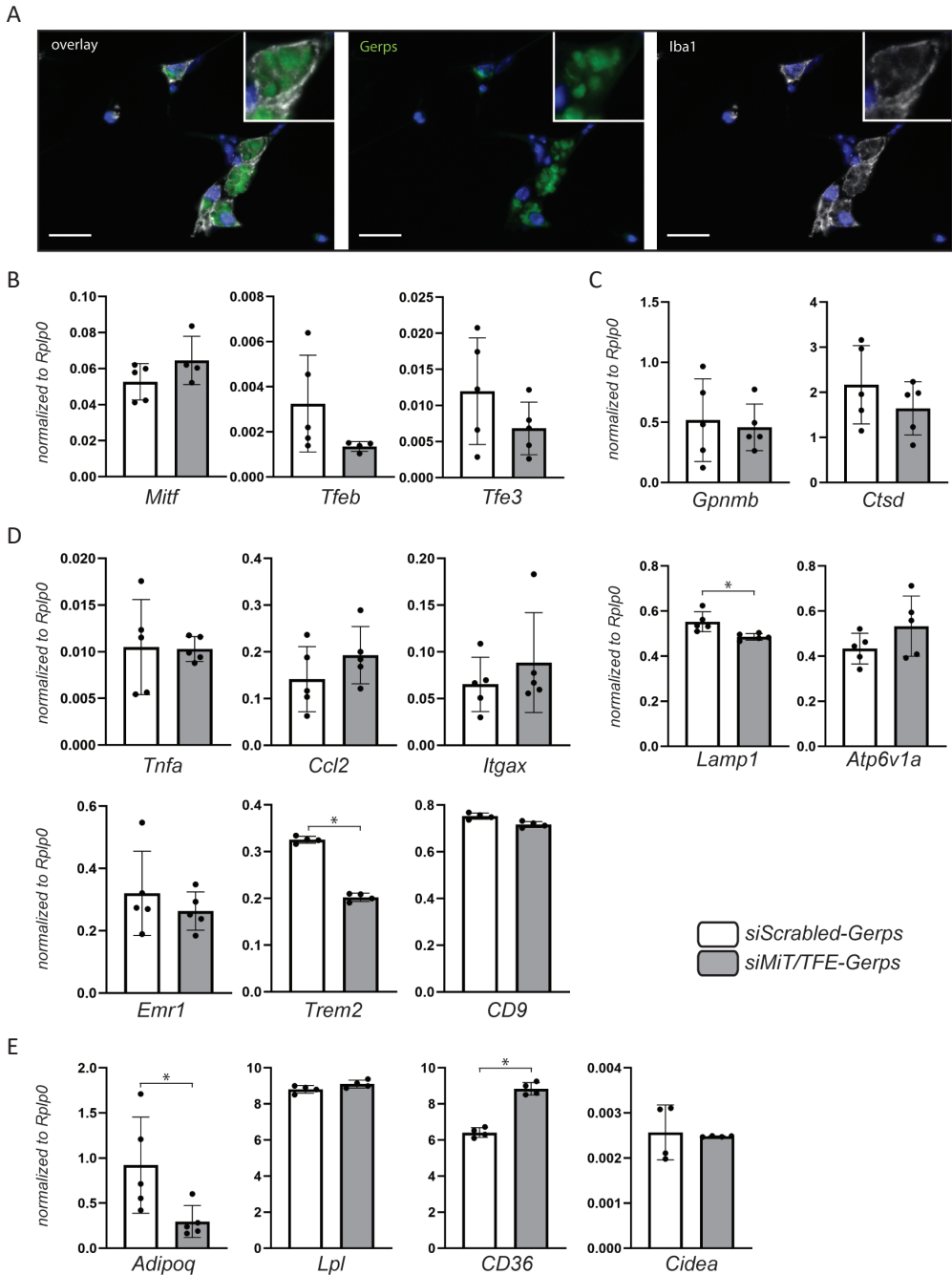


Figure 2. Validation of Gerp-siRNA complex treatment in RAW264.7 cells; (A) Fluorescence microscopy of RAW264.7 cells treated with FITC-labelled Gerp-siRNA particles; **(B)** Rt qPCR analysis of Mit/TFE genes in RAW264.7 macrophages subjected to Gerp-siRNA treatment.

Lowering of adiponectin expression in total EWAT upon treatment of obese mice with MiT/TFE siRNA Gerp particles

Since accumulating evidence suggests that obese ATMs exhibit increased lysosomal content, this methodology was employed to study the contribution of lysosomal biogenesis in ATMs to the integrity of adipose tissue and progression of obesity in leptin deficient mice (Ob/Ob). FITC-labelled Gerps were loaded with either scrambled siRNA or siRNA targeting *Mitf*, *Tfeb* and *Tfe3* simultaneously. The siRNA-Gerp complexes were injected daily into the peritoneal cavity of 9 weeks old leptin deficient mice for a period of 14 days. Fluorescence microscopy showed localization of Gerps inside CLSs (**Figure 3A**). Gene expression analysis on whole EWAT revealed that *Tfeb* and *Tfe3* tended to be reduced, whereas *Mitf* expression remained unchanged (**Figure 3B**). Although no differential RNA expression of *Gpnmb*, *Ctsd* and *Atp6via* could be detected, expression of the structural lysosomal protein *Lamp1* was significantly reduced (**Figure 3C**). Moreover, no difference in inflammatory status of epididymal fat was observed due to treatment, as measured by expression levels of cytokines *Ccl2*, *Tnfa* and macrophage markers *Emr1*(F4/8o) and *Itgax* (CD11c) (**Figure 3D**).



Recent studies on obesity in mice have identified a unique expression profile of ATM residing in CLSs that fundamentally differs from the classically activated macrophages.^{35,36} These ATMs are characterized by *CD9*, *CD36* and *TREM2* expression and are found to be specialized in lipid uptake and degradation.³⁶ Upon treatment with MiT/TFE targeting siRNA, *Trem2* expression was reduced in EWAT, but not *CD9* (**Figure 3D**). Characterization of lipid related signalling and scavenging in EWAT revealed a striking reduction in expression of the insulin sensitizing adipokine *Adipoq* (Adiponectin) and an increase in the lipid scavenging receptor *CD36*. Genes encoding the lipoprotein interacting protein lipoprotein lipase (*Lpl*) and the adipocyte specific lipid droplet marker cell death-inducing DNA fragmentation factor alpha-like effector A (*Cidea*) are aberrantly expressed upon obesity, but not altered in total EWAT upon Gerp-siRNA treatment.

Since ATM specific targeting was anticipated, CD11b-enriched fractions were analysed with respect to the specificity of the Gerp-siRNA treatment, as well as the macrophage specific changes. Fluorescence microscopy could readily detect enrichment of FITC-labelled Gerps in the CD11b-positive fraction (**Figure 4A**). Unexpectedly however, knock-down of *Mitf*, *Tfeb* and *Tfe3* was not observed in CD11b⁺-macrophage fraction (**Figure 4B**), while a trend towards lower expression of *Lamp1* was observed (**Figure 4C**). Other lysosomal genes did not show to be altered (**Figure 4C**). Pro-inflammatory markers *Ccl2*, *Tnfa* were not altered in the CD11b⁺-fraction (**Figure 4D**). Since the ATM population exhibits high plasticity, we speculated that targeted macrophages acquired a different metabolic state and phenotype. The markers of lipid-associated macrophages *Trem2* and *CD36* were not altered (**Figure 4D** and **E**). However, *CD9*, an additional marker that identifies macrophages involved in lipid uptake and degradation, was found to be significantly reduced (**Figure 4D**). In line with a potentially altered lipid uptake, CD11b specific *Lpl* expression was similarly reduced upon Gerp treatment targeting *Mitf*, *Tfeb* and *Tfe3* (**Figure 4E**).

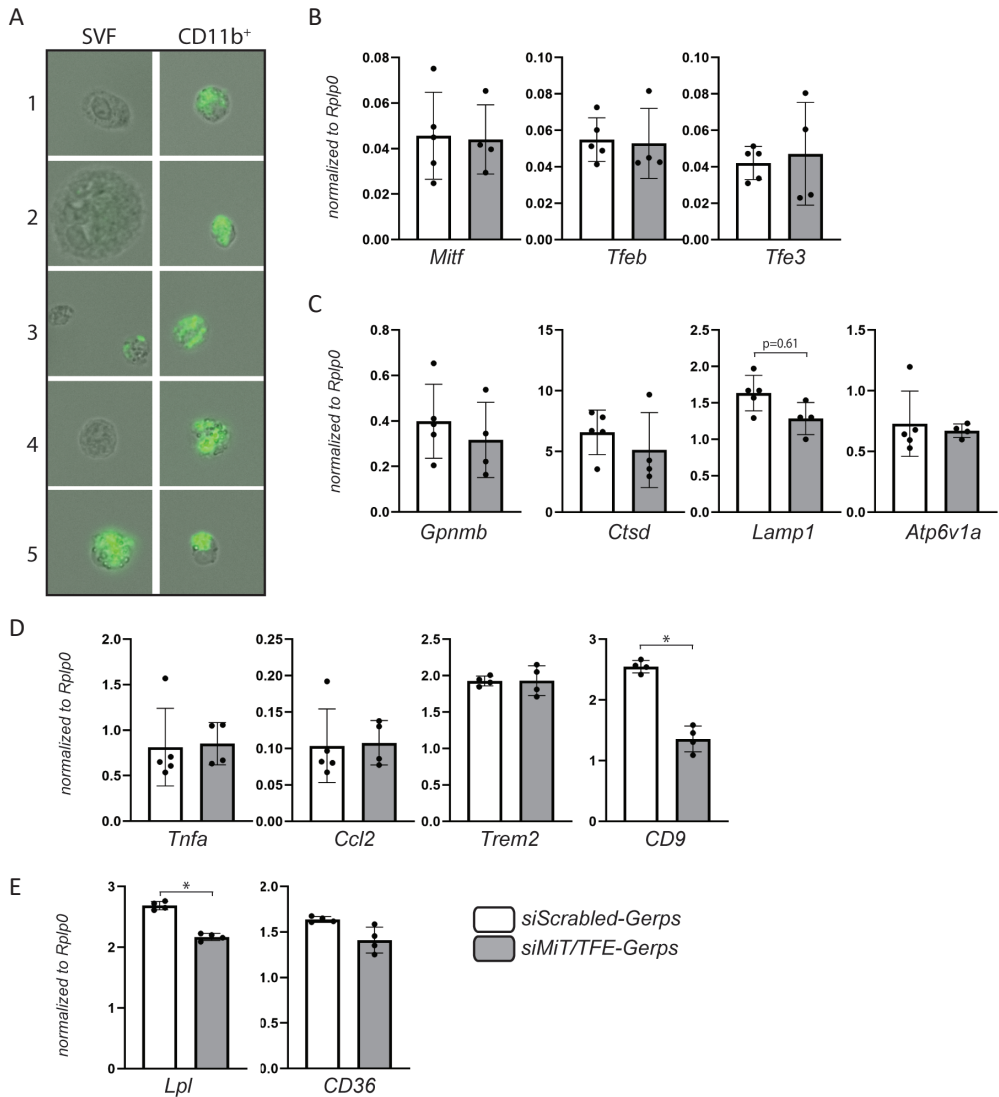


Figure 4. Characterization of EWAT obtained CD11b⁺ fraction from Gerp-siRNA treated obese mice; (A) Fluorescence microscopy analysis of CD11b⁺ fraction of Gerp-siRNA treated obese epididymal fat; Rt qPCR analysis of CD11b⁺ fraction of Gerp-siRNA treated obese epididymal fat on (B) MiT/TFE genes, (C) lysosomal genes, (D) inflammatory genes and (E) adiposity associated genes.

Treatment of obese mice by Gerp-MiT/TFE siRNA results in worsening of glucose tolerance RNA expression profiles suggest that ATM specific targeting of MiT/TFE members lowers lipid associated markers of macrophages. Furthermore, the expression of the adipokine adiponectin is reduced in EWAT, which possibly impacts on systemic insulin sensitivity. To further study the impact of the siMiT/TFE-Gerp treatment on progression of obesity, metabolic parameters of treated, obese mice were analysed. At start of the treatment, metabolic parameters between groups was not different (**Supplemental figure 3**).

Strikingly, glucose tolerance significantly reduced in groups treated with siRNA oligo's targeting MiT/TFE subfamily compared to scrambled siRNA after 14 days of siRNA-Gerp treatment (**Figure 5A and B**). Other metabolic parameters such as average weight, fat mass percentage were not altered (**Figure 5C and D**). Moreover, no difference was observed in fasting insulin levels and HbA1c (**Figure 5 E and F**).

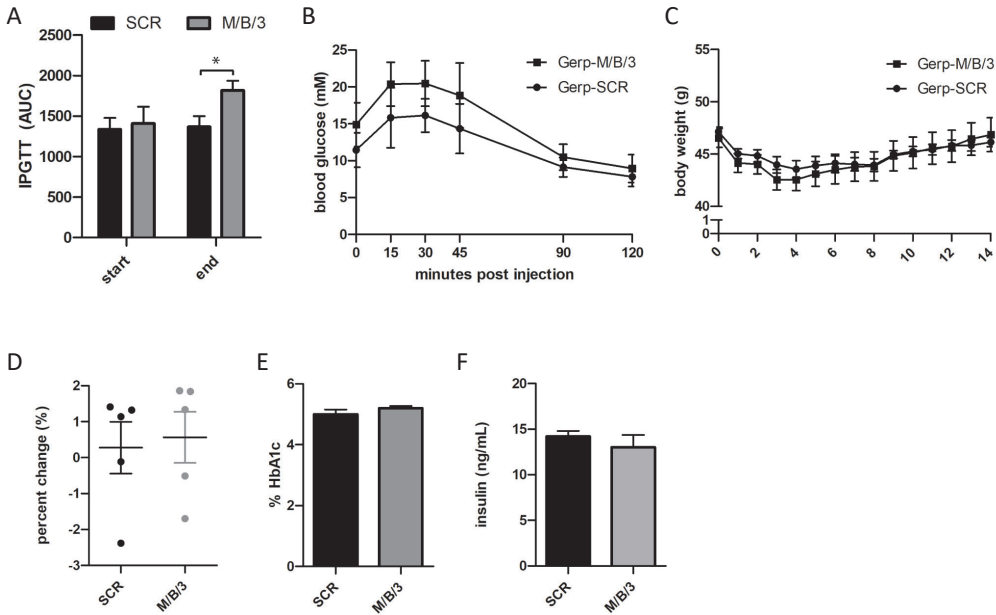


Figure 5. Metabolic characterization of Gerp-siRNA treated obese mice; (A) Area under the curves (AUC) of glucose tolerance of two weeks after treatment and (B) their respective curves; (C) Average body weight of scrambled treated group and triple knock-down group over 14 days of treatment; (D) Percent change in fat mass at 14 days of treatment compared to start; (E) Percentage change in HbA1c levels compared to start of the experiment; (F) Insulin levels at t=0 and t=14 of scrambled and triple siRNA treated groups.

Discussion

A major factor that currently drives the interest in the lysosome is its ubiquitous role in nutrient sensing and coordination of cellular metabolism.^{4,11} It has nevertheless remained enigmatic which of the known drivers of lysosomal biogenesis are redundant or crucial for their function. We previously reported transcriptional control by MITF, TFEB and TFE3 on the expression of several lysosomal genes (Chapter 2). Here, the regulatory profile of these TFs was extended by characterizing the individual and combinatorial effect of MITF, TEFB and TFE3 on expression of target genes. These data establish a compensatory feedback among MITF, TEFB and TFE3 that is dependent on the expression level of other members. Upon knock down of *Mitf* and *Tfe3* respectively, increased expression of untargeted MiT/TFE members was observed. In the case of *Mitf* targeted knock down, *Tfeb* and *Tfe3* were upregulated. In addition, regulation of target genes exhibited differential dependence on MiT/TFE members. Knock-down of *Mitf*, *Tfeb* and *Tfe3* did

not completely abolish lysosomal gene expression, which could be explained by the fact that no full knock-down was achieved. This could have allowed for residual transcriptional activity of knocked-down proteins.

Moreover, homologous MiT/TFE subfamily member TFEC is predominantly expressed in macrophages and may provide additional clues on the redundancy and exclusivity of MiT/TFE members in driving inflammatory and lysosomal gene expression. In addition to the homodimerization that occurs upon activation, heterodimerization among the MiT/TF factors has been described.³⁵ The cell specific presence of each TF, as well as the posttranscriptional (splicing) and posttranslational (phosphorylation, acetylation) processing, may determine self-regulation and promotor affinity of each subtype.^{13,37,38} Quantitative assessment of dimerization affinity and DNA-binding properties may shed light onto their cell-specific action.

Alternatively, presence of other transcription factors could have contributed to lysosomal biogenesis in the absence of MiT/TFE members, such as MYC, Signal transducer and activator of transcription 3 (Stat3) or zinc finger with KRAB and SCAN domains 3 (Zkscan3).^{39–42}

Intriguingly, combined knock down of *Tfeb* and *Tfe3* increased pro-inflammatory *Ccl2* gene transcription under basal and HEPES stimulated conditions. When *Mitf* was simultaneously knocked down, no increase *Ccl2* expression was observed. The significance of these findings remains unclear. Earlier observations by Pastore et al. revealed that upon LPS stimulation CCL2 secretion was compromised in a *Tfeb/Tfe3* double knock-out RAW264.7 model compared to the wild type cell line.⁴³

MiT/TFE regulation has been considered a main driver of lysosomal biogenesis, but the implication of this mechanism in tissue resident storage cells has remained incompletely understood. Moreover, a distinction between the role of these factors in ubiquitous lysosomal maintenance and compensatory (pathological) stimuli is not clear. Metabolically activated macrophages have emerged as storage cells that exhibit a unique gene expression profile along with increased lysosomal content.^{29,30,44–47} These cells have been shown to fundamentally differ from the classically activated M₁-macrophages that are assumed responsible for a chronic, low grade inflammatory state in obese individuals. Emerging data furthermore suggest that ATMs can serve a protective role within tissue by scavenging lipids and modulate inflammation.^{30,48} The Gerp-siRNA methodology provides a unique tool to study the impact of obese ATMs on whole body metabolism through transient interference with ATM gene expression.^{33,34} This way, compensatory lysosomal biogenesis in ATMs can be counteracted by interference in transcriptional regulation of lysosome genes. By fluorescence microscopy, localization of Gerps in Iba⁺-cells in EWAT was confirmed. Moreover, Gerp-positive cells were highly enriched in the CD11b⁺-fraction, which suggests that the delivery method was suitable for specific ATM targeting. A trend towards lower expression of target genes *Tfeb* and *Tfe3* was observed in the whole EWAT of MiT/TFE-Gerp treated mice, whereas no effect was observed in the CD11b⁺-fraction. Although effectivity and specificity of the technique was extensively validated *in vitro*, we cannot rule out additional technicalities such as limited reach of the entire ATM population in the epididymal fat. Recent data shows that during the progression towards obesity, murine adipose tissue acquired a *Trem2* positive, lipid associated subpopulation of macrophages as characterized by single-cell sequencing.³⁶

Obese *Trem2* knock-out mice manifest with dramatically increased adipocyte size and worsening of whole-body metabolism compared to obese wild type mice. Upon 14-days administration of MiT/TFE-Gerps, *Trem2* was found to be significantly lower in whole EWAT. Surprisingly, this effect was lost in the CD11b enriched fraction.^{36,45,46} In contrast, *CD9*, a marker strongly associated with *Trem2*⁺ LAM signature, was significantly reduced in the CD11b⁺-fraction, whereas reduction in *CD9* expression in whole AT was not significant. The presence of distinct macrophage subpopulations could provide an explanation to the discrepancies between EWAT and CD11b⁺-fractions. It is conceivable, for example, that the employed CD11b⁺-enrichment protocol may not have been sensitive enough to all ATM-populations, favouring extraction of *Trem2*⁺ CD11b⁺-macrophages due to either physical properties or protein expression. Since *CD9* is less exclusively associated with LAMs, a treatment-effect could still be observed in the enriched fraction, while variable expression in whole EWAT could dilute this effect. Alternatively, a differential uptake of Gerp-particles by different ATM-populations or suboptimal siRNA targeting of genes could explain a large variation in certain markers. The lack of treatment-effect on *Gpnmb* expression in EWAT and CD11b⁺-fraction is unexpected, since it proved the most sensitive to MiT/TFE regulation during *in vitro* validation. Again, the Gerp-siRNA particles may have reached only a subset of macrophages, diluting the effect of treatment. Expression of the ubiquitous lysosomal membrane protein *Lamp1* was however reduced in both EWAT and the CD11b⁺-fraction of Mi/TFE-Gerp treated mice. Taken together, the expression analysis revealed a significant reduction in several genes involved in lysosome function and lipid handling in EWAT, in the CD11b⁺-fraction or in both, concomitantly with impaired glucose clearance.

Aouadi et al. previously showed that Gerp-siRNA mediated knock-down of ATM derived lipoprotein lipase (LPL), the enzyme involved in de-esterification of lipoprotein derived lipids for cellular uptake, resulted in worsening of insulin sensitivity and a reduction in foam cell appearance, without exacerbation of the immune response.³⁴ Similarly, our data reveal an impaired insulin sensitivity upon interference in regulation of lysosome genes without apparent change in expression of canonical, pro-inflammatory markers *Ccl2* and *Tnfa*. The significant reduction in RNA encoding adiponectin in EWAT upon MiT/TFE knock down, an adipokine important in regulating systemic glucose metabolism, may therefore indicate that adipose tissue signalling, rather than inflammation underlies worsening of glucose sensitivity.⁴⁹ Adiponectin is exclusively produced by adipocytes and acts on many organs as potent insulin sensitizer and reducer of lipotoxicity.³² The link between lipid-associated macrophages and the adipose tissue however remains incompletely understood.

The current study suggests that reduced MiT/TE driven lysosomal biogenesis in obese ATMs causes a concomitant reduction in expression of lipid scavenging proteins, perturbed adipose tissue signalling and worsening of systemic glucose sensitivity, independent of inflammatory status. It would be of therapeutic value to study mechanisms through which lysosome and lipid scavenging capacity of ATMs can be improved.

Material and Methods

Animals

Leptin-deficient obese mice (C57BL/6J background) were obtained from Charles River (Italy). National and local ethical committee approval was obtained for conducting animal experiments and laboratory animal welfare rules were followed (AVD nr AVD1060020186607). Mice were kept on a chow diet for the duration of experiments. Body weight and food intake were measured weekly prior to start and daily from start of experiments on. Lean and fat mass were scanned at day 0, day 7 and day 14 by EchoMRI-100 analyzer (Echo MRI).

Preparation of Gerps

Gerp-siRNA complexes were prepared as previously described.⁵⁰ siRNA was functionalized by a 15 minutes incubation of 3 nmol siRNA (Dharmacon) with 50 nmoles Endo-Porter (Gene Tools) at room temperature, buffered in a total volume of 20 μ l by 30 mM sodium acetate pH 4.8. The functionalized siRNA solution was loaded into the glucan shells by resuspending 1 mg of FITC labelled glucan shells in the siRNA/endopporter solution, vortexed and incubated for 1 h. The siRNA-Gerp complexes were brought to a final concentration by PBS, homogenized by sonication and stored at -20°C.

Gerp-siRNA treatment of obese mice

9-weeks old mice were assigned to a treatment and control group (5 mice per group) based on fasting body weight and glucose levels. Daily, mice received intraperitoneal (i.p) treatment with one dose Gerp-siRNA up to fourteen days. One dose of prepared Gerps contained 0.2 mg of glucan shell, 10 nmol of Endo-Porter (Gene Tools) and 1 nmol of siRNA (Qiagen) in PBS (200 μ l). Organs were collected for assessment of specificity of the treatment and for metabolic and immunological profiling.

Monitoring metabolic parameters

Performance of the intraperitoneal glucose tolerance test (IPGTT) was performed by injection of 1.5g/kg body weight of a 20% glucose solution in PBS intraperitoneally. Blood was collected by tail bleeding at 0, 15, 30, 45, 90 and 120 minutes after injection of the glucose bolus to determine plasma glucose using either a portable glucometer or a glucose assay. In addition, body weight was determined.

Preparation of Stromal Vascular Fractions and CD11b⁺ fraction

Dissected epididymal white adipose tissue (EWAT) was minced and Krebs' buffer (2.4M NaCl; 96 mM KCl; 24mM KH₂PO₄; 24mM MgSO₄ in Milli-Q; pH 7.4) was added. An equal volume of 2x collagenase I (Sigma) buffer was added and fat pads were incubated for 1h at 37°C in a shaking incubator at 60 rpm. The collagenase I was washed by adding prewarmed PBS and the suspension was strained through repeated pipetting and filtering through a 200 μ m filter. The suspension was washed and allowed to stand for 10 minutes to allow the fat cell to float. The infranatant was collected with a syringe and an 18G needle for SVF collection. SVF fraction was centrifuged for 10 minutes at 350G at RT. CD11b⁺-cell isolation was performed through anti-CD11b antibody incubation conjugated to magnetic beads (Miltenyi Biotec). MACS columns were used to separate the stromal

vascular fraction (SVF) from the CD11b⁺-cell -fraction following the manufacturer's protocol.

RNA Extraction and Real-time PCR

Total RNA from total Epididymal fat, SVF, and CD11b⁺ fractions was obtained through TRIzol (Invitrogen) extraction and the NucleoSpin II extraction kit (Macherey Nagel) according to manufacturer's protocol. cDNA was synthesized based on the measured RNA concentration (DeNovix DS-1) according to the manufacturer's protocol (Invitrogen). Real time qPCR was performed using Bio-Rad CFX96 Touch™ real-time PCR detection system (Bio-Rad Laboratories). Acidic ribosomal phosphoprotein 36B4 expression (*Rplpo*) was used as reference.

Plasma parameters

For plasma preparations, blood samples were collected via tail cut and collected in heparin coated capillaries at day 0 and 14 after 4 hours of fasting. Capillaries were centrifuged at 1500 rpm at 4°C. Plasma was collected and stored at -80°C until assayed. Plasma insulin levels were measured by ELISA (Crystal Chem Inc.) Whole blood was separately obtained at end of the treatment HbA1c was determined by using a Mouse Glycated Hemoglobin Assay Kit according to the manufacturers protocol (Crystal Chem Inc.).

Cell Culture Experiments

The macrophage cell line RAW264.7 (American Type Culture Collection, TIB-71) was cultured in DMEM supplemented with 10% fetal calf serum (Thermo Fisher Scientific), 1% glutamax (Thermo Fisher Scientific) and 0,2% antibiotics (penicillin-streptomycin) at 37°C at 5% CO₂ in a humidified chamber. In assays employing lysosomal perturbation, RAW264.7 cells were subjected to 80mM sucrose (Sigma) or 25mM HEPES (Sigma) for at least 24 hours. For siRNA mediated knock down experiments, RAW264.7 cells were seeded at a confluency of 3x10⁵ cells/ml and allowed to rest at least 3h before transfection. siRNA oligonucleotides were obtained from Qiagen and contained two sequences per target for Mitf (Sequence: S102687692, S10270963), Tfeb (Sequence: S101444394, S101444408) and Tfe3 (Sequence: S101444415, S105181435) and control (scrambled/SCR) siRNA (S103650318). Cells were harvested 48 hours post-transfection and analysed on mRNA and protein expression.

Immunohistochemistry

EWAT was dehydrated in 70% ethanol overnight upon dissection, fixed in 4% formaline, phosphate-buffered at pH 7.0, and subsequently embedded in paraffin. Embedded tissue was cut in 4µm-thick sections, which were then deparaffinized by three 100% xylene washes and a subsequent 100% ethanol wash. Sections were rehydrated by washing subsequently in 96% ethanol, 70% ethanol and milliQ and heat induced epitope retrieval (HIER) was performed at 98°C for 10 minutes in 10mM citric acid (pH 6). Next, tissues were washed in PBS/0,1% Tween-20 (Sigma) and incubated with the following primary antibody rabbit-anti-Iba1 (Wako, 019-19741) diluted in PBS/5% antibody diluent (ScyTek Laboratories). Antibodies were visualized by Alexa Fluor™ 647 conjugated secondary anti rabbit antibody (Molecular Probes, A31573). For detection of transcription factors, cultured RAW264.7 on glass coverslips (VWR) were fixed in absolute methanol for 15

minutes at -20°C, blocked in 5% normal donkey serum (The Jackson Laboratory) diluted in 0.2% Tween/PBS. Cells were incubated with primary antibodies MITF (Exalpha Biologicals Inc, X1405M), TFEB (Bethyl Lab Inc, A303-673A) and TFE₃ (Sigma, HPA023881) for 1h and detected with secondary anti mouse or rabbit Alexa Fluor™ 488 conjugated antibodies (Molecular Probes, A2102 and A21206 resp.).

Western Blot Analysis

Cultured RAW264.7 cells and tissue samples were lysed in radio immunoprecipitation assay (RIPA) buffer (150 mmol/L NaCl, 50 mmol/L Tris-HCl pH 7.4, 2 mmol/L EDTA, 0.5% deoxycholate, 1 mmol/L Na₃VO₄, 20 mmol/L NaF, and 0.5% Triton X-100) containing protease and phosphatase inhibitors (Roche) and phenylmethylsulfonyl fluoride (PMSF; Sigma). Soluble lysate fraction was obtained by centrifugation at 12,000 x g for 15 minutes at 4°C. Protein concentrations were determined using the bicinchoninic acid assay (Thermo Fisher Scientific, 23225) and equal quantities of protein were denatured in Laemmli buffer at 95°C, separated on a 10% SDS-PAGE, and transferred to nitrocellulose (WELKE Biorad). Membranes were blocked in 5% (w:v) bovine serum albumin (Sigma, A1906) solution in PBS/0.1% Tween-20 (Sigma, P1379) for 1 h at room temperature (RT), and incubated overnight with respective antibodies at 4°C. Primary antibodies used MITF, TFEB and TFE₃ (see earlier) and detected by using specific secondary conjugated antibodies (Alexa Fluor™ 488/647) (Molecular Probes). Detection of immunoblots was performed using a Typhoon FLA 9500 fluorescence scanner (GE Healthcare)

Statistical Analysis

Values presented in figures represent means ± standard deviation. Statistical analysis of expression data on the Gerp-siRNA treated groups was performed by Student *t* test (two tailed).

IPGTT analysis

With respect to IPGTT analysis, significance was established when $p \leq 0.05$ for a given difference in area under the curve (AUC) between groups, and the power of the effect is 80%, tested by a two-way ANOVA for repeated measurements.

References

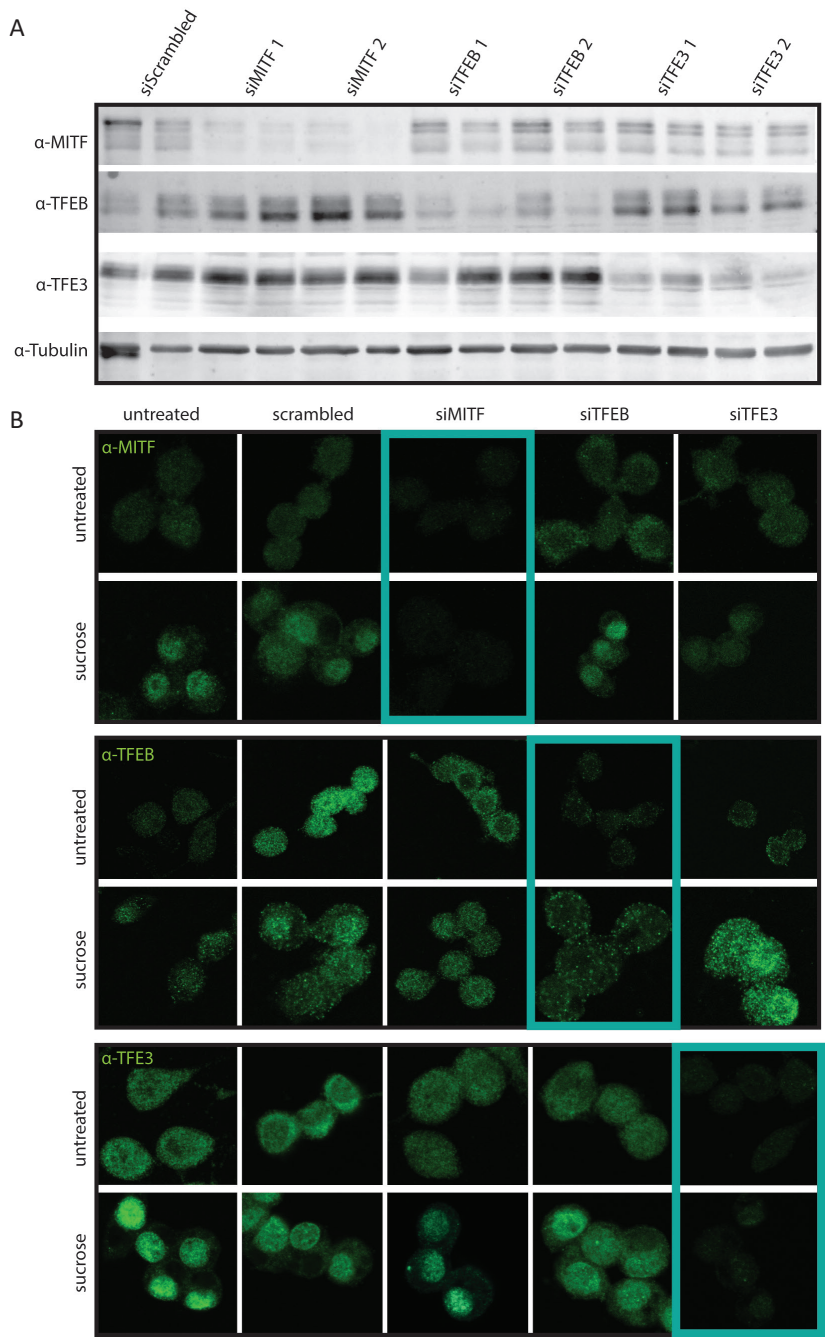
1. Meijer, A. J. & Codogno, P. Autophagy: Regulation and role in disease. *Autophagy, regulation, and disease*. A. J. Meijer and P. Codogno. *Crit. Rev. Clin. Lab. Sci.* **46**, 210–240 (2009).
2. Ballabio, A. & Bonifacio, J. S. Lysosomes as dynamic regulators of cell and organismal homeostasis. *Nat. Rev. Mol. Cell. Biol.* **21**, 101–118 (2020).
3. Steingrímsson, E., Copeland, N. G. & Jenkins, N. A. Melanocytes and the *Microphthalmia* transcription factor network. *Annu. Rev. Genet.* **38**, 365–411 (2004).
4. Sardiello, M., Palmieri, M., Ronza, A. di, Medina, D. L., Valenza, M., *et al.* A gene network regulating lysosomal biogenesis and function. *Science* **325**, 473–477 (2009).
5. Pogenberg, V., Ögmundsdóttir, M. H., Bergsteinsdóttir, K., Schepsky, A., Phung, B., *et al.* Restricted leucine zipper dimerization and specificity of DNA recognition of the melanocyte master regulator MITF. *Genes Dev.* **26**, 2647–2658 (2012).
6. Moore, K. J. Insight into the microphthalmia gene. *Trends Genet.* **11**, 442–448 (1995).
7. Kim, D. H., Sarbassov, D. D., Ali, S. M., King, J. E., Latek, R. R., Erdjument-Bromage, H., Tempst, P. & Sabatini, D. M. mTOR interacts with raptor to form a nutrient-sensitive complex that signals to the cell growth machinery. *Cell* **110**, 163–175 (2002).
8. Düvel, K., Yecies, J. L., Menon, S., Raman, P., Lipovsky, A. I., Souza, A. L., Triantafellow, E., Ma, Q., Gorski, R., Cleaver, S., Vander Heiden, M. G., MacKeigan, J. P., Finan, P. M., Clish, C. B., Murphy, L. O. & Manning, B. D. Activation of a metabolic gene regulatory network downstream of mTOR Complex 1. *Mol. Cell* **39**, 171–183 (2010).
9. Zoncu, R., Bar-Peled, L., Efeyan, A., Wang, S., Sancak, Y. & Sabatini, D. M. mTORC1 senses lysosomal amino acids through an inside-out mechanism that requires the vacuolar H⁺-ATPase. *Science* **334**, 678–683 (2011).
10. Condon, K. J. & Sabatini, D. M. Nutrient regulation of mTORC1 at a glance. *J. Cell Sci.* **132**, (2019).
11. Sancak, Y., Peterson, T. R., Shaul, Y. D., Lindquist, R. A., Thoreen, C. C., Bar-Peled, L. & Sabatini, D. M. The rag GTPases bind raptor and mediate amino acid signaling to mTORC1. *Science* **320**, 1496–1501 (2008).
12. Jin, J., Smith, F. D., Stark, C., Wells, C. D., Fawcett, J. P., Kulkarni, S., Metalnikov, P., O'Donnell, P., Taylor, P., Taylor, L., Zougman, A., Woodgett, J. R., Langeberg, L. K., Scott, J. D. & Pawson, T. Proteomic, functional, and domain-based analysis of in vivo 14-3-3 binding proteins involved in cytoskeletal regulation and cellular organization. *Curr. Biol.* **14**, 1436–1450 (2004).
13. Rocznik-Ferguson, A., Petit, C. S., Froehlich, F., Qian, S., Ky, J., Angarola, B., Walther, T. C. & Ferguson, S. M. The transcription factor TFEB links mTORC1 signaling to transcriptional control of lysosome homeostasis. *Sci. Signal.* **5**, ra42 (2012).
14. Martina, J. A. & Puertollano, R. Rag GTPases mediate amino acid-dependent recruitment of TFEB and MITF to lysosomes. *J. Cell Biol.* **200**, 475–491 (2013).
15. Martina, J. A., Diab, H. I., Brady, O. A. & Puertollano, R. TFEB and TFE3 are novel components of the integrated stress response. *EMBO J.* **35**, 479–495 (2016).
16. Martina, J. A., Chen, Y., Gucsek, M. & Puertollano, R. mTORC1 functions as a transcriptional regulator of autophagy by preventing nuclear transport of TFEB. *Autophagy* **8**, 903–914 (2012).
17. Bronisz, A., Sharma, S. M., Hu, R., Godlewski, J., Tzivion, G., Mansky, K. C. & Ostrowski, M. C. Microphthalmia-associated transcription factor interactions with 14-3-3 modulate differentiation of committed myeloid precursors. *Mol. Biol. Cell* **17**, 3897–3906 (2006).
18. Settembre, C., Di Malta, C., Polito, V. A., Aencibia, M. G., Vetrini, F., Erdin, S., Erdin, S. U., Huynh, T., Medina, D., Colella, P., Sardiello, M., Rubinstein, D. C. & Ballabio, A. TFEB links autophagy to lysosomal biogenesis. *Science* **332**, 1429–1433 (2011).

19. Settembre, C., Zoncu, R., Medina, D. L., Vetrini, F., Erdin, S. S. S., Erdin, S. S. S., Huynh, T., Ferron, M., Karsenty, G., Vellard, M. C., Facchinetti, V., Sabatini, D. M. & Ballabio, A. A lysosome-to-nucleus signalling mechanism senses and regulates the lysosome via mTOR and TFEB. *EMBO J.* **31**, 1095–1108 (2012).
20. Spampinato, C., Feeney, E., Li, L., Cardone, M., Lim, J.-A., Annunziata, F., Zare, H., Polishchuk, R., Puertollano, R., Parenti, G., Ballabio, A. & Raben, N. Transcription factor EB (TFEB) is a new therapeutic target for Pompe disease. *EMBO Mol. Med.* **5**, 691–706 (2013).
21. Song, W., Wang, F., Savini, M., Ake, A., di Ronza, A., Sardiello, M. & Segatori, L. TFEB regulates lysosomal proteostasis. *Hum. Mol. Genet.* **22**, 1994–2009 (2013).
22. Medina, D. L., Fraldi, A., Bouche, V., Annunziata, F., Mansueto, G., Spampinato, C., Puri, C., Pignata, A., Martina, J. A., Sardiello, M., Palmieri, M., Polishchuk, R., Puertollano, R. & Ballabio, A. Transcriptional activation of lysosomal exocytosis promotes cellular clearance. *Dev. Cell* **21**, 421–30 (2011).
23. Folick, A., Oakley, H. D., Yu, Y., Armstrong, E. H., Kumari, M., Sanor, L., Moore, D. D., Ortlund, E. A., Zechner, R. & Wang, M. C. Lysosomal signaling molecules regulate longevity in *Caenorhabditis elegans*. *Science* **347**, 83–86 (2015).
24. Peng, W., Minakaki, G., Nguyen, M. & Krainc, D. Preserving lysosomal function in the aging brain: insights from neurodegeneration. *Neurotherapeutics* **16**, 611–634 (2019).
25. Perera, R. M., Stoykova, S., Nicolay, B. N., Ross, K. N., Fitamant, J., Boukhali, M., Lengrand, J., Deshpande, V., Selig, M. K., Ferrone, C. R., Settlemann, J., Stephanopoulos, G., Dyson, N. J., Zoncu, R., Ramaswamy, S., Haas, W. & Bardeesy, N. Transcriptional control of autophagy–lysosome function drives pancreatic cancer metabolism. *Nature* **524**, 361–365 (2015).
26. Kimmelman, A. C. & White, E. Autophagy and tumor metabolism. *Cell Metabolism* **25**, 1037–1043 (2017).
27. Jaishy, B. & Abel, E. D. Lipotoxicity: Many roads to cell dysfunction and cell death lipids, lysosomes, and autophagy. *J. Lipid Res.* **57**, 1619–1635 (2016).
28. Gilleron, J., Gerdes, J. M. & Zeigerer, A. Metabolic regulation through the endosomal system. *Traffic* **20**, 552–570 (2019).
29. Xu, X., Grijalva, A., Skowronski, A., van Eijk, M., Serlie, M. J. J., Ferrante, A. W. W., van Eijk, M., Serlie, M. J. J. & Ferrante, A. W. W. Obesity activates a program of lysosomal-dependent lipid metabolism in adipose tissue macrophages independently of classic activation. *Cell Metab.* **18**, 816–830 (2013).
30. Gabriel, T. L., Tol, M. J., Ottenhof, R., van Roomen, C., Aten, J., *et al.* Lysosomal stress in obese adipose tissue macrophages contributes to MITF-dependent Gpnmb induction. *Diabetes* **63**, 3310–3323 (2014).
31. Van Der Lienden, M. J. C., Gaspar, P., Boot, R., Aerts, J. M. F. G. & Van Eijk, M. Glycoprotein non-metastatic protein B: An emerging biomarker for lysosomal dysfunction in macrophages. *Int. J. Mol. Sci.* **20** 66 (2019).
32. Wang, Z. V & Scherer, P. E. Adiponectin, the past two decades. *J. Mol. Cell Biol.* **8** 93–100 (2016).
33. Aouadi, M., Tencerova, M., Vangala, P., Yawe, J. C., Nicoloso, S. M., Amano, S. U., Cohen, J. L. & Czech, M. P. Gene silencing in adipose tissue macrophages regulates whole-body metabolism in obese mice. *Proc. Natl. Acad. Sci. USA.* **110**, 8278–8283 (2013).
34. Aouadi, M., Vangala, P., Yawe, J. C., Tencerova, M., Nicoloso, S. M., Cohen, J. L., Shen, Y. & Czech, M. P. Lipid storage by adipose tissue macrophages regulates systemic glucose tolerance. *Am. J. Physiol. - Endocrinol. Metab.* **307**, (2014).
35. Hill, D. A., Lim, H. W., Kim, Y. H., Ho, W. Y., Foong, Y. H., Nelson, V. L., Nguyen, H. C. B., Chegireddy, K., Kim, J., Habberthuer, A., Vallabhajosyula, P., Kambayashi, T., Won, K. J. & Lazar, M. A. Distinct macrophage populations direct inflammatory versus physiological

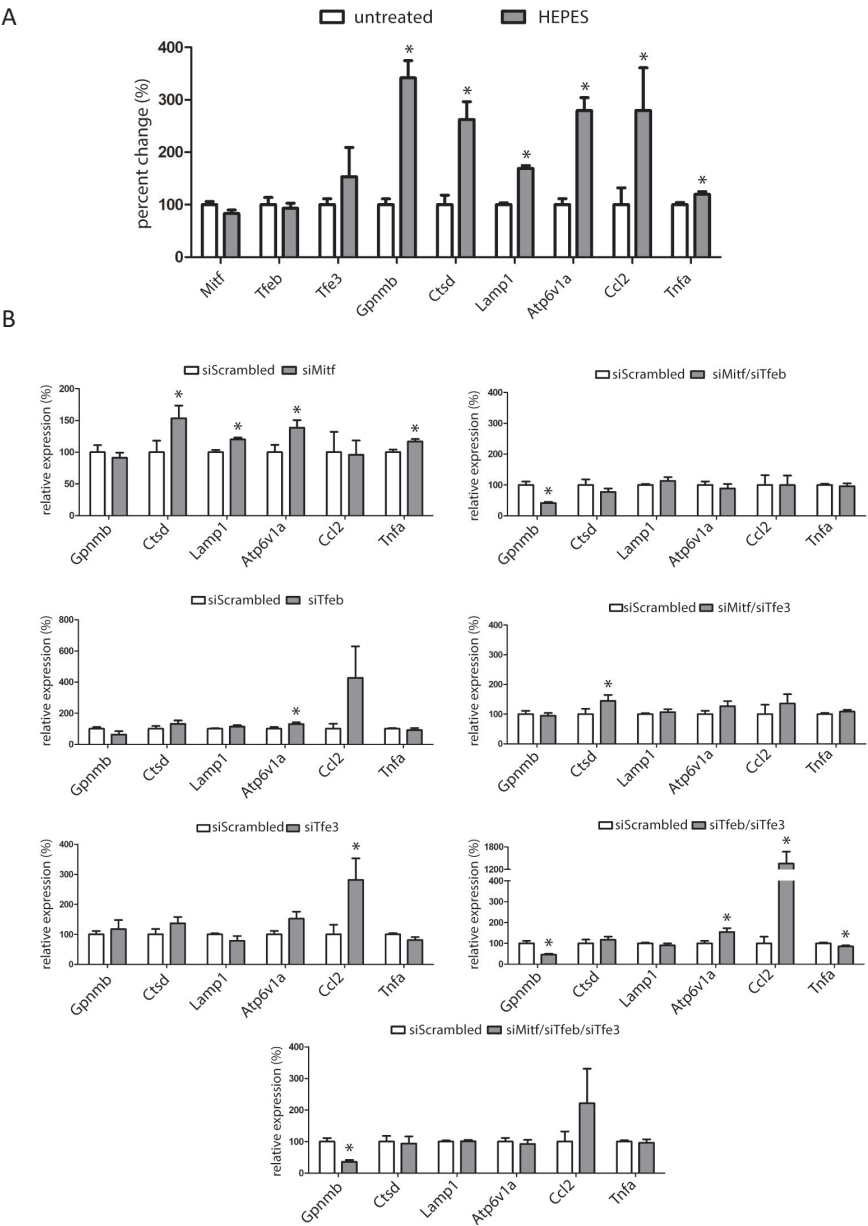
- changes in adipose tissue. *Proc. Natl. Acad. Sci. USA*. **115**, E5096–E5105 (2018).
36. Jaitin, D. A., Adlung, L., Thaïss, C. A., Weiner, A., Li, B., *et al.* Lipid-associated macrophages control metabolic homeostasis in a Trem2-dependent manner. *Cell* **178**, 686–698.e14 (2019).
37. Yasumoto, K. I., Amae, S., Udonon, T., Fuse, N., Takeda, K. & Shibahara, S. A big gene linked to small eyes encodes multiple Mitf isoforms: many promoters make light work. *Pigment Cell Res.* **11** 329–336 (1998).
38. Louphrasitthiphon, P., Siddaway, R., Loffreda, A., Pogenberg, V., Friedrichsen, H., *et al.* Tuning transcription factor availability through acetylation-mediated genomic redistribution. *Mol. Cell* (2020)
39. Martínez-Fábregas, J., Prescott, A., van Kasteren, S., Pedrioli, D. L., McLean, I., Moles, A., Reinheckel, T., Poli, V. & Watts, C. Lysosomal protease deficiency or substrate overload induces an oxidative-stress mediated STAT3-dependent pathway of lysosomal homeostasis. *Nat. Commun.* **9**, 1–16 (2018).
40. Chauhan, S., Goodwin, J. G., Chauhan, S., Manyam, G., Wang, J., Kamat, A. M. & Boyd, D. D. ZKSCAN3 Is a Master Transcriptional Repressor of Autophagy. *Mol. Cell* **50**, 16–28 (2013).
41. Li, Y., Xu, M., Ding, X., Yan, C., Song, Z., *et al.* Protein kinase C controls lysosome biogenesis independently of mTORC1. *Nat. Cell Biol.* **18**, 1065–1077 (2016).
42. Annunziata, I., van de Vlekkert, D., Wolf, E., Finkelstein, D., Neale, G., Machado, E., Mosca, R., Campos, Y., Tillman, H., Roussel, M. F., Andrew Weesner, J., Ellen Fremuth, L., Qiu, X., Han, M. J., Grosveld, G. C. & D'Azzo, A. MYC competes with MiT/TFE in regulating lysosomal biogenesis and autophagy through an epigenetic rheostat. *Nat. Commun.* **10**, 3623 (2019).
43. Pastore, N., Brady, O. A., Diab, H. I., Martina, J. A., Sun, L., Huynh, T., Lim, J.-A., Zare, H., Raben, N., Ballabio, A. & Puertollano, R. TFEB and TFE3 cooperate in the regulation of the innate immune response in activated macrophages. *Autophagy* **12**, 1240–1258 (2016).
44. Prieur, X., Mok, C. Y. L., Velagapudi, V. R., Núñez, V., Fuentes, L., Montaner, D., Ishikawa, K., Camacho, A., Barbarroja, N., O'Rahilly, S., Sethi, J. K., Dopazo, J., Orešič, M., Ricote, M. & Vidal-Puig, A. Differential lipid partitioning between adipocytes and tissue macrophages modulates macrophage lipotoxicity and M2/M1 polarization in obese mice. *Diabetes* **60**, 797–809 (2011).
45. Kratz, M., Coats, B. R., Hisert, K. B., Hagman, D., Mutskov, V., Peris, E., Schoenfelt, K. Q., Kuzma, J. N., Larson, I., Billing, P. S., Landerholm, R. W., Crouthamel, M., Gozal, D., Hwang, S., Singh, P. K. & Becker, L. Metabolic dysfunction drives a mechanistically distinct proinflammatory phenotype in adipose tissue macrophages. *Cell Metab.* **20**, 614–625 (2014).
46. Coats, B. R., Schoenfelt, K. Q., Barbosa-Lorenzi, V. C., Peris, E., Cui, C., Hoffman, A., Zhou, G., Fernandez, S., Zhai, L., Hall, B. A., Haka, A. S., Shah, A. M., Reardon, C. A., Brady, M. J., Rhodes, C. J., Maxfield, F. R. & Becker, L. Metabolically activated adipose tissue macrophages perform detrimental and beneficial functions during diet-induced obesity. *Cell Rep.* **20**, 3149–3161 (2017).
47. Russo, L. & Lumeng, C. N. Properties and functions of adipose tissue macrophages in obesity. *Immunology* **155**, 407–417 (2018).
48. Lee, Y. S., Wollam, J. & Olefsky, J. M. An integrated view of immunometabolism. *Cell* **172**, 22–40 (2018).
49. Stern, J. H., Rutkowski, J. M. & Scherer, P. E. Adiponectin, leptin, and fatty acids in the maintenance of metabolic homeostasis through adipose tissue crosstalk. *Cell Metab.* **23** 770–784 (2016).
50. Tesz, G. J., Aouadi, M., Prot, M., Nicoloso, S. M., Boutet, E., Amano, S. U., Goller, A., Wang, M., Guo, C.-A., Salomon, W. E., Virbasius, J. V., Baum, R. A., O'Connor, M. J., Soto, E.,

Ostroff, G. R. & Czech, M. P. Glucan particles for selective delivery of siRNA to phagocytic cells in mice. *Biochem. J.* **436**, 351–62 (2011).

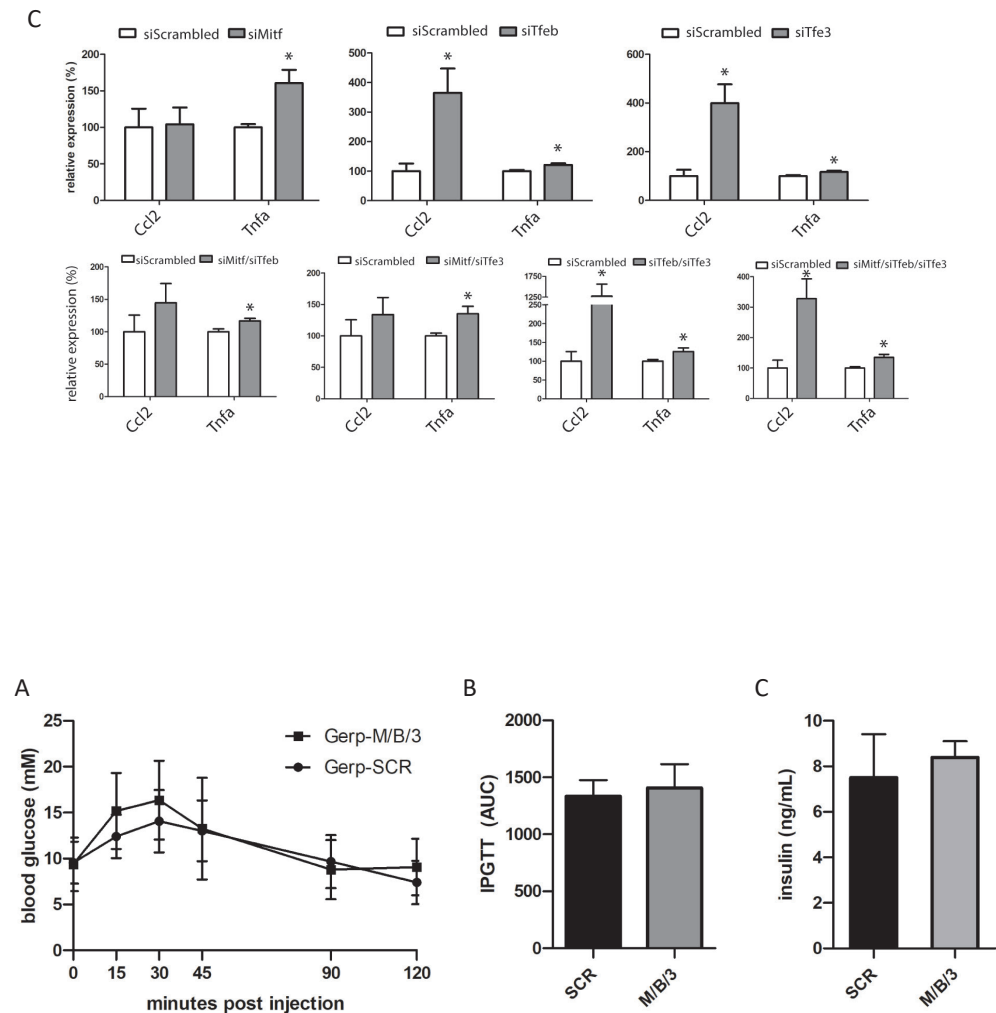
Supplemental Figures



Supplemental figure 1. Validation of siRNA mediated knock down of *Mitf*, *Tfeb* and *Tfe3* on protein level; (A) Verification of specificity target genes by two oligonucleotide sequences per gene. (B) Immunocytochemical validation of subcellular localization and intensity *Mit*/*TFE* members upon single knock down of either *Mitf*, *Tfeb* or *Tfe3*.



Supplemental figure 2. Gene expression analysis of lysosome related genes upon (A) HEPES addition to medium, (B) combinatorial knock down of Mitf, Tfeb and Tfe3 under (non-stressed) basal conditions; (C; Next page ->) inflammatory gene expression analysis during combinatorial knock down of Mitf, Tfeb and Tfe3 and (non-stressed) basal conditions



Supplemental figure 3. Metabolic parameters of mice at start of experiment; (A) Time curve of Intraperitoneal glucose tolerance test (IPGTT) of scrambled siRNA-Gerp and siMitf/TFE-Gerp treated group; **(B)** Area under the curve (AUC) of IPGTT; **(C)** Blood insulin levels

Chapter 7

Discussion and summary

Discussion

Historical and renewed interest in lysosomes

Since the seminal studies by De Duve and co-workers in the late fifties, cells are known to contain 100-200 distinct membrane enclosed acid compartments that are named lysosomes ('bodies of cleavage').¹ These organelles are responsible for fragmentation of intra- and extracellular macromolecules that enter lysosomes via endocytosis, macropinocytosis or autophagy. Fragmentation relies on the catalytic action of hydrolases that are assisted by accessory proteins and low luminal pH. The surrounding membrane of lysosomes is equipped with transporters that assist in export of degradation products, ion-channels and the v-ATPase that maintains the acid pH at the expense of ATP.² The interest in lysosomes was boosted in the sixties by the identification of genetic disorders that result in deficiencies in lysosomal hydrolases or supporting proteins.^{3,4} Since in most of these disorders the substrate of the deficient enzyme accumulates, inherited lysosomal deficiencies became collectively named as lysosomal storage diseases (LSDs). Presently, over 60 LSDs are known and also include genetic defects in non-enzymatic constituents of lysosomes such as transporters, activator proteins and other protein factors.⁵ In the case of inherited lysosomal enzymopathies, the corresponding enzymes were purified and characterized in the eighties and for most of these LSDs, the deficient gene has meanwhile been cloned. These developments revolutionized laboratory diagnosis and initiated research on therapies for lysosomal enzymopathies. Instrumental in this regard was the gained knowledge of biosynthesis, intracellular sorting and lectin-mediated uptake of lysosomal enzymes.⁶ From the late seventies onwards, attempts were made to treat lysosomal enzymopathies by administration of the lacking hydrolase: the breakthrough was enzyme replacement therapy (ERT) for type 1 Gaucher disease through chronic infusions with a mannose-terminated glucocerebrosidase ensuring lectin-receptor uptake by tissue macrophages.⁷ Such ERT was soon copied for other lysosomal enzyme deficiencies like Fabry disease and Pompe disease, albeit with limited clinical success. In the last two decades alternative therapies for some LSDs have been designed based on small compound drugs, e.g. substrate reduction therapy (SRT) and enzyme stabilizing chaperone therapies.^{8,9} At present, vast effort is paid to a variety of gene therapy approaches employing viral vectors (conventional gene therapies, RNA therapies and siRNA therapies).^{10,11} Interest in the cellular role of lysosomes was boosted by the appreciation of a key role for autophagy in maintenance of cell integrity, culminating in the Nobel prize that was recently awarded to Yoshio Oshumi.¹² In this millennium lysosome research got further, major momentum by the realization that the organelles not merely play a role in macromolecule fragmentation but are actively involved in the regulation of key cellular processes.¹³ It was discovered that two key regulatory kinases in cells, mTORC1 (master regulator of cell growth and metabolism mechanistic target of rapamycin [serine/threonine kinase] complex 1) and AMPK (AMP-activated protein kinase), can be associated with the surface of lysosomes and as such link metabolite supply from lysosomes with processes like cell growth and metabolism.¹³ Moreover, it has become apparent that mTORC1 regulates the activity of transcription factors of the MiT/TFE (microphthalmia-transcription factor E) family, a group of transcription factors that promote the expression of genes encoding lysosomal proteins and autophagy

components.¹⁴ In this way, supply of metabolites from lysosomes is intricately linked to *de novo* formation of lysosomes, autophagy and endocytosis. Knowledge on membrane proteins of lysosomes has been lagging for some time, but their composition on the lysosomal membrane surface and their functions is increasingly elucidated.^{15,16} Similarly, regulation of the membrane content of cells has been limitedly understood, but again crucially involves lysosomes. Turnover of membranes in cells takes place in lysosomes following formation of multi-vesicular bodies generated in endosomes as well through delivery via autophagy. By means of fission and fusion, lysosomes and endosomes dynamically interact with each other, as well as with the plasma membrane through endocytosis and phagocytosis. More recently, the relevance of exocytosis of lysosomes has begun to be appreciated.¹⁷ In specialized cells, lysosomes fulfil specific functions, attracting further attention of researchers. Examples of this are immune cells that phagocytose pathogens, antigens, senescent and apoptotic cells as well as osteoclasts involved in bone remodelling. In view of their amazingly broad functions lysosomes presently receive interest in various fields such as inherited and acquired metabolic disorders, infectious diseases, neurodegenerative diseases, cancer, and ageing.^{18–20}

This thesis aims to elucidate several aspects of lysosomes and their outcome is here further discussed.

Chapters 1 and 2 deal with perturbation of **lysosome function in general and that of lysosomal enzymes in cultured cells**. Cultured cells, and fibroblasts in particular, have been amply used as the biochemical confirmation of diagnosis of LSDs. In addition, they have been employed as models to study the biosynthesis, intracellular transport and uptake of lysosomal enzymes. The importance of the acidic lysosomal pH has also been elucidated by use of cultured cells. Lysosomotropic weak bases such as methylamine and chloroquine were used to increase endosomal and lysosomal pH and thus disrupt lysosomal processes in cultured cells. The mannose-6-phosphate receptor mediated sorting of newly formed lysosomal enzymes relies on low pH for the release of enzyme ligands from the receptors. Consequently, the presence of lysosomotropic weak bases in the cell culture medium also interferes with delivery of acid hydrolases to lysosomes.^{21,22} The effects of lysosomotropic bases illustrate that lysosomes of cultured cells can be markedly influenced by the culture medium composition.

Chapter 1 addresses the **impact of the presence of the zwitterionic buffer HEPES in cell culture medium on cultured cells**, nowadays a popular addition to stabilize medium pH. HEPES as buffer in biological systems was originally described by Good and co-workers. It was found to exert little effect on isolated mitochondria and purified bacterial enzymes.²³ Later studies reported no toxic effects of the presence of HEPES in cell culture medium and even noted an increase in growth rate as compared to bicarbonate supplemented medium.²⁴ However, as described in chapter 1, the presence of HEPES (25 mM) in culture medium does significantly influence lysosomes of cells. Since HEPES is a potent buffer with a pKa of 7.4, chronic exposure of cells to HEPES likely results in elevated lysosomal pH which impairs lysosomal function. A similar phenomenon is triggered by chloroquine and the v-ATPase inhibitor bafilomycin. Increased lysosomal pH is well known to reduce the activity of numerous lysosomal hydrolases and thus disturb

metabolic fluxes in cells.²⁵ In addition, membrane flow in the endolysosomal apparatus is impaired by pH changes induced by permeable weak bases and various low pH-dependent receptor-mediated endocytic mechanisms are reduced at such conditions.²⁶ It has been recently reported that perturbed lysosomal pH induces a rescue mechanism in which interaction of the STAT3 (Signal transducer and activator of transcription 3) protein with the ATP6V1A subunit of the lysosomal v-ATPase promotes reduction of lysosomal pH. Acidification of the cytosol or alkalinization of the lysosomal lumen triggers STAT3 to the lysosome, at the expense of STAT3-mediated transcription.²⁷

Exposure of cells to HEPES induces the translocation of MiT/TFE transcription factors, in turn promoting lysosome biogenesis and autophagy. This response likely constitutes an attempt to restore the catabolic flux in cells with impaired lysosomes. Remarkable is the finding that the MiT/TFE translocation upon HEPES stimulation proceeds independently of mTORC1, as phosphorylation of its prime substrates remained unaltered in HEPES exposed cells.²⁸ It therefore poses a paradox with respect to mTORC1 as a master regulator of anabolism.^{13,29,30} Indeed, MiT/TFE members are reported to be activated by several other proteins, including PKC, PKD, GSK3 β and phosphatases, and further research on cell specificity and redundancy of these pathways in regulating MiT/TFE members is required.^{31–35}

Chapter 2 illustrates how the **lysosomal enzyme glucocerebrosidase (GCase) acts as sensitive indicator for disturbances in lysosomes induced by the presence of HEPES in the culture medium**. GCase fundamentally differs from other soluble lysosomal hydrolases: it is not sorted to lysosomes via mannose-6-phosphate receptors, but it binds to the membrane protein LIMP2 in the endoplasmic reticulum soon after folding. As complex, LIMP2 and GCase are sorted to lysosomes where low local pH triggers dissociation. GCase is a glycoprotein containing 4 N-linked glycans that are largely converted in the Golgi apparatus from high mannose-structures to sialylated complex-type ones. These modifications are reflected by an increase in molecular weight of 62 kDa (ER) to 66 kDa (trans-Golgi). Upon delivery into the lysosome, exoglycosidases gradually trim the glycans of GCase resulting in stepwise formation of a 'mature' 58 kDa form of the enzyme. As such, the precise glycan composition of GCase does not influence its enzymatic activity.³⁶ Inside the lysosome, GCase is also subjected to proteolytic breakdown that is inhibitable by leupeptin. Exposing cultured cells to HEPES markedly reduces the maturation of 66 kDa GCase and its proteolytic degradation: accumulation of 66 kDa enzyme in less dense organelles occurs under these conditions. This is likely caused by a disturbed intralysosomal milieu that inhibits glycosidases and proteases. Since GCase turnover in lysosomes is relatively fast, a reduction in its intralysosomal degradation as induced by HEPES leads to a marked increase in cellular content on active enzyme molecules. This can be visualized with selective activity-based probes for GCase (see section below) and the measurement of enzyme activity in cell lysates. In other words, cells cultured in the presence of HEPES tend to show higher cellular GCase levels than when grown without buffer in the culture medium. This phenomenon is relevant for the enzymatic diagnosis of Gaucher disease with cultured cells as source of enzyme. A negative impact of the presence of HEPES in the culture medium is also observed for other lysosomal hydrolases such as acid alpha-glucosidase and beta-glucuronidase. This highlights that caution is warranted when interpreting data on lysosomes of cells that

are cultured in the presence of HEPES. Recently, GCase specific substrates have become available that can measure enzyme activity inside lysosomes of cultured living cells, providing alternative ways to measure GCase activity.³⁷

Besides accumulating protons, lysosomes also act as store for Ca^{2+} ions. Lysosomal Ca^{2+} concentration can be as high as 0.5 mM. Released Ca^{2+} from lysosomes is postulated to act as second messenger that activates calcium dependent cellular processes.^{38–40} TRPML1 (Mucolipin TRP channel 1) mediated calcium efflux from lysosomes has been linked to activation of the phosphatase calcineurin and subsequent dephosphorylation of TFEB (transcription factor EB).⁴¹ It is presently unknown whether the presence of HEPES in the culture medium impacts on lysosomal Ca^{2+} concentration besides H^+ concentration, and whether lysosomal Ca^{2+} release contributes to mTORC1-independent activation of MiT/TFE transcription factors. Lysosomal calcium is also crucially involved in the fusion of lysosomes with other organelles, as well as in lysosome exocytosis. SNAREs (Soluble N-ethylmaleimide-sensitive factor attachment protein receptors) form a parallel four-helix bundle called a *trans*-SNARE complex in a Ca^{2+} -dependent manner. This facilitates the merger of opposing membranes and exchange of content.⁴²

Chapter 3 focusses attention to the **composition of individual lysosomes in cells**. It has become clear that cellular lysosomes (>100) are heterogeneous of nature. Individual lysosomes in cells move inward (retrograde; towards the microtubule-organizing center (MTOC)) and outward (anterograde) along microtubules, assisted by adaptor proteins (dynein and kinesin, respectively).⁴³ The perinuclear lysosomes are found to be on average more acid and catabolically active than the peripheral located organelles.⁴⁴ During nutrient excess, anterograde outward movement is more frequent, whilst during nutrient shortage retrograde inward transport is more prominent. It is presently unknown whether the hydrolase composition of all lysosomes is similar. The recent design of cyclophellitol-based activity probes (ABPs) for various retaining glycosidases has led to tools allowing selective labelling of alpha- and beta-glucosidase, alpha- and beta-mannosidases, alpha- and beta-galactosidases, beta-glucuronidase, alpha-iduronidase and alpha-fucosidase.⁴⁵ Fluorophore-tagged ABPs allow labelling of corresponding active glycosidases and an unprecedented visualization of them in living cells. Chapter 3 describes the fluorescent labelling of active GCase molecules in intact fibroblasts. Correlative light and electron microscopy (CLEM) allows visualization of labelled GCase molecules in individual electron dense lysosomes. Labelling therapeutic enzyme with a different fluorophore-tagged ABP allows simultaneous detection of endogenous GCase and exogenous enzyme in mannose-receptor expressing cells exposed to the therapeutic agent. The study revealed that the majority of individual lysosomes was supplemented with therapeutic enzyme. The finding provides an explanation for the clinical success of enzyme replacement therapy of Gaucher disease and suggests the exchange of content among lysosomes. The CLEM technology could in principle employed to visualize multiple lysosomal glycosidases for the study of uniformity of lysosomes in cells exposed to various conditions (e.g. nutrients, hormones, lysosomotropic agents, hydrolase inhibitors). Another future application for ABPs is labelling of therapeutic recombinant enzyme with suitable tagged probes, followed by infusion and subsequent monitoring of tissue distribution with non-invasive scanning techniques, for example by PET-SCAN.⁴⁶

Chapters 4 and 5 are studies on **storage cells encountered in LSDs**. In many LSDs, tissue macrophages transform into storage cells. The particular vulnerability of these cells is not surprising given their role in ongoing phagocytosis and endocytosis of senescent and apoptotic cells as well as lipoproteins. These pathways imply high rates of lysosomal degradation of substrates and handling of products. Particularly in sphingolipid storage disorders the presence of lipid-laden macrophages is very prominent: examples of this are Gaucher cells in Gaucher disease (glucocerebrosidase deficiency) and Pick cells in Niemann-Pick diseases types A and B (acid sphingomyelinase deficiency). Factors that are produced by storage cells and released into the circulation have been actively searched for since these may be employed to assist diagnosis, to monitor progression of disease and to capture corrections by therapeutic interventions. At the forefront in this respect has been the detection of biomarkers for Gaucher disease, i.e. factors released by the glucosylceramide-laden macrophages. It was discovered that these Gaucher cells produce and secrete high quantities of the chitinase chitotriosidase and the chemokine CCL18, leading to strikingly elevated plasma levels in symptomatic patients, on average 1000-fold and 40-fold respectively.⁴⁵ Increased plasma levels of chitotriosidase are encountered in various LSDs, illustrating the common involvement of macrophages in storage accumulation in these disorders.⁴⁷ In many centres world-wide, plasma chitotriosidase measurement is nowadays employed as a first screen for the potential existence of a lysosomal storage disorder in a suspected individual.

Chapter 4 reviews the knowledge on **glycoprotein non metastatic protein B (GPNMB)**, a more recently identified marker for lysosomal dysfunction. GPNMB is a 110 kDa membrane protein that is selectively expressed, most prominently in melanocytes and in phagocytes subjected to lysosomal stressors.⁴⁸ GPNMB is excessively produced by Gaucher cells in spleen of GD patients, and remarkably also by RAW264.6 cells exposed to HEPES, a relative mild stressor of lysosomes. The protein has been reported to co-localize with phagosomes and lysosomes.⁴⁹ A soluble fragment of GPNMB is released by Gaucher cells, most likely via cleavage by ADAM10.^{50,51} The mechanism of active GPNMB shedding explains the more than tenfold elevated plasma levels encountered in symptomatic GD patients. The precise function of GPNMB and its soluble fragment in context of lysosome perturbation has still not been established.⁴⁸ It is presently thought that induction of GPNMB expression occurs in response to lysosomal storage, in particular through stress by excessive lipids. Consistent with this is the increased expression of GPNMB in lipid-laden macrophages of GD patients and in macrophages of patients and mice with Niemann Pick disease type C (NPC) showing lysosomal accumulation of sphingolipids and cholesterol resulting from impaired export of the sterol.^{52–54} In addition, elevated GPNMB has also been observed in acquired metabolic disorders characterized by lipid-stressed macrophages such as atherosclerosis and obesity.^{54,55} Finally, microglia, the resident brain macrophages, can also excessively produce GPNMB as was discovered in multiple sclerosis and neuronopathic Gaucher mice.^{56,57} It is presently unclear whether the upregulation of GPNMB serves some protection for stressed lysosomes. GPNMB has been described to mediate LC-3 dependent phagocytosis in macrophages, a process that utilizes aspects of the autophagy machinery.⁴⁹ Possibly, the increased intracellular GPNMB following perturbation of lysosomes reflects adaptations in the endolysosomal apparatus. GPNMB expression is known to be controlled by MITF, a member of the MiT/TFE transcription

factor family, further hinting to a role in the endolysosomal apparatus.^{54,58} In fact, the physiological relevance of the marked upregulation of chitotriosidase and CCL18 in Gaucher cells is neither identified yet.

Based on amino acid homology, GPNMB has been earlier proposed to contain a lectin-binding domain with some affinity to galactose structures.⁵⁹ Of interest, a genuine galactose-lectin, galectin 3, is also found to be modestly increased in GD patients, NPC mice, and individuals suffering from obesity, atherosclerosis, α -synucleinopathies, atherosclerosis and obesity.^{60–63} Galectin-3 has been shown to be involved in repair of lysosomal membrane permeabilization.^{64,65} In addition, it has been associated with membrane repair involving autophagy.^{65,66} Extracellular galectin-3 has been proposed to play a role in intercellular communication and was found to be associated with insulin resistance during obesity.⁶¹

Adaptations to lysosomal defects is characterized in *chapter 5*, which focusses on the liver of mice that are deficient in the cholesterol efflux transporter Niemann-Pick type C1 (NPC1^{-/-}). In certain LSDs, it has become apparent that a blockade in lysosomal catabolism due to an impaired hydrolase results in alternative metabolism. An example of this is offered by Gaucher disease. The deficiency of GCase causes lysosomal accumulation of glucosylceramide (GlcCer), but part of the lipid is converted by acid ceramidase to glucosylsphingosine (GlcSph).⁶⁷ The latter lipid is water-soluble and may leave lysosomes, cells and even the body via bile and urine. Similarly, alternative lysosomal deacylation of accumulating glycolipids occurs in other LSDs, e.g. formation of lysoGb3 (globotriaosylsphingosine in Fabry disease) and galactosylsphingosine in Krabbe disease.⁴⁵ Elevated deacylated sphingolipids (lyso-sphingolipids) are considered to be toxic. For example GlcSph has been proposed to induce osteopenia, α -synuclein aggregation, gammopathy and related multiple myeloma and to activate the complement cascade.⁴⁵ Likewise, lysoGb3 has been proposed to contribute to podocyturia, fibrosis and loss of nociceptive neurons in Fabry disease patients.⁴⁵ Finally, excessive galactosylsphingosine (originally named psychosine) in neurodegenerative Krabbe disease is thought to be neurotoxic.⁴⁵

An additional consequence of lysosomal enzyme deficiency can be the redistribution of substrate and altered destination of products. For example, the activity of the cytosol-facing GCase homologue glucosylceramidase (GBA2) is increased in GCase-deficient cells, along with extralysosomal GlcCer degradation and a concomitant formation of glucosylated cholesterol (GlcChol) via so-called transglucosylation.⁶⁸ A particularly intriguing LSD in this respect is NPC, which manifests with a primary lysosomal cholesterol accumulation but is accompanied by secondary accumulation of sphingomyelin and GlcCer. In addition, NPC patients show elevated levels of GlcChol that is formed by the transfer of the glucose moiety from GlcCer to cholesterol in lysosomes by GCase.⁶⁸ The modestly elevated GlcSph in NPC deficient patients and mice is likely caused by increased deacylation of excessive GlcCer, as in GD.⁶⁹

In *chapter 5*, the status of GCase was investigated in livers of mice lacking NPC1 protein. In the studied NPC livers, the most prominent pathological hallmark was the acquisition of characteristic lipid-laden storage macrophages. However, an altered ultrastructural appearance was also observed for hepatocytes. In total liver of NPC mice, a reduced enzyme activity as well GCase protein content was observed. In contrast, GBA2 levels tended to be

inversely correlated to GCase deficiency. There was variation among individual mice in the extent of the effect, but the changes in GCase and GBA2 levels were always reciprocal. Next, immunohistochemistry was used to study lysosomes in hepatocytes and Kupffer cells (resident macrophages) of 80 weeks old murine NPC liver. The investigation pointed to fundamentally distinct adaptations in hepatocytes compared to Kupffer cells. Increased levels of GPNMB, galectin-3 and the lysosomal protease cathepsin D were observed in the Kupffer cells, but not hepatocytes. In striking contrast, the hepatocytes in the NPC1-deficient liver showed a marked increase in LIMP2, a phenomenon not observed for the lipid-laden Kupffer cells. Recently it has been recognized by crystallography that LIMP2, the transporter of newly formed GCase to lysosomes, harbours a channel structure. Given structural similarity of LIMP2 with CD36, it is presently proposed that LIMP2 might act as a transporter for cholesterol.⁷⁰ Indeed, it has been observed that LIMP2 might assist export of cholesterol from lysosomes, as indicated by the finding that a double deficiency in NPC1 and LIMP2 results in a more prominent SREBP2-driven induction of HMGCoA reductase transcription, a classic readout for impaired cholesterol efflux from lysosomes.⁷¹ Based on these findings it seems conceivable that LIMP2 may facilitate transport of cholesterol from the lysosome when the regular NPC1-mediated pathway is absent. In theory, it cannot be excluded that LIMP2 might act as transporter of GlcChol. Depending on metabolite concentrations, GCase is known to be able to either catabolize GlcChol to glucose and cholesterol or to generate GlcChol from GlcCer and cholesterol. Moreover, the catalytic pocket of GCase bound to LIMP2 is relatively close to the presumed cholesterol channel of LIMP2. Of further note, NPC patients are presently treated with Miglustat (N-butyldeoxynojirimycin), a potent inhibitor of GBA2, the primary enzyme forming GlcChol in cells. The relevance of this with respect to export of cholesterol (or GlcChol) from lysosomes via LIMP2 is not established.

The location of LIMP2 in hepatocytes tends to be largely confined to the peribiliary region of the cytosol suggesting overlap with previously described location of lysosomes.^{72,73} Since lysosomes may excrete cargo into bile by exocytosis, we consider the possibility that the increased abundance of LIMP2 in NPC hepatocytes tells tales compensatory facilitation of cholesterol export into bile canaliculae.⁷⁴ In absence of NPC1, hepatocytes may thus be protected from cholesterol excess by LIMP2 upregulation.

Presently, NPC receives attention from many different research fields: researchers with an interest in cellular cholesterol homeostasis, investigators of lysosomal storage disorders and neuroscientists with an interest in degenerative conditions such as Alzheimer's disease.⁷⁵⁻⁷⁷ This illustrates the enormous cellular and physiological implications of a relatively simple monogenetic defect involving lysosomes.

Chapter 6 deals with the role of MiT/TFE transcription factors in lysosomal biogenesis in macrophages residing in adipose tissue of obese mice. The MiT/TFE subfamily of basic helix-loop-helix (bHLH) transcription factors consists of TFEB, TFE3 (transcription factor 3), MITF (melanogenesis associated transcription factor) and TFEC (transcription factor EC).⁷⁸ TFEB was the first to be identified as binding to a common sequence upstream of lysosomal genes, the so called Coordinated Lysosomal Expression and Regulation (CLEAR) element.⁷⁹ TFEB and TFE3 are ubiquitously expressed, whereas MITF is largely restricted to pigmented cells such as melanocytes and retinal epithelium cells, as well as myeloid cells of the immune system, osteoclasts, and stem cells of the hair

follicle.^{78,80} TFEC has been shown to be strictly expressed in macrophages.⁸¹ TFEB, TFE3 and MITF undergo phosphorylation by mTORC1, the master regulator of cell growth that resides at the cytosolic side of the lysosomal membrane.^{13,82–84} It is still unknown whether TFEC is also modified by mTORC1. Under basal, nutrient rich, conditions, heterodimeric RAG GTPases recruit mTORC1 to the lysosome, thereby facilitating its interaction with the activator protein RHEB (Ras homologue enriched in brain). Active mTORC1 phosphorylates a serine residue (Ser²¹¹) of TFEB that mediates cytosolic retention by 14-3-3 proteins.^{85,86} Likewise, the phosphorylation of a homologous serine (Ser¹⁷³) in MITF governs its cytosolic retention.⁸⁷ Inhibition of mTORC1 results in dephosphorylation of TFEB, MITF and TFE3 and their nuclear localization. Selective inhibition of mTORC1 by Torin 1 and lysosomal amino acid starvation promotes translocation of TFEB to the nucleus.^{79,85,88,89} Stressors of lysosomes such as the undegradable sucrose or lysosomotropic chloroquine induce the nuclear translocation of TFEB, MITF and TFE3.²⁸ During lysosomal deficiencies, increased transcriptional activity of TFEB and other TFs has been observed.^{79,90–93}

Transcriptional activity of MiT/TFE factors is complex. Homodimerization and heterodimerization among the MiT/TF factors have been described.^{78,94} The cell specificity of these TFs and their posttranscriptional (splicing) and posttranslational (phosphorylation, acetylation) processing impacts on transcriptional action.^{85,95,96} In bone marrow derived monocytes, MITF and TFE3 have been reported to be phosphorylated upon M-CSF (macrophage-colony stimulating factor) stimulation via ERK1/2 (extracellular-signal regulated kinase 1/2) / MAPK (mitogen-activated protein kinase).⁹⁷ Of note, phosphorylation of TFEB by ERK2 was found to result in cytosolic retention of TFEB.⁸⁸ Besides ERK1/2, MITF has also been reported to be serine-phosphorylated by the p38 MAPK.^{81,98} Moreover, the PI3K/AKT route has been described as an alternative pathway for activation of MITF in myeloid cells. IL-10 stimulation of dendritic cells causes nuclear translocation of MITF, triggering GPNMB expression through inhibition of PI3K/AKT and subsequent activation of GSK3 β .^{58,99} GSK3 β is thought to phosphorylate MITF on Ser²⁹⁸ and thereby allows MITF to transactivate promoter regions of target genes. Natural substitution of Ser²⁹⁸ in MITF to proline strongly affects binding affinity to consensus DNA target motifs and gives rise to Waardenburg Syndrome type 2, a syndrome characterized by a lack of skin pigmentation.^{99,100} Recently, acetylation has been added to the possible posttranslational modifications of MiT/TFE members. For example, MITF was shown to be subjected to MAPK/p300 dependent acetylation in melanocytes changing binding affinity to DNA-regions.⁹⁶

Other levels of regulation of MiT/TFE mediated transcription have become apparent. Mass spectrometry analysis of the nuclear binding partners of MITF has revealed an extensive interactome.¹⁰¹ Furthermore, recent studies point to a role of chromatin modifications in MiT/TFE mediated lysosomal biogenesis.¹⁰² In addition, HDACs (histone acetylases or deacetylases), particularly HDAC2, facilitate binding of c-Myc to the promoters of genes encoding lysosomal proteins, thus competing their MiT/TFE mediated transcription.¹⁰² Zkscan3 (zinc finger with KRAB and SCAN domains 3) has been proposed to act as a repressor of lysosomal biogenesis, likely by competing MiT/TFE mediated transcription.^{31,103} Thus, the chromatin landscape and other TFs may further regulate MiT/TFE mediated transcription.

The role of MiT/TFE in pathologies characterized by lipid-laden cells such as macrophages remains incompletely understood. Obesity is generally associated with a combination of pathologies (insulin resistance, hypertension, hypercholesterolemia and hypertriglyceridemia) that are classified as the metabolic syndrome.^{104,105} Obese adipose tissue tends to be inflamed and a macrophage orchestrated low-grade inflammation is generally considered to drive insulin resistance in diabetic obese individuals. It is assumed that communication between neighbouring macrophages with adipocytes in obese adipose tissue occurs. On the one hand, macrophages are involved in phagocytic clearance of apoptotic adipocytes, visible as so-called crown-like structures.^{106,107} On the other hand, macrophages respond to factors released by adipocytes, for example adiponectin, a hormone that sensitizes tissues for insulin and alleviates lipotoxicity and inflammation.¹⁰⁸ Xu et al. noted that obese adipose tissue macrophages (ATMs) have a foamy appearance suggesting lysosomal lipid stress.¹⁰⁹ In line with this, GPNMB, a marker for perturbation of lysosomes in macrophages, is dramatically increased in obese mice and, to a lesser extent, in men.^{48,54} In cultured macrophage-like RAW264.7 cells, MITF-mediated GPNMB expression is induced by feeding palmitate and chloroquine.⁵⁴

Given the previous findings regarding MiT/TFE driven induction of the lysosomal apparatus in macrophages upon lysosomal stress, we investigated the role of these transcription factors in macrophages residing in adipose tissue of obese mice. The key objective was to elucidate whether the MiT/TFE mediated response in the phagocytes is beneficial or harmful. To study this, use was made of siRNAs targeting MiT/TFE transcription factors and their selective delivery to macrophages in adipose tissue (ATM) through encapsulation in glucan particles (Gerps).¹¹⁰

First, the siRNAs targeting *Mitf*, *Tfeb* and *Tfe3* were examined regarding efficacy using cultured RAW264.7 cells. Using *Gpnmb* expression as readout, only simultaneous siRNA knockdown of *Mitf*, *Tfeb* and *Tfe3* mRNA resulted in marked reduction of *Gpnmb* mRNA. Next, mice were intraperitoneally treated with Gerps containing a mixture of siRNAs targeting the three MiT/TFE family members or Gerps containing scrambled siRNA2. After two weeks, the animals were sacrificed, and tissues and blood were collected for analyses. No significant reductions were observed in adipose tissue of mice treated with Gerps containing MiT/TFE siRNAs with respect to transcription factor mRNA levels and *Gpnmb* expression. However, there was marked variation among individual mice in both groups (Gerps with MiT/TFE siRNAs and those with scrambled siRNAs). Next, CD11b⁺-cells were isolated and examined, revealing again no significant changes in transcription factor mRNA levels and *Gpnmb* expression. In CD11b⁺-cells from MiT/TFE siRNA treated mice only *Cd9* and *Lpl* mRNA levels were found to be significantly reduced. CD9 is a tetraspanin that is associated with exosomes and is implicated in several biological processes including reproduction.^{111,112} Increased expression of CD9 and LPL mRNA has been found to be accompanied by increased expression of *TREM2* in macrophages (or microglia) cells.^{113,114} In obese adipose tissue *TREM2* positive, lipid laden macrophages have been identified by single-cell sequencing.¹¹³ Obese *Trem2* knock-out mice manifest with dramatically increased adipocyte size and worsening of whole-body metabolism compared to obese wild type mice.¹¹³ Upon administration of MiT/TFE-siRNA Gerps, *Trem2* levels were found to be significantly lower in epididymal white adipose tissue. The finding that *Gpnmb* expression was not prominently reduced in macrophages in adipose

tissue of MiT/TFE-siRNA Gerp treated obese mice is remarkable. Nevertheless, the treatment resulted in reduced glucose clearance in an intraperitoneal glucose tolerance test, suggesting increased insulin resistance. Moreover, the treated mice showed a reduced adiponectin expression in their adipose tissue. The reduction in adiponectin expression in adipose tissue is relevant since this adipokine is known to act as potent insulin sensitizer and protector against lipotoxicity.¹⁰⁸ The mechanism by which MiT/TFE suppression in macrophages effects adipocytes (adiponectin expression) is unknown.

It should be kept in mind that other transcription factors directly, or indirectly (c-Myc), play a major role in regulation of lysosomal biogenesis. Besides the MiT/TFE transcription factors, STAT3 has recently been reported to drive transcription of some lysosomal genes.¹¹⁵ Of note, STAT3 shares a 50 amino acid motif with MITF that binds PIAS3 (protein inhibitor of activated STAT3), suggesting common regulation.^{116,117}

Future questions

The described PhD investigations concerned lysosomes, in particular those in macrophages. Macrophages are well known to be heterogenous and generally two major phenotypes are distinguished: the inflammatory M1-macrophages and the alternatively activated M2-cells.¹¹⁸ It is assumed that lysosomal lipid accumulation promotes the differentiation of macrophages to the M2-phenotype, for example in spleen and liver of Gaucher disease patients and in adipose tissue of obese individuals (described in this thesis).¹¹⁹ A similar M1/M2 distinction is also made for the heterogeneous microglia in the brain.^{114,120} In general, M1-phagocytes are thought to promote pathology due to their inflammatory nature, whereas M2-cells dampen such processes and might exert beneficial roles in whole body metabolism in atherosclerosis and during obesity.^{113,121–123} It will be of interest to establish whether differences exist in lysosomal biogenesis and lysosome composition of M1-macrophages and their M2-counterparts. It has been reported that active mTORC1 promotes inflammatory M1-macrophages, whereas in M2-macrophages, TFEB transcriptional activity is high.^{124,125} In monocytes, MITF was shown to drive GPNMB expression as part of differentiation towards a M2-like, T-cell suppressive, phenotype.⁵⁸ Conceivably, and testable in future research, the M2-phenotype of tissue residing macrophages may be related to MiT/TFE transcription. If so, beneficial M2-macrophage differentiation could be promoted by (modest) lysosomal stress and/or lysosome perturbation.

Storage cells in inherited LSDs have been historically viewed as the major culprits in pathology. However, they might also modulate pathological processes, e.g. by containing toxic metabolites in storage material and through anti-inflammatory action. The occurrence of perturbed lysosomes not only has negative consequences for cells and their surroundings. It may lead to favourable induction of lysosomal biogenesis, promotion of autophagy and synthesis of anti-inflammatory cytokines. In other words, lysosomal accumulation of lipids in macrophages ('storage cells') within a tissue might give rise to various responses, including even beneficial ones. In view of this consideration, correcting the lysosomal storage in lipid-laden macrophages, present in inherited and acquired disorders and increasing with ageing, may render unforeseen outcomes.

References

1. De Duve, C. Lysosomes revisited. *Eur. J. Biochem.* **137**, 391–397 (1983).
2. Kissing, S., Saftig, P. & Haas, A. Vacuolar ATPase in phago(lyso)some biology. *Int. J. Med. Microbiol.* **308**, 58–67 (2018).
3. Neufeld, E. F., Lim, T. W. & Shapiro, L. J. Inherited disorders of lysosomal metabolism. *Annu. Rev. Biochem.* **44**, 357–376 (1975).
4. Hers, H. G. alpha-Glucosidase deficiency in generalized glycogenstorage disease (Pompe's disease). *Biochem. J.* **86**, 11–6 (1963).
5. Platt, F. M., d'Azzo, A., Davidson, B. L., Neufeld, E. F. & Tiffit, C. J. Lysosomal storage diseases. *Nat. Rev. Dis. Prim.* **4**, 27 (2018).
6. Neufeld, E. F. Lessons from genetic disorders of lysosomes. *Harvey Lect.* **75**, 41–60 (1979).
7. Brady, R. O., Murray, G. J. & Barton, N. W. Modifying exogenous glucocerebrosidase for effective replacement therapy in Gaucher disease. *J. Inherit. Metab. Dis.* **17**, 510–519 (1994).
8. Cox, T., Lachmann, R., Hollak, C., Aerts, J., van Weely, S., Hrebíček, M., Platt, F., Butters, T., Dwek, R., Moyses, C., Gow, I., Elstein, D. & Zimran, A. Novel oral treatment of Gaucher's disease with N-butyldeoxynojirimycin (OGT 918) to decrease substrate biosynthesis. *Lancet* **355**, 1481–1485 (2000).
9. Fan, J. Q., Ishii, S., Asano, N. & Suzuki, Y. Accelerated transport and maturation of lysosomal α -galactosidase A in fabry lymphoblasts by an enzyme inhibitor. *Nat. Med.* **5**, 112–115 (1999).
10. Dahl, M., Doyle, A., Olsson, K., Månsson, J. E., Marques, A. R. A., Mirzaian, M., Aerts, J. M., Ehinger, M., Rothe, M., Modlich, U., Schambach, A. & Karlsson, S. Lentiviral gene therapy using cellular promoters cures type 1 gaucher disease in mice. *Mol. Ther.* **23**, 835–844 (2015).
11. Kim, J., Hu, C., El Achkar, C. M., Black, L. E., Douville, J., *et al.* Patient-customized oligonucleotide therapy for a rare genetic disease. *N. Engl. J. Med.* **381**, 1644–1652 (2019).
12. Ohsumi, Y. Historical landmarks of autophagy research. *Cell Res.* **24**, 9–23 (2014).
13. Condon, K. J. & Sabatini, D. M. Nutrient regulation of mTORC1 at a glance. *J. Cell Sci.* **132**, (2019).
14. Napolitano, G. & Ballabio, A. TFEB at a glance. *J. Cell. Sci.* **129**, 2475–2481 (2016).
15. Schröder, B. A., Wrocklage, C., Hasilik, A. & Saftig, P. The proteome of lysosomes. *Proteomics* **10**, 4053–4076 (2010).
16. Schwake, M., Schröder, B. & Saftig, P. Lysosomal membrane proteins and their central role in physiology. *Traffic* **14**, 739–748 (2013).
17. Luzio, J. P., Hackmann, Y., Dieckmann, N. M. G. & Griffiths, G. M. The biogenesis of lysosomes and lysosome-related organelles. *Cold Spring Harb. Perspect. Biol.* **6**, a016840 (2014).
18. Ballabio, A. & Bonifacino, J. S. Lysosomes as dynamic regulators of cell and organismal homeostasis. *Nat. Rev. Mol. Cell Biol.* **21**, 101–118 (2020).
19. Peng, W., Minakaki, G., Nguyen, M. & Krainc, D. Preserving lysosomal function in the aging brain: insights from neurodegeneration. *Neurotherapeutics* **16**, 611–634 (2019).
20. Pattison, C. J. & Korolchuk, V. I. Autophagy: 'self-eating' your way to longevity. In *Subcell. Biochem.* **90**, 25–47 (2018).
21. Brown, W. J., Constantinescu, E. & Farquhar, M. G. Redistribution of mannose-6-phosphate receptors induced by tunicamycin and chloroquine. *J. Cell Biol.* **99**, 320–326 (1984).
22. Brown, W. J., Goodhouse, J. & Farquhar, M. G. Mannose-6-phosphate receptors for lysosomal enzymes cycle between the Golgi complex and endosomes. *J. Cell Biol.* **103**, 1235–1247 (1986).

23. Good, N. E. & Izawa, S. Hydrogen ion buffers. *Methods Enzymol.* **24**, 53–68 (1972).
24. Ferguson, W. J., Braunschweiger, K. I., Braunschweiger, W. R., Smith, J. R., McCormick, J. J., Wasmann, C. C., Jarvis, N. P., Bell, D. H. & Good, N. E. Hydrogen ion buffers for biological research. *Anal. Biochem.* **104**, 300–310 (1980).
25. Klionsky, D. J., Abdelmohsen, K., Abe, A., Abedin, M. J., Abeliovich, H., *et al.* *Guidelines for the use and interpretation of assays for monitoring autophagy (3rd edition)*. **12**, 1–222 (2016).
26. Schneider, Y. -J & Trouet, A. Effect of chloroquine and methylamine on endocytosis of fluorescein-labelled control IgG and of anti-(plasma membrane) IgG by cultured fibroblasts. *Eur. J. Biochem.* **118**, 33–38 (1981).
27. Liu, B., Palmfeldt, J., Lin, L., Colaço, A., Clemmensen, K. K. B. B., Huang, J., Xu, F., Liu, X., Maeda, K., Luo, Y. & Jäättelä, M. STAT3 associates with vacuolar H⁺-ATPase and regulates cytosolic and lysosomal pH. *Cell Res.* **28**, 996–1012 (2018).
28. Tol, M. J., van der Lienden, M. J. C. C., Gabriel, T. L., Hagen, J. J., Scheij, S., *et al.* HEPES activates a MiT/TFE-dependent lysosomal-autophagic gene network in cultured cells: A call for caution. *Autophagy* **14**, 1–13 (2018).
29. Chantranupong, L., Wolfson, R. L. & Sabatini, D. M. Nutrient-sensing mechanisms across evolution. *Cell* vol. 161 67–83 (2015).
30. Menon, S., Dibble, C. C., Talbott, G., Hoxhaj, G., Valvezan, A. J., Takahashi, H., Cantley, L. C. & Manning, B. D. Spatial control of the TSC complex integrates insulin and nutrient regulation of mTORC1 at the lysosome. *Cell* **156**, 771–785 (2014).
31. Li, Y., Xu, M., Ding, X., Yan, C., Song, Z., *et al.* Protein kinase C controls lysosome biogenesis independently of mTORC1. *Nat. Cell Biol.* **18**, 1065–1077 (2016).
32. Najibi, M., Labed, S. A., Visvikis, O. & Irazoqui, J. E. An Evolutionarily Conserved PLC-PKD-TFEB Pathway for Host Defense. *Cell Rep.* **15**, 1728–1742 (2016).
33. Ploper, D., Taelman, V. F., Robert, L., Perez, B. S., Titz, B., Chen, H. W., Graeber, T. G., Von Euw, E., Ribas, A. & De Robertis, E. M. MITF drives endolysosomal biogenesis and potentiates Wnt signaling in melanoma cells. *Proc. Natl. Acad. Sci. USA.* **112**, E420–E429 (2015).
34. Marchand, B., Arsenault, D., Raymond-Fleury, A., Boisvert, F. M. & Boucher, M. J. Glycogen synthase kinase-3 (GSK3) inhibition induces prosurvival autophagic signals in human pancreatic cancer cells. *J. Biol. Chem.* **290**, 5592–5605 (2015).
35. Wang, W., Gao, Q., Yang, M., Zhang, X., Yu, L., Lawas, M., Li, X., Bryant-Genevier, M., Southall, N. T., Marugan, J., Ferrer, M. & Xu, H. Up-regulation of lysosomal TRPML1 channels is essential for lysosomal adaptation to nutrient starvation. *Proc. Natl. Acad. Sci. USA.* **112**, E1373–E1381 (2015).
36. Weely, S. Van, Aerts, J. M. F. G., Leeuwen, M. B., Heikoop, J. C., Donker-Koopman, W. E., *et al.* Function of oligosaccharide modification in glucocerebrosidase, a membrane-associated lysosomal hydrolase. *Eur. J. Biochem.* **191**, 669–677 (1990).
37. Yadav, A. K., Shen, D. L., Shan, X., He, X., Kermode, A. R. & Vocadlo, D. J. Fluorescence-quenched substrates for live cell imaging of human glucocerebrosidase activity. *J. Am. Chem. Soc.* **137**, 1181–1189 (2015).
38. Lloyd-Evans, E., Morgan, A. J., He, X., Smith, D. A., Elliot-Smith, E., Sillence, D. J., Churchill, G. C., Schuchman, E. H., Galione, A. & Platt, F. M. Niemann-Pick disease type C1 is a sphingosine storage disease that causes deregulation of lysosomal calcium. *Nat. Med.* **14**, 1247–1255 (2008).
39. Christensen, K. A., Myers, J. T. & Swanson, J. A. pH-dependent regulation of lysosomal calcium in macrophages. *J. Cell Sci.* **115**, 599–607 (2002).
40. Ronco, V., Potenza, D. M., Denti, F., Vullo, S., Gagliano, G., Tognolina, M., Guerra, G., Pinton, P., Genazzani, A. A., Mapelli, L., Lim, D. & Moccia, F. A novel Ca²⁺-mediated

- cross-talk between endoplasmic reticulum and acidic organelles: Implications for NAADP-dependent Ca²⁺ signalling. *Cell Calcium* **57**, 89–100 (2015).
41. Medina, D. L., Di Paola, S., Peluso, I., Armani, A., De Stefani, D., Venditti, R., Montefusco, S., Scotto-Rosato, A., Prezioso, C., Forrester, A., Settembre, C., Wang, W., Gao, Q., Xu, H., Sandri, M., Rizzuto, R., De Matteis, M. A. & Ballabio, A. Lysosomal calcium signalling regulates autophagy through calcineurin and TFEB. *Nat. Cell Biol.* **17**, 288–299 (2015).
 42. Hesketh, G. G., Wartosch, L., Davis, L. J., Bright, N. A. & Luzio, J. P. The Lysosome and intracellular signalling. *Prog. Mol. Subcell. Biol.* **57** 151–180 (2018).
 43. Cabukusta, B. & Neeffjes, J. Mechanisms of lysosomal positioning and movement. *Traffic* **19**, 761–769 (2018).
 44. Johnson, D. E., Ostrowski, P., Jaumouillé, V. & Grinstein, S. The position of lysosomes within the cell determines their luminal pH. *J. Cell Biol.* **212**, 677–692 (2016).
 45. Aerts, J. M. F. G., Kuo, C. L., Lelieveld, L. T., Boer, D. E. C., van der Lienden, M. J. C., Overkleeft, H. S. & Artola, M. Glycosphingolipids and lysosomal storage disorders as illustrated by gaucher disease. *Curr. Opin. Chem. Biol.* **53** 204–215 (2019).
 46. McCarter, J. D., Adam, M. J. & Withers, S. G. Syntheses, radiolabelling, and kinetic evaluation of 2-deoxy-2-fluoro-2-iodo-d-hexoses for medical imaging. *Carbohydr. Res.* **266**, 273–277 (1995).
 47. Guo, Y., He, W., Boer, A. M., Wevers, R. A., de Bruijn, A. M., Groener, J. E. M., Hollak, C. E. M., Aerts, J. M. F. G., Galjaard, H. & van Diggelen, O. P. Elevated plasma chitotriosidase activity in various lysosomal storage disorders. *J. Inherit. Metab. Dis.* **18**, 717–722 (1995).
 48. Van Der Lienden, M. J. C., Gaspar, P., Boot, R., Aerts, J. M. F. G. & Van Eijk, M. Glycoprotein non-metastatic protein B: An emerging biomarker for lysosomal dysfunction in macrophages. *Int. J. Mol. Sci.* **20**, 66 (2019).
 49. Li, B., Castano, A. P., Hudson, T. E., Nowlin, B. T., Lin, S.-L., Bonventre, J. V., Swanson, K. D. & Duffield, J. S. The melanoma-associated transmembrane glycoprotein Gpnmb controls trafficking of cellular debris for degradation and is essential for tissue repair. *FASEB J.* **24**, 4767–4781 (2010).
 50. Rose, A. A. N., Annis, M. G., Dong, Z., Pepin, F., Hallett, M., Park, M. & Siegel, P. M. ADAM10 releases a soluble form of the GPNMB/Osteoactivin extracellular domain with angiogenic properties. *PLoS One* **5**, e12093 (2010).
 51. Hoashi, T., Sato, S., Yamaguchi, Y., Passeron, T., Tamaki, K. & Hearing, V. J. Glycoprotein nonmetastatic melanoma protein b, a melanocytic cell marker, is a melanosome-specific and proteolytically released protein. *FASEB J.* **24**, 1616–1629 (2010).
 52. Kramer, G., Wegdam, W., Donker-Koopman, W., Ottenhoff, R., Gaspar, P., Verhoek, M., Nelson, J., Gabriel, T., Kallemeijn, W., Boot, R. G., Laman, J. D., Vissers, J. P. C., Cox, T., Pavlova, E., Moran, M. T., Aerts, J. M. & van Eijk, M. Elevation of glycoprotein nonmetastatic melanoma protein B in type 1 Gaucher disease patients and mouse models. *FEBS Open Bio.* **6**, 902–913 (2016).
 53. Marques, A. R. A., Gabriel, T. L., Aten, J., Van Roomen, C. P. A. A., Ottenhoff, R., Claessen, N., Alfonso, P., Irún, P., Giraldo, P., Aerts, J. M. F. G. & Van Eijk, M. Gpnmb is a potential marker for the visceral pathology in Niemann-Pick type C disease. *PLoS One* **11**, e0147208 (2016).
 54. Gabriel, T. L., Tol, M. J., Ottenhof, R., van Roomen, C., Aten, J., *et al.* Lysosomal stress in obese adipose tissue macrophages contributes to MITF-dependent Gpnmb induction. *Diabetes* **63**, 3310–3323 (2014).
 55. Xu, J., Jüllig, M., Middleditch, M. J. & Cooper, G. J. S. Modelling atherosclerosis by proteomics: Molecular changes in the ascending aortas of cholesterol-fed rabbits. *Atherosclerosis* **242**, 268–76 (2015).
 56. Hendrickx, D. A. E., van Scheppingen, J., van der Poel, M., Bossers, K., Schuurman, K. G., van Eden, C. G., Hol, E. M., Hamann, J. & Huitinga, I. Gene expression profiling of multiple

- sclerosis pathology identifies early patterns of demyelination surrounding chronic active lesions. *Front. Immunol.* **8**, 1810 (2017).
57. Zigdon, H., Savidor, A., Levin, Y., Meshcheriakova, A., Schiffmann, R. & Futerman, A. H. Identification of a biomarker in cerebrospinal fluid for neuronopathic forms of Gaucher disease. *PLoS One* **10**, e0120194 (2015).
 58. Gutknecht, M., Geiger, J., Joas, S., Dörfel, D., Salih, H. R., Müller, M. R., Grünebach, F. & Rittig, S. M. The transcription factor MITF is a critical regulator of GPNMB expression in dendritic cells. *Cell Commun. Signal.* **13**, 19 (2015).
 59. Chung, J.-S., Yudate, T., Tomihari, M., Akiyoshi, H., Cruz, P. D. & Ariizumi, K. Binding of DC-HIL to dermatophytic fungi induces tyrosine phosphorylation and potentiates antigen presenting cell function. *J. Immunol.* **183**, 5190–5198 (2009).
 60. Cluzeau, C. V. M., Watkins-Chow, D. E., Fu, R., Borate, B., Yanjanin, N., Dail, M. K., Davidson, C. D., Walkley, S. U., Ory, D. S., Wassif, C. A., Pavan, W. J. & Porter, F. D. Microarray expression analysis and identification of serum biomarkers for Niemann–Pick disease, type C1. *Hum. Mol. Genet.* **21**, 3632–3646 (2012).
 61. Li, P., Liu, S., Lu, M., Bandyopadhyay, G., Oh, D., *et al.* Hematopoietic-derived galectin-3 causes cellular and systemic insulin resistance. *Cell* **167**, 973–984.e12 (2016).
 62. Nachtigal, M., Al-Assaad, Z., Mayer, E. P., Kim, K. & Monsigny, M. Galectin-3 expression in human atherosclerotic lesions. *Am. J. Pathol.* **152**, 1199–208 (1998).
 63. Jiang, P., Gan, M., Yen, S.-H., Mclean, P. J. & Dickson, D. W. Impaired endo-lysosomal membrane integrity accelerates the seeding progression of α -synuclein aggregates. *Sci. Rep.* **7**, 7690
 64. Aits, S., Krickler, J., Liu, B., Ellegaard, A.-M., Hämälistö, S., *et al.* Sensitive detection of lysosomal membrane permeabilization by lysosomal galectin puncta assay. *Autophagy* **11**, 1408–1424 (2015).
 65. Jia, J., Claude-Taupin, A., Gu, Y., Choi, S. W., Peters, R., Bissa, B., Mudd, M. H., Allers, L., Pallikkuth, S., Lidke, K. A., Salemi, M., Phinney, B., Mari, M., Reggiori, F. & Deretic, V. Galectin-3 coordinates a cellular system for lysosomal repair and removal. *Dev. Cell* **52**, 69–87.e8 (2020).
 66. Chauhan, S., Kumar, S., Jain, A., Ponpuak, M., Mudd, M. H., Kimura, T., Choi, S. W., Peters, R., Mandell, M., Bruun, J. A., Johansen, T. & Deretic, V. TRIMs and galectins globally cooperate and TRIM16 and galectin-3 co-direct autophagy in endomembrane damage homeostasis. *Dev. Cell* **39**, 13–27 (2016).
 67. Ferraz, M. J., Marques, A. R. A., Appelman, M. D., Verhoek, M., Strijland, A., Mirzaian, M., Scheij, S., Ouairy, C. M., Lahav, D., Wisse, P., Overkleeft, H. S., Boot, R. G. & Aerts, J. M. Lysosomal glycosphingolipid catabolism by acid ceramidase: formation of glycosphingoid bases during deficiency of glycosidases. *FEBS Lett.* **590**, 716–725 (2016).
 68. Marques, A. R. A., Mirzaian, M., Akiyama, H., Wisse, P., Ferraz, M. J., *et al.* Glucosylated cholesterol in mammalian cells and tissues: formation and degradation by multiple cellular β -glucosidases. *J. Lipid Res.* **57**, 451–63 (2016).
 69. Ferraz, M. J., Marques, A. R. A. A., Gaspar, P., Mirzaian, M., van Roomen, C., Ottenhoff, R., Alfonso, P., Irún, P., Giraldo, P., Wisse, P., Sá Miranda, C., Overkleeft, H. S. & Aerts, J. M. Lyso-glycosphingolipid abnormalities in different murine models of lysosomal storage disorders. *Mol. Genet. Metab.* **117**, 186–93 (2016).
 70. Neculai, D., Schwake, M., Ravichandran, M., Zunke, F., Collins, R. F., Peters, J., Neculai, M., Plumb, J., Loppnau, P., Pizarro, J. C., Seitova, A., Trimble, W. S., Saftig, P., Grinstein, S. & Dhe-Paganon, S. Structure of LIMP-2 provides functional insights with implications for SR-BI and CD36. *Nature* **504**, 172–176 (2013).
 71. Heybrock, S., Kanerva, K., Meng, Y., Ing, C., Liang, A., *et al.* Lysosomal integral membrane protein-2 (LIMP-2/SCARB2) is involved in lysosomal cholesterol export. *Nat. Commun.* **10**, 3521 (2019).

72. Groothuis, G. M., Hulstaert, C. E., Kalicharan, D. & Hardonk, M. J. Plasma membrane specialization and intracellular polarity of freshly isolated rat hepatocytes. *Eur. J. Cell Biol.* **26**, 43–51 (1981).
73. Elleder, M., Smíd, F., Hyniová, H., Čihula, J., Zeman, J. & Macek, M. Liver findings in Niemann-Pic disease type C. *Histochem. J.* **16**, 1147–1170 (1984).
74. Renaud, G., Hamilton, R. L. & Havel, R. J. Hepatic metabolism of colloidal gold-low-density lipoprotein complexes in the rat: Evidence for bulk excretion of lysosomal contents into bile. *Hepatology* **9**, 380–392 (1989).
75. Infante, R. E., Abi-Mosleh, L., Radhakrishnan, A., Dale, J. D., Brown, M. S. & Goldstein, J. L. Purified NPC1 protein: I. Binding of cholesterol and oxysterols to a 1278-amino acid membrane protein. *J. Biol. Chem.* **283**, 1052–1063 (2008).
76. Wraith, J. E., Baumgartner, M. R., Bembi, B., Covanis, A., Levade, T., Mengel, E., Pineda, M., Sedel, F., Topçu, M., Vanier, M. T., Widner, H., Wijburg, F. A. & Patterson, M. C. Recommendations on the diagnosis and management of Niemann-Pick disease type C. *Mol. Genet. Metab.* **98**, 152–165 (2009).
77. Nixon, R. A. Niemann-Pick Type C Disease and Alzheimer's Disease: The APP-endosome connection fattens up. *American Journal of Pathology* **164**, 757–761 (2004).
78. Steingrímsson, E., Copeland, N. G. & Jenkins, N. A. Melanocytes and the *Microphthalmia* transcription factor network. *Annu. Rev. Genet.* **38**, 365–411 (2004).
79. Sardiello, M., Palmieri, M., Ronza, A. di, Medina, D. L., Valenza, M., *et al.* A gene network regulating lysosomal biogenesis and function. *Science* **325**, 473–477 (2009).
80. Moore, K. J. Insight into the microphthalmia gene. *Trends Genet.* **11**, 442–448 (1995).
81. Rehli, M., Lichanska, A., Cassady, A. I., Ostrowski, M. C. & Hume, D. A. TFEC is a macrophage-restricted member of the microphthalmia-TFE subfamily of basic helix-loop-helix leucine zipper transcription factors. *J. Immunol.* **162**, 1559–1565 (1999).
82. Kim, D. H., Sarbassov, D. D., Ali, S. M., King, J. E., Latek, R. R., Erdjument-Bromage, H., Tempst, P. & Sabatini, D. M. mTOR interacts with raptor to form a nutrient-sensitive complex that signals to the cell growth machinery. *Cell* **110**, 163–175 (2002).
83. Düvel, K., Yecies, J. L., Menon, S., Raman, P., Lipovsky, A. I., Souza, A. L., Triantafellow, E., Ma, Q., Gorski, R., Cleaver, S., Vander Heiden, M. G., MacKeigan, J. P., Finan, P. M., Clish, C. B., Murphy, L. O. & Manning, B. D. Activation of a metabolic gene regulatory network downstream of mTOR complex 1. *Mol. Cell* **39**, 171–183 (2010).
84. Zoncu, R., Bar-Peled, L., Efeyan, A., Wang, S., Sancak, Y. & Sabatini, D. M. mTORC1 senses lysosomal amino acids through an inside-out mechanism that requires the vacuolar H⁺-ATPase. *Science* **334**, 678–683 (2011).
85. Roczniak-Ferguson, A., Petit, C. S., Froehlich, F., Qian, S., Ky, J., Angarola, B., Walther, T. C. & Ferguson, S. M. The transcription factor TFEB links mTORC1 signaling to transcriptional control of lysosome homeostasis. *Sci. Signal.* **5**, ra42 (2012).
86. Martina, J. A., Chen, Y., Gucek, M. & Puertollano, R. MTORC1 functions as a transcriptional regulator of autophagy by preventing nuclear transport of TFEB. *Autophagy* **8**, 903–914 (2012).
87. Bronisz, A., Sharma, S. M., Hu, R., Godlewski, J., Tzivion, G., Mansky, K. C. & Ostrowski, M. C. Microphthalmia-associated Transcription Factor Interactions with 14-3-3 Modulate differentiation of committed myeloid precursors. *Mol. Biol. Cell* **17**, 3897–3906 (2006).
88. Settembre, C., Di Malta, C., Polito, V. A., Arcibibia, M. G., Vetrini, F., Erdin, S., Erdin, S. U., Huynh, T., Medina, D., Colella, P., Sardiello, M., Rubinsztein, D. C. & Ballabio, A. TFEB links autophagy to lysosomal biogenesis. *Science* **332**, 1429–1433 (2011).
89. Settembre, C., Zoncu, R., Medina, D. L., Vetrini, F., Erdin, S. S., Erdin, S. S., Huynh, T., Ferron, M., Karsenty, G., Vellard, M. C., Facchinetti, V., Sabatini, D. M. & Ballabio, A. A lysosome-to-nucleus signalling mechanism senses and regulates the lysosome via mTOR

- and TFEB. *EMBO J.* **31**, 1095–1108 (2012).
90. Spampanato, C., Feeney, E., Li, L., Cardone, M., Lim, J.-A., Annunziata, F., Zare, H., Polishchuk, R., Puertollano, R., Parenti, G., Ballabio, A. & Raben, N. Transcription factor EB (TFEB) is a new therapeutic target for Pompe disease. *EMBO Mol. Med.* **5**, 691–706 (2013).
 91. Song, W., Wang, F., Savini, M., Ake, A., di Ronza, A., Sardiello, M. & Segatori, L. TFEB regulates lysosomal proteostasis. *Hum. Mol. Genet.* **22**, 1994–2009 (2013).
 92. Medina, D. L., Fraldi, A., Bouche, V., Annunziata, F., Mansueto, G., Spampanato, C., Puri, C., Pignata, A., Martina, J. A., Sardiello, M., Palmieri, M., Polishchuk, R., Puertollano, R. & Ballabio, A. Transcriptional activation of lysosomal exocytosis promotes cellular clearance. *Dev. Cell* **21**, 421–30 (2011).
 93. Martina, J. A., Diab, H. I., Brady, O. A. & Puertollano, R. TFEB and TFE₃ are novel components of the integrated stress response. *EMBO J.* **35**, 479–495 (2016).
 94. Pogenberg, V., Ögmundsdóttir, M. H., Bergsteinsdóttir, K., Schepsky, A., Phung, B., *et al.* Restricted leucine zipper dimerization and specificity of DNA recognition of the melanocyte master regulator MITF. *Genes Dev.* **26**, 2647–2658 (2012).
 95. Yasumoto, K. I., Amae, S., Udono, T., Fuse, N., Takeda, K. & Shibahara, S. A big gene linked to small eyes encodes multiple Mitf isoforms: many promoters make light work. *Pigment Cell Res.* **11**, 329–336 (1998).
 96. Louphrasitthiphol, P., Siddaway, R., Loffreda, A., Pogenberg, V., Friedrichsen, H., *et al.* Tuning transcription factor availability through acetylation-mediated genomic redistribution. *Mol. Cell.* **79**, 1–16 (2020).
 97. Weilbaecher, K. N., Motyckova, G., Huber, W. E., Takemoto, C. M., Hemesath, T. J., Xu, Y., Hershey, C. L., Dowland, N. R., Wells, A. G. & Fisher, D. E. Linkage of M-CSF signaling to Mitf, TFE₃, and the osteoclast defect in Mitf(mi/mi) mice. *Mol. Cell* **8**, 749–758 (2001).
 98. Mansky, K. C., Sankar, U., Han, J. & Ostrowski, M. C. Microphthalmia transcription factor is a target of the p38 MAPK pathway in response to receptor activator of NF- κ B ligand signaling. *J. Biol. Chem.* **277**, 11077–83 (2002).
 99. Takeda, K., Takemoto, C., Kobayashi, I., Watanabe, A., Nobukuni, Y., Fisher, D. E. & Tachibana, M. Ser298 of MITF, a mutation site in Waardenburg syndrome type 2, is a phosphorylation site with functional significance. *Hum. Mol. Genet.* **9**, 125–132 (2000).
 100. Tassabehji, M., Newton, V. E., Liu, X. Z., Brady, A., Donnai, D., Krajewska-walasek, M., Murday, V., Norman, A., Obersztyn, E., Reardon, W., Rice, J. C., Trembath, R., Wieacker, P., Whiteford, M., Winter, R. & Read, A. P. The mutational spectrum in waardenburg syndrome. *Hum. Mol. Genet.* **4**, 2131–2137 (1995).
 101. Laurette, P., Strub, T., Koludrovic, D., Keime, C., Le Gras, S., Seberg, H., Van Otterloo, E., Imrichova, H., Siddaway, R., Aerts, S., Cornell, R. A., Mengus, G. & Davidson, I. Transcription factor MITF and remodeler BRG1 define chromatin organisation at regulatory elements in melanoma cells. *Elife* **4**, e06857 (2015).
 102. Annunziata, I., van de Vlekkert, D., Wolf, E., Finkelstein, D., Neale, G., Machado, E., Mosca, R., Campos, Y., Tillman, H., Roussel, M. F., Andrew Weesner, J., Ellen Fremuth, L., Qiu, X., Han, M. J., Grosveld, G. C. & D'Azzo, A. MYC competes with MiT/TFE in regulating lysosomal biogenesis and autophagy through an epigenetic rheostat. *Nat. Commun.* **10** (2019).
 103. Chauhan, S., Goodwin, J. G., Chauhan, S., Manyam, G., Wang, J., Kamat, A. M. & Boyd, D. D. ZKSCAN3 is a master transcriptional repressor of autophagy. *Mol. Cell* **50**, 16–28 (2013).
 104. Gilleron, J., Gerdes, J. M. & Zeigerer, A. Metabolic regulation through the endosomal system. *Traffic* **20**, 552–570 (2019).
 105. Jaishy, B. & Abel, E. D. Lipotoxicity: Many roads to cell dysfunction and cell death lipids, lysosomes, and autophagy. *J. Lipid Res.* **57**, 1619–1635 (2016).

106. Weisberg, S. P., McCann, D., Desai, M., Rosenbaum, M., Leibel, R. L. & Ferrante, A. W. Obesity is associated with macrophage accumulation in adipose tissue. *J. Clin. Invest.* **112**, 1796–1808 (2003).
107. Xu, H., Barnes, G. T., Yang, Q., Tan, G., Yang, D., Chou, C. J., Sole, J., Nichols, A., Ross, J. S., Tartaglia, L. A. & Chen, H. Chronic inflammation in fat plays a crucial role in the development of obesity-related insulin resistance. *J. Clin. Invest.* **112**, 1821–1830 (2003).
108. Wang, Z. V & Scherer, P. E. Adiponectin, the past two decades. *J. Mol. Cell Biol.* **8**, 93–100 (2016).
109. Xu, X., Grijalva, A., Skowronski, A., van Eijk, M., Serlie, M. J. J., Ferrante, A. W. W., van Eijk, M., Serlie, M. J. J. & Ferrante, A. W. W. Obesity activates a program of lysosomal-dependent lipid metabolism in adipose tissue macrophages independently of classic activation. *Cell Metab.* **18**, 816–830 (2013).
110. Aouadi, M., Tencerova, M., Vangala, P., Yawe, J. C., Nicoloso, S. M., Amano, S. U., Cohen, J. L. & Czech, M. P. Gene silencing in adipose tissue macrophages regulates whole-body metabolism in obese mice. *Proc. Natl. Acad. Sci. USA.* **110**, 8278–8283 (2013).
111. Jankovičová, J., Neuerová, Z., Sečová, P., Bartáková, M., Bubeníčková, F., Komrsková, K., Postlerová, P. & Antalíková, J. Tetraspanins in mammalian reproduction: spermatozoa, oocytes and embryos. *Med. Microbiol. Immunol.* **209**, 407–425 (2020).
112. Wang, H. & Eckel, R. H. Lipoprotein lipase: From gene to obesity. *Am. J. Physiol. Endocrinol. Metab.* **297**, E271–288 (2009).
113. Jaitin, D. A., Adlung, L., Thaïss, C. A., Weiner, A., Li, B., *et al.* Lipid-associated macrophages control metabolic homeostasis in a Trem2-dependent manner. *Cell* **178**, 686–698.e14 (2019).
114. Loving, B. A. & Bruce, K. D. Lipid and lipoprotein metabolism in microglia. *Front Physiol.* **11**, 393 (2020).
115. Martínez-Fábregas, J., Prescott, A., van Kasteren, S., Pedrioli, D. L., McLean, I., Moles, A., Reinheckel, T., Poli, V. & Watts, C. Lysosomal protease deficiency or substrate overload induces an oxidative-stress mediated STAT3-dependent pathway of lysosomal homeostasis. *Nat. Commun.* **9**, 1–16 (2018).
116. Wan, P., Hu, Y. & He, L. Regulation of melanocyte pivotal transcription factor MITF by some other transcription factors. *Mol. Cell. Biochem.* **354**, 241–246 (2011).
117. Goding, C. R. & Arnheiter, H. Mitf—the first 25 years. *Genes Dev.* **33**, 983–1007 (2019).
118. van Beek, A. A., Van den Bossche, J., Mastroberardino, P. G., de Winther, M. P. J. & Leenen, P. J. M. Metabolic alterations in aging macrophages: Ingredients for inflammaging? *Trends Immunol.* **40**, 113–127 (2019).
119. Boven, L. A., van Meurs, M., Boot, R. G., Mehta, A., Boon, L., Aerts, J. M. & Laman, J. D. Gaucher cells demonstrate a distinct macrophage phenotype and resemble alternatively activated macrophages. *Am. J. Clin. Pathol.* **122**, 359–369 (2004).
120. Krasemann, S., Madore, C., Cialic, R., Baufeld, C., Calcagno, N., *et al.* The TREM2-APOE pathway drives the transcriptional phenotype of dysfunctional microglia in neurodegenerative diseases. *Immunity* **47**, 566–581.e9 (2017).
121. Cochain, C., Vafadarnejad, E., Arampatzi, P., Pelisek, J., Winkels, H., Ley, K., Wolf, D., Saliba, A. E. & Zernecke, A. Single-cell RNA-seq reveals the transcriptional landscape and heterogeneity of aortic macrophages in murine atherosclerosis. *Circ. Res.* **122**, 1661–1674 (2018).
122. McArdle, S., Buscher, K., Ghosheh, Y., Pramod, A. B., Miller, J., Winkels, H., Wolf, D. & Ley, K. Migratory and dancing macrophage subsets in atherosclerotic lesions. *Circ. Res.* **125**, 1038–1051 (2019).
123. Willemssen, L. & de Winther, M. P. J. Macrophage subsets in atherosclerosis as defined by single-cell technologies. *Journal of Pathology* path.5392 (2020).

124. Rizwan, H., Mohanta, J., Si, S. & Pal, A. Gold nanoparticles reduce high glucose-induced oxidative-nitrosative stress regulated inflammation and apoptosis via tuberlin-mTOR/NF- κ B pathways in macrophages. *Int. J. Nanomedicine* **12**, 5841–5862 (2017).
125. Yuan, Y., Li, L., Zhu, L., Liu, F., Tang, X., Liao, G., Liu, J., Cheng, J., Chen, Y. & Lu, Y. Mesenchymal stem cells elicit macrophages into M2 phenotype via improving transcription factor EB-mediated autophagy to alleviate diabetic nephropathy. *Stem Cells* **38**, 639–652 (2020).

Summary

The research described in this thesis combines the latest insights in lysosomal function with lysosome centred cell signalling. Novel imaging and labelling techniques are applied to provide in depth characterization of lysosome function in health and disease. An integrative approach was used to study the physiological role of the lysosome, characterizing the function of lysosomal hydrolases and signalling on a cellular level as well as within the context of tissue.

The general introduction covers the current knowledge on the composition and functions of lysosomes, with a focus on macrophages. Lysosomal hydrolases and corresponding inherited lysosomal storage disorders are introduced, with emphasis to glucocerebrosidase (GCase) and Gaucher disease. The effect of (MiT/TFE) transcriptional regulation of cellular content on lysosomes is described, as well as the role of lysosome-associated kinases in regulation of cellular metabolism with emphasis on lipid homeostasis. Excessive lipid accumulation as cause of metabolic derailment (lipotoxicity) is introduced and illustrated by inherited and acquired disorders.

Chapter 1 reports on an increase in lysosome biogenesis in cells cultured in medium containing the buffer HEPES, which is driven by the transcription factors of the Mi/TF family, TFEB, TFE₃ and MITF independently of mTORC1. In macrophage-like cells, exposure to HEPES results in an enlarged vacuolar compartment and alterations in lysosomal signalling, proteolytic capacity, autophagic flux, and inflammatory signalling. This is accompanied by an increase in GCase activity and GPNMB expression, a protein that is part of the cellular response to lysosomal perturbation. Altogether, the findings show that chemical buffering agents in cell culture media can potentially confound lysosomes.

Chapter 2 describes the impact of culture conditions on the maturation of GCase as measured with specific mechanism-based probes visualizing the enzyme. The zwitterionic buffer HEPES, earlier identified as lysosome stressor, is shown to reduce the normal maturation of GCase to its final 58kDa form by means of glycan modification in lysosomes by local glycosidases. The processing of other glycosidases such as alpha-glucosidase and beta-glucuronidase is also impaired by the presence of HEPES in the culture medium. In cells grown in the presence of HEPES, GCase markedly accumulates due to impaired degradation. This phenomenon potentially has impact on diagnosis of Gaucher disease when residual GCase activity in cultured cells is assessed. In fibroblasts of Gaucher disease patients grown in the presence of HEPES, the enzyme levels may be very close to those observed in control cells grown without the buffer. It is concluded that supplementation of HEPES to cell culture medium should be treated with caution when cultured cells are used to confirm the diagnosis of Gaucher disease.

Chapter 3 describes the visualization of active GCase molecules by means of correlative light and electron microscopy (CLEM). Cyclophellitol-derived activity-based probes (ABPs) with a fluorescent reporter are employed that irreversibly bind to the catalytic pocket of GCase. By combining electron microscopy and fluorescence microscopy, the subcellular localization of active GCase molecules can be visualized. This technique

confirmed that endogenous active GCase molecules reside in the electron dense lysosomes. Gaucher disease is currently treated by infusion of mannose receptor targeted, recombinant GCase. Pre-labelling of therapeutic enzyme with an ABP with a distinct fluorophore allowed the simultaneous visualization of endogenous and exogenous, therapeutic enzyme in cells expressing mannose-receptor. This method revealed the efficient delivery of recombinant GCase to lysosomal compartments that contain endogenous active enzyme in an unprecedented manner.

Chapter 4 reviews the current knowledge on glycoprotein non-metastatic protein B (GPNMB) as biomarker for macrophage-associated lysosomal storage disorders. The transmembrane glycoprotein has emerged as one of the most abundant proteins in lipid-laden macrophages accumulating in spleen of Gaucher patients. A soluble fragment of GPNMB is released from the storage cells which results in prominently elevated GPNMB levels in plasma of symptomatic Gaucher disease patients. GPNMB is also found to be markedly increased in storage cells in Niemann-Pick type C liver. The review extends the knowledge on lipid laden macrophages to other fields, including neurodegeneration and obesity, in which lipid storage by macrophages has also been reported to induce GPNMB expression.

Chapter 5 provides a molecular and biochemical characterization of the liver of mice suffering from a deficiency in the lysosomal protein NPC1, a condition that results in the lysosomal storage disorder Niemann-Pick type C. The transmembrane protein NPC1 is involved in export of cholesterol from lysosomes and its deficiency causes intralysosomal cholesterol accumulation, which is accompanied by accumulation of other lipids such as sphingomyelin and glucosylceramide. As previous reports suggested, analysis of the NPC1-deficient liver revealed a reduction in hepatic GCase protein along with reduced enzyme activity. Surprisingly, the hepatocytes of 80 weeks old NPC1-deficient liver showed a strong increase in LIMP2, the lysosomal membrane protein that transport GCase to lysosomes and that is speculated to also act as cholesterol channel in the lysosomal membrane. The upregulation of LIMP2 was not observed in cholesterol-laden Kupffer cells in the same NPC1-deficient livers. These findings might point to compensatory role for LIMP2 in cholesterol transport during deficiency of the NPC1-mediated pathway.

Chapter 6 reports on the molecular and metabolic consequences of interfering in lysosomal biogenesis of obese adipose tissue macrophages. An siRNA-based approach was employed to elucidate the role of three Mi/TFE members, MITF, TFEB and TFE3, in regulating lysosome and inflammatory gene expression in macrophages. In cultured cells, a biomarker of lysosomal stress, GPNMB, was found to be highly dependent on Mi/TFE mediated transcription. The simultaneous knock down of all three Mi/TFE members was required for optimal reduction in GPNMB response to lysosomal perturbations, pointing to redundancy among the transcription factors. Delivery vehicles called glucan encapsulated particles were loaded with siRNAs targeting MITF, TFEB and TFE3 simultaneously. These were used to selectively interfere with macrophages in the adipose tissue of obese mice. The treatment resulted in worsening of glucose tolerance and reduced production of beneficial by adipocytes. Based on these results, the Mi/TFE driven induction of gene expression in macrophages present in obese adipose tissue seems

Summary

a favourable response limiting metabolic abnormalities and not a driver of pathology.

The discussion considers the major findings made during the investigations. The findings are discussed in view of recent literature.

Appendices

Summary in Dutch

List of publications

Curriculum Vitae

Acknowledgements

Samenvatting

Het onderzoek in dit proefschrift combineert nieuwe inzichten met betrekking tot lysosomale functie en signalering vanuit lysosomen. Nieuwe visualisatie- en labelingstechnieken zijn gebruikt om lysosomale functie tijdens welzijn en ziekte in kaart te brengen. Middels een integratieve benadering is de fysiologische functie van het lysosoom als organel bestudeerd, in de context van de cel en het weefsel.

De algemene introductie beslaat de huidige kennis over de samenstelling en functie van lysosomen, met een focus op de rol van het lysosoom in de macrofaag. In deze context worden lysosomale hydrolases geïntroduceerd met de daaraan gekoppelde aangeboren lysosomale stapelingsziektes. Glucocerebrosidase en de ziekte van Gaucher worden uitgelicht als voorbeeld van een aandoening waarin lysosomale lipidenstapeling zich manifesteert in de macrofaag. Beschreven wordt hoe de status van het lysosoom gekoppeld is aan transcriptionele regulatie van het celmetabolisme via lysosoom-geassocieerde kinases. Verstoord lipidenmetabolisme, en lysosomale lipidenafbraak in het bijzonder, wordt uitgelicht als belangrijk voorbeeld van lysosomale disfunctie. De consequenties van excessieve blootstelling aan lipiden (lipotoxiciteit) worden geïntroduceerd en de gerelateerde aangeboren en verkregen metabole aandoeningen worden besproken.

Hoofdstuk 1 beschrijft de veranderde biogenese van lysosomen in gekweekte cellen door toedoen van de veelgebruikte celkweek buffer HEPES. De toename in lysosomale genexpressie wordt toegeschreven aan drie transcriptiefactoren die behoren tot de MiT/TFE familie, TFEB, TFE3 en MITF. Het effect werd onafhankelijk bevonden van mTORC1, een lysosoom-geassocieerde kinase dat MiT/TFE leden post-translationeel modificeert. In gekweekte cellen die model staan voor de macrofaag resulteert blootstelling aan HEPES in een vergroting van de vacuolaire compartiment en veranderingen in lysosomale signalering, proteolytische capaciteit, autofage flux en inflammatiesignalering. Deze veranderingen worden geïllustreerd door een verhoogde activiteit van lysosomaal glucocerebrosidase en expressie van GPNMB, een eiwit dat verhoogd is als reactie op lysosomale disfunctie. Deze bevindingen laten zien dat buffers die gebruikt worden tijdens *in vitro* kweek van cellen potentieel lysosomale functie kunnen verstoren.

In **Hoofdstuk 2** is de invloed van kweekcondities op de maturatie van GCase geanalyseerd aan de hand van een synthetisch suicide substraat met een fluorescent label, een activity-based probe (ABP). De zwitterionische buffer HEPES, eerder geïdentificeerd als lysosomale stressor, verstoort de glycaanmodificatie van GCase, waardoor de uiteindelijke 58 kDa variant niet wordt gevormd tijdens de gebruikelijke maturatie in lysosomen. Fysiologische maturatie van andere glycosidasen zoals alpha-glucosidase en beta-glucuronidase is ook verstoord in aanwezigheid van HEPES in kweekmedium. GCase accumuleert in aanwezigheid van HEPES door verminderde proteolytische afbraak. Dit fenomeen heeft potentieel gevolgen voor diagnose van Gaucherpatiënten wanneer enzymactiviteit wordt gemeten in gekweekte cellen. De GCase-activiteit in patiënt-verkregen fibroblasten die gekweekt zijn in bijzijn van HEPES kan vergelijkbaar hoog zijn met die in fibroblasten afkomstig van gezonde individuen zonder de buffer. Concluderend, voorzichtigheid moet in acht moet genomen worden bij het gebruik van HEPES bij het kweken van cellen, en in het bijzonder bij gebruik van gekweekte cellen

voor diagnose van de ziekte van Gaucher.

Hoofdstuk 3 beschrijft de visualisatie van actieve GCase moleculen door middel van correlatieve licht- en elektronenmicroscopie (CLEM). Hierbij is gebruik gemaakt van ABPs die irreversibel binden in het katalytische domein van GCase. Door fluorescentiemicroscopie met elektronenmicroscopie te combineren kan de subcellulaire lokalisatie van GCase worden vastgesteld. Het signaal van gelabeld endogeen GCase kon worden gelokaliseerd in electrodichte (endo)lysosomen. De huidige behandeling van de ziekte van Gaucher bestaat uit recombinant GCase met affiniteit voor de mannose receptor. Door therapeutisch GCase te pre-labelen met een afwijkend fluorescente ABP kon zowel endogeen als exogeen, therapeutisch enzym simultaan gelabeld worden in cellen met overexpressie van de mannose receptor. Deze methode beschrijft voor het eerst een efficiënte aflevering van recombinant GCase in individuele lysosomen die tevens endogeen GCase bevatten.

Hoofdstuk 4 geeft een overzicht van de huidige kennis over glycoproteïne non-metastatische proteïne B (GPNMB) als biomarker voor lysosomale stapelingsziekten waarin de macrofaag een centrale rol speelt. Het geglycosyleerde transmembraan eiwit is een van de meest voorkomende eiwitten in lipide-geladen macrofagen die zich ophopen in de milt van Gaucherpatiënten. Bovendien is een prominente verhoging gevonden in de hoeveelheid van een oplosbaar GPNMB-fragment in plasma van symptomatische Gaucher patiënten. In andere lysosomale stapelingsziekten waarbij stapelingscellen voorkomen is GPNMB ook (lokaal en systemisch) verhoogd, bijvoorbeeld Niemann-Pick type C. De kennis aangaande stapelingscellen in andere ziektebeelden wordt besproken, waaronder die in neurodegeneratieve aandoeningen en obesitas, waarbij lipide stapelende macrofagen ook een verhoogde expressie van GPNMB tonen.

In **Hoofdstuk 5** is de lever van muizen die deficiënt zijn in het lysosomale eiwit NPC1 gekarakteriseerd op histologisch, biochemisch en moleculair niveau. NPC1 is betrokken bij de export van lysosomaal cholesterol en een deficiëntie in dit eiwit resulteert in de lysosomale stapelingsziekte Niemann-Pick type C. De ziekte is gekarakteriseerd door lysosomale cholesterol accumulatie dat ook gepaard gaat met stapeling van andere lipiden zoals sphingomyeline en glucosylceramide. Histologische analyse bevestigde de aanwezigheid van karakteristieke stapelingsmacrofagen en morfologische veranderingen in de lever van 80 dagen oude NPC-muizen. De levers bevatten een verlaagde hoeveelheid GCase eiwit wat gepaard gaat met verlaagde enzymactiviteit in leverlysaten van NPC1-deficiënte muizen, in lijn met eerder gepubliceerde data betreffende een verlaagde GCase activiteit bij NPC-deficiëntie. Western blot analyse gaf een verhoogde aanwezigheid van lysosoom geassocieerde eiwitten te zien, waaronder GPNMB, Galectine-3 en LIMP2. Immunohistochemische analyse wees uit dat LIMP2 verhoogd was in de hepatocyt, maar niet in de lipide geladen macrofagen van dezelfde lever. LIMP2 is verantwoordelijk voor het transport van nieuw gesynthetiseerd GBA naar het lysosoom en is tevens beschreven als lysosomaal exportkanaal voor cholesterol, als alternatief voor NPC1. De in dit hoofdstuk beschreven bevindingen suggereren dat LIMP2 in de hepatocyt bij een NPC1-deficiëntie als een compensatie opgereguleerd wordt.

Hoofdstuk 6 beschrijft de moleculaire en metabole consequenties van verstoorde

lysosomale biogenese in obese adipose weefselmacrofagen. Door middel van siRNA werd de expressie van drie leden van de MiT/TFE transcriptiefactorfamilie, MITF, TFEB en TFE₃, gereduceerd in gekweekte cellen. Hiermee werd beoogd de algehele expressie van lysosomale en autofagie genen te remmen. Een van de meest afhankelijke eiwitten van MiT/TFE regulatie bleek GPNMB, een gevoelige marker voor lysosomale stress. Echter, een simultane knock-down van MITF, TFEB en TFE₃ was nodig voor opheffing van verhoogde GPNMB-expressie ten gevolge van lysosomale perturbatie, wat duidt op overlappende regulatie van genexpressie. *In vivo* siRNA-experimenten werden uitgevoerd met behulp van glucanomhulsels geladen met siRNA specifiek voor MITF, TFEB en TFE₃. Deze methode werd toegepast voor de specifieke levering van siRNA in de vetweefselmacrofagen van obese muizen. De siRNA-behandeling resulteerde in verslechtering van glucosetolerantie en in verminderde productie van adiponectine door het vetweefsel. Concluderend lijkt de MiT/TFE-gedreven transcriptie in de obese vetweefselmacrofaag een gunstige bijdrage te leveren aan de glucosegevoeligheid tijdens obesitas.

De discussie beschouwt de belangrijkste bevindingen uit dit proefschrift en plaatst deze in de context van de huidige literatuur.

List of publications

1. Aerts, J.M.F.G., Ferraz M.J., Mirzaian M., Gaspar P., van Oussoren S., Wisse P., Kuo C.-L., Lelieveld L.T, Kytidou K., Hazeu M.D., Boer D.E.C., Meijer R., van der Lienden M.J.C., Chao D.H.M., Gabriel T.L., Aten J., Overkleeft H.S., van Eijk M., Boot R.G. & Marques A.R.A. Lysosomal storage diseases. For better or worse: adapting to defective lysosomal glycosphingolipid breakdown. *eLS* 1–13 (2017).
2. Tol, M. J., van der Lienden, M. J. C., Gabriel, T. L., Hagen, J. J., Scheij, S., Veenendaal, T., Klumperman, J., Donker-Koopman, W.E., Verhoeven, A.J., Overkleeft H.S., Aerts, J.M.F.G., Argmann, C.A. & van Eijk, M. HEPES activates a MiT/TFE-dependent lysosomal-autophagic gene network in cultured cells: A call for caution. *Autophagy* **14**, 1–13 (2018).
3. Artola, M., Kuo, C.-L., McMahon, S. A., Oehler, V., Hansen, T., van der Lienden, M., He, X., van den Elst, H., Florea, B. I., Kermode, A. R., van der Marel, G. A., Gloster, T. M., Codée, J. D. C., Overkleeft, H. S. & Aerts, J. M. F. G. New irreversible α -1 -iduronidase inhibitors and activity-based probes. *Chemistry - A European Journal* **24**, 19081–19088 (2018).
4. van der Lienden, M. J. C., Gaspar, P., Boot, R., Aerts, J. M. F. G. & van Eijk, M. Glycoprotein non-metastatic protein B: an emerging biomarker for lysosomal dysfunction in macrophages. *International Journal of Molecular Sciences*, **20**, 66 (2018).
5. van Meel, E., Bos, E., van der Lienden, M. J. C., Overkleeft, H. S., van Kasteren, S. I., Koster, A. J. & Aerts, J. M. F. G. Localization of active endogenous and exogenous β -glucocerebrosidase by correlative light-electron microscopy in human fibroblasts. *Traffic* **20**, 346–356 (2019).
6. Aerts, J. M. F. G., Kuo, C. L., Lelieveld, L. T., Boer, D. E. C., van der Lienden, M. J. C., Overkleeft, H. S. & Artola, M. Glycosphingolipids and lysosomal storage disorders as illustrated by gaucher disease. *Current Opinion in Chemical Biology* **53** 204–215 (2019).

Curriculum vitae

Martijn van der Lienden was born on December 3rd 1990 in Gouda, The Netherlands. During his high school years (VWO, Emmouscollege in Rotterdam), he became interested in molecular biology through his specialization in the life sciences. In 2009, he started his bachelor Biomedical Sciences at the Leiden University Medical Centre. As part of an exchange program, he studied human physiology and immunology at Karolinska Instituted in Stockholm in the second year of his BSc. After a minor internship at the department of Rheumatology at the LUMC, he dedicated his bachelor thesis to immunological characteristics of colorectal tumours at the department of Surgery of the LUMC.

Martijn continued at the LUMC with a research-oriented Master study, of which the first year was centred around his internship at the department of Virology in the LUMC. Under supervision of Dr. H. Mikkers, he worked on improving the quality of hematopoietic stem cells with respect to lymphoid differentiation, originating from immunocompromised patient-derived induced pluripotent stem cells. He meanwhile guided a student swimming society in the capacity as secretary of swimming. The second internship during his Master's was performed at the University of Cambridge at the John van Geest Centre for Brain Repair (Addenbrooke's hospital). He conducted molecular studies on the relation between morphological and immunological responses of astrocytes upon neuron damage and in tauopathies under supervision of Dr. A. Lakatos.

After graduation, Martijn initiated his doctoral studies in at Medical Biochemistry in 2015 under supervision of Dr. M. van Eijk and Prof. Dr. J.M.F.G. Aerts. The aim was to study lysosomal function and signalling within the context of disease in cells and within the body. Research covered by this thesis was presented at the ESGLD meetings (2017 in Lyon, France and 2019 in Vic, Spain, oral presentations), the Dutch conference for Diabetes, ADDRm in Oosterbeek, The Netherlands(2018, oral presentation), EMBO Lysosome and Metabolism in Naples, Italy (2018, poster presentation) and the EWGGD in Clermont-Ferrand, France (2019, oral presentation).

Martijn is currently performing postdoctoral research at the Academic Medical Centre in Amsterdam, continuing studies on lipid-laden macrophages in inherited metabolic disorders.

Acknowledgements

This thesis is the work of many. I wouldn't have been able to do anything without the environment of the lab, the input of the collaborations and last but not least, the never ceasing support of my family and friends.

I would like to thank first and before all my promotors **Marco** and **Hans**. **Marco**, thank you for choosing me to study lysosomal stress in obese adipose tissue macrophages. You have introduced me to the world of obesity and lysosomal storage disorders, always encouraged me to engage myself with the scientific community and to critically think about the next steps in the countless (too many) projects. Besides that, I will remember the conversations Rotterdam, Hausmagger and other music, fish, football, and 'what further came on the table'. **Hans**, thank you for making me aware of the bigger picture through thorough consideration of every project. I especially value the Thorn-sessions in which every project got the attention it deserved, along with the necessary wine from the sunny hills of Thorn. **Jan**, thank you for being the third supervisor and for conveying the enthusiasm for histology. Without your input and effort, it wouldn't have been possible to write this thesis.

I am incredibly grateful to have spent four years among my colleagues from the department of Medical Biochemistry, who all created an incredibly pleasant atmosphere to work in. **Maria**, **Daphne** and **Marc**, thank you for being the Party office. I will miss the talks on exciting projects, the complaining about less exciting things, and I know, everything is my fault! **Lindsey**, **Kim**, **Kassi**, **Saskia**, **Rianne**, **Ethan**, **Bas**, **Marta**, **Rebecca** and **Remco**, it was great to work with you in the lab, share ups and downs, and for the (perhaps more than) occasional incubation time small talk. **Rolf**, I highly valued your critical input on every project, but perhaps even more I valued the occasional talk on the latest (or oldest) obscure music bands. **Wouter**, **Mina**, **Judith**, **Eline**, the lab I knew when I started has changed, but your expertise and contribution in the lab were incredibly inspiring and have taught me a lot. Dear **Marri**, you have been the driving force of almost everything in the lab. Thank you for managing everyone to keep track of whatever reagent they finished, and especially for the great vibe the lab.

Larissa, **Yvonne**, **Sant**, **Daniël**, it was a pleasure to have you as students and you have taught me a lot, including about myself. I hope our lab was a place that inspired you to choose whatever you are passionate about, and to leave whatever wasn't interesting at all.

Dear **Marc** and **Tanit**, you paved the way for me to work on lysosomal stress. It was great to meet you both and talk about science. Your scientific contributions have inspired me throughout the last four years and will keep on doing so.

During my projects, I have had the pleasure to work with people from several different institutes. Thank you, **Bruno** for listening to our idea, for your constructive and valuable input on our animal protocols, and for offering the infrastructure and resources to perform mouse experiments. Dear **Patrick**, I am very grateful for the days you sacrificed for guiding me in mouse experiments, and for being the perfect talking buddy during those days and on the yearly diabetes meetings. I value our conversations during those days, and I hope we can keep that up. Many thanks to **Myriam** and the lab at Karolinska Institutet, for the interest you showed in our project, and to go along with our project based on our mutual interest in the obese adipose

tissue macrophages and Kupffer cells. Your contributions allowed us to do the pivotal experiments for my diabetes type 2 project. **Nike, Roelof**, thank you for the incredibly valuable contributions to mouse and tissue related projects, and for the pleasant chats in the AMC. Of course, I would like to thank everyone from 'upstairs': **Tom, Annelot, Thomas, Timo, Bobby, Daniël, Floor**, it was great to pop by, troubleshoot, supervise practica, organize the 'Biosyn-Medical biochemistry combination' football team, complain (mostly about cell culture), dine, bowl, and borrel.

I would also like to thank **Andras** and **Giulia**, who allowed me to perform research within a very motivating atmosphere and giving me the freedom to develop as a researcher. In addition, **Patri, Jessica, Sebastian**, and the BRC-crew, it was great to meet you all, it provided me with an extra push to do a PhD.

I would also like to thank everyone outside my scientific bubble. Special thanks to **Ingmar**, for being a great housemate, it was a challenge to find common time to eat, but there was always time to chat and relax. Everyone from the 'Sweden-group': **Sanne, Jaeike, Elleke, Aster, Meghna, Marloes, Kirsten**, even though it gets more and more difficult to meet, we always manage somehow. Thanks for being there throughout our studies and beyond. To **Patrick** who has seen me unexpectedly often since you defended in Prague, despite the distance I hope we can keep the great dinners and visits up. Also thank you and **Dijana**, for making me feel at home, for the great chats, dinners, and parties. **Sander, Tycho, Robin, Luuk**, you were basically there since I can remember things, and sometimes until the moment I remember things, so to many bro-nights to come;)

Ik ben enorme dank verschuldigd aan **mijn familie**, en in het bijzonder **mijn ouders**: zonder jullie open blik was ik überhaupt nooit in staat geweest in de levenswetenschappen door te gaan en als promovendus te beginnen. **Joris en Corné**, met een onbevangen blik hebben we allemaal een plek gevonden in de levenswetenschappen, en die blik is volgens mij het mooiste om te blijven houden.

Finally, and especially, I would like to thank my love, **Sravya**. As the most passionate, talented, engaging, happy, loving, and caring person I know, you are in so many ways my example and completion of what I do. As our first chats were about dissection techniques and X-inactivation, we might also be one of the nerdiest couples on the planet. I am the happiest, to have you at my side and to share all the milestones we will achieve in our live.

Martijn

'My final point concerns the value of serendipity and, especially, of its necessary correlate, the freedom to follow a new trail opened by chance, irrespective of previous commitments. It is noteworthy that in the paper in which lysosomes are first mentioned, the Lilly Research Laboratories are acknowledged for their financial support, despite the fact that their major interest, insulin, is conspicuously absent from the paper. One could only wish that funding agencies might show the same liberal attitude today.'

de Duve, C. The lysosome turns fifty. *Nat. Cell Biol.* 7, 847-849 (2005).

